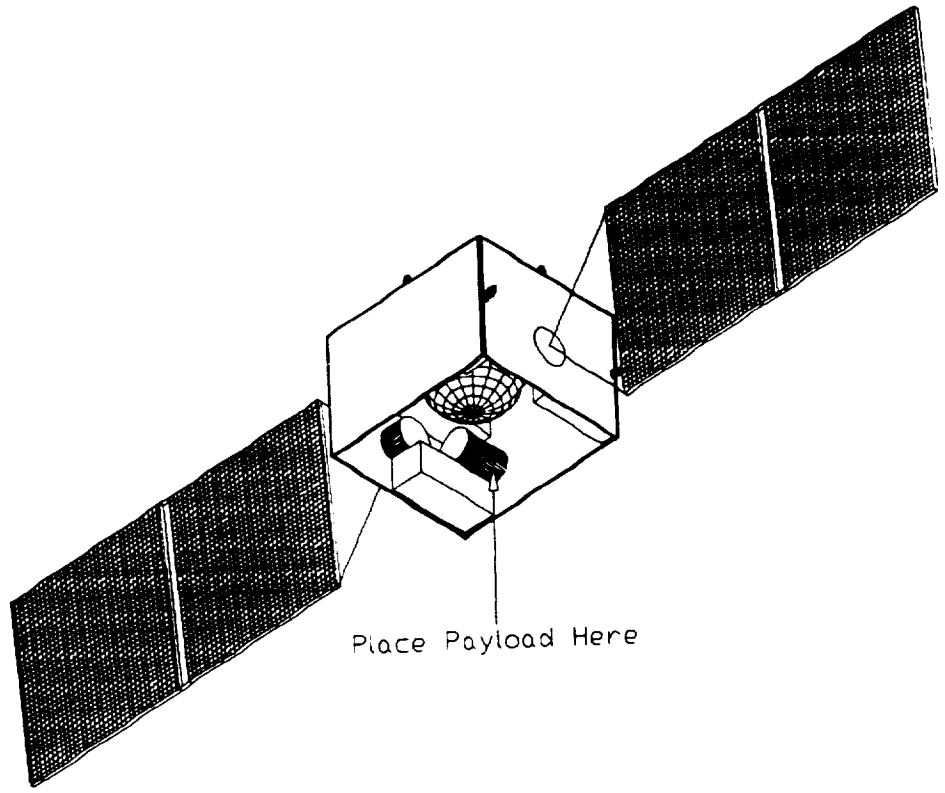


M 3-12
73733

p-270

SPACECRAFT DESIGN PROJECT MULTIPURPOSE SATELLITE BUS

MPS



DECEMBER 1990

NAVAL POSTGRADUATE SCHOOL

MONTEREY, CALIFORNIA

(NASA-CR-190009) SPACECRAFT DESIGN PROJECT
MULTIPURPOSE SATELLITE BUS MPS (Naval
Postgraduate School) 270 p

N92-27555

Unclas
G3/18 0073933

1990 SPACECRAFT PROJECT TEAM

Lyle Kellman

John Riley

Michael Szostak

Joseph Watkins

Joseph Willhelm

Gary Yale

COURSE

AE 4871

Advanced Spacecraft Design

Fall 1990

Course Instructor

Prof Brij Agrawal

This project was sponsored in part by NASA / University Space Research Association

Advanced Design Program

ACKNOWLEDGEMENTS

The 1990 design project team would like to thank Prof Brij Agrawal for his guidance and assistance throughout the 11 week quarter. His continuous support was sincerely appreciated and ensured the success of the project. We are also indebted to Profs G. Myers, T. Ha, D. Wadsworth, and R. Adler of the Naval Postgraduate School, who consistently made themselves available to answer our questions. Mike Brown, Charlie Merk, Shannon Coffey, Mike Zedd, Robert Morris, Paul Carey, and Nick Davinic of the Naval Research Laboratory also contributed to the success of the project. Bill Cummings of MIT Lincoln Laboratory and Lin Flinn, Richard Sudol and Perri-Anne Stiffler of Space Applications also made significant contributions. Finally, we appreciate the continued interest of Mr. J. Burke, our NASA representative from the Jet Propulsion Laboratory.

TABLE OF CONTENTS

1990 SPACECRAFT PROJECT TEAM.....	ii
ACKNOWLEDGEMENTS.....	iii
TABLE OF CONTENTS	iv
LIST OF TABLES	x
LIST OF FIGURES	xii
I. INTRODUCTION.....	1
A. BUS DESCRIPTION.....	2
B. PAYLOAD OVERVIEW	5
1. Advanced Very High Resolution Radiometer (AVHRR).....	5
2. Extremely High Frequency (EHF) Mission.....	6
C. LAUNCH VEHICLE DESCRIPTION	8
1. PEGASUS Air Launched Vehicle (ALV).....	8
2. TAURUS Single Stage Launch Vehicle (SSLV).....	9
II. BUS CONFIGURATION.....	11
A. EQUIPMENT LAYOUTS.....	13
1. Earth Face.....	13
a. AVHRR.....	13
b. EHF.....	14
2. Anti-Earth Face.....	15
3. North Face.....	16
4. South Face	17
5. East Face.....	18
6. West Face	19
7. Stowed Configuration.....	20

a.	AVHRR.....	20
b.	EHF.....	22
B.	SPACECRAFT BUS CONFIGURATIONS/SUMMARIES	24
1.	Mass Summaries.....	24
2.	Electrical Power Summaries.....	25
3.	Propellant Budget/Summary.....	27
III.	PAYLOADS.....	28
A.	AVHRR.....	28
1.	Functional Description.....	28
B.	Extremely High Frequency (EHF)	33
1.	EHF Bandwidth Allocation	34
2.	EHF Antenna	36
3.	Pointing Losses	42
4.	EHF Communications Repeater.....	46
5.	Dehop Circuit.....	49
6.	Command Check Circuit	51
7.	Hopping Circuit	52
IV.	ORBITAL DYNAMICS	54
A.	SELECTION OF ORBITS	54
1.	AVHRR.....	54
2.	EHF.....	56
B.	ORBIT ANALYSIS.....	57
1.	AVHRR	57
a.	Sun Angles on the Satellite	57
b.	Sun Angles on the Solar Arrays	63
c.	Eclipse Periods.....	70
2.	EHF.....	72

a.	Worst Case Eclipse.....	72
b.	Altitude as a Function of Time.....	73
C.	ORBIT MAINTENANCE.....	74
V.	SUBSYSTEMS.....	76
A.	ELECTRICAL POWER SUBSYSTEM.....	76
1.	Functional Description.....	76
a.	Solar Array Design.....	77
b.	Battery Design.....	79
2.	Detailed Mass Summary.....	81
B.	ATTITUDE CONTROL SUBSYSTEM.....	82
1.	Attitude Determination and Control System.....	82
a.	Precision Sensor Subsystem.....	82
b.	Basic Sensor System.....	83
c.	Attitude Control Subsystem.....	84
2.	Design Considerations.....	85
3.	Basic and Precision Subsystem Summary.....	86
4.	System Parameters.....	87
5.	System Performance.....	87
6.	Detailed Mass Summary.....	88
C.	THERMAL CONTROL SUBSYSTEM.....	89
1.	Design Considerations.....	89
2.	Optical Solar Radiator Sizing.....	90
3.	Solar Array Temperature.....	91
4.	Thermal Analysis Using PC-ITAS.....	93
5.	Conclusions.....	98
D.	PROPULSION SUBSYSTEM.....	99
1.	Functional Description.....	99

a. Requirements.....	99
b. Summary of Subsystem	100
c. Summary of Subsystem Operations.....	103
2. Detailed Mass/Power Summary	104
E. TELEMETRY AND TRACKING SUBSYSTEM	105
1. Functional Description.....	105
F. STRUCTURAL SUBSYSTEM.....	112
1. Functional Description.....	112
2. Requirements	112
3. Summary of Subsystem Operations	113
a. Frame Construction	113
b. Honeycomb Panels.....	113
c. Payload Mechanical Interface	114
d. Earth Face	115
e. Fuel Tank Support.....	115
4. Margins of Safety	116
5. Detailed Mass Summary.....	116
REFERENCES.....	118
APPENDIX A.....	120
ORBITAL DYNAMICS.....	120
Appendix A.1	120
Appendix A.2	147
Appendix A.3	165
Appendix A.4	178
APPENDIX B.....	184
A. BATTERY DESIGN.....	184
B. SOLAR ARRAY DEGRADATION.....	186

1. EHF Payload	186
2. AVHRR Payload	190
C. SOLAR ARRAY PANEL SIZING	192
APPENDIX C	193
ATTITUDE CONTROL CALCULATIONS	193
1. Moment of Inertia Calculations	193
2. Disturbance Torques	196
a. Solar Torque	196
b. Magnetic Torque	199
c. Aerodynamic Torque	200
3. Equations of Motion	200
APPENDIX D	209
THERMAL CONTROL CALCULATIONS	209
APPENDIX E	224
PROPULSION CALCULATIONS	224
APPENDIX F	225
AXIAL LOADS	225
1. Frame Beams	225
2. Honeycomb Panel	225
BENDING LOADS	226
1. Maximum Deflection	226
2. Maximum Bending Stress	227
3. Maximum Shear Stress	228
HONEYCOMB PANELS	228
1. Fundamental Natural Frequency Calculations	228
2. Stress Due to Dynamic Acceleration	229
APPENDIX H	230

COMMUNICATIONS SUBSYSTEM TABLES	230
APPENDIX J.....	235
LINK ANALYSIS.....	235
APPENDIX K.....	251
DEFENSE ADVANCED RESEARCH PROJECTS AGENCY STATEMENT OF WORK	251

LIST OF TABLES

TABLE 1.1	Molniya Type Orbits for SSLV Ballasted Vehicle	9
TABLE 2.1	Mass Summary Comparison	24
TABLE 2.2	Electrical Power Summary - AVHRR.....	25
TABLE 2.3	Electrical Power Summary - EHF Comm.....	26
TABLE 2.4	Propellant Budget Summary.....	27
TABLE 3.1	AVHRR Channels	29
TABLE 4.1	Summary of Orbital Parameters.....	54
TABLE 4.2	Sun Angles on Satellite Faces for an 8:30 PM Orbit.....	60
TABLE 4.3	Sun Angles on Satellite Faces for a 3:30 PM Orbit	62
TABLE 4.4	Eclipse Duration for EHF Mission.....	73
TABLE 4.5	Perturbations on EHF Mission Orbit	75
TABLE 5.1	System Power Summaries (Normal Operations).....	76
TABLE 5.2	Solar Cell Characteristics	78
TABLE 5.3	Solar Array Summaries	78
TABLE 5.4	Battery Summary	80
TABLE 5.5	Radiation Annual Fluence Summary	81
TABLE 5.6	Detailed Mass Summary of EPS	81
TABLE 5.7	Reaction Wheel Parameters (AVHRR).....	87
TABLE 5.8	Mass Summary of ADCS.....	88
TABLE 5.9	Typical Equipment Temperature Limits	90
TABLE 5.10	Solar Array Operating Temperatures.....	92
TABLE 5.11	AVHRR Model and Node Assignment.....	94
TABLE 5.12	EHF Model and Node Assignment	94
TABLE 5.13	AVHRR Material Selection and Heat Dissipation	96
TABLE 5.14	EHF Material Selection and Heat Dissipation	97

TABLE 5.15	Thruster Operations.....	99
TABLE 5.16	Summary of Propulsion Equipment.....	102
TABLE 5.17	Propellant/Pressurant Tank Characteristics.....	103
TABLE 5.18	Mass/Power Summary of Propulsion Subsystem.....	104
TABLE 5.19	Accelerations at Payload Interface.....	112
TABLE 5.20	Margins of Safety.....	116
TABLE 5.21	Mass Summary of Structural Subsystem.....	117

LIST OF FIGURES

FIGURE 1.1	MPS Bus in AVHRR Configuration	6
FIGURE 1.2	MPS Bus in EHF Configuration.....	7
FIGURE 1.3	Pegasus Dynamic Shroud.....	8
FIGURE 1.4	Taurus Dynamic Shroud	10
FIGURE 2.1	Multiple Purpose Satellite Bus	11
FIGURE 2.2	Earth Face With the AVHRR Mounted.....	13
FIGURE 2.3	Earth Face With the EHF Payload Mounted.....	14
FIGURE 2.4	Anti-Earth Face.....	15
FIGURE 2.5	North Face.....	16
FIGURE 2.6	South Face.....	17
FIGURE 2.7	East Face.....	18
FIGURE 2.8	West Face.....	19
FIGURE 2.9	Side view of MPS Bus w/AVHRR Payload in Folded Configuration.....	20
FIGURE 2.10	Top view of MPS Bus w/AVHRR Payload in Folded Configuration.....	21
FIGURE 2.11	Side view of MPS Bus w/EHF Payload in Folded Configuration.....	22
FIGURE 2.12	MPS Bus with Solar Array Deploying	23
FIGURE 3.1	Microstrip Element.....	30
FIGURE 3.2	Six-Element Microstrip Array	32
FIGURE 3.3	EHF Payload Configuration.....	33
FIGURE 3.4	EHF Bandwidth Allocation.....	35
FIGURE 3.5	Feedhorn Arrangement.....	37
FIGURE 3.6	Gain Versus Beamwidth	39

FIGURE 3.7	Beamwidth versus Altitude	40
FIGURE 3.8	Beamwidth versus Time After Perigee	41
FIGURE 3.9	Gain Versus Altitude	41
FIGURE 3.10	Gain Versus Time After Perigee	42
FIGURE 3.11	Pointing Losses	43
FIGURE 3.12	Gain Versus Off Axis Angle.....	45
FIGURE 3.13	Gain Versus Scan Angle	45
FIGURE 3.14	TWTA Characteristics.....	47
FIGURE 3.15	Communications Repeater	48
FIGURE 3.16	Dehopping Circuit	50
FIGURE 3.17	Command Check Circuit.....	52
FIGURE 3.18	Hopping Circuit.....	53
FIGURE 4.1	First Day of Winter Sun Angles on S/C Faces vs Orbital Position	58
FIGURE 4.2	Sun Angle on +Roll Face vs Orbital Position	59
FIGURE 4.3	Solar Array Illumination Geometry.....	65
FIGURE 4.4	Solar Array Rotation Angle vs Orbital Position and Season.....	66
FIGURE 4.5	Solar Array Sun Angle vs Orbital Position and Season	68
FIGURE 4.6	Worst Case Solar Array Sun Angles vs Time of Year.....	69
FIGURE 4.7	Eclipse Duration vs Time of Year.....	70
FIGURE 4.8	Eclipse Location in the S/C Orbit vs Time of Year.....	71
FIGURE 4.9	Time Since Perigee vs True Anomaly	74
FIGURE 5.1	Functional Diagram of Precision Sensor Subsystem	83
FIGURE 5.2	Functional Diagram of Basic Sensor Subsystem.....	84
FIGURE 5.3	Functional Diagram of Attitude Control Subsystem	85
FIGURE 5.4	Location of Thrusters.....	100
FIGURE 5.5	Schematic Diagram of Propulsion System.....	101
FIGURE 5.6	TT&C Package.....	106

FIGURE 5.7	Remote Tracking Unit.....	107
FIGURE 5.8	Remote Command Unit.....	109
FIGURE 5.9	Cross-section of Tubular Frame	113
FIGURE 5.10	Typical Honeycomb Panel.....	114
FIGURE 5.11	Marmon Clamp Design.....	115

I. INTRODUCTION

This spacecraft design project is the output of AE 4871, an advanced spacecraft design course taught as the culmination of the Space Engineering Curriculum at the Naval Postgraduate School (NPS). The intent of the course is to provide students with both satellite system and subsystem design experience as well as the experience of working on a project team. Due to the small number of students taking the course in 1990 (6), each student was given responsibility for one primary subsystem and to assist in at least one other subsystem. The Naval Research Laboratory, Washington D.C., was again asked to augment the Naval Postgraduate School faculty. Analysis and design of each subsystem was done to the extent possible within the constraints of an eleven week quarter and considering the limited number of team members.

Rather than pursue an academic design for this year's course, the project team at the suggestion of the instructor, Professor Brij Agrawal, decided instead to design a multimission spacecraft bus based on a Statement of Work issued by Defense Advanced Research Projects Agency (DARPA). The SOW called for a " proposal to design a small, low cost, lightweight, general purpose spacecraft bus capable of accommodating any of a variety of mission payloads. Typical payloads envisioned include those associated with meteorological, communication, surveillance and tracking, target location, and navigation mission areas". The two payloads chosen for the Multipurpose Satellite (MPS) bus design were a multi-spectral meteorological payload called the Advanced Very High Resolution Radiometer (AVHRR), and an EHF communications package. MPS was designed with excess internal volume to expand easily and also to be able to accommodate future, unspecified payloads in the other mission areas.

A. BUS DESCRIPTION

The thrust of this project was to design not a single spacecraft, but to design a multimission bus capable of supporting several current payloads and unnamed, unspecified future payloads. Spiraling costs of spacecraft and shrinking defense budgets necessitated a fresh look at the feasibility of a multimission spacecraft bus. The design team chose two very diverse and different payloads, along with them two vastly different orbits, to show that multimission spacecraft buses are an area where indeed more research and effort needs to be made. Tradeoffs, of course, were made throughout the design, but optimization of subsystem components limited weight and volume penalties, performance degradation, and reliability concerns. Simplicity was chosen over more complex, sophisticated and usually more efficient designs. Cost of individual subsystem components was not a primary concern in the design phase, but every effort was made to chose flight tested and flight proven hardware. Significant cost savings could be realized if a standard spacecraft bus was indeed designed and purchased in finite quantities.

Throughout this document, justification for subsystem choices will be made where clarification is necessary. Detailed analyses in all subsystem areas can be found in the appendices. The AVHRR and the EHF comm payloads previously mentioned were suggested by DARPA as typical payloads and the launch vehicle was given as PEGASUS, the new air-launched vehicle built by Orbital Science Corporation and the Hercules Aerospace Company. This choice of launch vehicle constrained the volumetric dimensions of the bus. In order to get the AVHRR payload to its design altitude of 450 NM and 98.75° inclination, Pegasus performance characteristics limited the bus and payload to 350 lbs. This fact constrained the MPS bus mass to approximately 285 lbs. Every effort was made to get the EHF package into the Pegasus shroud and to boost it to an 8 hour Molniya type orbit. Unfortunately however, performance limitations would not allow this to be done without launching a marginally capable spacecraft. Orbital Sciences Corporation

has already recognized this need and has a fourth stage/perigee kick motor for Pegasus in the works. Until the advent of this modification though, design work on the EHF payload assumed that TAURUS, the small Standard Launch Vehicle (SSLV) would be the launch platform.

The Multipurpose Satellite bus is modular in the fact that the various payloads would "bolt on" the earth face and several other components could also be removed, added or modified according to the payload's needs. Because of the SOW's requirement that the spacecraft be able to launch within 72 hours, this modularity is limited to select equipment. Equipment such as the one million dollar plus celestial sensor and the solar array panels are examples. The expensive star sensor would be installed only on missions that necessitated high degree of pointing accuracy. The number of solar array panels would depend on the power requirements of the mission payload and the orbit. Fuel would be added in the amount required, if any, just prior to launch.

The MPS bus, regardless of the payload, is a 3 axis stabilized, nadir pointing, dual solar array spacecraft. The various payloads would attach to the earthface of the bus in the orientation necessary for that payload. The basic bus is a rectangular aluminum frame 32" x 28" x 23" with five load supporting panels (four sides and anti-earth face). Attitude control is maintained with a 4 reaction wheel system to accommodate the vast number and types of possible orbits. One wheel is placed on each of the primary axes and a standby wheel 45° from each axis is also installed. Two magnetic torque rods are installed to unload the reaction wheels.

Pointing accuracy to $\pm .01^\circ$ is necessitated by the AVHRR payload. This degree of accuracy can only be accomplished with a celestial star sensor. This extremely expensive sensor could be removed for the EHF payload where a sun/earth sensor combination could achieve $\pm 0.5^\circ$ pointing accuracy. The solar array subsystem consists of two 34 in. x 32 in. panels per side for these two payloads. An additional panel can be added on each side for a future payload; if additional power is required. The arrays are single degree of

freedom positioned along the roll axis, and can rotate about this axis to maximize sun angle. With the EHF package installed, the satellite rotates about its yaw axis so as to maintain the solar panel axis (roll axis) normal to the sun while providing maximum solar power efficiency. This yaw motion provides a second degree of freedom for the solar arrays.

The Electric Power Subsystem (EPS) is taken from the High Latitude Communication Satellite design, NPS's 1989 design course project, with few exceptions. The 28 volt single bus, the sixteen 12 Amp-hour batteries and the power converter equipment remain the same. The solar array area has changed however because of the different orbits, the different power requirements, and the different launch vehicle influencing the stowed configuration. Thermal control was designed to be completely passive. Because most of the support equipment is on continually, thought was given to distribute high power dissipators so that the bus's internal temperature was uniform. The payloads are by far the biggest power dissipators and are provided with their own radiators. The AVHRR radiator is part of the payload and is positioned to radiate to deep space 180° from the sun. There is an additional radiator mounted on the bus to radiate thermal energy from the internal equipment to supplement the radiator on the AVHRR. The EHF payload, on the other hand, is configured with optical solar reflectors (OSR) along the north face of its Earth face panel. Because of the different orbits, various coverings/paint schemes and insulation will have to be used.

The propulsion system consists of a single 16 inch diameter hydrazine tank with a nitrogen diaphragm blow down system. Six 0.2 lb thrusters are located to desaturate the reaction wheels (secondary to magnetic torque rods), for orbit maintenance, for orbit stationkeeping, minor orbit changes or ASAT avoidance. The weight penalty incurred if the payload does not require a propellant/propulsion system is considered minimal.

B. PAYLOAD OVERVIEW

1. Advanced Very High Resolution Radiometer (AVHRR)

The AVHRR is an operational radiometer designed to provide meteorological data from the year 1990 to the year 2000. The AVHRR scans the earth's surface several times each day in the spectral regions from 0.7 to 0.12 microns. These six spectral bands can be downlinked in either high or low resolution modes. Operating 24 hours a day, the AVHRR can provide land, water, and cloud imaging; sea surface temperature; and ice concentration and coverage.

The AVHRR would be launched by Pegasus into a 450 NM (833 km) 0830 descending or 1530 ascending sun synchronous orbit at a 98.75° inclination. Orbit period is 101 minutes with worst case 37 minute eclipse occurring during the summer. Average eclipse time is on the order of 33 minutes. The AVHRR is mounted on the earth face so that the bus is nadir pointing and the bus is 'flown' so that the solar arrays are positioned along the roll axis. Rather than incurring an increase in the cost and complexity of two degree of freedom solar arrays, the solar arrays are single degree of freedom and oversized to to compensate for the cosine effect of the sun's rays in relation to the orbit plane. Although the AVHRR requires only a nominal amount of power, the fact that it is in eclipse for greater than one third of its orbit necessitates a large power requirement for battery charging. Negligible radiation damage and orbit altitude degradation is experienced at 450 NM. The MPS bus with the AVHRR mounted is depicted in Figure 1.1.

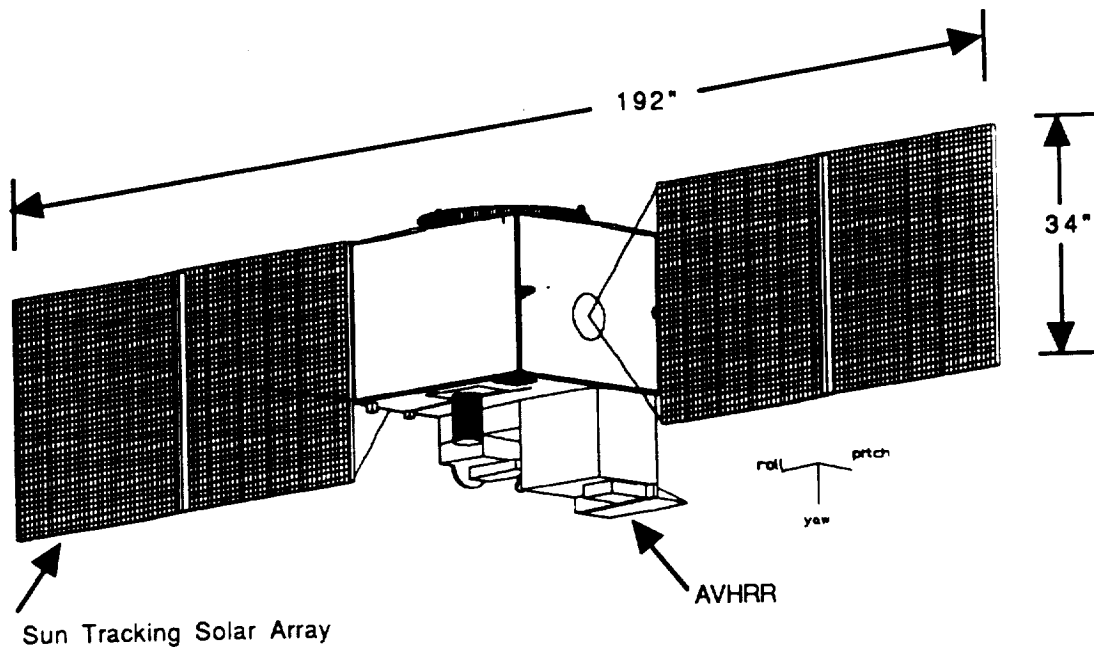


FIGURE 1.1 MPS Bus in AVHRR Configuration

2. Extremely High Frequency (EHF) Mission

The EHF payload is to be used to supplement the existing communication facilities of the operational forces in time of crisis. The payload was designed to be quickly mated with the MPS bus and launched within 72 hours. The antenna/feedhorn arrangement was designed and provided by Lincoln Laboratory.

The EHF communications payload is to be launched by Taurus (SSLV) into a six, eight, or twelve hour Molniya type orbit. For this design, an eight hour Molniya type orbit was chosen with a 500 km perigee and a 27,000 km apogee. Worst case eclipse for this orbit is 52 minutes. The EHF payload consists of a 32" x 28" x 6" structural box that supports the EHF antenna structure and houses the EHF R/T and the TT&C equipment. The EHF and TT&C antennas and the earth sensor are located on the earth face of this box that is affixed to the earth face of the MPS bus. Optical solar reflectors are mounted on the

north face of the structural box and provide the necessary cooling for the travelling wave tube amplifiers (TWTA). The solar array configuration for the EHF consists of the same panels as the AVHRR. The MPS bus with the EHF payload is depicted in Figure 1.2.

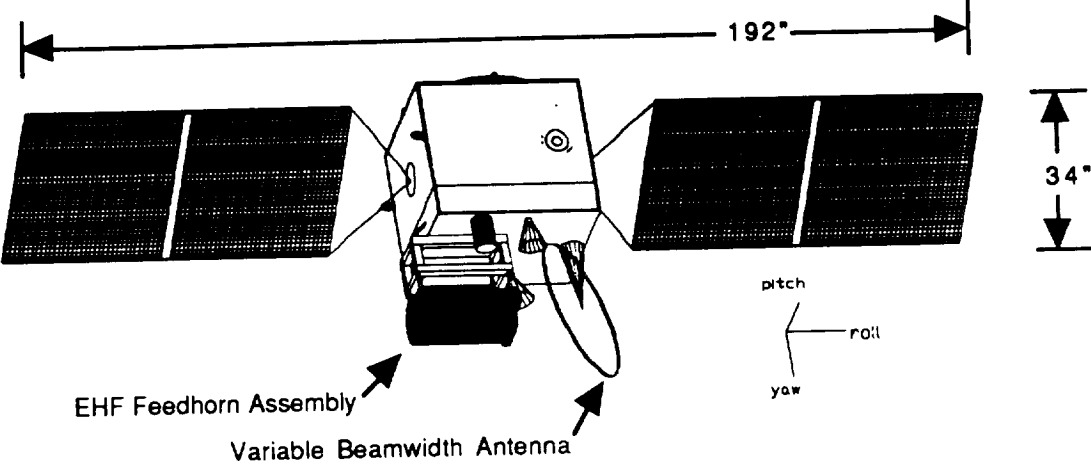


FIGURE 1.2 MPS Bus in EHF Configuration

C. LAUNCH VEHICLE DESCRIPTION

1. PEGASUS Air Launched Vehicle (ALV)

The Pegasus air launched booster is a three stage solid propellant winged rocket designed specifically for the insertion of small payloads into orbit. The 50 foot long, 50 inch diameter booster weighs 42,000 lbs and is carried aloft by a conventional transport/bomber-class aircraft (B-52, B-747, L-1011). Once oriented along the desired orbit direction, level at approximately 42,000 feet, and flying at high subsonic speed, the parent aircraft releases the Pegasus booster. The booster freefalls with active guidance to clear the carrier aircraft while executing a pitch-up maneuver to place it in the proper attitude for motor ignition. After first stage ignition, the vehicle follows a lifting-ascent trajectory to orbit. The dynamic payload envelope is detailed in Figure 1.3

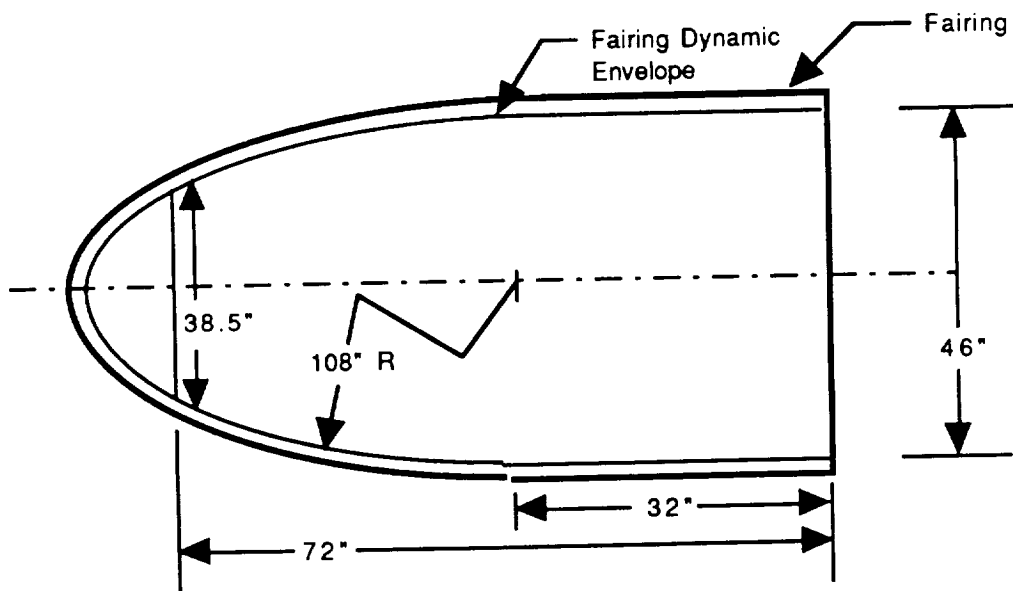


FIGURE 1.3 Pegasus Dynamic Shroud

2. TAURUS Standard Small Launch Vehicle (SSLV)

Taurus is a four-stage, inertially-guided, 3-axis stabilized, solid propellant launch vehicle proposed by Orbital Science Corporation . The design incorporates a Pegasus first, second, and third stage atop a Peacekeeper ICBM. Taurus is fully transportable with rapid launch site establishment and launch call up. Initial performance estimates are described in Table 1.1.

Perigee	Apogee	Period	Payload	Enhanced
270 nm	21400 nm	12 Hrs	194 Lb	458 Lb
270 nm	14773 nm	8 Hrs	277 Lb	573 Lb
270 nm	10945 nm	6 Hrs	362 Lb	694 Lb
270 nm	6658 nm	4 Hrs	542 Lb	953 Lb

TABLE 1.1 Molniya Type Orbits for SSLV Ballasted Vehicle

Because Pegasus is unable to propel an EHF payload into an 8 hour Molniya type orbit, Taurus would be the launch vehicle of choice for this payload. The 50 inch diameter x 90 inch long dynamic envelope of the shroud allows for the addition of a third solar array panel per side if needed (the 46" diameter shroud of Pegasus allows only two panels per side). The Taurus dynamic shroud is depicted in Figure 1.4.

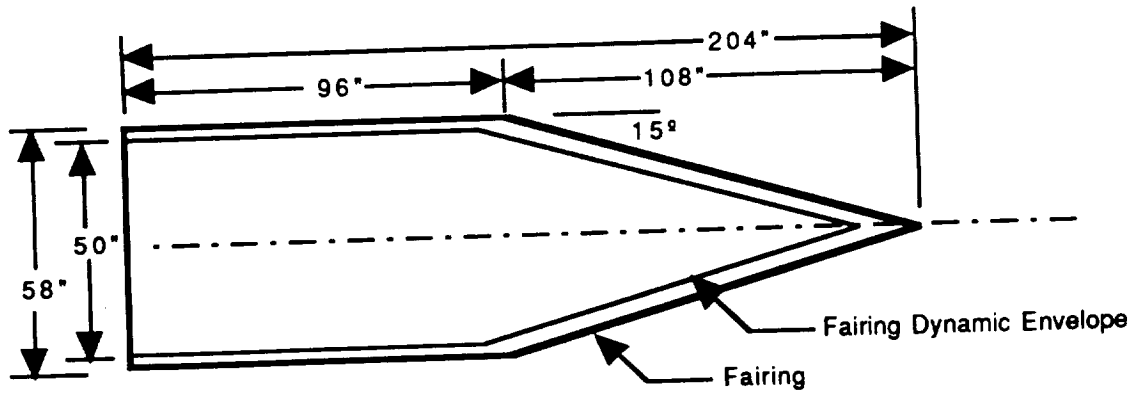


FIGURE 1.4 Taurus Dynamic Shroud

II. BUS CONFIGURATION

The MPS bus as previously mentioned, is not alone an operational spacecraft, but a vehicle used in conjunction with a number of various payloads to form a spacecraft. The bus itself as depicted in Figure 2.1, is a 270 lb rectangular box with all the subsystems necessary to fly a variety of orbits and missions.

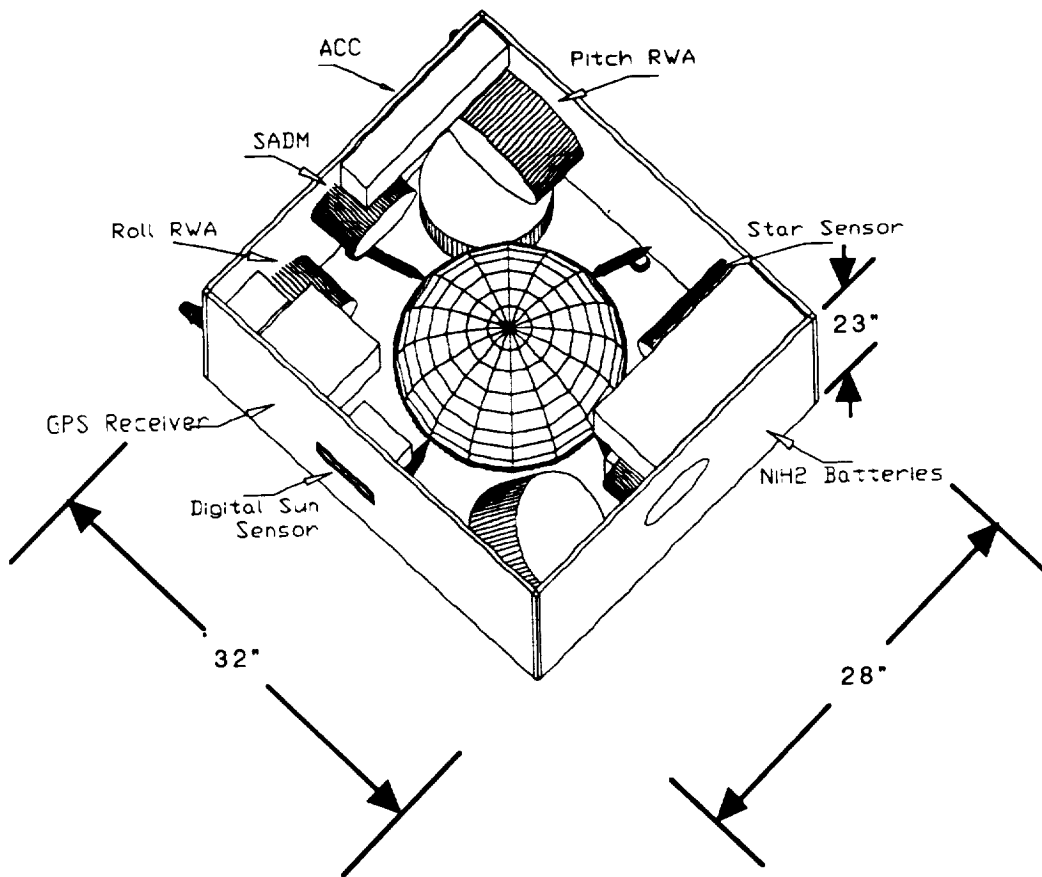


FIGURE 2.1 Multiple Purpose Satellite Bus

The choice of equipment and its location within the bus will be detailed in the various subsections to follow. The main feature of the bus is its ability to support a variety

of 'bolt on' payloads. With the advent of programmable circuitry, equipment such as reaction wheels, solar array drive motors and power control electronics can be adapted to almost any orbit or mission. It is feasible to program the entire bus to support the payload, regardless of the desired orbit. This programming would be performed after payload mating to the bus and just prior to launch. Figures 2.2 and 2.3 show the earth faces of both the AVHRR and the EHF payloads while the five load supporting panels standard to the MPS bus are depicted in Figures 2.4 to 2.8. A side view of the folded configuration of both payloads as well as the top view of the AVHRR is depicted in Figures 2.9 to 2.11. Lastly, a view of the solar arrays unfolding is depicted in Figure 2.12.

A. EQUIPMENT LAYOUTS

1. Earth Face

a. AVHRR

Figure 2.2 shows the earth face in the AVHRR configuration. Mounted also on the earth face are the earth sensor, two dipole antenna and a six element microstrip array antenna. Mounted on the underside of the face are the RTU and the RCU.

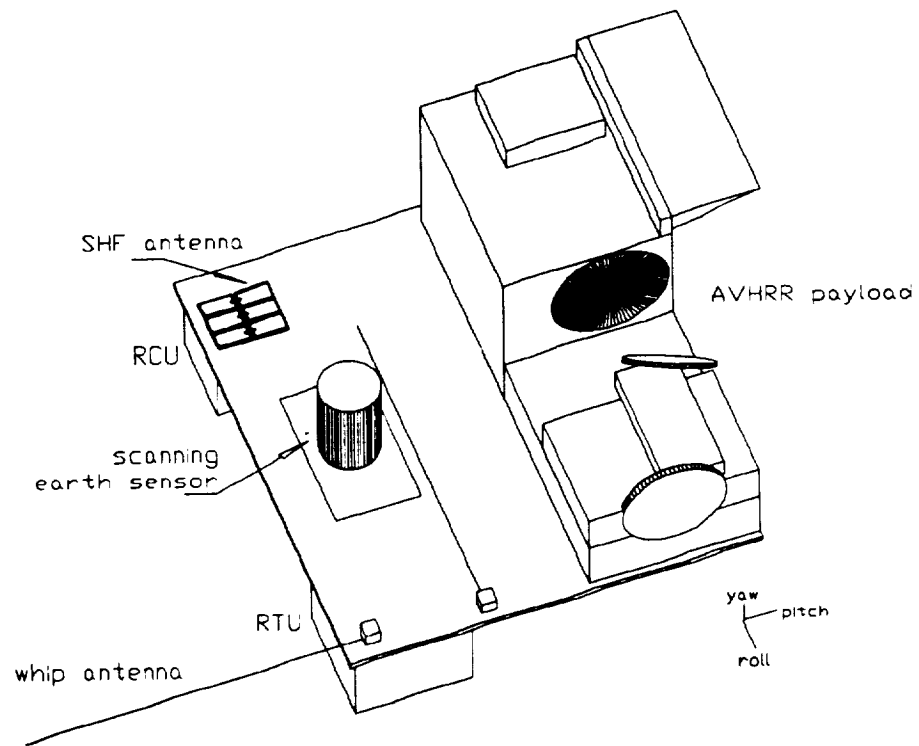


FIGURE 2.2 Earth Face With the AVHRR Mounted

b. EHF

Figure 2.3 depicts the EHF antenna structure mounted on its 6" x 32" x 28" frame. Seen are the 22 and 44 Ghz feedhorns, the variable beamwidth antenna, two earth coverage feedhorns and the scanning earth sensor. Unseen on the underside are the RTU and RCU units and the EHF travelling wave tube amplifiers. Also not shown in this diagram are the optical solar reflectors located on the north face of this frame.

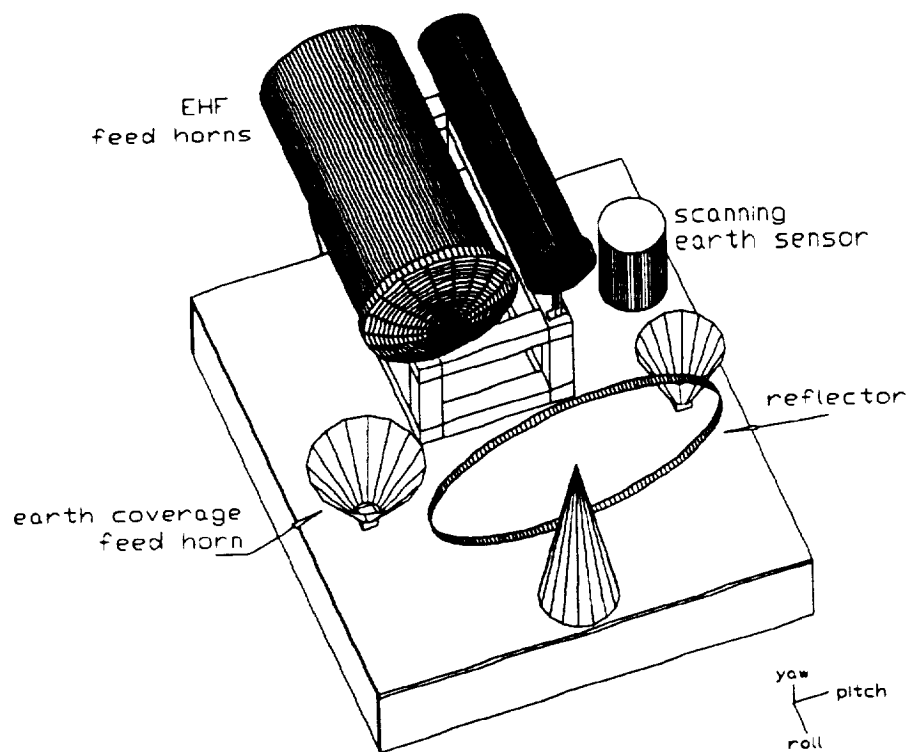


FIGURE 2.3 Earth Face With the EHF Payload Mounted

2. Anti-Earth Face

Mounted on the anti-earth face are the yaw reaction wheel assembly and the 16 inch diameter fuel tank . The fuel tank supports attach to a waistband on the fuel tank and then again to the rectangular frame. Not depicted is a 22 inch diameter, one sixteenth inch thick disk used to transmit the axial load of the fuel tank to the Marmon clamp assembly directly below this panel. Also not shown on the underside of this panel is a digital sun sensor and four thrusters. The anti-earth face is depicted in Figure 2.4.

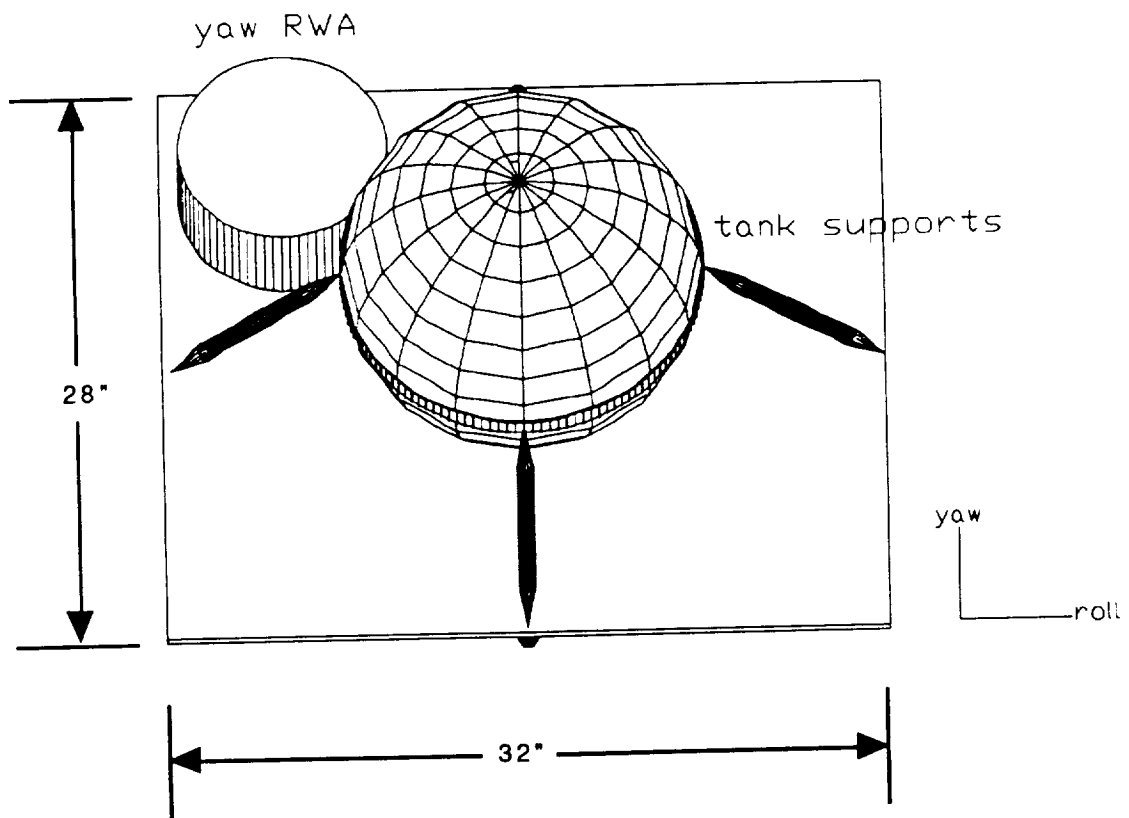


FIGURE 2.4 Anti-Earth Face

3. North Face

Affixed to the north face are the Global Positioning System microreceiver, the second digital sun sensor, and the backup reaction wheel. The backup reaction wheel is skewed 45° to the primary axes of the spacecraft. The north face is shown in Figure 2.5.

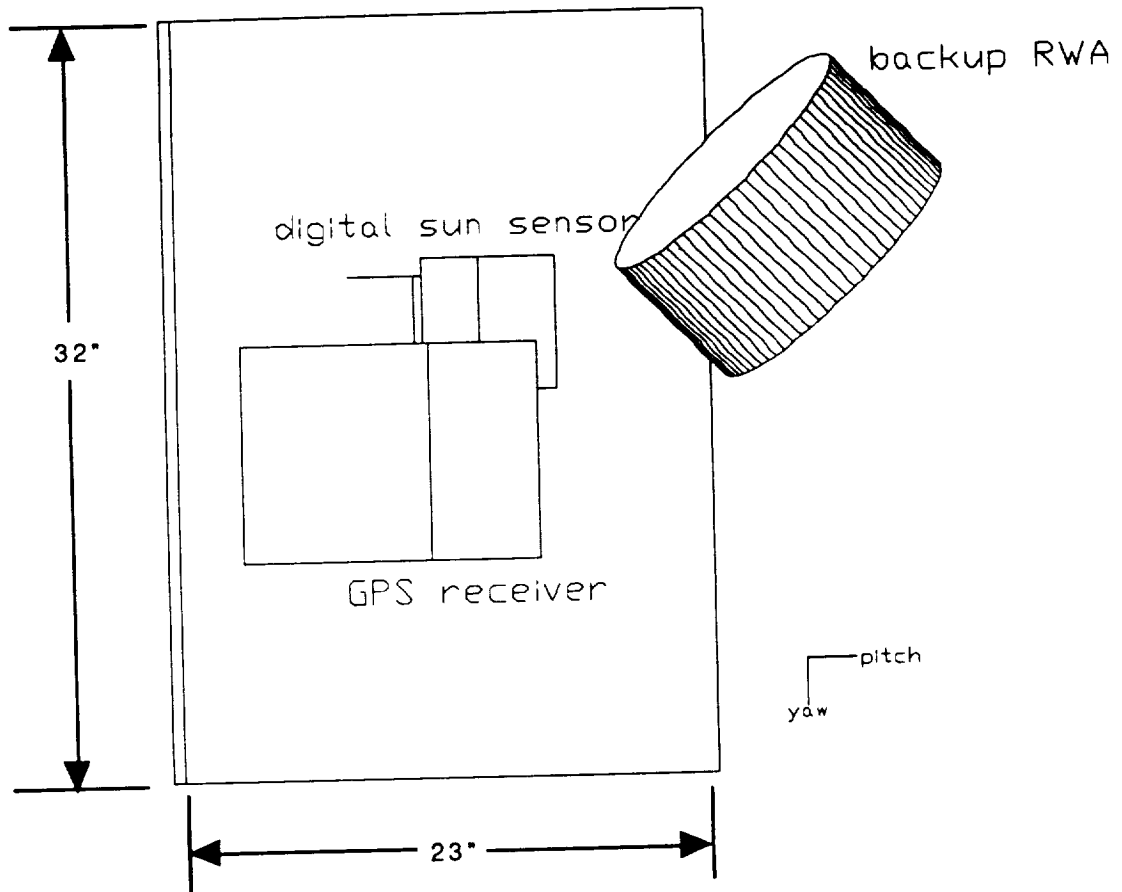


FIGURE 2.5 North Face

4. South Face

Attached to the south face are the celestial sensor assembly and pitch reaction wheel assembly. The south face is depicted in Figure 2.6.

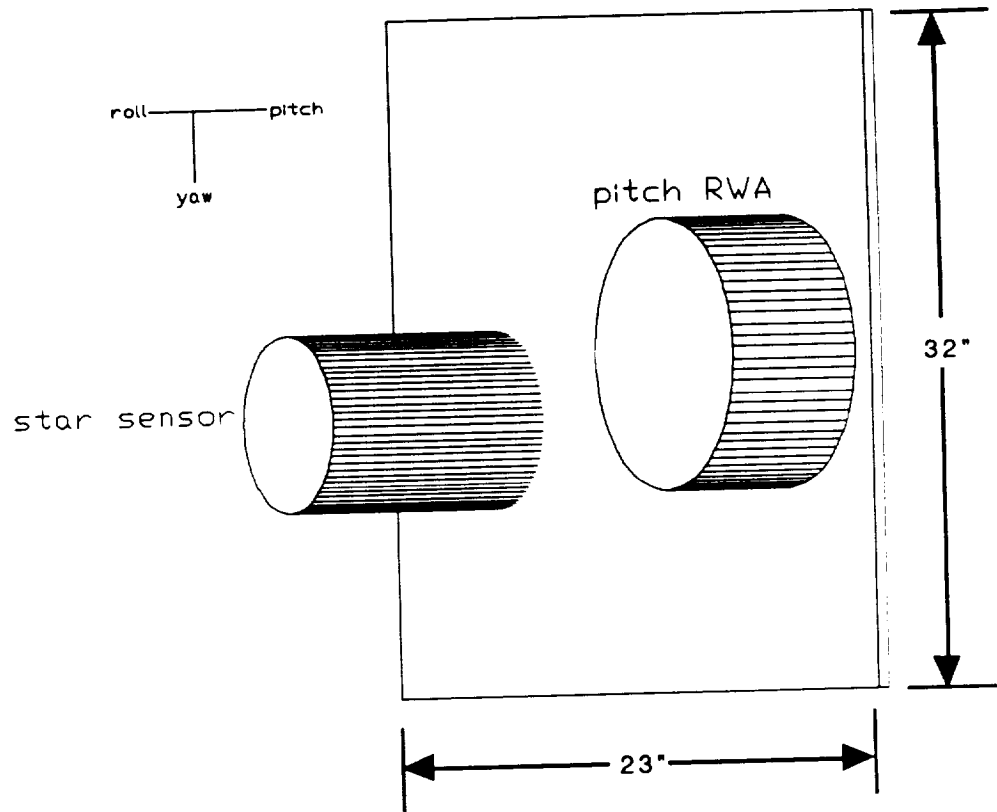


FIGURE 2.6 South Face

5. East Face

Mounted on the east face are the roll reaction wheel assembly, a solar array drive motor (SADM), the gyro assembly, and the attitude control computer. In addition, two thrusters are mounted through this face. The east face is depicted in Figure 2.7.

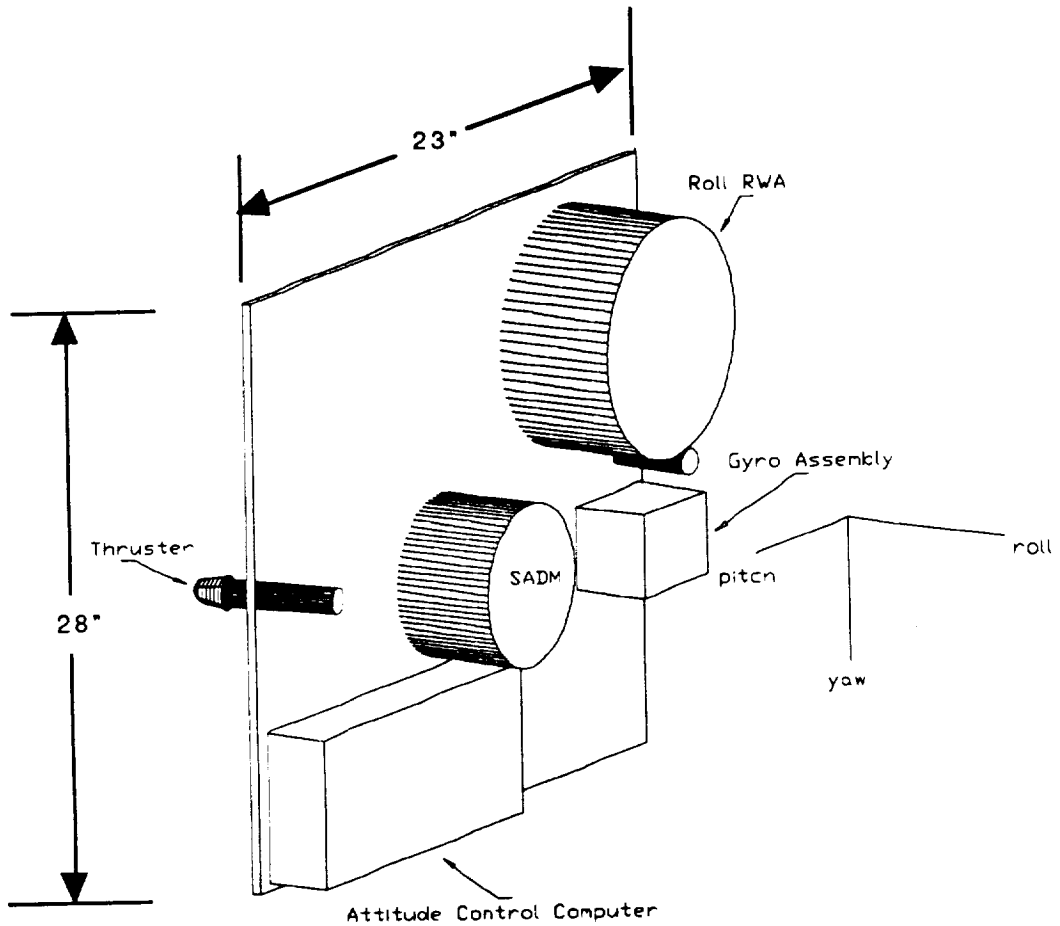


FIGURE 2.7 East Face

6. West Face

The west face has mounted to it a SADM, the power control electronics, and sixteen NiH₂ battery cells. The batteries are contained in eight common pressure vessels but are depicted as a box for simplicity. The west face is depicted in Figure 2.8.

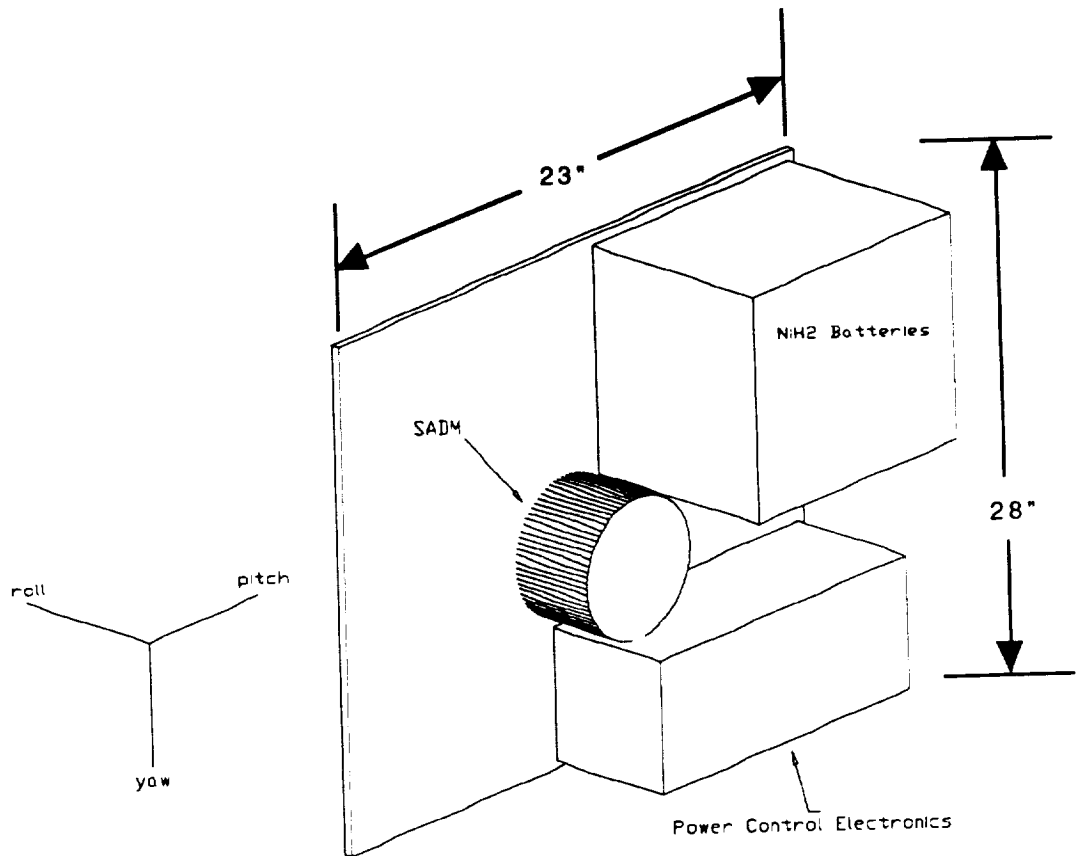


FIGURE 2.8 West Face

7. Stowed Configuration

a. AVHRR

The launch vehicle for the AVHRR is Pegasus. A stowed AVHRR is shown in the Pegasus dynamic shroud in Figure 2.9. A top view of the AVHRR in the Pegasus dynamic shroud is depicted in Figure 2.10.

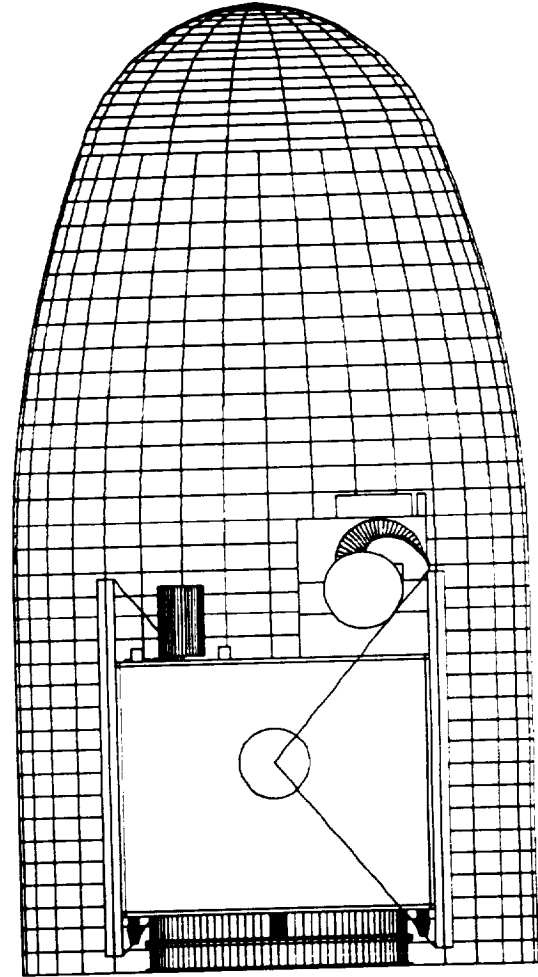


FIGURE 2.9 Side view of MPS Bus w/AVHRR Payload in Folded Configuration

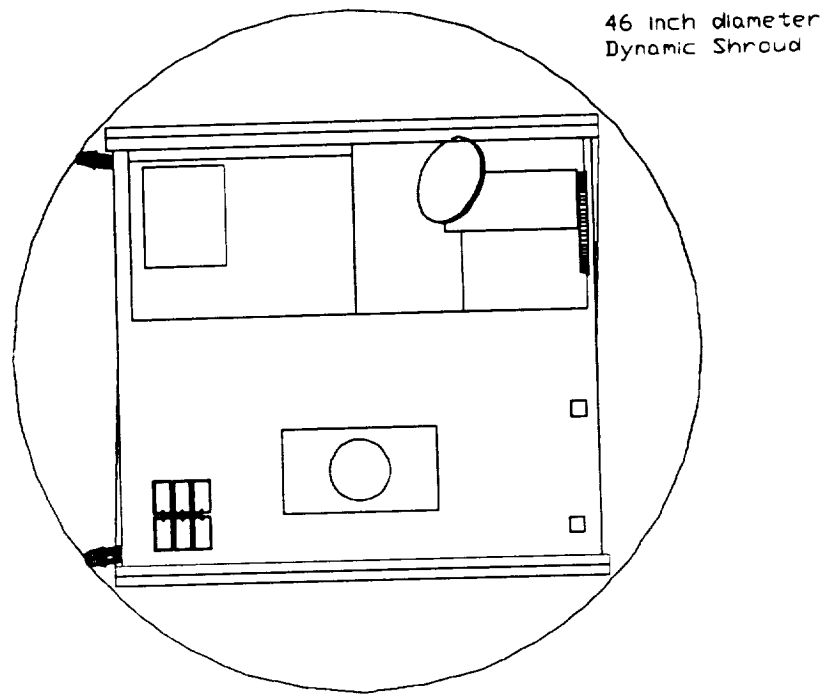


FIGURE 2.10 Top view of MPS Bus w/AVHRR Payload in Folded Configuration

b. EHF

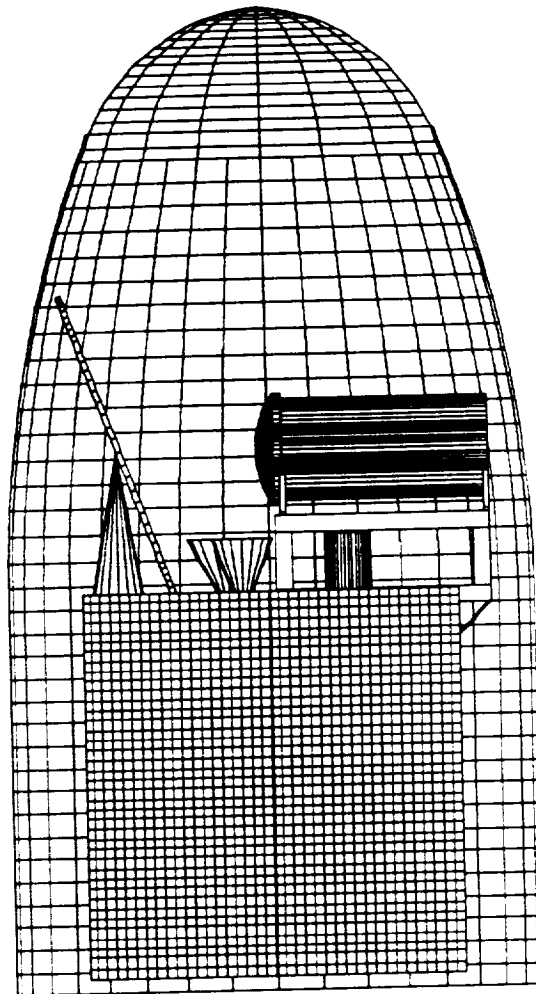


FIGURE 2.11 Side view of MPS Bus w/EHF Payload in Folded Configuration

Figure 2.12 depicts the MPS bus deploying its solar arrays. The solar arrays are affixed to the east and west faces of the bus, but are folded over onto the north and south faces while in the stowed configuration. The two solar panels per side are stowed such that the solar cells are positioned outboard, in the event that electrical power is needed prior to their deployment. The Y shaped yokes provide a 16 inch clearance from the bus. This view is looking at the anti-earth face, with the marmon clamp assembly clearly visible.

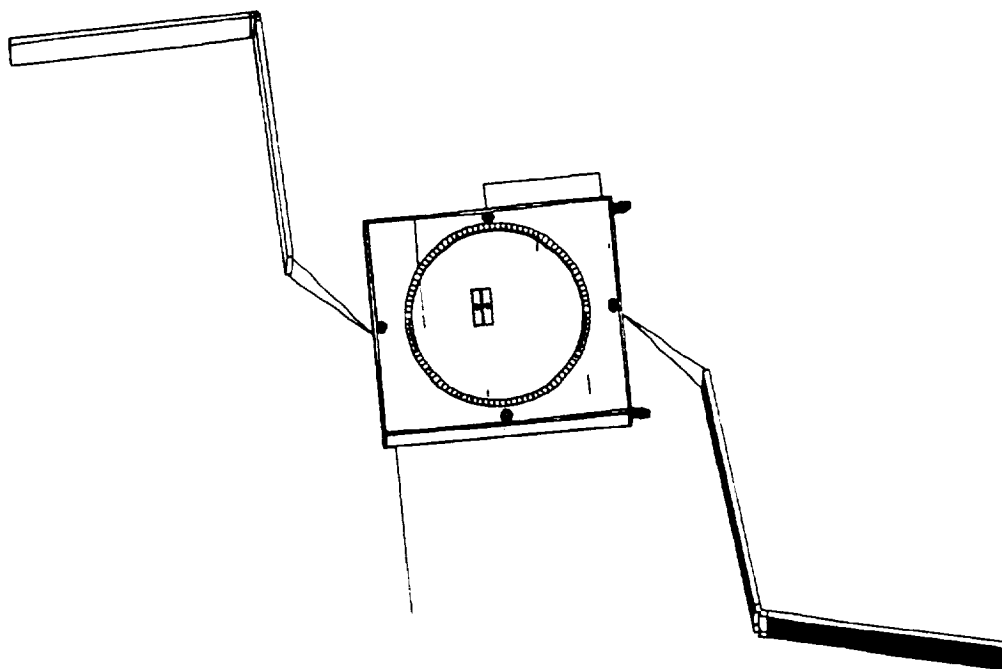


FIGURE 2.12 MPS Bus with Solar Array Deploying

B. SPACECRAFT BUS CONFIGURATIONS/SUMMARIES

The basic spacecraft bus just described is used with payloads that will have different power, structural and propulsion requirements. A mass, electrical power, and propellant summary is provided in Table 2.1 through Table 2.4 describing the requirements for the AVHRR and EHF payloads. Fuel loads are assumed to be nominal.

1. Mass Summaries

	AVHRR	EHF COMM
SUBSYSTEM	Mass (kg/lb)	Mass (kg/lb)
Mass of S/C structure	20.75 / 45.75	27.13 / 59.81
Dry Mass Reaction Control System	15.20 / 33.51	15.20 / 33.51
Mass of Attitude Control System	24.72 / 54.50	21.55 / 47.51
Mechanical Integration Mass	1.00 / 2.20	1.00 / 2.20
Electrical Power Subsystem Mass	37.06 / 81.70	37.06 / 81.70
Thermal Control Subsystem Mass	2.54 / 5.60	5.50 / 12.13
Telemetry and Control Mass	4.50 / 9.92	4.50 / 9.92
Payload	29.32 / 64.64	38.18 / 84.17
Mass Margin	13.51 / 29.78	15.01 / 33.09
Dry Spacecraft Mass	135.09 / 297.82	150.12 / 330.96
Propellant/Pressurant	11.02 / 24.29	13.02 / 28.70
Spacecraft Mass At Separation	159.62 / 351.89	178.15 / 392.75

TABLE 2.1 Mass Summary Comparison

2. Electrical Power Summaries

	Normal Ops (W)	Launch/Ascent (W)	Activation (W)	Eclipse (W)
Battery Charging	76.0	0.0	0.0	0.0
TT&C	11.2	11.2	11.2	11.2
Attitude Control	54.0	4.1	54.0	54.0
Sun/Earth/Star Sensors	4.4	0.0	4.4	4.4
Propulsion	6.1	42.1	42.1	0.0
Solar Array Drives	10.0	0.0	10.0	0.0
Power Control	4.1	2.0	4.1	4.1
Bus Harness Losses	4.0	3.0	3.0	3.0
Payload	28.0	4.0	4.0	28.0
System Reserve	4.0	0.0	0.0	0.0
Total	201.8	66.4	132.8	104.7
EOL w/ cosine effect	313.9			

TABLE 2.2 Electrical Power Summary - AVHRR

	Normal Ops (W)	Launch/Ascent (W)	Activation (W)	Eclipse (W)
Battery Charging	25.0	0.0	0.0	0.0
TT&C	11.2	11.2	11.2	11.2
Attitude Control	54.0	4.1	54.0	54.0
Sun/Earth/Star Sensors	4.4	0.0	4.4	4.4
Propulsion	6.1	42.1	42.1	6.1
Solar Array Drives	10.0	0.0	10.0	10.0
Power Control	4.1	2.0	4.1	4.1
Bus Harness Losses	4.0	3.0	3.0	3.0
Payload	115.0	4.0	4.0	57.5
System Reserve	4.0	0.0	0.0	0.0
Total	237.8	66.4	132.8	150.3

TABLE 2.3 Electrical Power Summary - EHF Comm

3. Propellant Budget/Summary

The propellant budgets were estimated as:

	AVHRR	EHF
Maneuver	(kg)	(kg)
Stationkeeping	6.0	8.0
Orbit Maintenance	3.42	3.42
Desaturation	1.0	1.0
Margin	0.1	0.1
Orbit Deboost	0.5	0.5
Total	11.02	13.02

TABLE 2.4 Propellant Budget Summary

III. PAYLOADS

A. AVHRR

1. Functional Description

The Advanced Very High Resolution Radiometer (AVHRR) provides data for transmission to both Automatic Picture Transmission (APT) and High Resolution Picture Transmission (HRPT) users. The AVHRR is a scanning radiometer which is sensitive in six spectral regions. In these spectral regions, the payload monitors data for day and night cloud mapping, sea surface temperature mapping, and other oceanographic and hydrologic applications. The HRPT data is full resolution (1.1 km) while APT data is at a reduced resolution to maintain allowable bandwidth. The APT transmission is maintained for use by ground terminals that do not have HRPT capability (i.e. third world countries).

Specific design considerations (such as pointing accuracy and thermal control) that are driven by the AVHRR payload are discussed later in appropriate subsystem sections.

Communications:

For the communications design considerations of the AVHRR payload; HRPT, APT, and TT&C data must be transmitted and received in a format that is compatible with existing TIROS HRPT ground stations. Also, the TT&C and command uplink channels are designed to be more rigid to insure that control could always be maintained even in the event of an attitude control failure resulting in a tumbling satellite. In order to accomplish this, data had to be formatted at the following frequencies, data rates, and modulation formats:

Type	Data Rate	Carrier Freq	Modulation
HRPT	665 kbps	1.707 GHZ	BPSK
APT	2 kbps	137.5 MHz	AM/FM
TT&C	8.32 kbps	136.77 MHz	BPSK
COMMAND	1 kbps	148.56 MHz	FSK/AM

TABLE 3.1 AVHRR Channels

Table J.2 in Appendix J shows the link analysis for each of these data channels. The design is for a 10^{-6} BER with a 2 dB link margin (The command uplink and TT&C use a 3 dB margin). Free space losses at these frequencies are relatively low due to the lower orbit of the AVHRR payload. This allowed an ample margin in the link analysis and led to lower gain antennas and lower transmitted powers.

To transmit and receive at these frequencies, two antennas were needed because no one antenna has a bandwidth wide enough to cover all of the carrier frequencies.

1. One antenna can cover all three of the VHF frequencies from 136-149 MHz. It will have to have a wide beamwidth so that the satellite will be able to receive a command uplink if the attitude control system fails and the satellite starts tumbling. Because the wavelengths at these frequencies are on the order of two meters and because a very low gain antenna was acceptable, two whip antennas mounted in such a way that they would be orthogonal to each other but parallel to the earth face were chosen as shown in Figure 2.1. The whips are 23 inches long in order to resonate at a quarter wavelength. This gives a low gain, lightweight antenna system with an omnidirectional beam pattern that could be completely stowed for launch.

2. The second antenna had to be able to transmit at 1.7 GHz with a gain of 4 dB. (See Table 3.1 and Table J.2) The beamwidth did not have to be wide nor was a high antenna gain needed. The design criteria was weight. With this in mind, a Microstrip Antenna was chosen. Figure 3.1 shows one element of this antenna.

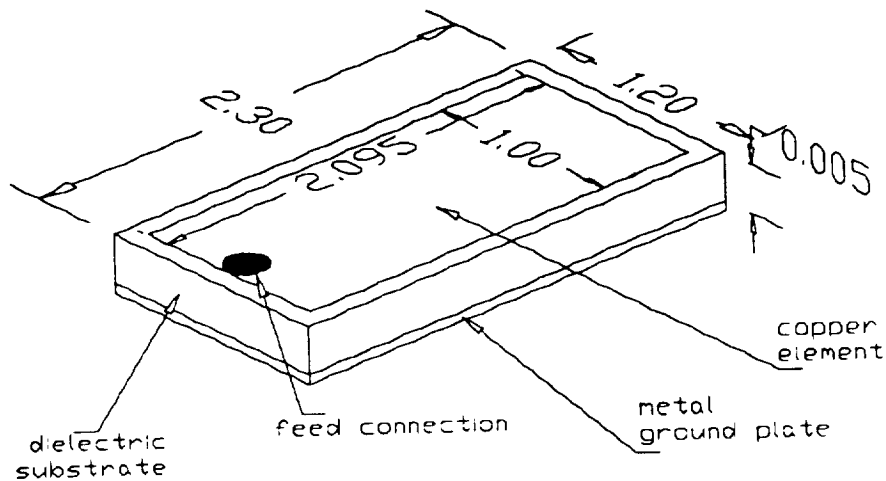


FIGURE 3.1 Microstrip Element
(dimensions in inches)

The advantages of a microstrip antenna are:

1. Low cost due to inexpensive mass production procedures.
2. Very thin and conformal to the earth face of the satellite.
3. Negligible weight
4. Surprisingly efficient (typically 80% - 90%)
5. Very reliable since the antenna is essentially one continuous piece of copper. The most common failure

is at the point where the feed pin is soldered to the microstrip element.

The metal ground plate for this antenna is simply the aluminum earth face of the satellite. The dielectric substrate is teflon-fiberglass which is commonly used. The microstrip element is copper etched from one side of a printed circuit board. The dimensions and characteristics of this antenna follow:

Bandwidth: The bandwidth is a function of the thickness of the dielectric substrate by the following formula:

$$BW = 4f^2 \frac{t}{1/32} \quad (3.1)$$

With a thickness of .005 inches, the bandwidth is 1.849 MHz which more than adequately covers the signal bandwidth of 1.33 MHz.

Length (L): The Length of the microstrip element is roughly one-half of the wavelength through the dielectric substrate as calculated with the following formula:

$$L \approx 0.49 \frac{\lambda_o}{\sqrt{\epsilon_r}} \quad (3.2)$$

where $\epsilon_r = 2.45$ and $\lambda_o = 6.69$ inches. Therefore $L = 2.095$ inches.

Width (W): The width of the microstrip element must be less than a wavelength in the dielectric. The width was chosen to be 1 inch.

Array Dimensions: In order to get sufficient gain, six microstrip elements were needed in an array as shown in Figure 3.2.

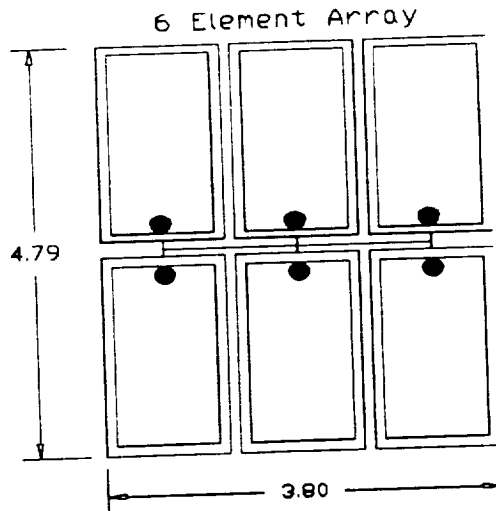


FIGURE 3.2 6-Element Microstrip Array
(dimensions in inches)

Gain (G): The gain of the antenna can be approximated with the following formula:

$$\text{Gain} \approx 10 \log \frac{4\pi A}{\lambda_0^2} - \frac{\alpha}{2} (D_1 + D_2) \quad (3.3)$$

where $A = D_1 * D_2$, $D_1 =$ effective width of array, $D_2 =$ height of array, and $a =$ attenuation (0.4 dB/ft for a 50 W microstrip line on 1/32 in Teflon fiberglass at 2.2 GHz)

$$D_1 = 4.2 \text{ inches}$$

$$D_2 = 3.02 \text{ inches}$$

$$A = 12.684 \text{ inches}$$

therefore $G = 4.072 \text{ dB}$ which is adequate to close the link.

B. Extremely High Frequency (EHF)

The basic design for the EHF Payload is shown in Figure 3.3. It includes the antennas required to support the communications payload, an attitude control package receiving commands from the RCU, a communications repeater and a TT&C package.

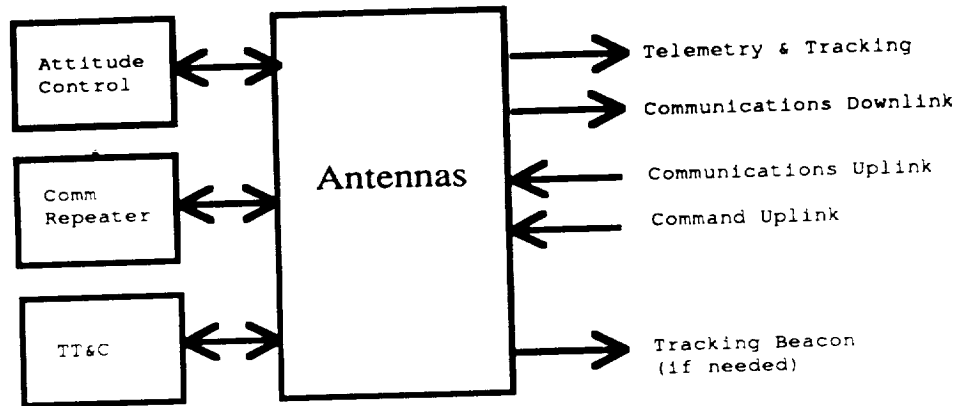


FIGURE 3.3 EHF Payload Configuration

1. EHF Bandwidth Allocation

The payload was designed to be compatible with MIL STD 1582 at the unclassified level. This drove the selection of uplink and downlink frequencies as well as bandwidth, modulation techniques and several other circuit parameters. Figure 3.4 shows what the signal waveform will look like. The signal has a bandwidth of 7.84 MHz. This waveform will be hopping at a rate of 3000 hops per second over 255 different hop frequencies. This fills a bandwidth of 2 GHz as illustrated in Equation 3.4 where B is the total bandwidth and b is the bandwidth of a single hop. The resulting processing gain is 24.06 dB as shown in Equation 3.6. This translates as immunity to jamming since, even though the signal only takes up a bandwidth of 7.84 MHz, the jammer would have to jam a significant portion of the 2 GHz bandwidth in order to cause real damage to the integrity of the link. Frequency hopping also provides protection from multipath fading since, by the time a signal could reach the antenna by an alternate path to introduce fading, the transmitter will have already hopped to a different frequency.

$$\text{Number of hop frequencies} = \frac{B}{b} = 255 \quad (3.4)$$

$$b = 245 \text{ KHz} * 32 \text{ channels} = 7.84 \text{ MHz} \quad (3.5)$$

$$\text{Processing gain} = 10 \log \frac{B}{b} = 24.06 \text{ dB} \quad (3.6)$$

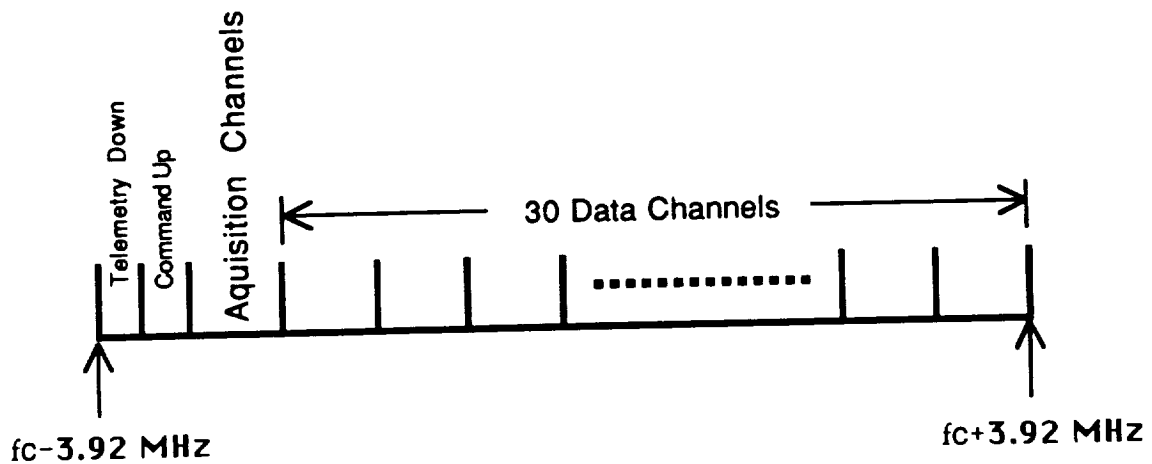


FIGURE 3.4 EHF Bandwidth Allocation

Figure 3.4 shows that the signal will contain 32 channels where the center frequencies are spaced 245 KHz apart. This gives a channel bandwidth of 7.84 MHz as shown in Equation 3.5. With a data rate of 2.4 kbps, this will give a substantial guard band and inter-symbol interference will be negligible. Of these 32 channels, 30 of them will be used by the customer to transmit data from one earth terminal to another by a "Bent Pipe" approach.

The satellite will not transform the data channels. However, the customer should use FSK modulation to transmit the data. PSK requires that coherent phase knowledge be maintained and this is very difficult in a Frequency Hopping channel. MIL STD 1582 should be consulted for the requirements for low data rate transmission. Encryption, error correction coding, and other safeguards are required and are the responsibility of the customer.

The lowest frequency channel will be partitioned in half for telemetry downlink signals and command uplink signals. The command check circuit pulls out the command channel and checks for a command signal. Then the telemetry signal is inserted.

The remaining channel is used for channel acquisition so that the customer may gain access to the link and be assigned a channel to use. Acquisition is done using acquisition codes contained in MIL STD 1582. The Net Control Unit (NCU) monitors the acquisition channel and reads all incoming acquisition messages. When link access is requested, the NCU will assign the next open data channel. The customer will be given a channel which is his to use until either party terminates the link or the link is preempted by higher priority traffic.

2. EHF Antenna

A number of studies are ongoing in the field of EHF antennas. For example, Electro Magnetic Sciences is building a Spherical Lens Multi-beam Antenna that will operate 271 separate feeds. These feeds will travel through extensive switch trees to 211 ports at the lens assembly. The interesting thing about this project is that the discovery of a flangeless interconnect method for lightweight, smaller sized switches has made it possible to package many feeds into a much smaller package for more detailed beamforming than was ever before possible.

Another example is the Variable Beamwidth Antenna (VBWA) that is under study by MIT Lincoln Lab. The MPS EHF payload was designed to accommodate the Variable Beamwidth Antenna both in weight and power requirements. The data for the Variable Beamwidth Antenna as presented by MIT Lincoln Lab is listed below:

Weight = 14.57 lbs

Power required = 20 watts

Efficiency = 0.75%

Gain Versus Beamwidth = See Figure 3.6

The basic idea behind this antenna assembly is to allow the capability to vary the beamwidth of the antenna with a cluster of feedhorns in order to maintain a constant coverage area on the earth while maximizing the gain of the antenna. For a circular orbiting satellite with a nadir-pointing antenna there will be little advantage while on station, but if the satellite is in an elliptical orbit or the beam is scanning away from a nadir position, the VBWA will allow for higher antenna gains at higher altitudes and wider beamwidths at lower altitudes.

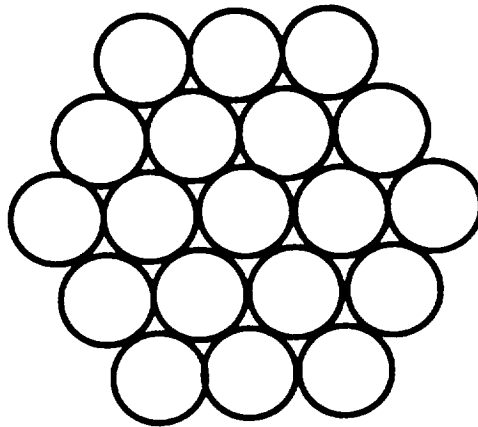


FIGURE 3.5 Feedhorn Arrangement

The MIT assembly as shown in Figure 2.3 has a feedhorn cluster of 19 feedhorns arranged as shown in Figure 3.5. When the center feedhorn is the only one in operation, the beamwidth will be 4° (to the -3 dB point) and the gain will be 32 dB. As the satellite draws closer to the earth, a wider beamwidth will be needed to maintain the same swath width. As this happens, power will be switched to the middle ring of feedhorns to gradually widen the beamwidth and maintain the swath width. At some point in the orbit, the middle ring of feedhorns will reach a maximum power and it will become necessary to

begin switching power to the outer ring of feedhorns. Once the outer ring of feedhorns have reached maximum power, the antenna will be at a maximum beamwidth of 28° and a minimum gain of 20 dB. The following paragraphs will discuss the operation of the Variable Beamwidth Antenna in an 8 hour Molniya orbit as designed for the MPS EHF payload.

The following points of operation for beamwidth versus gain were given.

<u>Beamwidth</u>	<u>Gain</u>
4°	32 dB
8°	27 dB
12°	24 dB
22°	22 dB
28°	20 dB

The above data was assumed to be piecewise linear and Figure 3.6 was generated. In actuality, the plot of beamwidth versus gain will not be linear, but this approximation will serve to illustrate the advantages of having a variable beamwidth antenna.

Gain VS. Beamwidth
(Using known points)

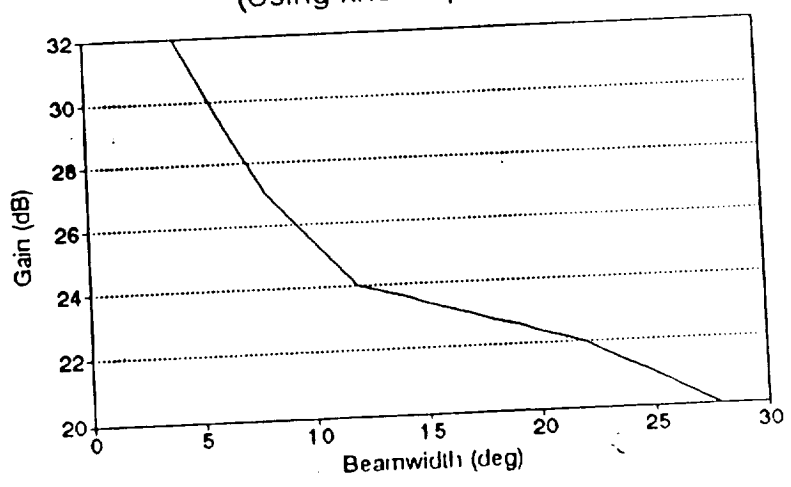


FIGURE 3.6 Gain Versus Beamwidth

Beamwidth VS Altitude (for several Swath Widths)

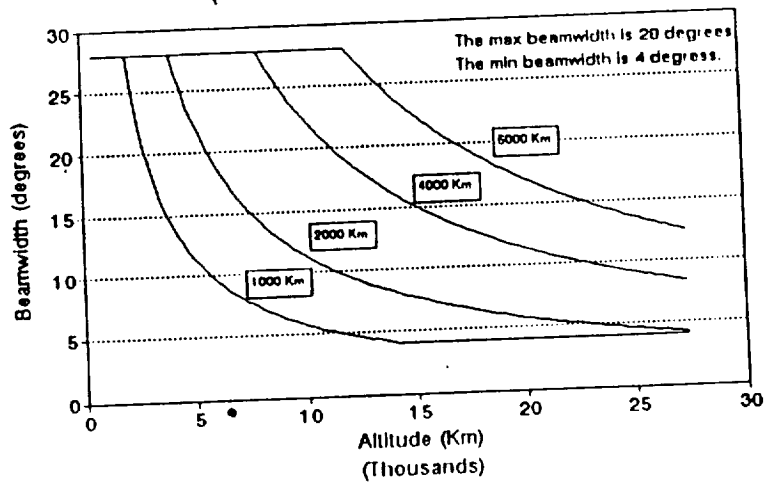


FIGURE 3.7 Beamwidth versus Altitude

Figure 3.7 shows a plot of the beamwidth vs. altitude needed to maintain various swath widths. The plot assumes a flat earth and clips at the maximum and minimum beamwidths. It can be seen that certain swath widths can not be maintained from an apogee of 27,358 km to a perigee of 500 km. The best case scenario appears to be the 2000 km swath width. It can be achieved at a 4000 km altitude and maintained all the way to apogee at a 4.19° beamwidth. The 1000 km swath width will reach the minimum beamwidth at 14500 km altitude, while the 6000 km swath width can not be achieved until a 12000 km altitude and will never take advantage of the minimum beamwidth.

Beamwidth VS Time after Perigee (for several Swath Widths)

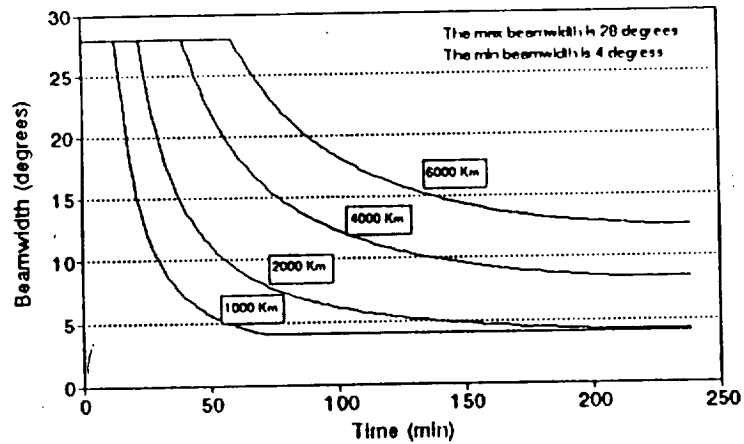


FIGURE 3.8 Beamwidth versus Time After Perigee

Figure 3.8 illustrates the requirements for beamwidth versus time after perigee that will have to be programmed into an onboard processor to maintain a desired swath width. This processor can receive a command uplink from a ground terminal to update the antenna operation or perhaps change to a different mode of operation.

Gain VS Altitude (for Several Swath Widths)

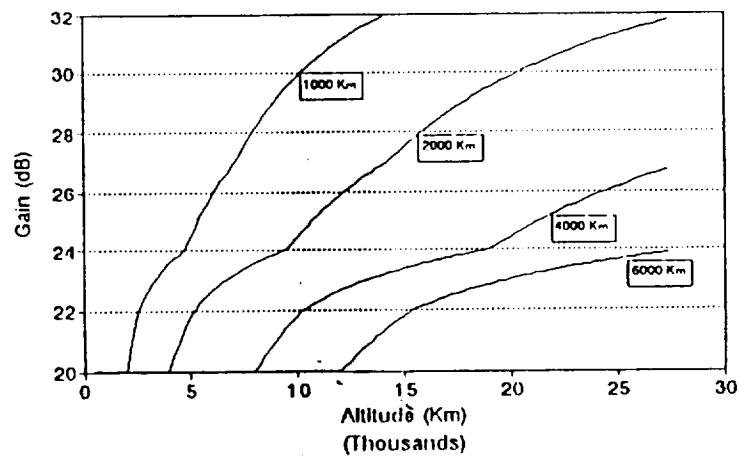


FIGURE 3.9 Gain Versus Altitude

Gain VS Time after Perigee (for Several Swath Widths)

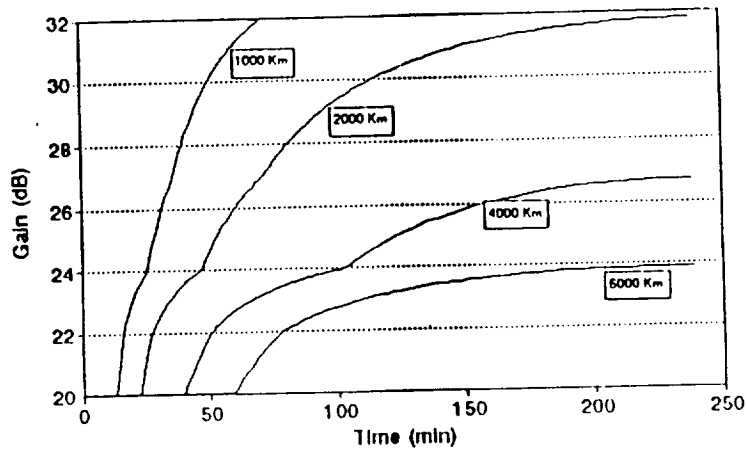


FIGURE 3.10 Gain Versus Time After Perigee

Using the information from Figure 3.6 about the behavior of the antenna gain with changing beamwidth, Figure 3.9 and 3.10 are generated to show what will happen to the gain as a function of altitude and time after perigee.

3. Pointing Losses

One problem that should be considered when designing an antenna satellite system is the possibility of losses due to pointing inaccuracies or pointing losses. These losses are usually considered in the earth station, but they should also be considered in the satellite.

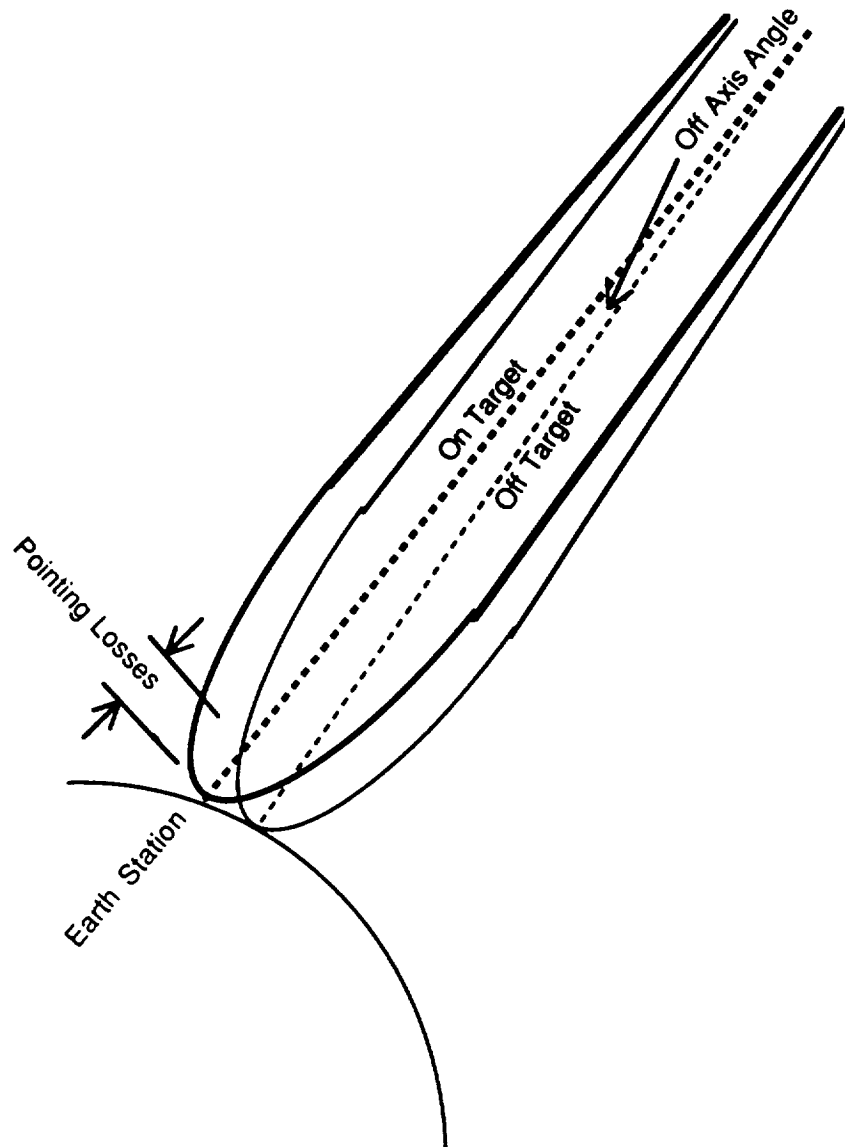


FIGURE 3.11 Pointing Losses

Figure 3.11 shows an illustration of what constitutes pointing losses. From this illustration, it can be seen that pointing losses are a function of the off axis angle from the target. For the VBWA, the shape of the beam obeys a Gaussian equation (as calculated in Equation 3.7) for each feedhorn. Therefore this equation can be used to analyze the

pointing losses for the satellite operating at its minimum beamwidth. The wider beamwidths will exhibit a flatter beamshape giving lower pointing losses and therefore the minimum beamwidth will be the worst case.

$$G = G_0 e^{-k\theta^2} \quad (3.7)$$

Figure 3.12 shows the shape of the beam as a function of off axis angle. It can be seen that an off axis angle of 2° gives 3 dB of pointing losses. The pointing accuracy should be maintained at less than 1° to ensure a good link margin. In satellite design it is easier to maintain low roll and pitch errors than it is to maintain low yaw errors. MPS is designed to have a roll error of 0.1° , a pitch error of 0.1° , and a yaw error of 0.5° . Most of the pointing losses for MPS will be due to yaw error. Since the satellite will most often be nadir pointing and since the beamshape is symmetric about its center axis, yaw error will have no effect on pointing losses most of the time. However, the antenna reflector assembly does have two degrees of freedom and can scan up to 50° off the nadir. When the reflector is not nadir pointing, yaw error will give some pointing losses. To see this effect, first use Equation 3.8 to convert max yaw error (ϕ) and scan angle (ψ) into off axis angle (θ). Figure 3.13 shows the pointing losses as a function of scan angle for various yaw errors. The worst case scenario for MPS is when yaw error is at 0.5° and the antenna reflector is scanning out to 50° . From Figure 3.13, this translates to a pointing loss of $-3.3(10^{-5})$ dB. Therefore, pointing losses from the MPS Bus should not be a problem.

$$\sin^2(\psi) (1 - \cos \phi) = (1 - \cos \theta) \quad (3.8)$$

Gain vs Off Axis Angle (For one feed horn)

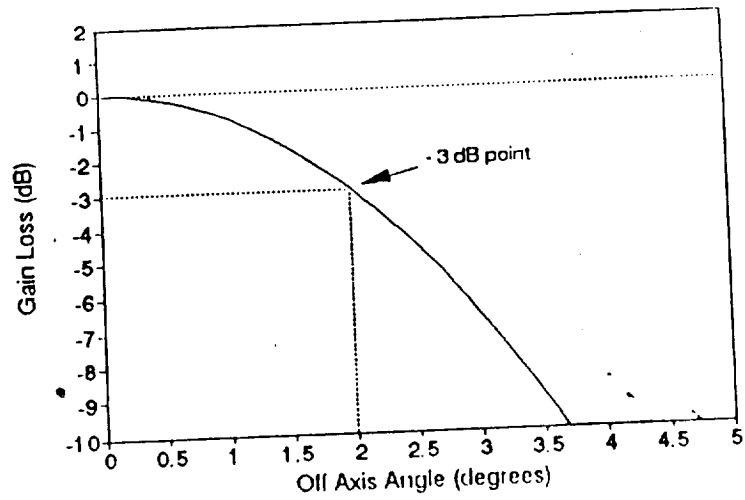


FIGURE 3.12 Gain Versus Off Axis Angle

Gain vs Scan Angle (various Yaw Errors)

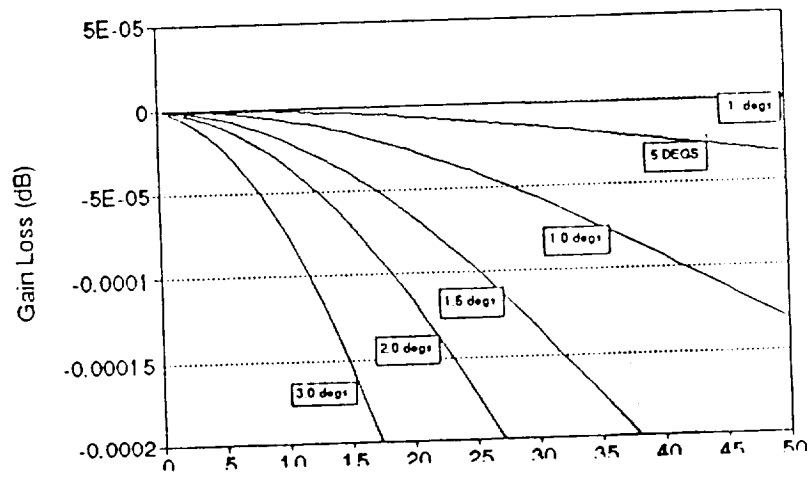


FIGURE 3.13. Gain Versus Scan Angle

4. EHF Communications Repeater

The Communications Repeater will perform the following functions:

1. Receive a 44 GHz signal with a 2 GHz bandwidth.
2. Down convert the signal to an IF frequency that will still allow for 2 GHz bandwidth.
3. Demodulate the frequency hopping pattern.
4. Down convert to another IF frequency.
5. Check the signal for a command uplink signal and send it to the TT&C package.
6. Check the signal for an acquisition control message and act accordingly.
7. Incorporate a telemetry downlink signal.
8. Up convert the signal to 20 GHz.
9. Frequency hop the signal back to 2 GHz bandwidth.
10. Amplify the power up to 20 watts.
11. Transmit a 20 GHz signal with a 2 GHz bandwidth.

Figure 3.15 shows a simple block diagram of the communications repeater. It can be seen that each of the above requirements are met. The signal is received from the antenna and amplified. Then it is downconverted to 8 GHz where it is dehopped to 100 MHz at a 7.98 MHz bandwidth. Then the command channel is filtered out and sent to the RTU in the TT&C package. At this point, telemetry information will be inserted into the telemetry channel of the signal for downlink to the earth station. Then the signal is upconverted to 20 GHz. The signal is then frequency hopped back to 2 GHz bandwidth and amplified for transmission to earth.

The repeater has two Traveling Wave Tube Amplifiers (TWTA's) for redundancy. Figure 3.14 shows the operating characteristics of this amplifier. It can be seen from the figure that the optimum operating point is at the peak of the curve. If the input power

varies either way (especially to the right), a loss of efficiency will result. For this reason, each TWTA is preceded by a hard limiter to insure that the input power stays at the operating point.

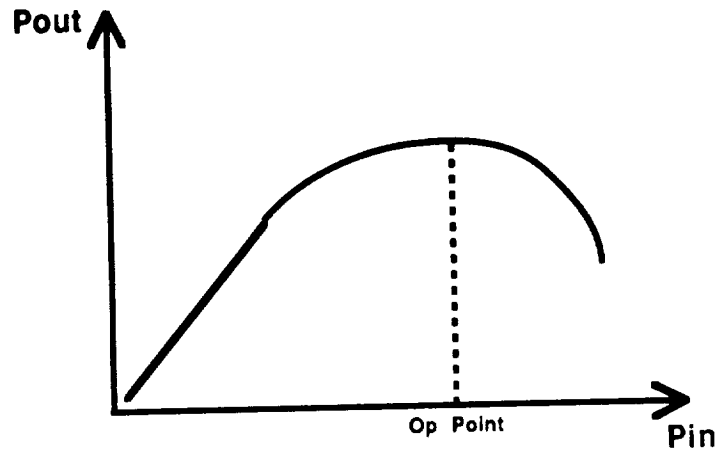


FIGURE 3.14 TWTA Characteristics

Within the Communications Receiver are several more complicated circuits that are shown in Figures 3.16, 3.17, and 3.18. These circuits are discussed in more detail.

Communications Repeater

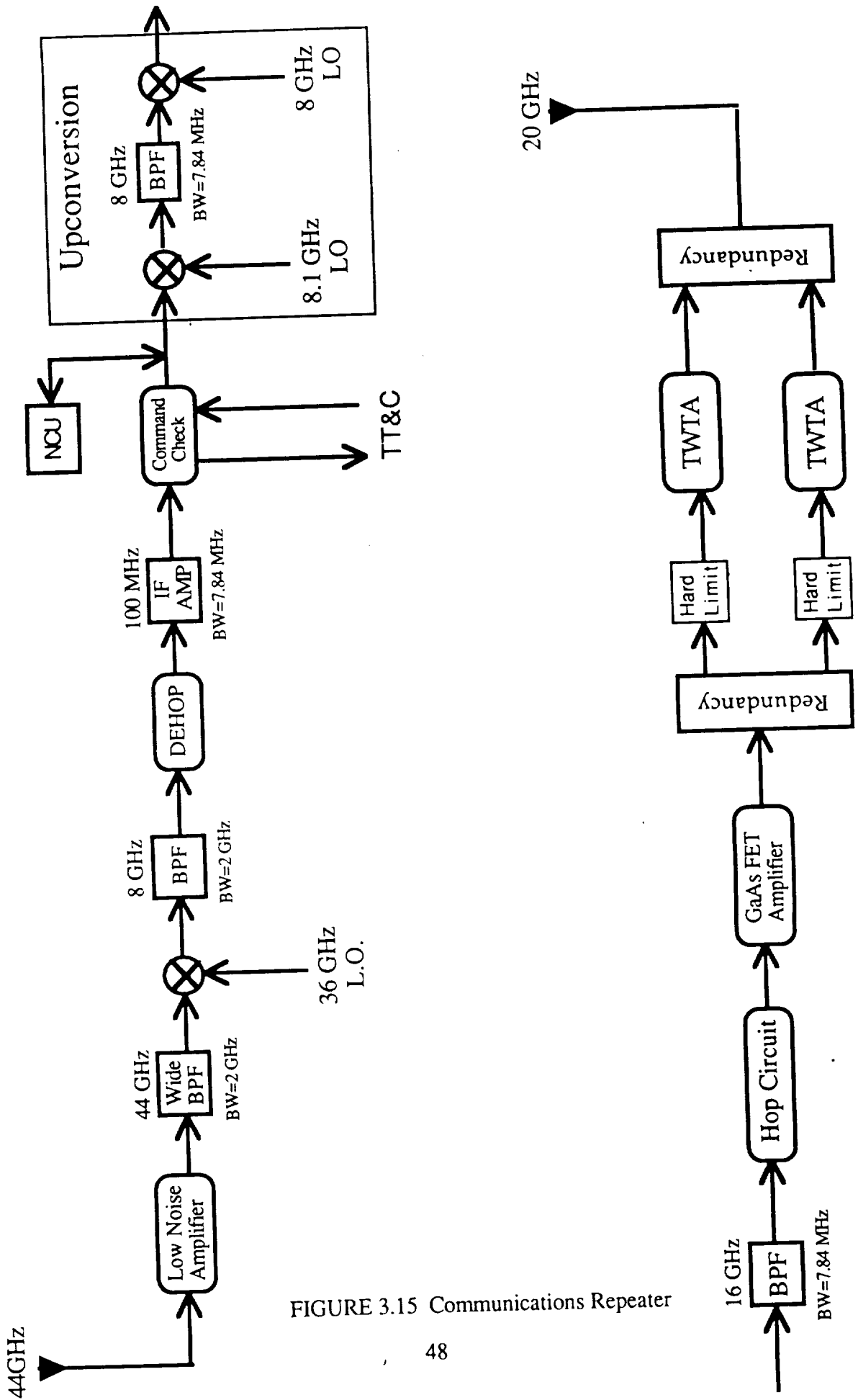


FIGURE 3.15 Communications Repeater

5. Dehop Circuit

Figure 3.16 shows a block diagram of the dehopping circuit. The hopping signal comes into the circuit with a bandwidth of 2 GHz which consists of 255 different hop frequencies. The trap filter is a narrow band filter that is waiting for one particular hop to occur. When the target hop occurs, the signal is sent to the envelope detector which is essentially a low pass filter where the signal will become a pulse that is the same duration as the target hop. The threshold detector takes the energy present within the target hop band and sends a short pulse to the feedback shift register (FSR) that will reset it to the location in the hop code that corresponds to the target hop. The incoming signal is now synchronized.

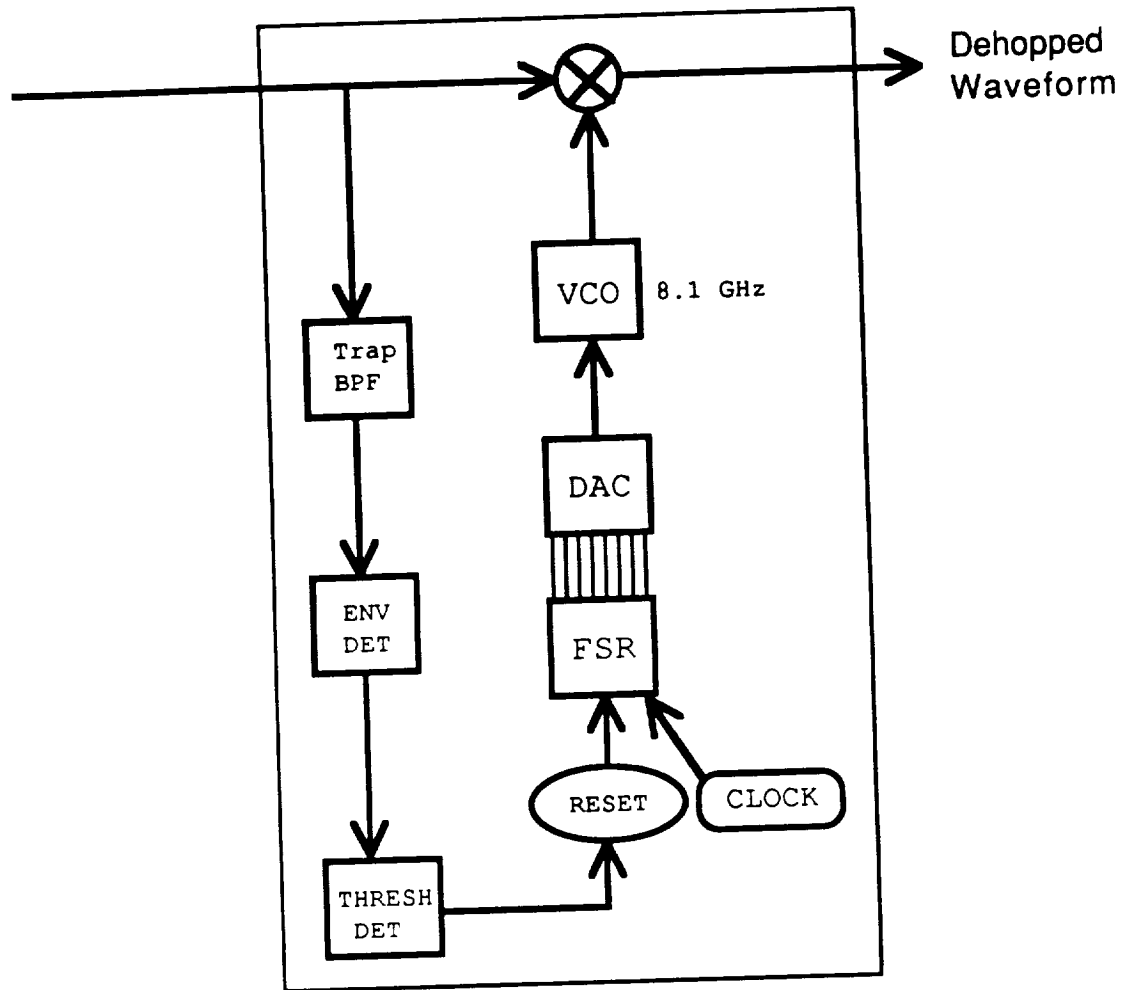


FIGURE 3.16 Dehopping Circuit

The FSR is an 8 bit device which is constructed using a modulo two addition between the output and input to create an 8 bit pseudorandom code that is non repeating for a 255 step cycle. This 8 bit code is sent through a digital to analog converter (DAC) where it becomes a 255 level voltage hopping signal. This signal is sent to the voltage controlled oscillator (VCO) which operates around 8.1 GHz to convert the signal that is hopping in voltage to a signal that is hopping in frequency. This signal is mixed with the received

signal. Since the hops are perfectly synchronized, the difference frequency out of the mixer will occur at 100 MHz and will be dehopped.

6. Command Check Circuit

Figure 3.17 shows a block diagram of the command check circuit. This circuit filters out the the command channel.and modulates it to 1.763721 GHz before sending it to the TT&C package On the telemetry side of the circuit, the telemetry data from the TT&C package is modulated to 96.21 MHz and inserted in the received signal. The RCU in the bus will have an algorithm that is dedicated to the control of the switches in the command check circuit. This will allow the ground terminals to switch the mode of operation of the TT&C package from the VBWA to the E/C antennas. This switching should take place at the SHF frequencies so that further modulation is not required.

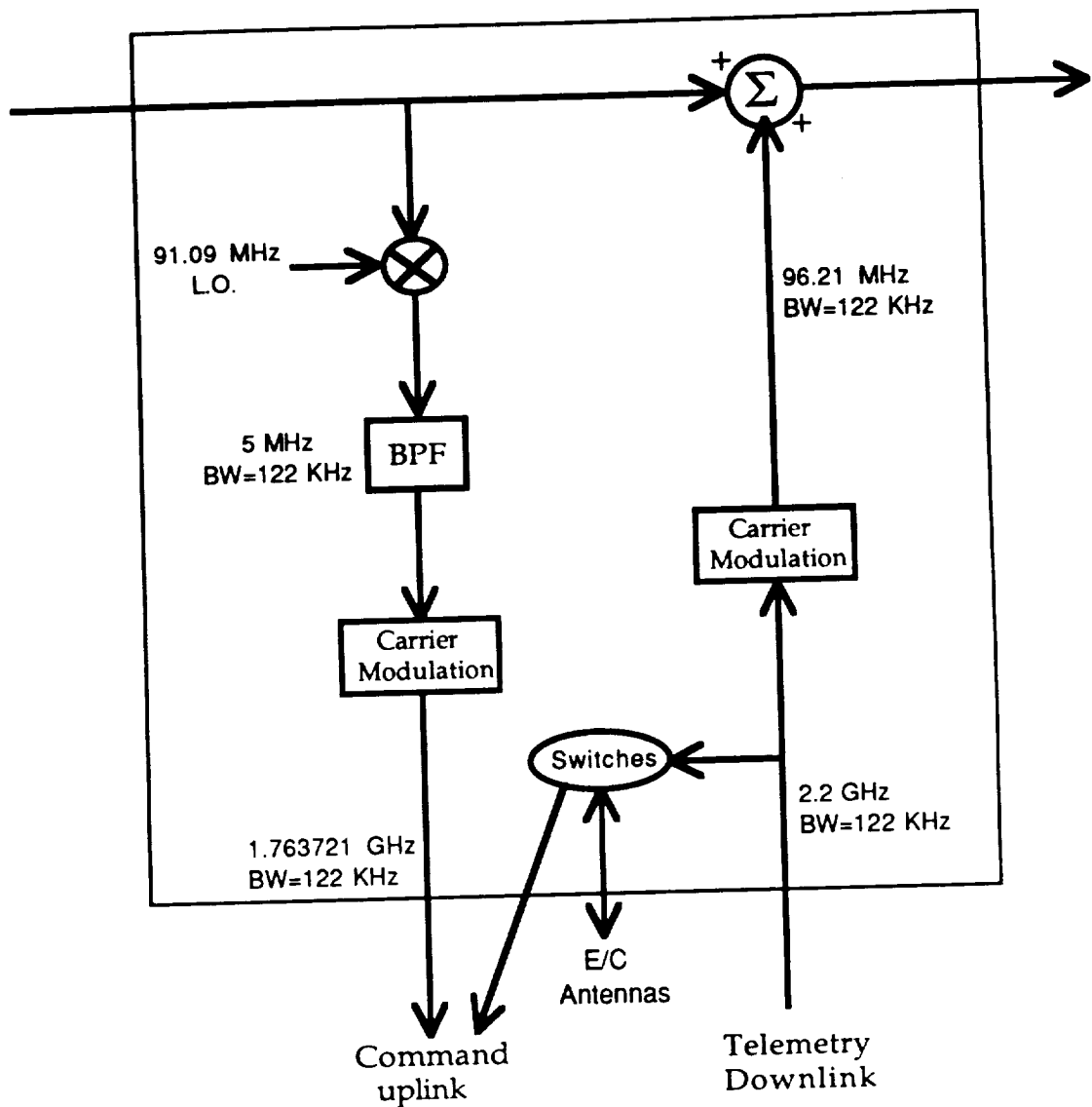


FIGURE 3.17 Command Check Circuit

7. Hopping Circuit

Figure 3.18 shows a block diagram of the frequency hopping circuit which is similar to the dehopping circuit except that synchronization is not necessary. The FSR simply sends the 8 bit pseudorandom code to the DAC which sends a hopping voltage to the VCO. The VCO (centered about 4 GHz) sends a frequency hopping signal to the mixer

where the signal is frequency hopped to 2 GHz bandwidth and upconverted to 20 GHz for transmission.

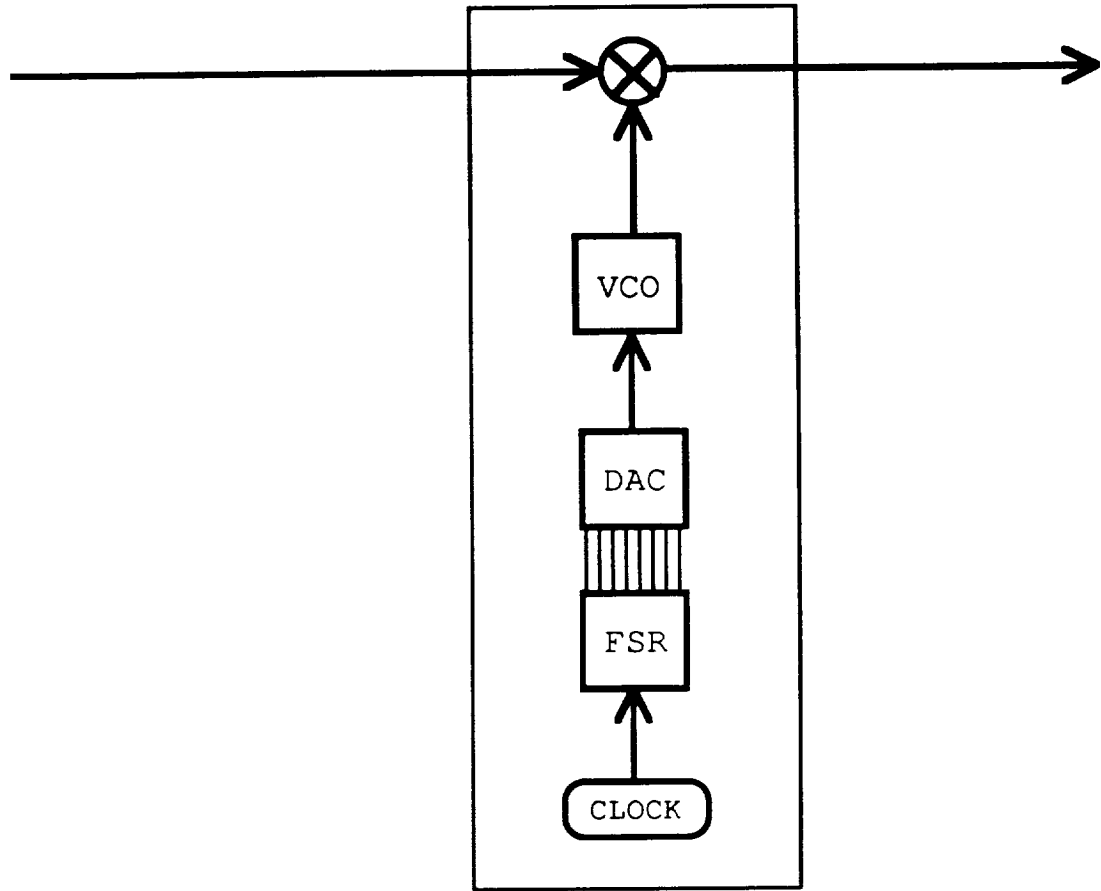


FIGURE 3.18 Hopping Circuit

IV. ORBITAL DYNAMICS

A. SELECTION OF ORBITS

Payload	AVHRR	EHF Communications
Orbit Type	Sunsynchronous	Molniya
Period	101.5 min	8 hr
Semimajor Axis	7212 km	20,307 km
Eccentricity	0.0	0.661
Inclination	98.75 deg	63.43 deg
Ascending Node	3:30 PM/8:30 PM	N/A
Argument of Perigee	N/A	270 deg

TABLE 4.1 Summary of Orbital Parameters

1. AVHRR

Orbit choices are naturally driven by the mission. In the case of the AVHRR, the mission is IR scanning and the sensor is designed to operate at 450 nautical miles altitude. To make the sensor useful everywhere in the orbit, the altitude has to be constant. These requirements dictate a circular orbit. Table 4.1 contains values for the period, semimajor axis, and eccentricity of this orbit. Because the orbit is circular, argument of perigee is undefined. The desire for global coverage coupled with the low altitude lead to a highly inclined orbit. Careful selection of the inclination produces a sunsynchronous orbit. Finally, spacecraft currently performing missions similar to the AVHRR mission locate

their ascending nodes within a couple of hours of the earth's terminator line (the line which separates the sunlit side from the dark side). This design follows suit and is within two and a half hours of the terminator line. This information is also provided in Table 4.1.

2. EHF

The EHF Communications mission produced an entirely different orbit. The statement of work required a Molniya type orbit. Guidance from DARPA indicated that at least tentatively, DARPA was most interested in the 8 hr orbit. Consequently, that is the orbit that we focused on. Although geosynchronous communications satellites provide continuous coverage over regions of the earth, their performance degrades at the higher latitudes. This shortcoming is more noticeable as one moves along the spectrum of radio frequencies towards higher frequencies. Therefore, we envision our EHF Communications mission as one that addresses this deficiency in geosynchronous missions. In order to provide high latitude coverage, we have a high inclination, a very eccentric orbit, and perigee located at the southern most point in the orbit. The high eccentricity gives us a longer loiter time over the northern hemisphere. In fact, the satellite will spend nearly 90% of its time in the northern hemisphere and almost two thirds of its time at a high enough altitude and latitude to be providing communications service (see the section on EHF Payload for a specific discussion). Parameters of this orbit are summarized in Table 4.1. The orbit has a 500 km perigee altitude. The choice of inclination was based on the critical inclination to remove rotation of the line of apsides. Such a choice minimizes the effects of perturbations on the orbital elements making the orbit easier to maintain. Although perigee is at 270 deg, it can just as easily be located at 90 deg if one wants coverage at the extreme southern latitudes. For purposes of this design, northern hemisphere coverage is assumed. If one wants southern hemisphere coverage instead, the general conclusions from the northern hemisphere analysis still apply but the specific points in the orbit where significant events occur are rotated 180 degrees.

B. ORBIT ANALYSIS

1. AVHRR

The AVHRR orbit analysis focused on the relationship between the satellite and the sun. This mission uses a sunsynchronous orbit. However, such an orbit does not imply that the geometry between the satellite and the sun is a constant. Sun-synchronous indicates that the longitude of the ascending node moves along the earth's equator rather than remaining fixed in inertial space. The rate of change in the longitude of the ascending node is such that in the course of one year, the node will travel once around the equator. If the plane of the equator and the plane of the ecliptic were coplanar, then the sun would remain in the same relative location with respect to the orbit. Since these planes are not coplanar the location of the sun depends on the season. The AVHRR orbit analysis was directed at determining sun angles on the satellite, sun angles on the solar arrays, and eclipse periods.

a. Sun Angles on the Satellite

The primary motivation for this analysis is to ensure that the placement of the AVHRR payload on the spacecraft will prevent sunlight from shining in the sensor field of view and to prevent illumination of the thermal radiator. The basic approach is to define vectors normal to each of the satellite's faces. These vectors are essentially the roll, pitch, and yaw axes and their negatives. Another vector is defined to point from the satellite directly at the sun. The angle of incidence of sunlight striking a satellite face is the angle between the sun vector and the vector normal to the satellite face. This angle shall be referred to as the sun angle of a particular face. If the sun angle is zero degrees, then the sun is shining directly on the satellite face. If the sun angle is greater than 90 degrees, then the satellite face is oriented away from the sun and has no incident sunlight.

The program developed to perform this investigation propagates the satellite through one revolution around the earth on the first day of each season. The most extreme

values for sun angles are not guaranteed to occur on any of these four days. However, these days do illustrate the seasonal variation of the sun angles. Because the duration of one orbit is 101.5 minutes and the ascending node moves 360 degrees in one year, we made the simplifying assumption that the orbit is fixed in inertial space for the interval of time defined by one orbit. The consequences of this assumption is that the angle between the sun vector and the vector normal to the orbital plane remains constant. Since the satellite's pitch axis is parallel to the orbit normal vector, the sun angle on the satellite's pitch and negative pitch faces remains constant for that orbit. The sun angles on the remaining four faces vary sinusoidally. All four faces experience the same sun angle profile with the only difference being a shift in time. Table 4.2 summarizes the results on all six faces and for all four seasons. Figure 4.1 illustrates how the sun angles on the satellite faces vary as the satellite moves through one revolution.

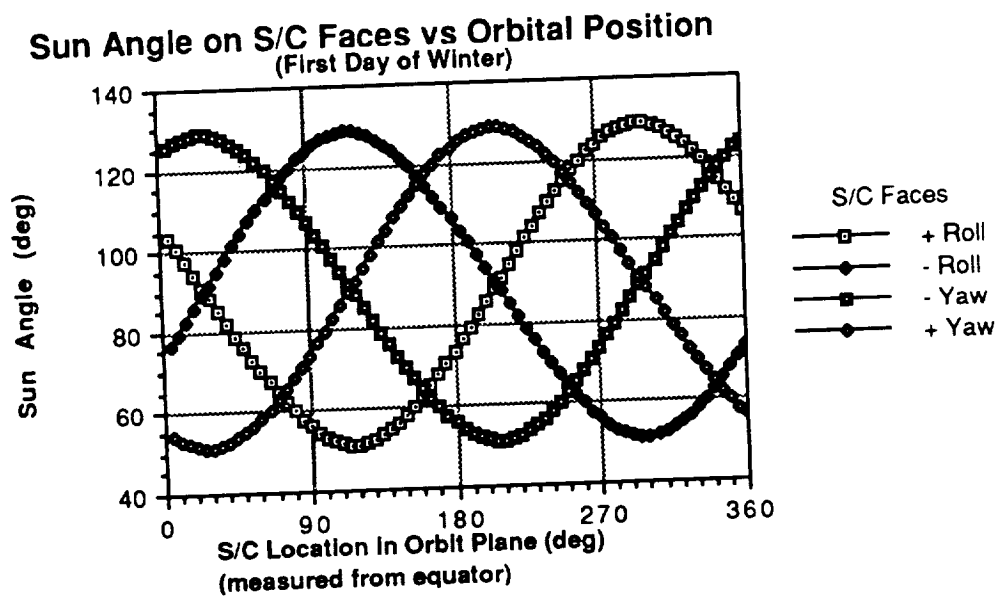


FIGURE 4.1 First Day of Winter Sun Angles on S/C Faces vs Orbital Position (8:30 PM Ascending Node)

Figure 4.1 is for the first day of winter and the orbit's ascending node is at 8:30 PM. The plots for the other seasons are similar in general shape but contain a phase shift and a change in amplitude. Figure 4.2 examines these changes by plotting the sun angle profile on the +Roll face for the first day of all four seasons.

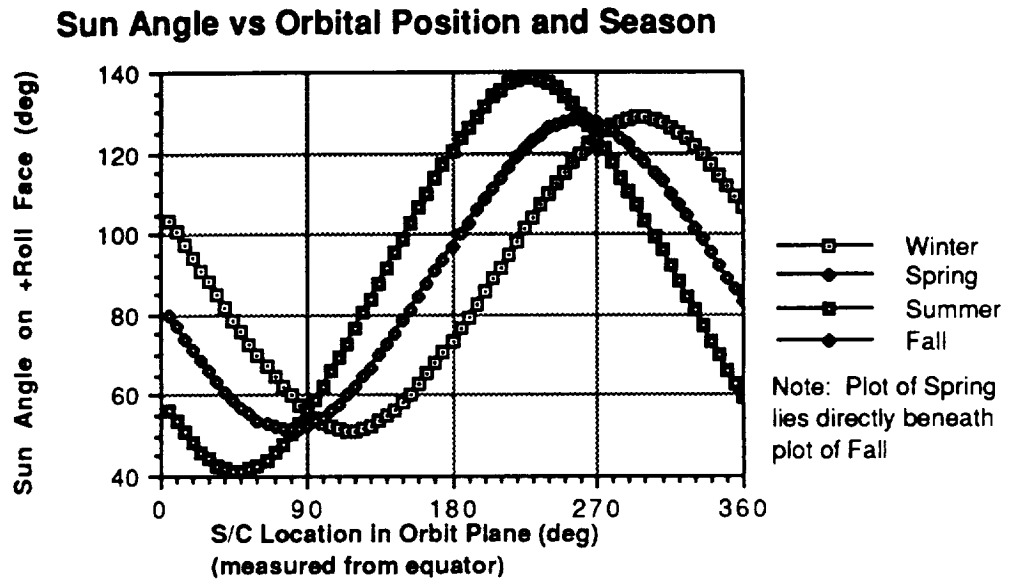


FIGURE 4.2 Sun Angle on +Roll Face vs Orbital Position
(8:30 PM Ascending Node)

The data in Table 4.2 is for an 8:30 PM ascending node orbit.

	Arg. of Latitude (deg)	Sun Angle on _____ Face (deg)					
		+ Pitch	- Pitch	+ Roll	- Roll	+ Yaw	- Yaw
First Day of Winter	25	141.2	38.8	91.2	88.8	51.3	128.7
	115	141.2	38.8	51.3	128.7	88.8	91.2
	205	141.2	38.8	88.8	91.2	128.7	51.3
	295	141.2	38.8	128.7	51.3	91.2	88.8
First Day of Spring	80	141.6	38.4	51.7	128.4	90.8	89.250
	170	141.6	38.4	90.8	89.2	128.4	51.7
	260	141.6	38.4	128.4	51.7	89.2	90.8
	350	141.6	38.4	89.2	90.8	51.7	128.4
First Day of Summer	50	131.2	48.8	41.2	138.8	91.6	88.4
	140	131.2	48.8	91.6	88.4	138.8	41.2
	230	131.2	48.8	138.8	41.2	88.4	91.6
	310	131.2	48.8	88.4	91.6	41.2	138.8
First Day of Fall	80	141.6	38.4	51.7	128.4	90.8	89.250
	170	141.6	38.4	90.8	89.2	128.4	51.7
	260	141.6	38.4	128.4	51.7	89.2	90.8
	350	141.6	38.4	89.2	90.8	51.7	128.4

TABLE 4.2 Sun Angles on Satellite Faces for an 8:30 PM Orbit

Argument of latitude is the angle from the ascending node to the satellite position measured in the direction of satellite motion. Table 4.2 lists four values for argument of latitude for each of the four orbits. The values listed in the table are the locations in the orbit where one face experiences a minimum sun angle for that orbit and its opposite face experiences a maximum sun angle. Notice that the orbit locations of the minimum and maximum sun angles vary with season as well as the values of the sun angles. This behavior is because the orbit does not maintain constant geometry with respect to the sun. The orbit is precessing around the earth's spin axis while the motion of the sun with respect to the earth is inclined 23.5 degrees. This disparity is irrelevant at the equinoxes when the earth's spin axis is perpendicular to the sun vector which lies in the plane of the equator. Notice that the table entries are identical for the equinoxes. In addition, the plots for Spring and Fall in Figure 4.2 lie one on top of the other. The most surprising data is that at the solstices. Because the orbit is sunsynchronous and retrograde, the orbit plane is closer to being parallel with the plane of the ecliptic during summer than during winter. That geometry makes the minimum and maximum sun angles more extreme in summer. One might expect that winter would represent the other end of the spectrum. However, the values for winter are very nearly the same as those for the equinoxes. This result is caused by a combination of the sunsynchronous nature of the orbit and the ascending node's displacement away from the terminator line. If the displacement had been zero, then winter would represent the other extreme.

Season	Arg. of	Sun Angle on _____ Face (deg)					
	Latitude (deg)	+ Pitch	- Pitch	+ Roll	- Roll	+ Yaw	- Yaw
First Day of Winter	65	141.2	38.8	128.7	51.3	88.8	91.2
	155	141.2	38.8	88.8	91.2	51.3	128.8
	245	141.2	38.8	51.3	128.7	91.2	88.8
	335	141.2	38.8	91.2	88.8	128.8	51.3
First Day of Spring	10	141.6	38.4	89.3	90.7	128.4	51.7
	100	141.6	38.4	128.4	51.7	90.7	89.3
	190	141.6	38.4	90.7	89.3	51.7	128.4
	280	141.6	38.4	51.7	128.4	89.3	90.7
First Day of Summer	40	131.2	48.8	88.4	91.6	138.8	41.2
	130	131.2	48.8	138.8	41.2	91.6	88.4
	220	131.2	48.8	91.6	88.4	41.2	138.8
	310	131.2	48.8	41.2	138.8	88.4	91.6
First Day of Fall	10	141.6	38.4	89.3	90.7	128.4	51.7
	100	141.6	38.4	128.4	51.7	90.7	89.3
	190	141.6	38.4	90.7	89.3	51.7	128.4
	280	141.6	38.4	51.7	128.4	89.3	90.7

TABLE 4.3 Sun Angles on Satellite Faces for a 3:30 PM Orbit

Table 4.3 presents the same information as Table 4.2, but the orbit under consideration has its ascending node at 3:30 PM. The two possible locations for the ascending node are symmetrical with respect to the terminator line. This geometry causes the values for the sun angles to be the same regardless of which of the ascending nodes is being used. The orbit locations for the specific sun angles vary but not the values for the sun angles. Close comparison of the values in the two tables will turn up some differences in the tenth's digit. One can attribute this to the method for generating the data rather than the physics of the problem. The data was generated by propagating the satellite through its orbit in five degree steps. The sun angles are only available at these points. Rerunning the program with a finer resolution should produce identical sun angles for orbits that are symmetrical about the terminator line.

b. Sun Angles on the Solar Arrays

The next area of investigation concerns the sun angles on the solar arrays. The solar arrays can rotate freely about the roll axis. To obtain the maximum amount of power out of the solar arrays, they need to rotate in a manner that minimizes their sun angles. These calculations were performed by the same program as was used to generate the sun angles in the previous section. At each evaluated point in the orbit, the same sun vector is still valid. That sun vector and the satellite roll axis define a plane. Let's refer to that plane as the sun vector roll axis plane (SVRA Plane). The solar arrays have a normal vector hereafter referred to as the solar array normal vector (SAN Vector). The sun angle on the solar arrays is minimized when the SAN Vector lies in the SVRA Plane. A vector normal to this plane is easily obtained by crossing the +Roll Axis Vector with the Sun Vector.

$$\text{SVRA Normal} = (+\text{Roll Axis}) \times (\text{Sun Vector})$$

These vectors and the other elements of the solar array sun angle geometry are presented in Figure 4.3.

The two angles that are desired are 1) the angle that the solar arrays should rotate to bring the SAN Vector into the SVRA Plane and 2) the sun angle on the solar arrays that results from that rotation. The angle that the solar arrays should rotate is the angle between the SAN Vector and its projection in the SVRA Plane. This angle is complementary with the angle between the SAN Vector and the SVRA Normal Vector. Once the rotation angle is found, the program rotates the solar arrays and then measures the resulting sun angle. This angle is the minimum sun angle possible for that orbit location. Notice that this angle is smaller than the original sun angle on the unrotated solar arrays. Two situations of interest can be seen from Figure 4.3. The first is when the SAN Vector is in the SVRA Plane to begin with. Under these circumstances the rotation angle will be zero degrees. The second interesting situation is when the +Roll Axis is perpendicular to the Sun Vector. When that happens, it is possible to rotate the solar arrays so that the resulting sun angle is zero degrees. Because the angle between Sun Vector and the +Roll Axis is constantly changing as the satellite moves through one orbit, the solar array rotation angle will change as well. The profile of how the solar array rotation angle changes is illustrated in Figure 4.4.

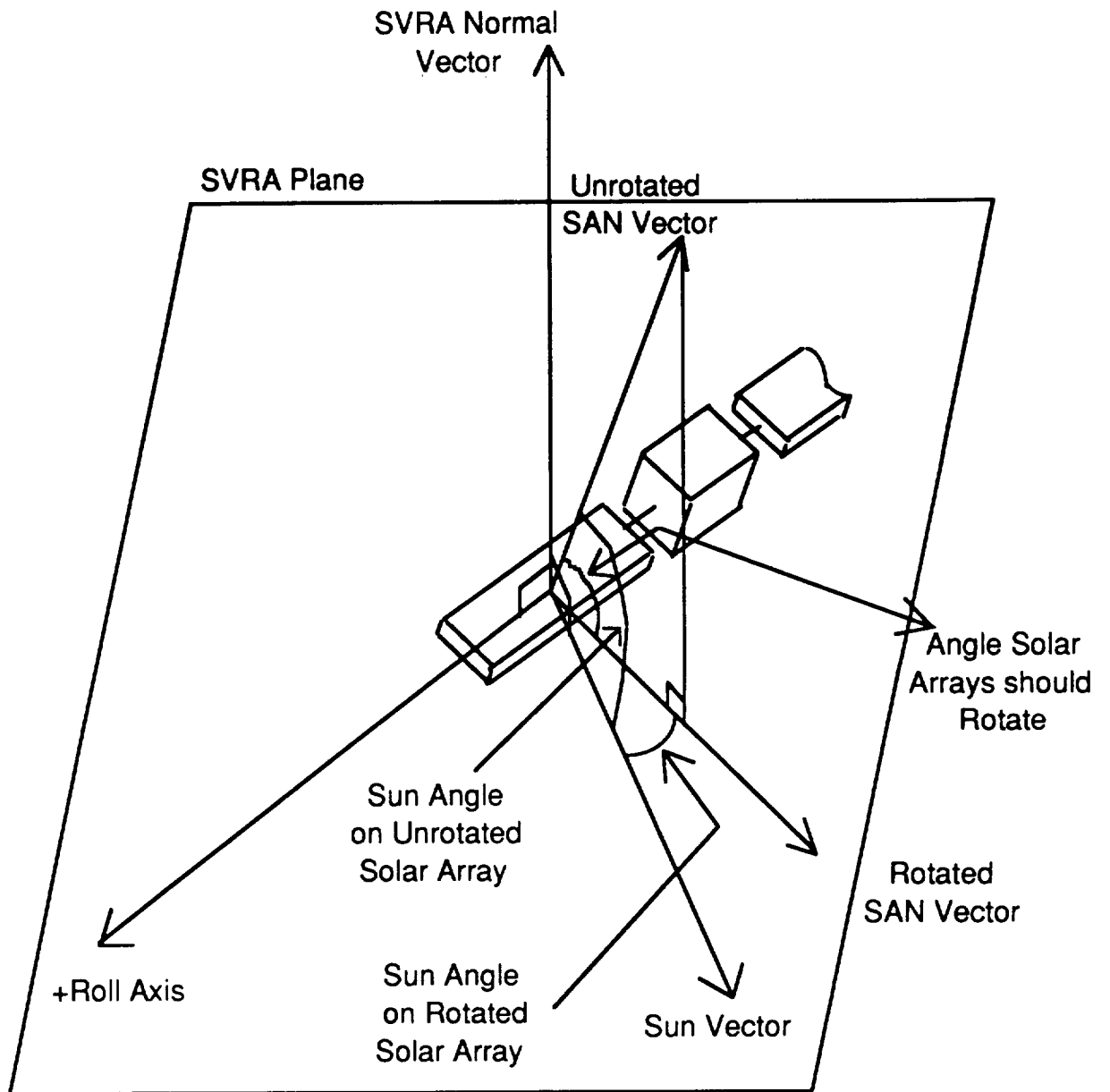


FIGURE 4.3 Solar Array Illumination Geometry

Seasonal Solar Array Rotation Angles

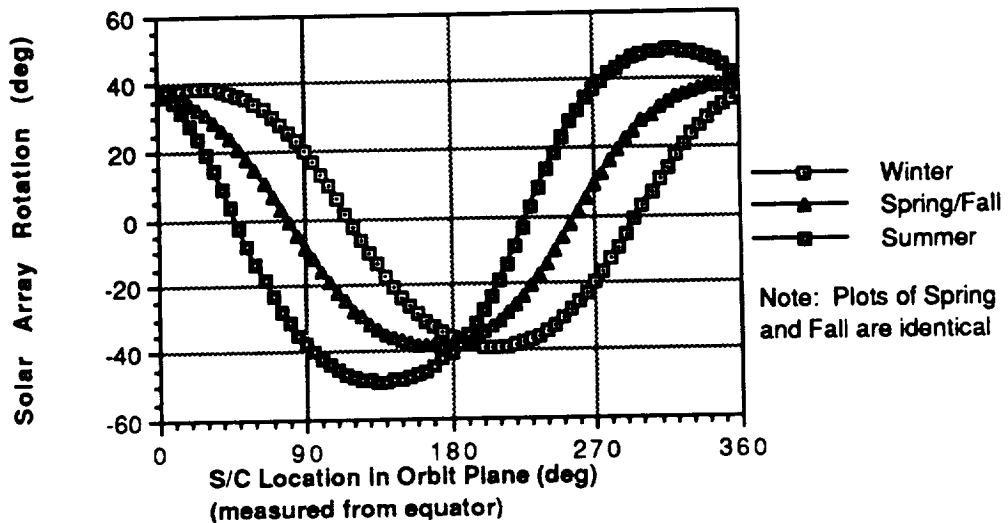


FIGURE 4.4 Solar Array Rotation Angle vs Orbital Position and Season

As one can see in Figure 4.4, for every orbit, there are two locations in the orbit where the solar array rotation angle is zero. These are the locations where the SAN Vector is already in the SVRA Plane. These locations are on opposite sides of a given orbit. Furthermore, these locations are not fixed with respect to the equator. They occur in different places depending on the time of year. This necessitates at least a phase shift in rotation angle profiles. There is also a change in amplitude that is seasonally dependent. All of the plots are centered with respect to zero rotation angle. The reference orientation for zero rotation is when the SAN Vector is parallel to the Negative Pitch Axis. Positive rotation is defined by the right hand rule and the +Roll Axis. The lack of a constant rotation angle profile dictates either a sensor on board the solar arrays to minimize the sun angle or regular contact with the satellite to upload a new rotation angle profile before the current one reduces solar array output beyond an acceptable level. Once again, the plots for

the equinoxes are identical. The season with the largest rotation angles is Summer. This is still because that is the season when the orbital plane is most nearly parallel to the plane of the ecliptic. Although there are still two locations requiring no rotation, the orbital positions 90 degrees away are worse than for any other season.

Figure 4.5 shows what the resulting sun angles are on the solar arrays if the rotation profiles from Figure 4.4 are used. As before, Spring and Fall produce the same plot and Summer has the largest excursion away from zero. Each orbit has two locations where the resulting sun angle is zero degrees. The only circumstances that permit this situation are when the Sun Vector and +Roll Axis are perpendicular to each other. Referring back to Figure 4.2 confirms that the orbital positions that produce a sun angle of 90 degrees on the +Roll Axis are the same orbital positions that have a rotation angle of zero for the solar arrays. Furthermore, because the plots in Figure 4.2 are centered vertically about 90 degrees, every orbit, not just the four representing the first day of each season, will have two points where the angle of incidence after rotation is zero. Of course, one of those points may be in eclipse, but that issue is discussed later. When comparing Figures 4.4 and 4.5, it is also interesting to note that the points in the orbit requiring zero rotation of the solar arrays are also the points with the worst sun angles for that orbit. At these points, there is not any rotation about the +Roll Axis that can improve the sun angle. Conversely, the points that require the most rotation correspond to the locations with a resulting sun angle of zero degrees. Finally, the values for maximum rotation in a given orbit and worst case solar array sun angle in the same orbit are equal to each other but are staggered 90 degrees apart. A quick check back in Table 4.2 reveals that the sun angle on the -Pitch Face is also the same value as the maximum rotation angle and the worst case solar array sun angle for a given day.

These scenarios can be summarized by defining a new plane. This plane contains the Sun Vector and the Pitch Axis. Because the Pitch Axis is assumed to remain fixed in inertial space during one orbit, this plane is also fixed. The Roll Axis completes a full 360

degree rotation around the Pitch Axis during one orbit. Whenever the Roll Axis is perpendicular to Sun Vector Pitch Axis Plane, the solar array rotation angle will be a maximum and the resulting solar array sun angle will be zero. Whenever the Roll Axis is in the Sun Vector Pitch Axis Plane, rotation of the solar arrays away from their reference only makes the sun angle worse. The rotation angle is zero but the solar array sun angles are a maximum. This consequence is used in developing the next program to investigate the orbit.

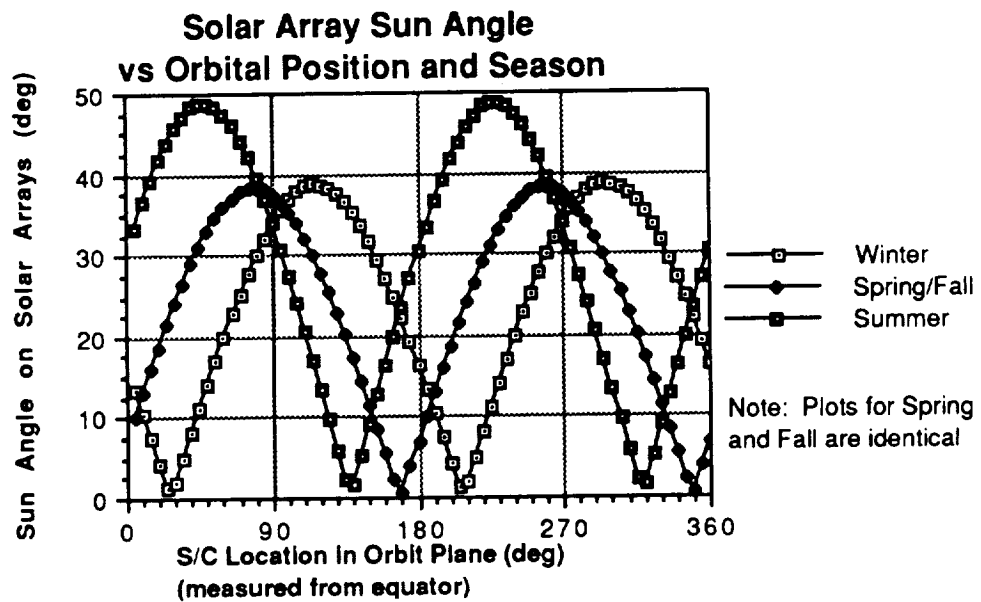


FIGURE 4.5 Solar Array Sun Angle vs Orbital Position and Season

To ensure that the solar arrays are sized large enough, the absolute worst case sun angle on the solar arrays is required. To provide this information, a different program had to be developed. This program propagates the earth around the sun and the orbit's ascending node around the earth's equator. For each point in the earth's orbit, the worst case solar array sun angle is tabulated. As mentioned above, this worst case angle is the

same as the sun angle on the -Pitch Axis. This avoids the need to propagate the satellite through its orbit at each of the locations of the earth. Figure 4.6 summarizes the results. It is essentially a plot of the maximum values from the four plots in Figure 4.5 plus intermediate values for days other than the first day of each season. The data still represents the 8:30 PM ascending node orbit. The data points are in five degree increments of the earth's orbit around the sun.

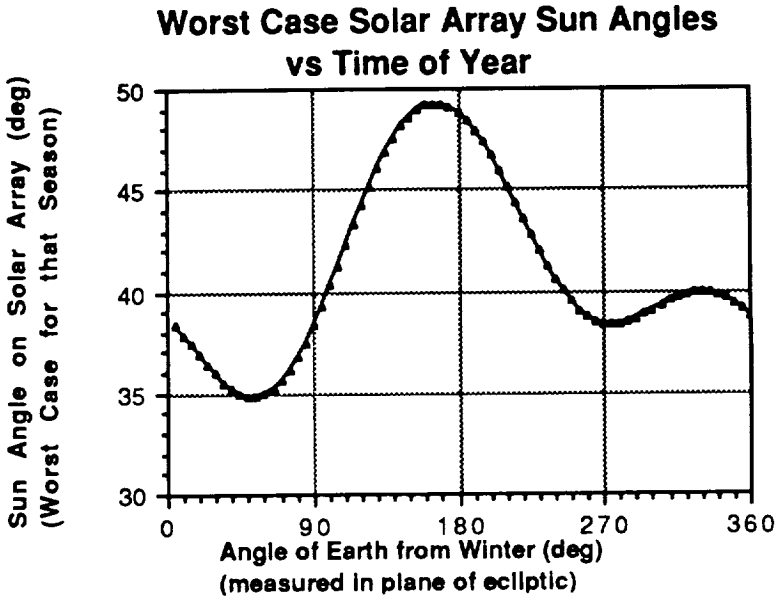


FIGURE 4.6 Worst Case Solar Array Sun Angles vs Time of Year

Figure 4.6 illustrates that for solar array sizing purposes, the worst case sun angles occur slightly before the first day of summer. However, the value for the worst case angle is only 0.4 degrees more than the value on the first day of summer.

c. Eclipse Periods

Eclipse duration influences design of the satellite most directly in terms of sizing the batteries and the solar arrays. The same program that calculated the worst case solar array sun angles also calculated the length of the eclipses. The program propagates the satellite through an orbit. At each step, the program looks to see if the satellite is over the sunlit side or the dark side of the earth. This is determined by looking at the angle between the Sun Vector and the Satellite Position Vector. If this angle is less than 90 degrees the satellite is above the sunlit side. If the angle is greater than 90 degrees, the satellite is above the dark side. If the satellite is over the dark side, it is in eclipse only if the component of the Position Vector perpendicular to the Sun Vector is less than the radius of the earth. This model assumes that the earth's shadow is a uniform cylinder parallel to the Sun Vector. By keeping track of when the satellite enters eclipse as well as when it exits, the eclipse duration is found. The program then propagates the earth one step in its orbit around the sun and performs the same series of eclipse calculations for this new geometry. Results for the 8:30 PM ascending node orbit are in Figure 4.7.

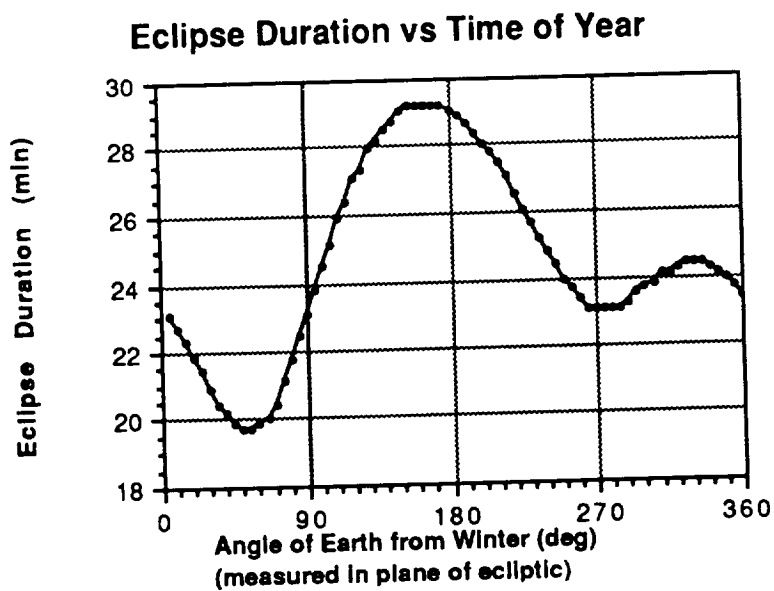


FIGURE 4.7 Eclipse Duration vs Time of Year

These results were obtained by stepping the satellite through its orbit in 0.5 degree increments. This produces a potential error in the predicted duration of just under the amount of time required to move through one degree in the orbit. This value is less than 20 seconds. Smaller step sizes should smooth out the curve. Figure 4.8 shows how the location of the eclipse in the satellite's orbit varies through the year. This is attributable to the apparent motion of the sun 23.5 degrees above and below the equator.

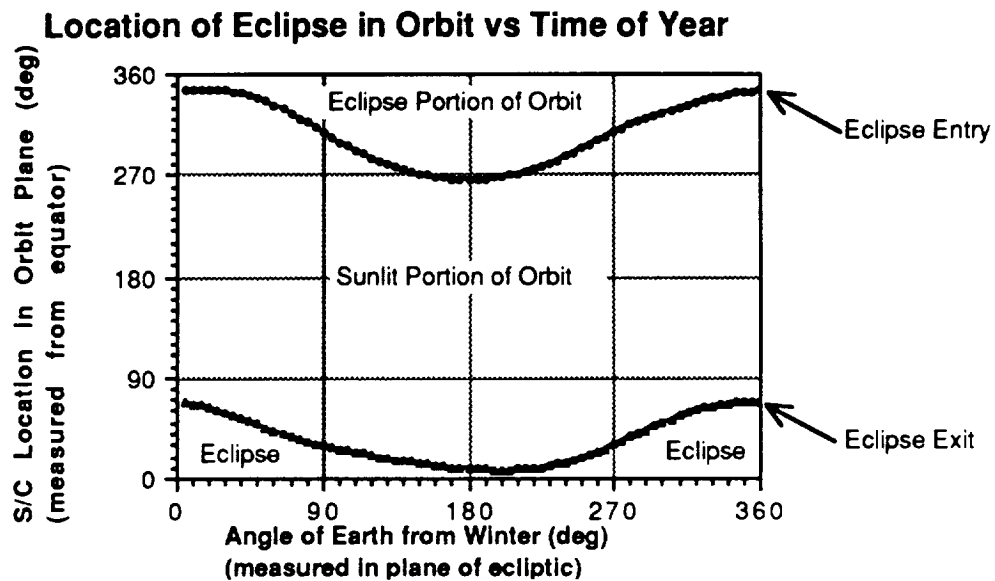


FIGURE 4.8 Eclipse Location in the S/C Orbit vs Time of Year

2. EHF

The analysis of the EHF Communications orbit does not require the same level of analysis as the AVHRR orbit. The advantage that the EHF mission enjoys is that the satellite is free to rotate around the Yaw Axis. This being the case, it is possible for the satellite to position its solar arrays with zero angle of incidence everywhere in the orbit. An analysis that has not been performed that probably should be done is to see what that angle of rotation around the Yaw Axis should be as a function of where the satellite is in its orbit. This analysis would be analogous to the solar array rotation profile for the AVHRR mission. The analysis that was done was to find the worst case eclipse and to find the time spent in specific altitude windows.

a. Worst Case Eclipse

Unlike the circular orbit of the AVHRR, the EHF mission's elliptical orbit means that the satellite travels at a nonconstant angular rate. The worst case eclipse in terms of duration is when the portion of the orbit in eclipse passes directly through the center of the earth's shadow cylinder. This condition is a function of longitude of the ascending node. Since we have no way of knowing in advance where a user will want the orbit placed, we must assume that our orbit may pass through the center of the cylinder. Another necessary condition for the worst possible eclipse is when the eclipse is centered around apogee. We can never create that geometry because we have assumed an inclination of 63.43 degrees and an argument of perigee of 270 degrees. Our worst case is when the portion of the orbit in eclipse is as close to apogee as the geometry will allow. With perigee at the southern most point in the orbit, the worst case scenario is created on the first day of winter. The center of the eclipse occurs 113.5 degrees past perigee. The shadow cylinder cannot be any farther north because the sun cannot be any farther south.

The program uses an iterative approach to find the values for true anomaly which correspond to eclipse entry and eclipse exit. At both of these points, the component of the satellite position vector perpendicular to the sun line is equal to the radius of the earth. Time spent in eclipse is found by converting the true anomalies of eclipse entry and eclipse exit into eccentric anomalies and then using Kepler's equation. Specific values for the EHF orbit are in Table 4.4.

True Anomaly at Eclipse Entry (deg)	70.587
True Anomaly at Eclipse Exit (deg)	131.715
Eclipse Duration (min)	52.079

TABLE 4.4 Eclipse Duration for EHF Mission

b. Altitude as a Function of Time

The principle motivation behind this analysis is to permit an estimate of the radiation environment on the solar arrays. This analysis is necessary because the radiation environment is dependent on altitude and on the amount of time the spacecraft spends at that altitude. This program simply accepts an altitude step size from the user and then breaks the orbit from perigee to apogee into segments. Each segment, with the possible exception of the first and last, represents a change in altitude specified by the user. Similar to the eclipse calculations, these satellite position radii can be converted into true anomaly, eccentric anomaly, and a time from a reference. Results are depicted in Figure 4.9.

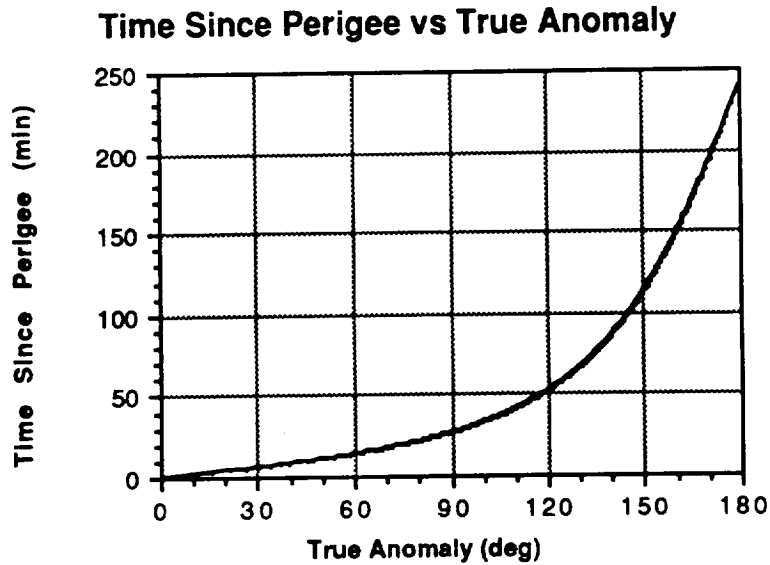


FIGURE 4.9 Time Since Perigee vs True Anomaly

As the slope of the curve in Figure 4.9 increases, so does the time spent near that altitude. Obviously, near apogee represents the longest loiter time. Since the figure is valid from perigee to apogee, total time spent in an altitude window during one orbit is twice the value off of the graph. Time spent in an altitude window during one day is six times the graph value, and so on.

C. ORBIT MAINTENANCE

Orbit selection for both missions was done so as to eliminate the orbit maintenance requirements. The AVHRR mission is patterned after an existing system. The Defense Meteorological Satellite System (DMSP) uses the same orbit as the AVHRR mission. DMSP has several payloads, one of which is very similar to AVHRR. DMSP performs no orbit maintenance during its lifetime. Because any changes in the orbit as a result of natural

perturbations seem to be acceptable to the present DMSP user community, the AVHRR mission will also include no orbit maintenance.

The EHF communications mission has an inclination of 63.435 degrees. This value is the critical inclination that prevents the line of apsides from changing. Perigee is located at the orbit's southern most point to give good coverage in the northern hemisphere. Perturbation analysis was performed using zonal harmonics J_2 through J_7 . The results of this analysis indicate that the orbit changes very little over the course of a satellite's lifetime. Perigee will rotate completely around the orbit in about 500 years. Our mission design life is only three years. During the mission lifetime, perigee will move less than 2.5 degrees. The change in inclination and eccentricity are likewise very small during a satellite's lifetime. Both of these changes are periodic. Results are summarized in Table 4.5. The table shows how the values are altered if inclination is within 0.1 degrees of nominal. The delta columns show how far inclination and eccentricity will change from their original values. Orbit maintenance fuel is not needed to counter any of these perturbations.

Inclination	Period (years)	Δi (deg)	Δe
63.335	243.2	0.2	0.006
63.435	377.4	0.3	0.002
63.535	262.9	0.15	0.004

TABLE 4.5 Perturbations on EHF Mission Orbit

V. SUBSYSTEMS

A. ELECTRICAL POWER SUBSYSTEM

1. Functional Description

The electrical power subsystem (EPS) will provide power to the spacecraft for the AVHRR and EHF payloads. The AVHRR payload will require continuous power during all phases of the mission, while the EHF communications equipment requires operating power when the spacecraft is 20° above the horizon and housekeeping power during the entire orbit. In addition to supplying power for the payloads, the EPS will be required to support electrical accessories such as the power control electronics; telemetry, tracking, and control (TT&C); sensors; and propulsion systems.

In general, the electrical subsystem will consist of solar panels of silicon photovoltaic cells and Ni-H₂ batteries. The spacecraft bus will operate off a single 28 volt bus. Power summaries of each configuration are listed in Table 5.1.

ELEMENT	AVHRR (W)	EHF (W)
MPS Bus Subtotal	166.4	114.8
Mission Instruments	28.0	115.0
MMS Harness Loss	4.0	4.0
System Reserve	4.0	4.0
Satellite Total	201.8	237.8
With cosine effect	313.9	n/a

TABLE 5.1 System Power Summaries (Normal Operations)

a. Solar Array Design

The MPS bus was designed to have two symmetric solar arrays of either two or three panels each. The Pegasus shroud will only be able to accommodate two panels per side while the Taurus shroud will accommodate three. The AVHRR and EHF configurations require two solar arrays of two panels each. The solar arrays on the EHF payload will be sun tracking to maintain panel orientation perpendicular to the sun's rays. This is accomplished through freedom of movement about the longitudinal axis of the arrays and through satellite rotation about the yaw axis. The AVHRR solar panels will, as nearly as possible, be oriented perpendicular to the sun's rays. The AVHRR operational requirements do not allow for the rotation of the spacecraft about the yaw axis. Therefore some loss of potential power is introduced due to the effect of the angle of incidence which reaches a maximum of 50° .

Silicon cells were chosen for cost and reliability, the cells selected were the same as those used in INTELSAT VI and are described in Table 5.2.

CHARACTERISTICS	K7 SILICON CELL
Power BOL (28°C) (mW)	307.8
Power EOL (28°C) (mW)	230.8
BOL	
I_{mp} (A)	0.644
V_{mp} (V)	0.478
I_{sc} (A)	0.6887
V_{oc} (V)	0.590
Size (cm)	2.5 X 6.2
Thickness (cm)	0.02
Material	Si
Base Resistivity Ω -cm/type	10/N/P
Front junction depth (μ m)	0.2
Back surface field	Yes
Back surface reflector	Yes
Contact metallization	TiPdAg
Front contact width (cm)	0.06
Antireflective coating	$TiO_xAl_2O_3$
Cover type	cmx microsheet with antireflective coating
Cover thickness (cm)	0.021
Cover adhesive	DC 93-500
Cover front surface	Textured

TABLE 5.2 Solar Cell Characteristics

Using the data from Table 5.1 and the cell characteristics from Table 5.2, the actual array panel area was determined and the results are summarized in Table 5.3. Supporting calculations can be found in Appendix B.

	AVHRR	EHF
Number cells series	22	22
Number cells parallel	68	80
Total number cells	1496	1760
Area needed (ft ²)	24.9	29.3
Area available (ft ²)	30.2	30.2

TABLE 5.3 Solar Array Summaries

b. Battery Design

The battery for eclipse power is the same as selected for HILACS, that is, 12 amp hour nickel hydrogen battery manufactured by Eagle Picher. The battery are made in a two cell common pressure vessel (CPV). Dimensions of each CPV are approximately 3.5 inches in diameter and 6 inches in height. Utilizing a 28 volt bus with constant current charge, the number of CPV cells is limited to eight. NiH₂ battery were chosen because of the high number of charge/discharge cycles the bus may experience. The AVHRR payload because of its 450 NM low earth orbit (LEO), for example, will experience over 15,000 cycles in its three year design life. The number of charge/discharge cycle this EHF payload will experience on the other hand may only be 1000. Because the bus was designed to accommodate these and other payloads in various orbits, the battery recharge requirements will vary. For this reason, the recharge circuitry must have the capability to be selectable or be comprised of modular components.

The AVHRR payload configuration draws 100.6 Watts during eclipse. Because this eclipse is roughly one third of the orbit, the recharge rate must be high enough to replenish the amount of power removed during the sunlight period. For a low earth orbit satellite with numerous charge and discharge cycles, an additional 10% on top of that power removed should also be replaced. For example, if 10 amps are drawn from the battery for 1 hour, the recharge cycle must provide an equivalent 11 amp hour for the charge period. Knowing the duration of the sunlight period and the power removed determines the recharging rate. Assuming that 90% of the sunlight period was used to recharge the battery, the AVHRR charge rate was chosen to be C/4, this is only slightly below the maximum recommended charge rate of C/3, where C is the battery capacity in amp-hours.

The EHF payload utilizes only 80.7 Watts during eclipse. Because of the longer sunlight periods and smaller power drawn, the charging rate of this configuration is only C/10. There are seasons where the Molniya type orbit would have no eclipse and then the battery would be trickle charged.

	AVHRR	EHF
Charge required	76.8 W	30.7 W
Charging rate	C/4	C/10
Charge time	59 min	6.5 hrs
Available sun	64 min	7.1 hrs
Battery capacity	12 A-hr	12 A-hr

TABLE 5.4 Battery Summary

Radiation effects and shielding requirements were examined for the AVHRR's circular orbit and the EHF's eight hour Molniya orbit. The degradation for the AVHRR configuration was based on an annual equivalent of 1 MeV electron fluence assuming solar maximum for the three year mission. The eight hour Molniya orbit posed significant challenges to the analysis of the radiation effects. Apogee for this orbit extended into the Van Allen belts exposing the solar cells to large fluences. Appendix B lists the equivalent 1 MeV fluences in five minute increments of orbital time for this orbit. Total fluence per orbit, per year, and three year lifetime were derived and the impact on the solar cells calculated. The radiation effect on both orbits are summarized in Table 5.5.

	AVHRR		EHF	
	Isc	Voc, Pmax	Isc	Voc, Pmax
Trapped electrons	4.59E+11	4.59E+11	3.18E+13	3.18E+13
Trapped protons	8.64E+12	1.47E+13	3.82E+15	1.59E+15
Totals	9.10E+12	1.52E+13	3.85E+15	1.62E+15

TABLE 5.5 Radiation Annual Fluence Summary

Power control electronics will maintain bus voltage at 28 volts. The bus will be fully regulated by employing a shunt regulator for periods of solar array operations and will utilize a boost regulator during periods of battery operations. This arrangement is discussed in detail in the HILACS project report.

2. Detailed Mass Summary

A detailed mass summary of the Electrical Power Subsystem components is listed in Table 5.6.

Components	Mass (kg)
Array Structural and Cells	13.00
Batteries	7.12
Wire Harness	3.00
Mechanical Integration	2.00
Solar Array Drive Electronics	1.00
Solar Array Drive Motors	8.00
Power Electronics	2.00
Shunt Resistor Bank	0.94
Total	37.06

TABLE 5.6 Detailed Mass Summary of EPS

B. ATTITUDE CONTROL SUBSYSTEM

1. Attitude Determination and Control System

The function of the attitude determination and control system, (ADCS), is to provide precise attitude pointing for the AVHRR or similar payload in a low (450 NMI) circular orbit, and a less accurate determination for the EHF or other communications payload in a Molniya-type orbit. This dual objective is met by using two subsystems for the different requirements, the Precision Sensor Subsystem, PSS, and the Basic Sensor Subsystem or BSS. The PSS and BSS are used for precise positioning, whereas the BSS alone can be used for less stringent requirements. Both subsystems consists of sensors to determine attitude, an on-board processor for control, and an inertial reference system consisting of an assembly of 3 orthogonal gyros, (GA). The BSS and PSS share the same components where possible. The Attitude Control Subsystem ,(ACS), is driven by either the PSS or BSS and consists of 3 primary reaction wheel assemblies, (RWA), with a fourth skewed wheel to provide redundancy, and two magnetic torque rods, (MTR), for momentum dumping. The six 0.2 lb thrusters can be utilized for momentum dumping in case of failure of the MTR's or if excessive momentum buildup occurs. The two subsystems are described below.

a. Precision Sensor Subsystem

The Precision Sensor Subsystem relies primarily on a Celestial Sensor Assembly, (CSA), for attitude determination. Figure 5.1 provides a functional block diagram of the system. The CSA is a strap-down star mapper with a 10.4 degree field of view. The CSA is the same sensor used aboard the DMSP Block 5D-3 satellite, (ref DMSP). The star sensor measures star transits across a detector and provides an input to the attitude control computer, (ACC). The user will be required to uplink to the satellite, approximately once per day, the 80 brightest stars that will be in view of the CSA. The ACC also receives input from the GA and an on-board GPS receiver. The ACC uses the

b. Basic Sensor System

The Basic Sensor Subsystem consists of a conical scanning earth sensor, (ES), a digital sun sensor, (DS), the GA, RWAs, ACC, GPS receiver, and MTRs. A scanning ES is required by the great range of possible altitudes that the satellite may achieve. The ES scans the 14 to 16 micrometer infrared radiance profile of the earth to determine pitch and roll error, while the DS determines the angle between the pitch axis and the sun. This information together with the ephemeris data from the ACC and GPS receiver provides yaw error. The BSS can provide better than 0.5 degree accuracy in each of the three axis. Figure 5.2 is a functional block diagram of the subsystem.

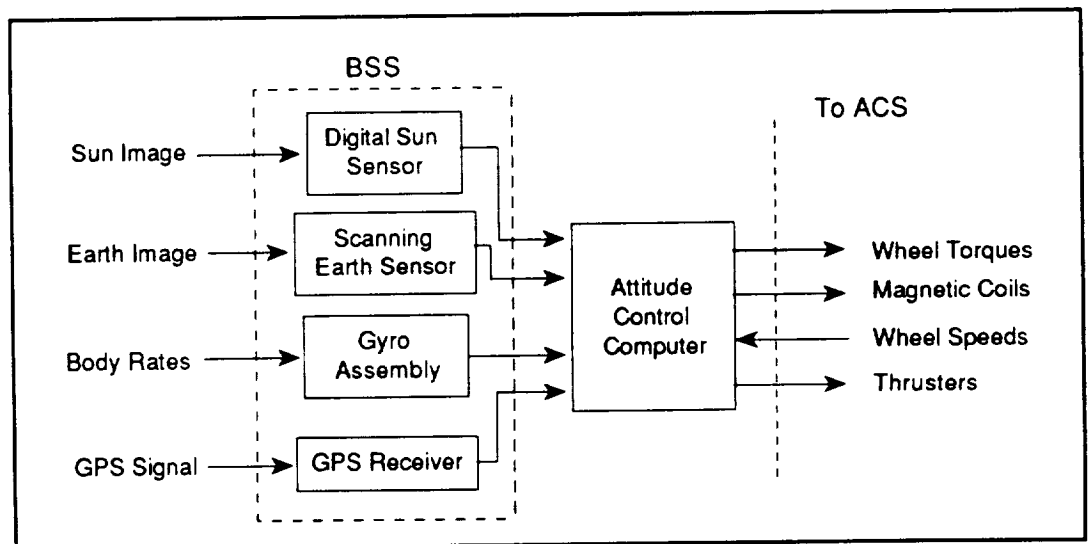


FIGURE 5.2 Functional Diagram of Basic Sensor Subsystem

c. Attitude Control Subsystem

The Attitude Control Subsystem, (ACS), is driven by the output of the ACC. The ACC sends commands to the RWAs to correct attitude errors. The RWAs' input to the ACC is the load current and wheel speed. The current is used to determine if an overload condition exists in which case the ACC shuts down the wheel and starts the backup RWA. The wheel speed is used as feedback and to determine if momentum dumping is required. When the momentum reaches the maximum for the wheel, the torque coils are commanded on to dump the excess momentum. In case of excessive rate buildup, as determined by differentiators in the circuitry, thrusters are fired to slow the rate to within acceptable limits. The block diagram for the ACS is given below.

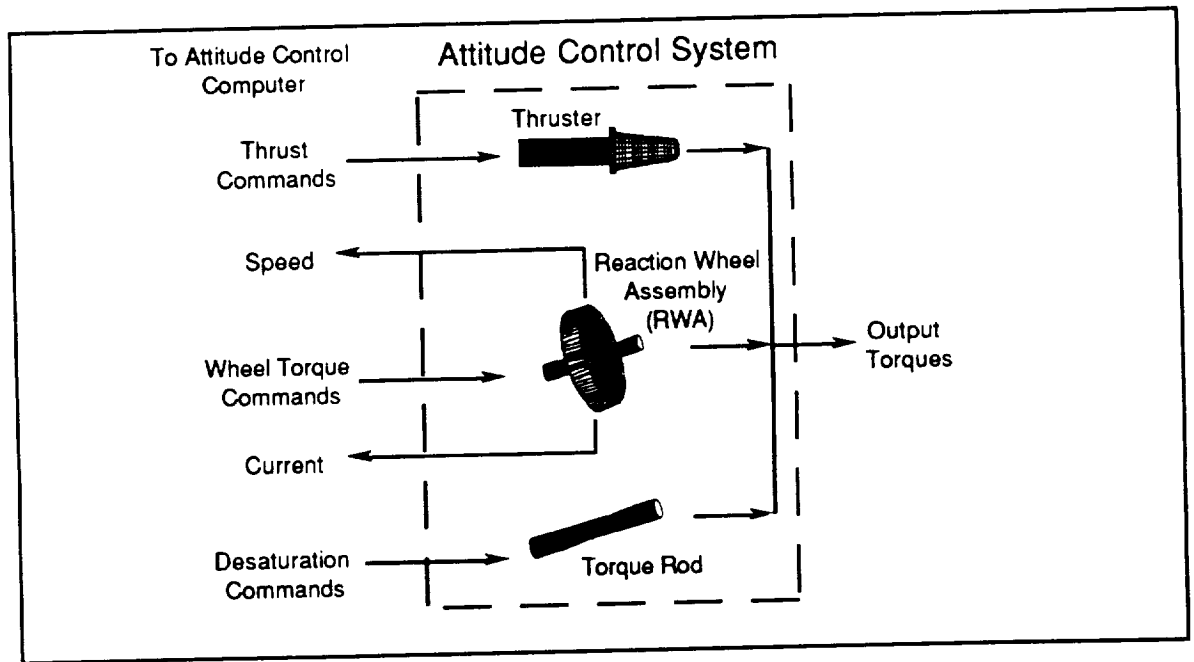


FIGURE 5.3 Functional Diagram of Attitude Control Subsystem

2. Design Considerations

For the first order accurate approximation, the spacecraft is modeled as a rigid body with nonrotating and rigid solar arrays. During the on-orbit mode, the disturbance torques are solar, gravity gradient, magnetic, and aerodynamic. The calculations, programs and resulting wheel speeds and attitude errors are given in Appendix C. The yaw motion of the satellite in the Molniya-type orbit is modeled as in HILACS, (see ref HILACS). The attitude control of the meteorological payload is treated in this report.

During the acquisition mode, the sun sensor on the anti-earth face acquires the sun. After the ACC commands the RWAs accordingly, the earth is acquired and the BSS begins operation. This is accomplished as follows: first, the RWAs are commanded to null the yaw rate, this fixes the yaw axis in inertial space in an unknown attitude, next, the spacecraft begins a slow rotation about the pitch axis until a sun observation occurs. If a sun observation does not occur in 5 revolutions, the pitch rate is nulled and the spacecraft begins a rotation about the roll axis. Utilizing this sun line and GPS receiver data, attitude is determined and error correction by the ACC commences. Once the pitch, yaw, and roll rates are nulled, the solar arrays are deployed. After sun and earth sensor updates to the GA occurs, the system is switched over to the PSS if precision is required, otherwise the BSS continues to control attitude. In the EHF payload the PSS is not available and the BSS will be the on-orbit mode.

3. Basic and Precision Subsystem Summary

The following is a break-down of the components of the BSS and the PSS. The AVHRR payload will require both the BSS and the PSS while the EHF payload will require only the BSS.

Component	AVHRR	EHF	PWR	Manufacturer
	(kg)	(kg)	(W)	
Attit. Ctrl. Computer	2.5	2.5	6	Barnes
Roll RWA	2.4	2.4	18	Honeywell
Pitch RWA	2.4	2.4	18	Honeywell
Yaw RWA	2.4	2.4	18	Honeywell
Backup RWA	2.4	2.4	N/A	Honeywell
Spring Restraining Gyro Assembly	1.2	1.2	19	INTELSAT V Heritage
Earth Sensor	3.77	3.77	4	Barnes
Sun Sensor North Face	0.04	0.04	1	Adcole
Sun Sensor Anti-Earth Face	0.04	0.04	1	Adcole
Roll-Yaw Torque Rods	0.40	0.40	0.6	Ithaco
Pitch Torque Rods	0.4	0.4	0.6	Ithaco
GPS Receiver	3.6	3.6	4	Motorola
Celestial Sensor	3.17	N/A	2.15	DMSP Heritage
Total	24.72	21.55	92.35	

Note: the EHF payload will require 2.15 W less of power than the AVHRR payload.

TABLE 5.7 Basic and Precision Subsystem Summary

4. System Parameters

The system parameters are computed in Appendix C. The RWAs are mounted so as to provide torque along each of the spacecraft's principle axis of inertia with the backup wheel mounted to provide torque equally along each of the principle axes. The worst case disturbance torque in the normal mode of operations is the interaction of the magnetic torque rods with the Earth's magnetic field during desaturation of the RWAs. The RWA parameters for the AVHRR payload are given below:

	Roll	Pitch	Yaw
Momentum Storage	1.9 Nms	1.9 Nms	1.9 Nms
Gain	0.885 Nm/rad	0.710 Nm/rad	0.621 Nm/rad
Time Constant	4 sec	8 sec	8 sec

TABLE 5.8 System Constants

5. System Performance

The wheels will be desaturated at approximately 100 RPM. The torque rods will provide a 10 AMP-m² magnetic dipole which will result in 0.006 N-m of torque over the earth's geomagnetic poles for the 450 nmi altitude of the circular orbit. The pitch torque rod will be energized within +/- 30 deg of the north and south geomagnetic poles and the roll-yaw rod when within +/- 30 deg of the geomagnetic equator. The desaturation scheme for the Molniya-type orbit is dependent upon the longitude of the ascending node. Basically, the roll-yaw rod will be used near the equatorial crossing and the pitch rod near perigee. As can be seen from the plot of the wheel speeds in Appendix C, the pitch wheel will require periodic desaturation. The roll - yaw wheels should rarely, if ever, require desaturation due to the cyclic nature of the disturbance torques. The satellite will maintain a 0.01 deg pointing accuracy during desaturation.

C. THERMAL CONTROL SUBSYSTEM

Thermal analysis of a spacecraft requires precise information concerning equipment placement, operating temperature limits, structural materials, and amount of power dissipated by the equipment. The conceptual EHF and AVHRR payloads for the MPS bus proposed in this study will not necessarily determine the final configuration. Because of this, the analysis performed on these configurations will be considered as an initial analysis with the understanding that as more detailed information and configuration revisions are incorporated, the analysis will be updated.

1. Design Considerations

The thermal control of each configuration is to be done utilizing passive techniques. The requirements to conserve mass in the design of the spacecraft were such that if passive techniques could be employed the impact on the mass of the spacecraft would be minimal. Therefore the goal is to use optical solar reflectors (OSR's), insulation, conductive transfer, and paints and coatings to regulate the temperature of the equipment.

The typical equipment operating limits listed in Table 5.9 were used as guidelines in the thermal analysis procedures:

Subsystem/Equipment	Thermal Design Temperature Limits (°C), Min/Max	
	Nonoperating/Turn-on	Operating
Communications		
Receiver	-30/+55	+10/+45
Input multiplex	-30/+55	-10/+30
Output multiplex	-30/+55	-10/+40
TWTA	-30/+55	-10/+55
Antenna	-170/+90	-170/+90
Electric power		
Solar array wing	-160/+80	-160/+80
Battery	-10/+25	0/+25
Shunt assembly	-45/+65	-45/+65
Attitude control		
Earth/sun sensor	-30/+55	-30/+50
Angular rate assembly	-30/+55	+1/+55
Momentum wheel	-15/+55	+1/+45
Propulsion		
Solid apogee motor	+5/+35	--
Propellant tank	+10/+50	+10/+50
Thruster catalyst bed	+10/+120	+10/+120
Structure		
Pyrotechnic mechanism	-170/+55	-115/+55
Separation clamp	-40/+40	-15/+40

TABLE 5.9 Typical Equipment Temperature Limits

2. Optical Solar Radiator Sizing

Based on the power summaries of the spacecraft an initial analysis was conducted to determine the approximate area required to radiate the thermal energy generated. The thermal energy dissipated by the EHF payload was estimated to be 148 Watts and for the AVHRR payload, 115 Watts. It is felt that these estimates are conservative and would reflect lower temperatures than might actually be encountered. Because space is such a good heat sink, any additional thermal load could be removed by limiting the insulation and/or altering the surface coatings.

The heat balance equation is:

$$\epsilon \sigma T^4 \eta A = \alpha_S A S \sin(\theta) + P$$

where

ϵ = emittance of the radiator (0.8)

σ = Stefan-Boltzmann constant

η = efficiency

A = area of the radiator

T = maximum desired operating temperature (310 K)

α_S = solar absorptance EOL (0.12)

S = solar intensity at winter solstice (1397 W/m²)

θ = solar aspect angle (23.5°)

P = thermal load to be dissipated in Watts

The area required for the radiator for the EHF configuration is 744 in² and for the AVHRR configuration it is 573.5 in². It should be noted that the AVHRR assembly comes with approximately 300 in² in OSR's installed.

3. Solar Array Temperature

The solar arrays of the EHF configuration will remain perpendicular to the solar flux. The AVHRR solar arrays will, as nearly as possible, be perpendicular to the solar flux. The positioning of the EHF solar arrays is accomplished by rotation about the roll axis by the solar array drive motors and about the yaw axis by attitude control of the spacecraft. The AVHRR solar array, due to equipment requirements, only has rotation about the roll axis by use of the solar array drive motors. This introduces some loss in power but is compensated for in the sizing of the arrays. The greatest angular displacement is approximately 50° inclination from perpendicular.

The effective solar absorptance (α_{SE}) is:

$$\alpha_{SE} = \alpha_S - F_p \eta$$

where

α_S = average solar cell array absorptance (0.8)

F_p = solar cell packing factor (0.95)

η = solar cell operating efficiency

The steady state operating temperature (T_{op}) of the solar array is given by:

$$T_{op} = \left[\frac{\alpha_{SE} A_F S \cos(\alpha)}{(\epsilon_F A_F + \epsilon_B A_B) \sigma} \right]^{1/4}$$

where

A_F = array front side area (30.2 ft²)

A_B = array back side area (30.2 ft²)

ϵ_F = emittance of array front side (0.8)

ϵ_B = emittance of array back side (0.7)

S = solar constant

σ = Stefan-Boltzmann constant

α = angle of incidence of sunlight

The operating temperatures of each of the solar arrays are summarized as follows:

T_{op}	EHF	AVHRR
Summer Solstice	45.3° C	12° C
Winter Solstice	50.4° C	34.6° C

TABLE 5.10 Solar Array Operating Temperatures

4. Thermal Analysis Using PC-ITAS

The Integrated Thermal Analysis System for personal computers (PC-ITAS) is a menu driven software package produced by ANALYTIX Corporation. The thermal analyzer has the ability to accept various inputs concerning the spacecraft. Among these inputs are spacecraft configuration, operations, and orbital parameters. After entering this data the analyzer will generate steady state or transient output temperatures. It can be used to rapidly analyze changes in configuration or material properties during the design phase.

PC-ITAS allows the user to represent the spacecraft with a model. The model building menu has various geometric shapes which can be dimensioned to satisfy any requirements. Each geometric shape will constitute one or more surfaces. The software limits the user to 550 surfaces although expanded versions are available. Caution must be exercised in choosing geometries as the more surfaces used, the more memory and computer running time are needed. It was determined that, for the computer system currently in use by the design team, approximately 165 surfaces could be generated for analysis without any overflow problems. Because this is a preliminary design analysis this did not pose a significant problem. Some equipment was not modelled in detail due to this limitation so there was a trade off between computer capability and depth of analysis. To get an accurate, in depth analysis would require a final design and complete thermal characteristics of each piece of equipment.

Each surface constitutes a node in the thermal analysis phase. A box, for example, would have six surfaces therefore it has six nodes. The following tables outline the components modelled and the geometric shapes selected to represent them, as well as the number of each nodes assigned to that component.

Component	Geometric Model	Assigned Nodes
MPS Bus	5 sided box	1 - 5
Power control	Box	6 - 11
Batteries	Box	12 - 17
Attitude control	Box	18 - 23
Fuel tank	18 sided sphere	24 - 41
AVHRR	5 sided box	42 - 46
RTU	Box	47 - 52
RCU	Box	53 - 58
OSR shield	Polygon	59
AVHRR side panels (2)	Polygon	60, 61
AVHRR OSR's	Polygon	62
Bus OSR's	Polygon	63
Yaw RWA	12 sided cylinder, capped	64 - 87
Pitch RWA	12 sided cylinder, capped	88 - 111
Roll RWA	12 sided cylinder, capped	112 - 135
MPS Bus south panel	Polygon	136
Solar array drive motor - east	5 sided box	137 - 141
Solar array drive motor - west	5 sided box	142 - 146

TABLE 5.11 AVHRR Model and Node Assignment

Component	Geometric Model	Assigned Nodes
MPS Bus	5 sided box	1 - 4
Power control	Box	5 - 10
Batteries	Box	11 - 16
Attitude control	Box	17 - 22
Fuel tank	18 sided sphere	23 - 40
Yaw RWA	12 sided cylinder, capped	41 - 64
Pitch RWA	12 sided cylinder, capped	65 - 88
Roll RWA	12 sided cylinder, capped	89 - 112
Solar array drive motor - east	5 sided box	113 - 117
Solar array drive motor - west	5 sided box	118 - 122
OSR's	Polygon	123
MPS Bus south panel	Polygon	124
Connector	5 sided box	125 - 129
EHF Feedhorn assembly	Box	130 - 135
RF reflector	6 sided disc	136 - 141
Reflector support	4 sided cone, capped	142 - 149
EHF Electronic I	Box	150 - 155
EHF Electronics II	Box	156 - 161

TABLE 5.12 EHF Model and Node Assignment

After generating the model, the orbital parameters were entered. PC-ITAS will generate graphics so that the user may see the spacecraft in the orbit specified and will use this data in the generation of view factors and shadow factors. The EHF payload was analyzed for a Molniya orbit and the AVHRR payload for a circular, nearly polar orbit. Orbit parameters are entered through the orbital analysis parameters menu and can be rapidly changed to conduct analysis for any number of orbits the user desires.

Included with the PC-ITAS software are physical and optical properties of numerous materials. The user may select from these tables or enter the requirements in the appropriate blocks within the menu. Optical properties of the surfaces modelled must be selected for analysis. The analyzer will automatically calculate view factors between surfaces for use in the radiative heat transfer equation. The user may, if it is so desired, link nodes by either radiation or conduction. Unless there is a specific need to do so, radiation links need not be established as they are generated automatically. Conduction transfers, where known, should be entered as part of the data. Should certain equipment be operated for a set time duration and off for other periods, the analyzer is capable of handling this condition. The power profile definitions menu will allow the entering of these equipments along with a listing of their on and off times.

Equipment which dissipates heat can be indicated at the time the optical parameters are designated. Any heat dissipated will become part of the environment and incorporated into the thermal analysis. Because detailed information on the thermal energy generated by the equipment and specific locations of that generation is not available, the heat dissipated by a piece of equipment was estimated and then applied equally to all surfaces of the geometric representation of that component.

The following table lists the materials selected, optical properties, and heat dissipated per surface (node) of each payload.

AVHRR		Optical Properties		Heat Dissipated Per Surface (W)
Component	Material	α	ϵ	
Bus	Anodized Aluminum 7075-T6	0.30	0.80	
Power control	Sandblasted Aluminum 2024	0.42	0.21	0.1
Batteries	Polished Stainless Steel 302	0.38	0.19	9.0
Attitude control	Sandblasted Aluminum 2024	0.38	0.19	0.3
Fuel tank	Polished Nickel Coating	0.44	0.05	0.2
AVHRR	Anodized Aluminum Low A/E	0.25	0.72	1.5
RTU	Sandblasted Aluminum 2024	0.38	0.19	0.3
RCU	Sandblasted Aluminum 2024	0.38	0.19	0.3
Shield	Bare, Clean Aluminum	0.19	0.08	
OSR's	Ag-SiO ₂	0.05	0.8	
RWA's	Anodized Aluminum 2024	0.68	0.48	0.5
SADM's	Anodized Aluminum 2024	0.68	0.48	0.7

TABLE 5.13 AVHRR Material Selection and Heat Dissipation

EHF		Optical Properties		Heat Dissipated Per Surface (W)
Component	Material	α	ϵ	
Bus	Anodized Aluminum 7075-T6	0.30	0.80	
Power control	Sandblasted Aluminum 2024	0.38	0.19	0.1
Batteries	Polished Stainless Steel 302	0.38	0.19	3.0
Attitude control	Sandblasted Aluminum 2024	0.38	0.19	0.3
Fuel tank	Polished Nickel Coating	0.44	0.05	0.2
RWA's	Anodized Aluminum 2024	0.68	0.48	0.5
SADM's	Anodized Aluminum 2024	0.68	0.48	0.7
OSR's	Ag-SiO ₂	0.05	0.8	
Connector	Anodized Aluminum 7075-T6	0.30	0.80	
EHF Feedhorn	Anodized Aluminum 7075-T6	0.30	0.80	0.16
RF reflector	Reflector	0.10	0.10	
Reflector Support	Flame Sprayed Aluminum Oxide Rokide A	0.27	0.75	
EHF Elex I	Anodized Aluminum, Gray	0.56	0.60	3.3
EHF Elex II	Anodized Aluminum, Gray	0.56	0.60	10.0

TABLE 5.14 EHF Material Selection and Heat Dissipation

After all parameters have been entered the thermal analysis can be initiated. The results are placed in an output file and will include the parameters entered, all default settings, and steady state temperatures for each node at the end of one orbit. The output for each payload can be found in Appendix D.

5. Conclusions

The results of the thermal analysis on both payloads are indicative of a specific set of conditions with estimations by the available data. This preliminary analysis indicates that, with proper selection of coatings and materials, the temperatures of the various equipments can be maintained within operating ranges. There are specific nodes which are too cold or too hot, but since these are identified corrective action can be implemented. Corrective action in these cases would be to insulate or link by conduction to the radiator. To do this next step would require more detailed information in order to calculate path lengths to be used in the conduction linking. Before a more refined analysis and implementation of any corrective action there is a need to select the individual pieces of equipment which will actually be used in the spacecraft systems.

D. PROPULSION SUBSYSTEM

1. Functional Description

The propulsion subsystem consists of one propellant tank with a 20 kg capacity, six .2 lbf thrusters and associated valves and tubing. Installed primarily as a backup system for reaction wheel desaturation, orbit maintenance, and orbit stationkeeping, the system is provided with no redundancy. The fuel is hydrazine monopropellant with catalytic beds. The center mounted spherical tank is filled to the amount required by the mission just prior to launch.

a. Requirements

After separation from the Pegasus launch vehicle, the propulsion system will be used to correct minor errors in the orbit. On orbit the system will provide delta V for stationkeeping. See Table 5.15 for thruster operation and axis effect and Figure 5.4 for thruster location..

Operation	Thruster Number
Delta V Yaw	1A/2A 1C/2C
Delta V Roll	1B/2B
Positive Roll (+X)	1A
Negative Roll (-X)	2A
Positive Yaw (+Z)	1B
Negative Yaw (-Z)	2B
Positive Pitch (+Y)	1C
Negative Pitch (-Y)	2C

TABLE 5.15 Thruster Operations

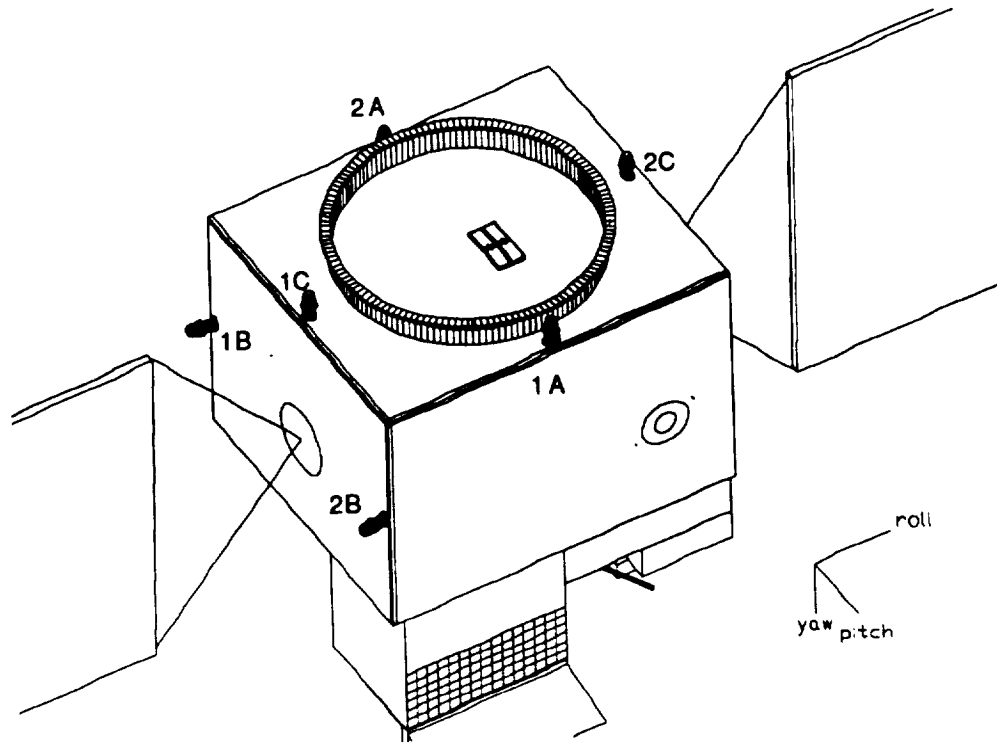


FIGURE 5.4 Location of Thrusters

b. Summary of Subsystem

The propulsion subsystem consists of six 0.2 lbf thrusters. The thrusters recommended are the Rocket Research MR103C. These particular thrusters were chosen for the design because the MR103C has a design that minimizes space required for mounting. The MR103C is also the lightest of the .2 lbf thrusters considered for the requirements of the satellite. The six thrusters along with the rest of the propulsion system are depicted in a schematic in Figure 5.5. Note also that a 8 micron filter is incorporated to screen the impurities remaining in the fuel. There is one pressure transducer and one pressure regulator to monitor the pressure throughout the system.

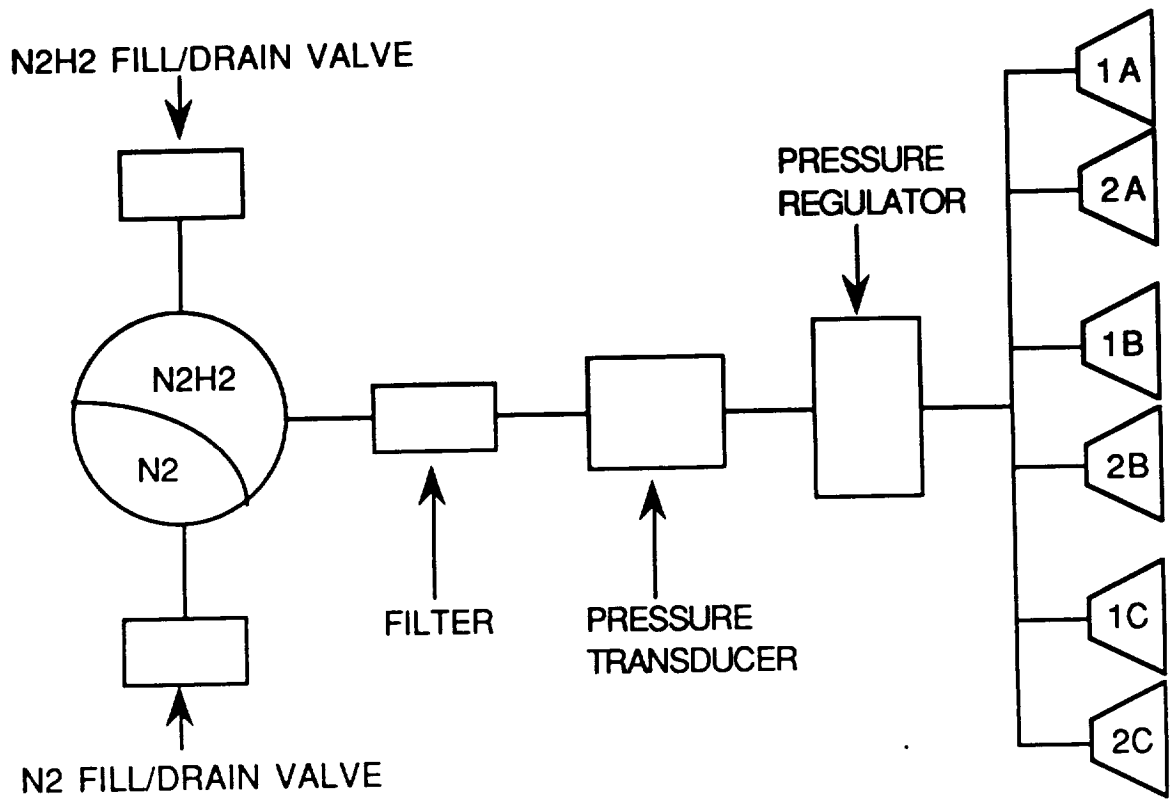


FIGURE 5.5 Schematic Diagram of Propulsion System

Thruster characteristics are detailed in Table 5.16.

Design Characteristic	
Catalyst	Shell 405
Thrust, steady state (lbf)	.252 - .042
Feed press (psia)	420 - 70
Chamber press (psia)	370 - 60
Expansion Ratio	100:1
Flow rate (lbm/sec)	.001 - .0002
Valve	Wright
Valve power	9 Watts
Weight	0.73
Engine	0.28
Valve	0.45
Demonstrated Performance	SATCOM
Specific impulse	227 - 206
Total impulse (lbf - sec)	35625
Total pulses	410000
Minimum impulse bit	.001
Steady state firing (sec)	64800

TABLE 5.16 Summary of Propulsion Equipment

The 16 inch diameter tank is made of titanium alloy and made by TRW Pressure Systems Inc. An elastomeric diaphragm inside the tank separates the nitrogen gas pressurant from the propellant. Maximum capacity of the tank is 20 kgs. Table 5.17 lists the characteristics of the tank.

Internal Volume	1352 sq in
Operating Pressure	480 psia
Operating Temp	70 degree F
Proof Pressure	590 psia
Burst Pressure	960 psia

TABLE 5.17 Propellant/Pressurant Tank Characteristics

The fill and drain valves are used to service the propulsion subsystem during system functional evaluation to include leakage and cleanliness tests, loading and unloading, and prelaunch operations. The valves are manually operated and self contained.

The lines consist of titanium alloy tubing and fittings and interconnect the tank and thrusters via a pressure transducer and regulator. The transducer and regulator measure and maintain the proper inlet pressure to the operating thruster.

c. Summary of Subsystem Operations

Thruster operations can be performed with or without the solar arrays deployed. Thrust can be applied to desaturate the reaction wheels along any axis but ΔV for orbit maintenance can only be provided in the positive yaw or the positive roll directions. The positive roll thrusters are placed to provide ΔV for orbit maintenance without the need for reorientation of the spacecraft. Major orbit changes will require reorientation of the spacecraft to align the flight path of the spacecraft along the positive Z axis. Mission instrument deactivation may be required during major orbit corrections. The two thrusters along the east face could possibly impinge on the solar panels, depending on the angular position of the arrays. A electronic cutout cam would have to installed to prevent accidental firing and subsequent damage to the arrays. It is unlikely that this would effect AVHRR operations as the arrays operate $\pm 50^\circ$ degrees of the roll / yaw plane. The EHF payload however, sometimes requires the arrays to rotate $\pm 90^\circ$ roll / yaw plane necessitating close

management of solar array and thruster operations. As an additional precaution, the thrusters along the positive roll axis are canted out at an angle of 8°.

2. Detailed Mass/Power Summary

A detailed mass/power summary of the propulsion subsystem is provided in Table

5.18.

Element	Mass/kg	Power/W
0.2 lb Thruster (6)	4.4	54 (max)
Propellant Tank	5.9	0
Transducer/ Regulator	1.4	4
Tubing	1	0
Electronics	1.5	4
Drain/Fill Valves	1	0
Total	15.2	62

TABLE 5.18 Mass/Power Summary of Propulsion Subsystem

E. TELEMETRY AND TRACKING SUBSYSTEM

1. Functional Description

The TT&C package for the MPS Bus is designed to be compatible with the Air Force SGLS system for satellite control. TT&C is designed in the bus to operate at SHF frequencies that correspond to channel 1 of the SGLS ground terminal as follows:

Command Uplink: 1.763721 GHz

Telemetry Downlink: 2.2 GHz

Carrier 1: 2.2025 GHz

Carrier 2: 2.1975 GHz

The TT&C package sends and receives data from the payload and/or the anti-earth face antenna through command controlled switches that allow the ground terminal to shift between payload antennas and the anti-earth face antenna. The anti-earth face antenna is a four element microstrip antenna that uses the same elements as the AVHRR antenna shown in Figure 3.2 and has a gain of 2.5 dB. The switches will probably be aligned so that during launch and activation, TT&C will be accomplished with the SGLS system channel 1 to the anti-earth face antenna. Once the satellite is on station, the payload TT&C will have been activated and the anti-earth face telemetry downlink can be put in standby. The anti-earth face command receiver will remain active to provide a failsafe in case the satellite attitude control system fails.

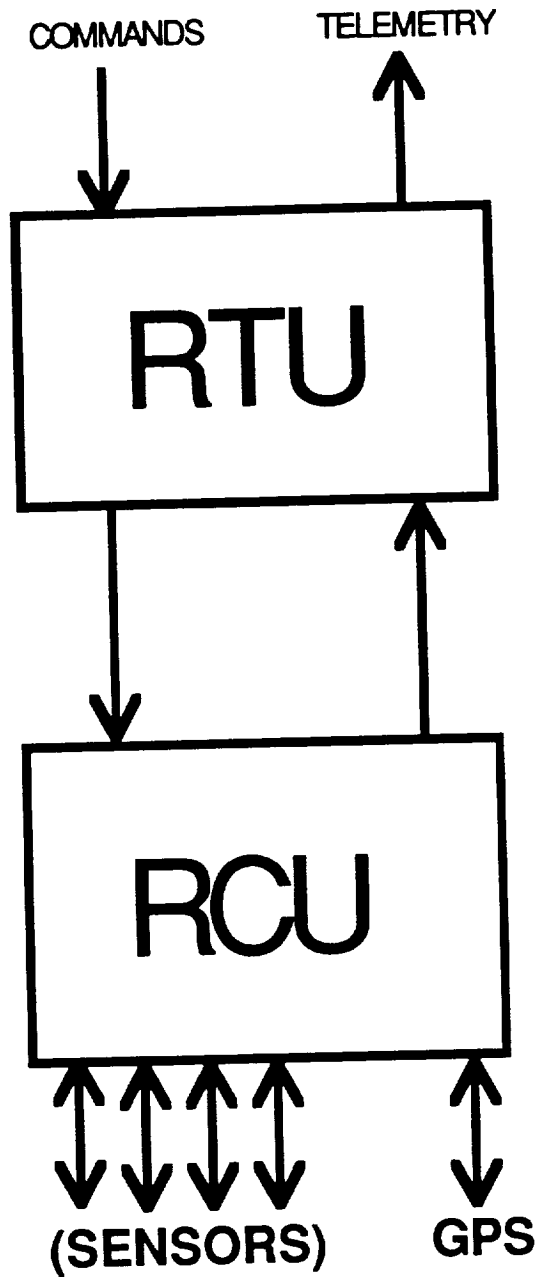


FIGURE 5.6 TT&C Package

The TT&C consists of two major components as shown in Figure 5.6. These components are the remote tracking unit (RTU) and the remote command unit (RCU). The RTU is the interface between the TT&C antenna systems and the RCU. The function of

the RTU is to take commands from the antennas and payload in the SGLS format and demodulate and decode them to the point where they can be handled by the RCU. The RTU also takes telemetry signals from the RCU, modulates and encodes them and sends them on to antennas.

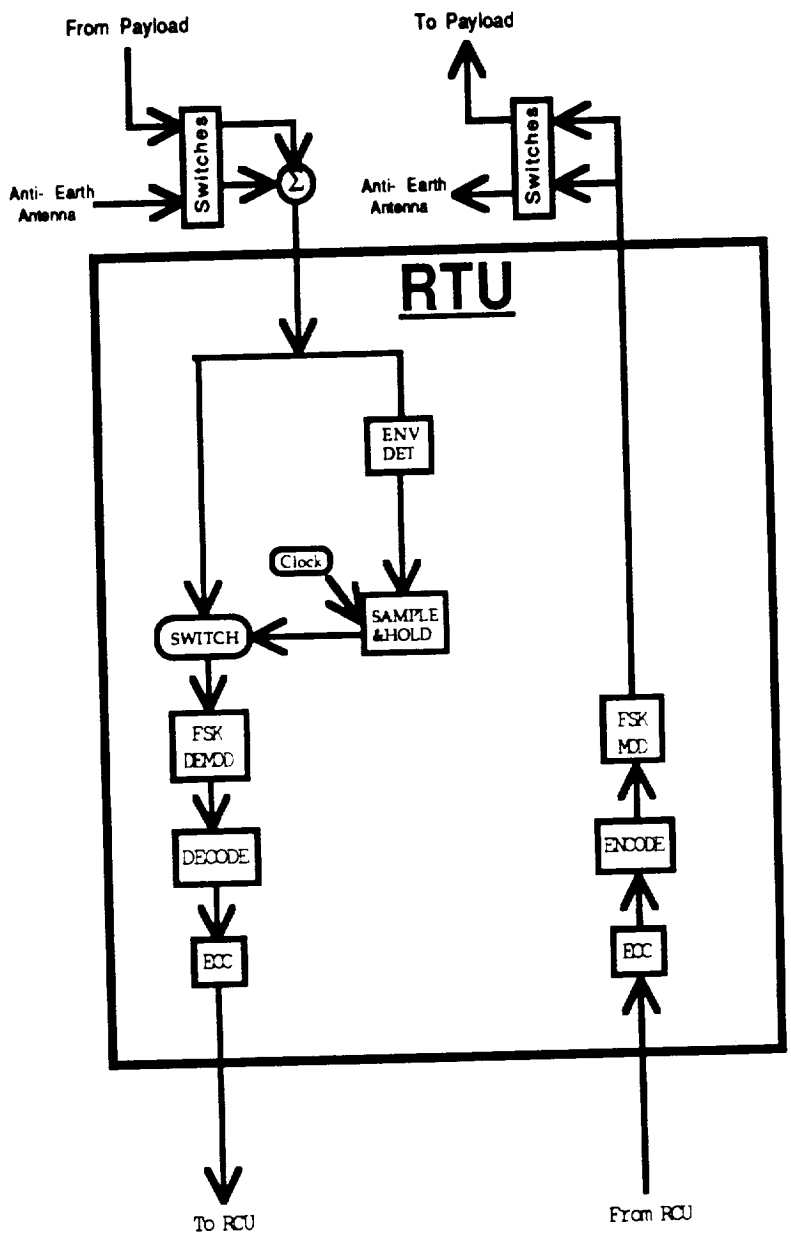


FIGURE 5.7 Remote Tracking Unit

Figure 5.7 shows a block diagram of the RTU. On the command side of the circuit, the first function performed by the circuit is to check for a signal. The antennas and/or payload have filtered the command channel and modulated it to 1.763721 GHz. If the channel contains energy, the envelope detector and sample and hold circuit will use this energy to hold open an electronic switch to send the command signal on to the FSK demodulator. It is demodulated and decoded and sent on to a small processor that will check the error correction coding (ECC) of the signal.

ECC is a process in which bits are added to each symbol to provide redundancy in the data. A primary goal of ECC is to recognize a bit error in order to prevent improper commands being executed, but for low bit error rates the ECC could be redundant enough to actually correct bit errors. An example of ECC is the Hamming Code. The Hamming code is a process in which check bits are inserted in a data stream that tell whether a group of bits has an odd or even number of 1's. (odd or even parity). If the check bit says that a group of data bits should have even parity and the receiver counts an odd number of 1's in that group, then a bit error has occurred. With redundant check bits, the bit in error may be deduced and corrected. If there are not enough check bits or too many bit errors, then the data will have to be retransmitted. MIL STD 1582 requires that ECC be used to allow for higher bit error rates and prevent improper TT&C commands. This report will not explore them in detail.

On the telemetry downlink side of the RTU, the telemetry signal comes from the RCU. ECC is inserted in the data, the data is encoded and the FSK modulator prepares it to be sent to the antennas at 2.2 GHz. The RTU only handles data that is compatible with channel 1 of SGLS. Therefore, if another format or frequency is desired, the payload will have to modulate and process the data itself. This allows for the MPS bus to be somewhat modular.

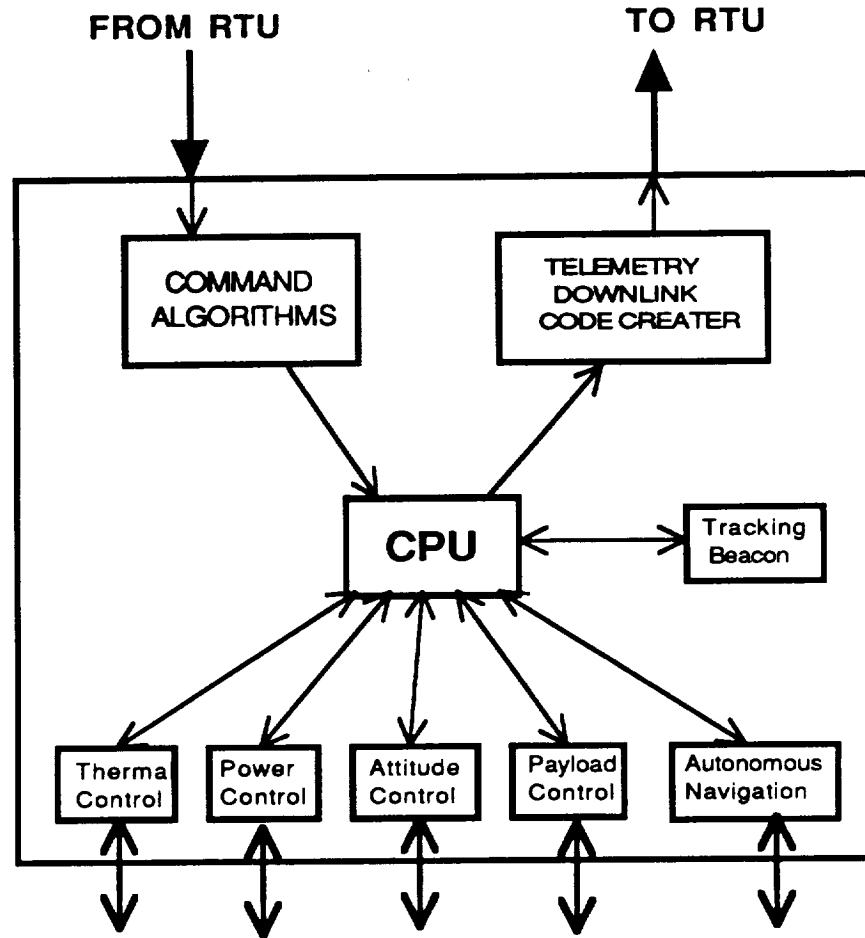


FIGURE 5.8 Remote Command Unit

Figure 5.8 shows a block diagram of the RCU. On the command side of the circuit, the signal comes from the RTU and goes through a processor that contains all the recognizable command algorithms. The signal will be compared to these algorithms and, when a match is found, the CPU executes the command. On the telemetry side of the circuit, data is gathered from all the sensors throughout the satellite (including the payload) and compiled into a telemetry downlink signal that is sent to the RTU.

The MPS bus has a GPS microreceiver onboard that operates with the GPS satellite system to triangulate the position of the receiver using a method known as Time Difference

of Arrival. If four GPS satellites are in view, the position of the satellite can be determined to as close as 50 ft. This means that a tracking beacon will not be necessary and the navigation of the satellite will be autonomous. One problem with GPS is that it is a downlooking satellite and is designed to link with ground based systems. A satellite system will have to lock onto the GPS satellites while they are pointed at the earth. The satellite will most likely be receiving lower powered side-lobes and will require a significant antenna gain in order to achieve the 34 dB C/N ratio that is required to receive analog data. If one GPS satellite can be tracked then a solution can be determined, but it may take some time. Also, MPS with an EHF payload will spend some time above the orbital altitude of GPS and, therefore, may not be able to provide navigation information while the satellite is above 20000 Km. The orbit determination will have to be done at lower altitudes.

In the event that the GPS receiver is not accurately predicting the position of the satellite, a tracking beacon in the RCU can be turned on with a command signal and manual range and range rate tracking can be accomplished. For manual tracking, the accuracy is ranging to 50 ft and range rate to .120 ft/sec. The tracking beacon is a pseudonoise code which is transmitted by the ground station, downconverted in the satellite, and retransmitted. It is anticipated that the GPS microreceiver will be reliable and the tracking beacon will remain in standby for most of the design life.

Table J.1 shows the link analysis data for the telemetry and command signals. For the EHF payload, the payload sends TT&C data through either the VBWA or two earth coverage feedhorns mounted on the earth face of the payload with the VBWA assembly as shown in Figure 2.3. One E/C feedhorn is sized for 1.763721 GHz and the other is sized for 2.2 GHz. If the variable beamwidth antenna fails, TT&C can be accomplished with the E/C antennas. The link margin at apogee for the E/C feedhorns is 6.31 dB on the uplink and 16.66 dB on the downlink. The link margin for the Variable Beamwidth Antennas is above 20 dB for almost all of the orbit.

For the AVHRR payload, the link analysis is shown in Table J.2 and is compatible with the TIROS-N earth station. The analysis shows that the satellite will have excess margin to close the link.

F. STRUCTURAL SUBSYSTEM

1. Functional Description

The spacecraft bus structure was designed to fit within the 46 inch diameter Pegasus shroud with two folding solar panels and to fit within the Taurus shroud with three. Pentagonal, hexagonal, and octagonal shapes for the bus were explored, but a rectangular design was chosen for simplicity and ease of assembly. The bus is built on a rectangular frame that is comprised of hollow rectangular cross-section tubing made from 6061-T6 aluminum. Fastened to this frame are five load supporting honeycomb panels with aluminum faceskins, one panel being the Anti-earth face. The sixth side of the spacecraft bus is the earth/payload face. The entire spacecraft is mounted to Pegasus with a standard Marmon clamp assembly. Total weight of the dry standard bus structure is 45 pounds for the AVHRR configuration and 59 pounds for the EHF configuration.

2. Requirements

The goal of modularity was balanced with the requirement to launch within 72 hours. This requirement to be launched within 72 hours severely limited the amount of modularity to interchanging the payload face and perhaps removing or adding very select equipment. Therefore, the panels are not removable and are permanently fastened to the frame. The frame and panel construction was designed to withstand Pegasus launch loads as depicted in Table 5.19.

Flight Mode	X (Roll) (g)	Y (Pitch) (g)	Z (Yaw) (g)
Captive Carry	+0.9	+0.822	+3.5
	-0.68	-0.922	-1.4
Powered Flight	+0	+0.5	+2.8
	-8.5	-0.5	-1.0

TABLE 5.19 Accelerations at Payload Interface

3. Summary of Subsystem Operations

a. Frame Construction

The rectangular frame is comprised of aluminum rectangular tubing. The frame is designed to withstand the axial and lateral loads of the Pegasus launch while the honeycomb panels are designed for equipment mounting only. The axial tubing has a cross sectional area of 1 1/2 x 2 inches O.D. and an average wall thickness of .125 inches. The lateral tubing has cross sectional dimensions of 1 x 1 1/2 O.D. with .125 inch thickness. The factor of safety used for both lateral and axial loads was 1.5. The axial tubing is oriented so the 2 inch length is parallel to the +Z direction. This is to maximize the area moment of inertia and to minimize deflection of the beam. A cross sectional view of an axial frame member is depicted in Figure 5.9

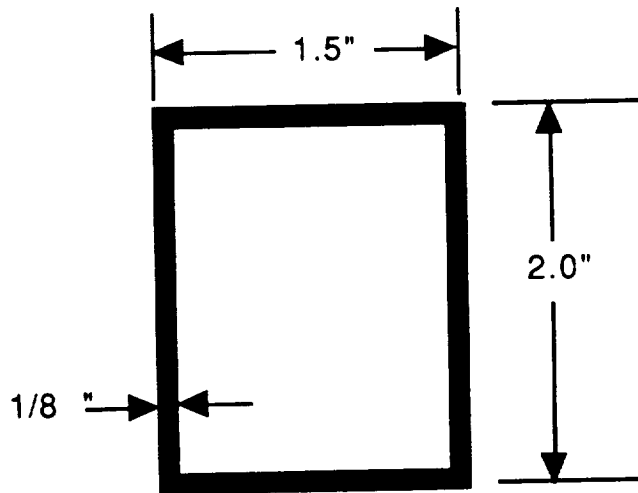


FIGURE 5.9 Cross-section of Tubular Frame

b. Honeycomb Panels

The 0.375 inch honeycomb panels with 0.004 inch faceskins are designed to meet design criteria for minimum natural frequency and for stress due to dynamic loads. The

primary purpose of the panel design is to be have the surface area to mount equipment. The honeycomb panels are not designed to absorb either the axial or lateral loads of launch. The honeycomb panels are simply supported along their four sides. A typical honeycomb panel is depicted in Figure 5.10.

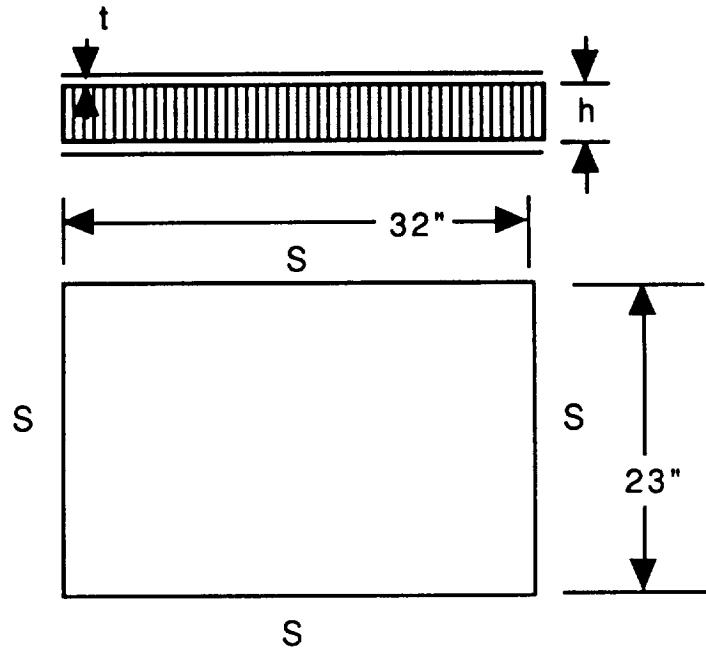


FIGURE 5.10 Typical Honeycomb Panel

c. Payload Mechanical Interface

For the separable payload interface, the MPS bus uses a slightly modified Orbital Science Corporation Marmon clamp design. The OSC design was modified to allow clearance for thrusters on the anti-earth face. The design still attaches directly to the Pegasus Stage 3 avionics deck, but the clearance between the avionics shelf and the payload attachment plane is increased from three to five inches. The design uses a standard bolt cutter separation system with four springs supplying an initial push-off force of 330 N (75 lbf). The Marmon clamp is depicted in Figure 5.11.

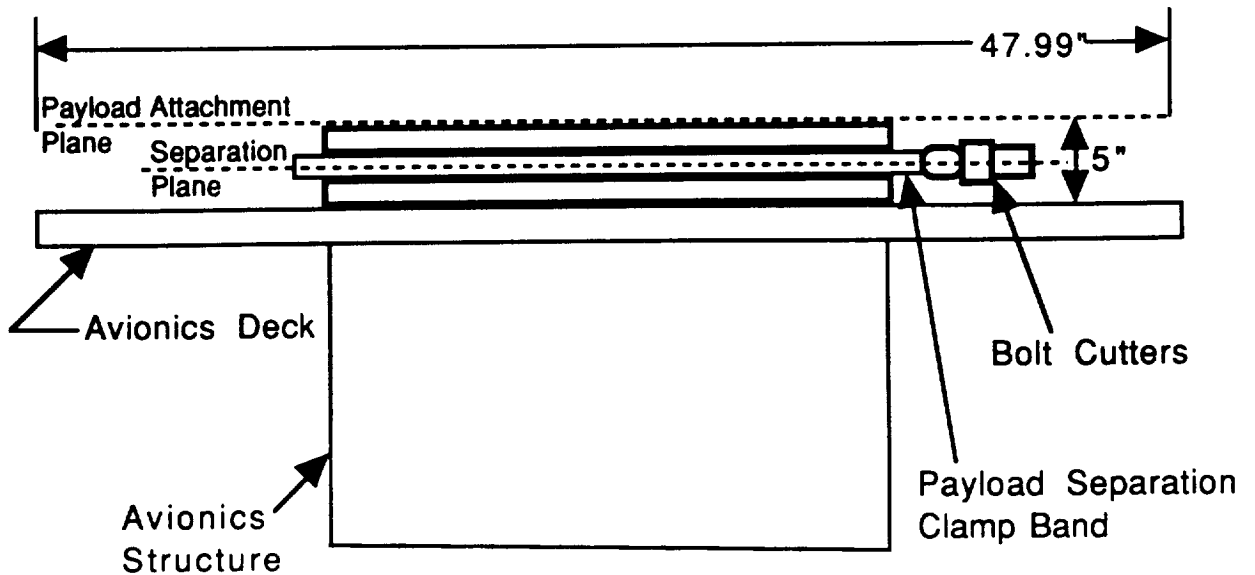


FIGURE 5.11 Marmon Clamp Design

d. Earth Face

The mass and structural requirements of this face are dependent of the payload chosen. The 62 lb AVHRR is affixed directly to a 1 inch honeycomb panel whereas the 85 lb EHF payload is supported by a 6" x 32" x 28" aluminum frame. The thickness of the aluminum face skin is .1 mm. The frame for the EHF configuration supports the EHF feedhorn assembly , the variable beam antenna, the EHF and TT&C R/Ts, and the Optical Solar Reflectors.

e. Fuel Tank Support

The fuel tank is supported at its base and by four structural members attached to a waistband. The base support affixes the fuel tank to the anti-earth face of the bus. It is a 22 inch diameter flat disc that transmits the axial force of the fuel tank during launch

directly to the Marmon clamp. The support members are 1 inch aluminum round tubing capable of supporting the lateral loads of launch.

4. Margins of Safety

The margins of safety for the frame/panel design are summarized in Table 5.20.

Component	Expected Max Load	Yield Load	Margin of Safety
Aluminum Frame	12,600 psi (compression)	37,000 psi	32
Aluminum Frame	900 psi (bending)	37,000 psi	1.9
Aluminum Frame	1,000 psi (shear)	30,000 psi	29
Honeycomb panel	20 g	37,000 psi	1.1
Honeycomb panel	11,406 psi (facing stress)	24,000 psi	1.1

TABLE 5.20 Margins of Safety

5. Detailed Mass Summary

The components of the structural subsystem are listed in Table 5.21. Figures listed with an asterisk are to be read AVHRR/ EHF

Component	Mass (kg)
Lateral Rectangular Tubing (8)	6.01
Axial Rectangular Tubing(4)	3.40
Honeycomb panels (5)	.85
Fuel tank waist band	.68
Fuel tank base	1.36
Fuel tank structural supports (4)	.73
Marmon clamp assembly	5.27
Earth Face	.18 / 6.61 *
Misc.Hardware	2.27
Total	20.75 / 27.13 *

TABLE 5.21 Mass Summary of Structural Subsystem

REFERENCES

Koczor, Ronald J., *Multispectral Sensing with the AVHRR*, ITT Aerospace/Optical Division, Fort Wayne, IN, Presented at the North American NOAA Polar Orbiters Users Group Meeting, Boulder, CO, July 14-16, 1987.

Owens, Larry; Cechowski, Donald; and Ames, Alan J., *Characteristics of the AVHRR/3 and HIRS/3 for NOAA-K,L,M*, ITT Aerospace/Optical Division, Fort Wayne, IN, Presented at the Fourth Conference on Satellite Meteorology and Oceanography, San Diego, May 16-19, 1989.

Thompson, W. David, Spectrum Research, Inc., *The Mini METSAT: A Small Low-Cost Advanced Technology Weather System*, Presented at the Third Annual AIAA/USU Conference on Small Satellites, Utah State University, Logan, UT, September 26-28, 1989.

Jackson, John H. and Wirtz, Harold G., *Theory and Problems of Statics and Strength of Materials*, McGraw-Hill, 1983.

Agrawal, Brij N., *Design of Geosynchronous Spacecraft*, Prentice-Hall, 1986.

Ha, Tri T., *Digital Satellite Communications*, New York, Macmillan, 1986.

Johnson, Richard C. and Jasik, Henry, *Antenna Engineering Handbook*, 2d Ed, New York, 1984

Tada, H. Y., et. al., *Solar Cell Radiation Handbook*, Third Edition, JPL Publication 82-69. November 1, 1982.

JPL and NASA, *Solar Cell Array Design Handbook*, Volumes 1 and 2., JPL Publication SP 43-38. October 1976.

Josefson, C. et. al., *Spacecraft Design Project; High Latitude Communications Satellite*, Naval Postgraduate School, December 1989.

National Oceanic and Atmospheric Administration Technical Report NESDIS, *Final Report On The Modulation And EMC Considerations For The HRPT Transmission System In The Post NOAA-M Polar Orbiting Satellite Era.*, U.S. Dept. of Commerce, Washington D.C., June 1989.

Hussey, W. John, *The Tiros-N/NOAA Operational Satellite System.*, U.S. Dept of Commerce, NOAA, Washington D.C., May 1979

Air Force Military Standard 1582, *Low Data Rate EHF Communication Standards*, 18 April, 1990

Space Systems Control Division, Space Flight Operations, *Air Force Satellite Control Facility Space/Ground Interface*, Aerospace Report No. TOR-0059(6110-01)-3 Reissue H., June 1987

APPENDIX A

ORBITAL DYNAMICS

Appendix A.1

Program SUN_ANGLE2

Listing and Sample Output



C Third Axis: Perpendicular to Ecliptic (+ "North")
 C Second Axis: Complete Right Hand Coordinate System
 C Principle Plane: Ecliptic
 C
 C System: Season (Denoted by "Season")
 C Origin: Center of Earth
 C Principle Axis: Sun vector projected into equatorial plane
 C Third Axis: Perpendicular to equator (North)
 C Second Axis: Complete Right Hand Coordinate System
 C Principle Plane: Equatorial plane
 C
 C System: Intermediate (Denoted by "I")
 C Origin: Center of Earth
 C Principle Axis: Intersection of S/C orbit plane and equator
 C (Ascending Node)
 C Third Axis: Perpendicular to equator (North)
 C Second Axis: Complete Right Hand Coordinate System
 C Principle Plane: Equatorial plane
 C
 C System: Orbit Normal (Denoted by "O")
 C Origin: Center of Earth
 C Principle Axis: Intersection of S/C orbit plane and equator
 C (Ascending Node)
 C Third Axis: Perpendicular to S/C orbit plane
 C Second Axis: Complete Right Hand Coordinate System such that
 C second axis is 90 deg from principle axis
 C measured in the direction of S/C motion
 C Principle Plane: S/C orbit plane
 C
 C System: Body (Denoted by "B")
 C Origin: Center of S/C
 C Principle Axis: Out S/C Top (Away from Earth) (Yaw)
 C Second Axis: Out S/C Front (Along velocity vector) (Roll)
 C Third Axis: Out S/C Left (Pitch)
 C Principle Plane: Local Horizontal
 C



EXTERNAL ANGLE
EXTERNAL DOT

CHARACTER*1 AGAIN

INTEGER I, POINTS, SEASON

REAL*8 ANGLE, DOT
 REAL*8 TILT, NEG TILT, DEG2RAD, RAD2DEG
 REAL*8 INCL, OMEGA
 REAL*8 SunS(4), SunSeason(4)
 REAL*8 LeftB(4), RightB(4), FrontB(4), RearB(4), TopB(4), BotB(4)
 REAL*8 SunLeft, SunRight
 REAL*8 SunFront(360), SunRear(360), SunTop(360), SunBot(360)
 REAL*8 SARotate(360), SunSA(360)
 REAL*8 THETA, Front, Rear, Top, Bot, SARot, SA

```
OPEN (UNIT = 8, FILE = 'Sun Angle2.Out', STATUS = 'NEW')
```

```
.....
```

```
C
```

```
C Useful Constants
```

```
C
```

```
C DEG2RAD: Conversion Factor from Degrees to Radians
```

```
C RAD2DEG: Conversion Factor from Radians to Degrees
```

```
C TILT: Tilt of Earth's spin axis wrt normal to the ecliptic
```

```
C NEG TILT: Negative of TILT
```

```
C
```

```
.....
```

```
DEG2RAD = PI / 180.0D0  
RAD2DEG = 180.0D0 / PI  
TILT = 23.5D0 * DEG2RAD  
NEG TILT = -1.0D0 * TILT
```

```
.....
```

```
C
```

```
C Get the input values
```

```
C Echo check them to the output file
```

```
C
```

```
.....
```

```
5 WRITE(*,*)'Orbit Inclination (deg)?'
```

```
READ(*,*) INCL
```

```
WRITE(*,*)'Orbit Longitude of the Ascending Node (deg)'
```

```
WRITE(*,*) ' on the first day of winter?'
```

```
READ(*,*) OMEGA
```

```
WRITE(*,*)'Number of points to evaluate in one orbit'
```

```
READ(*,*)POINTS
```

```
WRITE(8,1000)
```

```
WRITE(8,1020) INCL
```

```
WRITE(8,1030) OMEGA
```

```
WRITE(8,1040) POINTS
```

```
.....
```

```
C
```

```
C Convert the angles to radians
```

```
C
```

```
.....
```

```
INCL = INCL * DEG2RAD  
OMEGA = OMEGA * DEG2RAD
```

```
.....
```

```
C
```

```
C Write the header information to the output file
```

```
C
```

```
.....
```

```
WRITE(*,1090)
WRITE(8,1090)
```

```

C
C   Initialize the season counter
C

```

```
SEASON = 0
```

```

C
C   The next line begins the loop that cycles through the seasons
C   beginning with Winter
C

```

```
100 SEASON = SEASON + 1
    GO TO (1, 2, 3, 4), SEASON
1 CONTINUE
```

```

C
C   WINTER Calculations
C

```

```

C
C   Direction of the sun vector expressed in sun coordinates
C       SunS = (1)S1 + (0)S2 + (0)S3
C
C   Define the sun vector for the first day of Winter
C

```

```
SunS(1) = 1.0D0
SunS(2) = 0.0D0
SunS(3) = 0.0D0
CALL MAG(SunS)
CALL ROT2(SunS, NEG TILT, SunSeason)
GOTO 10
```

```
2 CONTINUE
```

```

C
C   SPRING Calculations
C

```

.....
C
C Direction of the sun vector expressed in sun coordinates
C SunS = (1)S1 + (0)S2 + (0)S3
C
C Define the sun vector for the first day of Spring
C
.....

SunS(1) = 1.0D0
SunS(2) = 0.0D0
SunS(3) = 0.0D0
CALL MAG(SunS)
CALL ROT1(SunS, NEG TILT, SunSeason)
GO TO 10

3 CONTINUE

.....
C
C SUMMER Calculations
C
.....

.....
C
C Direction of the sun vector expressed in sun coordinates
C SunS = (1)S1 + (0)S2 + (0)S3
C
C Define the sun vector for the first day of Summer
C
.....

SunS(1) = 1.0D0
SunS(2) = 0.0D0
SunS(3) = 0.0D0
CALL MAG(SunS)
CALL ROT2(SunS, TILT, SunSeason)
GO TO 10

4 CONTINUE

.....
C
C FALL Calculations
C
.....

.....
C
C Direction of the sun vector expressed in sun coordinates
C SunS = (1)S1 + (0)S2 + (0)S3
C
C Define the sun vector for the first day of Fall
C


```

C
C The sun angles to the other S/C faces vary with the location in
C the orbit. The next DO LOOP converts those angles at the various
C orbit locations to degrees before writing. The following angles
C are written to a table:
C
C THETA: Location of S/C in orbit measured in direction of S/C
C motion from the point where the S/C crosses the plane
C of the ecliptic in a northerly direction
C FRONT: Sun angle to the S/C front face
C REAR: Sun angle to the S/C rear face
C TOP: Sun angle to the S/C top face
C BOT: Sun angle to the S/C bottom face
C SAROT: Angle the solar arrays should rotate to maximize
C power output
C SA: Sun angle to the solar arrays after they have rotated
C

```

```

DO 40 I = 1, POINTS
  THETA = I * 360.0D0 / POINTS
  Front = SunFront(I) * RAD2DEG
  Rear = SunRear(I) * RAD2DEG
  Top = SunTop(I) * RAD2DEG
  Bot = SunBot(I) * RAD2DEG
  SARot = SARotate(I) * RAD2DEG
  SA = SunSA(I) * RAD2DEG
  WRITE(*,1080) I,THETA,Front,Rear,Top,Bot,SARot,SA
  WRITE(8,1080) I,THETA,Front,Rear,Top,Bot,SARot,SA

```

```

40 CONTINUE

```

```

C
C Check to see if the season just calculated was the last season
C for this case
C

```

```

IF (SEASON .NE. 4) THEN
  GO TO 100
ENDIF

```

```

C
C See if there is another case to run
C

```

```

WRITE(*,*) ' Do You have another case? Y/N'
READ(*,*) AGAIN
IF ( (AGAIN .EQ. "Y") .OR. (AGAIN .EQ. "y") ) THEN

```


.....

FrontB(1) = 0.0D0
FrontB(2) = 1.0D0
FrontB(3) = 0.0D0
CALL MAG(FrontB)

RearB(1) = 0.0D0
RearB(2) = -1.0D0
RearB(3) = 0.0D0
CALL MAG(RearB)

TopB(1) = 1.0D0
TopB(2) = 0.0D0
TopB(3) = 0.0D0
CALL MAG(TopB)

BotB(1) = -1.0D0
BotB(2) = 0.0D0
BotB(3) = 0.0D0
CALL MAG(BotB)

.....

C
C Rotate the spacecraft through one orbit to find the angles between
C the sun vector and the other spacecraft faces. The rotation begins
C at the ascending node. The rotation actually converts the sun
C vector from the orbit normal coordinate system to the body
C coordinate system.
C
C BETA: Location of the S/C measured from the ascending node
C FRONT: Angle between Sun Vector and the S/C's Front side
C REAR: Angle between Sun Vector and the S/C's Rear side
C TOP: Angle between Sun Vector and the S/C's Top side
C BOTTOM: Angle between Sun Vector and the S/C's Bottom side
C

.....

DO 10 I = 1, TRIALS
BETA = I * (2.0D0 * PI / TRIALS)
CALL ROT3(SunO, BETA, SunB)
FRONT(I) = ANGLE(SunB, FrontB)
REAR(I) = ANGLE(SunB, RearB)
TOP(I) = ANGLE(SunB, TopB)
BOTTOM(I) = ANGLE(SunB, BotB)

.....

C
C Find the vector normal to the plane containing
C the roll axis and the sun vector
C

.....

CALL CROSS(FRONTB, SunB, SVRAN)

~~~~~

C  
C  
C  
C  
C  
C  
C  
C  
C  
C  
C  
C  
C  
C  
C  
C  
C  
C  
C  
C  
C

The power output from the solar arrays is maximized when the vector normal to the solar arrays is in the same plane as the one defined by the sun vector and the S/C roll axis. Without any rotation, the solar array normal vector is parallel to the vector normal to the S/C left face. The angle the solar arrays should rotate to bring their normal vector into the plane containing the roll axis and the sun vector is complementary with the angle between the solar array normal vector and the vector normal to the plane containing the sun vector and the S/C roll axis.

Find the angle the solar arrays should rotate to maximize power output then rotate the solar arrays through that angle.

~~~~~

```
ROTATE(I) = PI / 2.0D0 - ANGLE(LeftB, SVRAN)
CALL ROT2(LEFTB, ROTATE(I), SANF)
```

~~~~~

C  
C  
C  
C  
C  
C  
C  
C  
C  
C  
C  
C  
C  
C  
C  
C  
C  
C  
C  
C  
C

If the solar array normal vector rotated in the correct direction, the vector will be in the same plane as the roll axis and the sun vector. If this is true, then the normal to that plane and the solar array normal vector are perpendicular. This can be verified by looking at their dot product. If the dot product isn't zero, the direction of rotation should be reversed. The code rechecks the dot product. If it still isn't equal to zero, there is an error somewhere. The code indicates this by assigning a value of 4\*pi radians. The user must recognize this value is he/she sees it in the output.

~~~~~

```
CHECK = DOT(SVRAN, SANF)
IF(DABS(CHECK) .GT. 0.01D0) THEN
  ROTATE(I) = -1.0D0 * ROTATE(I)
  CALL ROT2(LEFTB, ROTATE(I), SANF)
  CHECK = DOT(SVRAN, SANF)
  IF(DABS(CHECK) .GT. 0.01D0) THEN
    ROTATE(I) = 4.0D0 * PI
  ENDIF
ENDIF
ARRAY(I) = ANGLE(SANF, SunB)
10 CONTINUE
RETURN
END
```



```

C   fourth position
C
C   INPUT VARIABLES:
C
C   A: First vector in the vector cross product
C   B: Second vector in the vector cross product
C
C   OUTPUT VARIABLES:
C
C   C: Result of the vector cross product
C
C   LOCAL VARIABLES: NONE
C

```



```

REAL*8 A(4), B(4), C(4)
C(1) = A(2) * B(3) - A(3) * B(2)
C(2) = A(3) * B(1) - A(1) * B(3)
C(3) = A(1) * B(2) - A(2) * B(1)
CALL MAG(C)
RETURN
END

```

FUNCTION ANGLE (VECTA, VECTB)



```

C
C   AUTHOR: Gary E. Yale
C
C   DATE: Nov 90
C
C   OBJECTIVE: Find the angle between two vectors using the property
C   of the dot product (the angle is the inverse cosine of the dot
C   product divided by the product of their magnitudes)
C
C   SUPPORT MODULES: DOT
C
C           ////////// VARIABLE DEFINITIONS  //////////
C
C   All vectors have three components and their magnitude is in the
C   fourth position
C
C   INPUT VARIABLES:
C
C   VECTA: One of the vectors defining an angle
C   VECTB: Second vector defining an angle
C
C   OUTPUT VARIABLES:
C
C   ANGLE: The angle between the two vectors (rad)
C
C   LOCAL VARIABLES: NONE
C

```


98.750 Orbit Inclination (deg)
 37.500 Orbit Longitude of the Ascending Node (deg)
 on the first day of Winter
 72 Number of points to evaluate in one revolution

DEFINITIONS:

OrbAng: Angle between equator and S/C in orbital plane
SunFront: Sun Angle to S/C Front Side
SunRear: Sun Angle to S/C Rear Side
SunTop: Sun Angle to S/C Top Side
SunBot: Sun Angle to S/C Bottom Side
S/A Rotate: Angle S/A Should Rotate for min Sun Angle
SunSA: Sun Angle to Solar Array after Array Rotation

The following angles apply for WINTER

38.763 Sun Angle to S/C Left Side
 141.237 Sun Angle to S/C Right Side

Point	OrbAng	SunFront	SunRear	SunTop	SunBot	S/A Rotate	SunSA
1	5.000	103.515	76.485	125.510	54.490	36.683	13.515
2	10.000	100.497	79.503	126.799	53.201	37.532	10.497
3	15.000	97.428	82.572	127.778	52.222	38.155	7.428
4	20.000	94.324	85.676	128.429	51.571	38.559	4.324
5	25.000	91.200	88.800	128.737	51.263	38.747	1.200
6	30.000	88.070	91.930	128.696	51.304	38.722	1.930
7	35.000	84.949	95.051	128.307	51.693	38.484	5.051
8	40.000	81.852	98.148	127.578	52.422	38.029	8.148
9	45.000	78.794	101.206	126.525	53.475	37.354	11.206
10	50.000	75.790	104.210	125.168	54.832	36.452	14.210
11	55.000	72.858	107.142	123.531	56.469	35.314	17.142
12	60.000	70.016	109.984	121.641	58.359	33.932	19.984
13	65.000	67.283	112.717	119.525	60.475	32.294	22.717
14	70.000	64.681	115.319	117.212	62.788	30.389	25.319
15	75.000	62.232	117.768	114.725	65.275	28.210	27.768
16	80.000	59.962	120.038	112.090	67.910	25.748	30.038
17	85.000	57.897	122.103	109.330	70.670	23.002	32.103
18	90.000	56.064	123.936	106.465	73.535	19.976	33.936
19	95.000	54.490	125.510	103.515	76.485	16.684	35.510
20	100.000	53.201	126.799	100.497	79.503	13.151	36.799
21	105.000	52.222	127.778	97.428	82.572	9.414	37.778
22	110.000	51.571	128.429	94.324	85.676	5.523	38.429
23	115.000	51.263	128.737	91.200	88.800	1.538	38.737
24	120.000	51.304	128.696	88.070	91.930	-2.473	38.696
25	125.000	51.693	128.307	84.949	95.051	-6.442	38.307
26	130.000	52.422	127.578	81.852	98.148	-10.302	37.578
27	135.000	53.475	126.525	78.794	101.206	-13.995	36.525
28	140.000	54.832	125.168	75.790	104.210	-17.475	35.168
29	145.000	56.469	123.531	72.858	107.142	-20.706	33.531
30	150.000	58.359	121.641	70.016	109.984	-23.668	31.641
31	155.000	60.475	119.525	67.283	112.717	-26.348	29.525
32	160.000	62.788	117.212	64.681	115.319	-28.743	27.212

33	165.000	65.275	114.725	62.232	117.768	-30.858	24.725
34	170.000	67.910	112.090	59.962	120.038	-32.699	22.090
35	175.000	70.670	109.330	57.897	122.103	-34.277	19.330
36	180.000	73.535	106.465	56.064	123.936	-35.601	16.465
37	185.000	76.485	103.515	54.490	125.510	-36.683	13.515
38	190.000	79.503	100.497	53.201	126.799	-37.532	10.497
39	195.000	82.572	97.428	52.222	127.778	-38.155	7.428
40	200.000	85.676	94.324	51.571	128.429	-38.559	4.324
41	205.000	88.800	91.200	51.263	128.737	-38.747	1.200
42	210.000	91.930	88.070	51.304	128.696	-38.722	1.930
43	215.000	95.051	84.949	51.693	128.307	-38.484	5.051
44	220.000	98.148	81.852	52.422	127.578	-38.029	8.148
45	225.000	101.206	78.794	53.475	126.525	-37.354	11.206
46	230.000	104.210	75.790	54.832	125.168	-36.452	14.210
47	235.000	107.142	72.858	56.469	123.531	-35.314	17.142
48	240.000	109.984	70.016	58.359	121.641	-33.932	19.984
49	245.000	112.717	67.283	60.475	119.525	-32.294	22.717
50	250.000	115.319	64.681	62.788	117.212	-30.389	25.319
51	255.000	117.768	62.232	65.275	114.725	-28.210	27.768
52	260.000	120.038	59.962	67.910	112.090	-25.748	30.038
53	265.000	122.103	57.897	70.670	109.330	-23.002	32.103
54	270.000	123.936	56.064	73.535	106.465	-19.976	33.936
55	275.000	125.510	54.490	76.485	103.515	-16.684	35.510
56	280.000	126.799	53.201	79.503	100.497	-13.151	36.799
57	285.000	127.778	52.222	82.572	97.428	-9.414	37.778
58	290.000	128.429	51.571	85.676	94.324	-5.523	38.429
59	295.000	128.737	51.263	88.800	91.200	-1.538	38.737
60	300.000	128.696	51.304	91.930	88.070	2.473	38.696
61	305.000	128.307	51.693	95.051	84.949	6.442	38.307
62	310.000	127.578	52.422	98.148	81.852	10.302	37.578
63	315.000	126.525	53.475	101.206	78.794	13.995	36.525
64	320.000	125.168	54.832	104.210	75.790	17.475	35.168
65	325.000	123.531	56.469	107.142	72.858	20.706	33.531
66	330.000	121.641	58.359	109.984	70.016	23.668	31.641
67	335.000	119.525	60.475	112.717	67.283	26.348	29.525
68	340.000	117.212	62.788	115.319	64.681	28.743	27.212
69	345.000	114.725	65.275	117.768	62.232	30.858	24.725
70	350.000	112.090	67.910	120.038	59.962	32.699	22.090
71	355.000	109.330	70.670	122.103	57.897	34.277	19.330
72	360.000	106.465	73.535	123.936	56.064	35.601	16.465

The following angles apply for SPRING

38.361 Sun Angle to S/C Left Side
 141.639 Sun Angle to S/C Right Side

Point	OrbAng	SunFront	SunRear	SunTop	SunBot	S/A Rotate	SunSA
1	5.000	80.021	99.979	126.579	53.421	37.235	9.979
2	10.000	77.023	102.977	125.349	54.651	36.421	12.977
3	15.000	74.090	105.910	123.834	56.166	35.378	15.910
4	20.000	71.239	108.761	122.058	57.942	34.094	18.761
5	25.000	68.491	111.509	120.048	59.952	32.561	21.509
6	30.000	65.864	114.136	117.831	62.169	30.769	24.136
7	35.000	63.382	116.618	115.432	64.568	28.709	26.618
8	40.000	61.069	118.931	112.877	67.123	26.372	28.931
9	45.000	58.949	121.051	110.189	69.811	23.756	31.051
10	50.000	57.049	122.951	107.389	72.611	20.863	32.951
11	55.000	55.397	124.603	104.496	75.504	17.704	34.603
12	60.000	54.017	125.983	101.529	78.471	14.299	35.983
13	65.000	52.934	127.066	98.505	81.495	10.681	37.066
14	70.000	52.170	127.830	95.440	84.560	6.894	37.830
15	75.000	51.738	128.262	92.349	87.651	2.992	38.262
16	80.000	51.650	128.350	89.247	90.753	-0.960	38.350
17	85.000	51.905	128.095	86.148	93.852	-4.896	38.095
18	90.000	52.500	127.500	83.068	96.932	-8.750	37.500
19	95.000	53.421	126.579	80.021	99.979	-12.462	36.579
20	100.000	54.651	125.349	77.023	102.977	-15.981	35.349
21	105.000	56.166	123.834	74.090	105.910	-19.270	33.834
22	110.000	57.942	122.058	71.239	108.761	-22.302	32.058
23	115.000	59.952	120.048	68.491	111.509	-25.061	30.048
24	120.000	62.169	117.831	65.864	114.136	-27.541	27.831
25	125.000	64.568	115.432	63.382	116.618	-29.743	25.432
26	130.000	67.123	112.877	61.069	118.931	-31.672	22.877
27	135.000	69.811	110.189	58.949	121.051	-33.337	20.189
28	140.000	72.611	107.389	57.049	122.951	-34.748	17.389
29	145.000	75.504	104.496	55.397	124.603	-35.914	14.496
30	150.000	78.471	101.529	54.017	125.983	-36.844	11.529
31	155.000	81.495	98.505	52.934	127.066	-37.548	8.505
32	160.000	84.560	95.440	52.170	127.830	-38.032	5.440
33	165.000	87.651	92.349	51.738	128.262	-38.300	2.349
34	170.000	90.753	89.247	51.650	128.350	-38.354	0.753
35	175.000	93.852	86.148	51.905	128.095	-38.196	3.852
36	180.000	96.932	83.068	52.500	127.500	-37.824	6.932
37	185.000	99.979	80.021	53.421	126.579	-37.235	9.979
38	190.000	102.977	77.023	54.651	125.349	-36.421	12.977
39	195.000	105.910	74.090	56.166	123.834	-35.378	15.910
40	200.000	108.761	71.239	57.942	122.058	-34.094	18.761
41	205.000	111.509	68.491	59.952	120.048	-32.561	21.509
42	210.000	114.136	65.864	62.169	117.831	-30.769	24.136
43	215.000	116.618	63.382	64.568	115.432	-28.709	26.618
44	220.000	118.931	61.069	67.123	112.877	-26.372	28.931
45	225.000	121.051	58.949	69.811	110.189	-23.756	31.051
46	230.000	122.951	57.049	72.611	107.389	-20.863	32.951
47	235.000	124.603	55.397	75.504	104.496	-17.704	34.603
48	240.000	125.983	54.017	78.471	101.529	-14.299	35.983

49	245.000	127.066	52.934	81.495	98.505	-10.681	37.066
50	250.000	127.830	52.170	84.560	95.440	-6.894	37.830
51	255.000	128.262	51.738	87.651	92.349	-2.992	38.262
52	260.000	128.350	51.650	90.753	89.247	0.960	38.350
53	265.000	128.095	51.905	93.852	86.148	4.896	38.095
54	270.000	127.500	52.500	96.932	83.068	8.750	37.500
55	275.000	126.579	53.421	99.979	80.021	12.462	36.579
56	280.000	125.349	54.651	102.977	77.023	15.981	35.349
57	285.000	123.834	56.166	105.910	74.090	19.270	33.834
58	290.000	122.058	57.942	108.761	71.239	22.302	32.058
59	295.000	120.048	59.952	111.509	68.491	25.061	30.048
60	300.000	117.831	62.169	114.136	65.864	27.541	27.831
61	305.000	115.432	64.568	116.618	63.382	29.743	25.432
62	310.000	112.877	67.123	118.931	61.069	31.672	22.877
63	315.000	110.189	69.811	121.051	58.949	33.337	20.189
64	320.000	107.389	72.611	122.951	57.049	34.748	17.389
65	325.000	104.496	75.504	124.603	55.397	35.914	14.496
66	330.000	101.529	78.471	125.983	54.017	36.844	11.529
67	335.000	98.505	81.495	127.066	52.934	37.548	8.505
68	340.000	95.440	84.560	127.830	52.170	38.032	5.440
69	345.000	92.349	87.651	128.262	51.738	38.300	2.349
70	350.000	89.247	90.753	128.350	51.650	38.354	0.753
71	355.000	86.148	93.852	128.095	51.905	38.196	3.852
72	360.000	83.068	96.932	127.500	52.500	37.824	6.932

The following angles apply for SUMMER

48.820 Sun Angle to S/C Left Side
131.180 Sun Angle to S/C Right Side

Point	OrbAng	SunFront	SunRear	SunTop	SunBot	S/A Rotate	SunSA
1	5.000	56.529	123.471	120.807	59.193	37.877	33.471
2	10.000	53.554	126.446	117.525	62.475	35.064	36.446
3	15.000	50.796	129.204	114.117	65.883	31.823	39.204
4	20.000	48.296	131.704	110.607	69.393	28.126	41.704
5	25.000	46.098	133.902	107.016	72.984	23.962	43.902
6	30.000	44.251	135.749	103.361	76.639	19.339	45.749
7	35.000	42.802	137.198	99.658	80.342	14.295	47.198
8	40.000	41.795	138.205	95.923	84.077	8.907	48.205
9	45.000	41.263	138.737	92.167	87.833	3.287	48.737
10	50.000	41.225	138.775	88.405	91.595	-2.421	48.775
11	55.000	41.682	138.318	84.647	95.353	-8.064	48.318
12	60.000	42.619	137.381	80.908	99.092	-13.496	47.381
13	65.000	44.004	135.996	77.200	102.800	-18.598	45.996
14	70.000	45.793	134.207	73.537	106.463	-23.288	44.207
15	75.000	47.941	132.059	69.934	110.066	-27.523	42.059
16	80.000	50.398	129.602	66.411	113.589	-31.290	39.602
17	85.000	53.120	126.880	62.986	117.014	-34.599	36.880
18	90.000	56.064	123.936	59.683	120.317	-37.476	33.936
19	95.000	59.193	120.807	56.529	123.471	-39.951	30.807
20	100.000	62.475	117.525	53.554	126.446	-42.058	27.525
21	105.000	65.883	114.117	50.796	129.204	-43.830	24.117

22	110.000	69.393	110.607	48.296	131.704	-45.297	20.607
23	115.000	72.984	107.016	46.098	133.902	-46.483	17.016
24	120.000	76.639	103.361	44.251	135.749	-47.410	13.361
25	125.000	80.342	99.658	42.802	137.198	-48.095	9.658
26	130.000	84.077	95.923	41.795	138.205	-48.550	5.923
27	135.000	87.833	92.167	41.263	138.737	-48.784	2.167
28	140.000	91.595	88.405	41.225	138.775	-48.801	1.595
29	145.000	95.353	84.647	41.682	138.318	-48.600	5.353
30	150.000	99.092	80.908	42.619	137.381	-48.179	9.092
31	155.000	102.800	77.200	44.004	135.996	-47.530	12.800
32	160.000	106.463	73.537	45.793	134.207	-46.640	16.463
33	165.000	110.066	69.934	47.941	132.059	-45.495	20.066
34	170.000	113.589	66.411	50.398	129.602	-44.072	23.589
35	175.000	117.014	62.986	53.120	126.880	-42.349	27.014
36	180.000	120.317	59.683	56.064	123.936	-40.294	30.317
37	185.000	123.471	56.529	59.193	120.807	-37.877	33.471
38	190.000	126.446	53.554	62.475	117.525	-35.064	36.446
39	195.000	129.204	50.796	65.883	114.117	-31.823	39.204
40	200.000	131.704	48.296	69.393	110.607	-28.126	41.704
41	205.000	133.902	46.098	72.984	107.016	-23.962	43.902
42	210.000	135.749	44.251	76.639	103.361	-19.339	45.749
43	215.000	137.198	42.802	80.342	99.658	-14.295	47.198
44	220.000	138.205	41.795	84.077	95.923	-8.907	48.205
45	225.000	138.737	41.263	87.833	92.167	-3.287	48.737
46	230.000	138.775	41.225	91.595	88.405	2.421	48.775
47	235.000	138.318	41.682	95.353	84.647	8.064	48.318
48	240.000	137.381	42.619	99.092	80.908	13.496	47.381
49	245.000	135.996	44.004	102.800	77.200	18.598	45.996
50	250.000	134.207	45.793	106.463	73.537	23.288	44.207
51	255.000	132.059	47.941	110.066	69.934	27.523	42.059
52	260.000	129.602	50.398	113.589	66.411	31.290	39.602
53	265.000	126.880	53.120	117.014	62.986	34.599	36.880
54	270.000	123.936	56.064	120.317	59.683	37.476	33.936
55	275.000	120.807	59.193	123.471	56.529	39.951	30.807
56	280.000	117.525	62.475	126.446	53.554	42.058	27.525
57	285.000	114.117	65.883	129.204	50.796	43.830	24.117
58	290.000	110.607	69.393	131.704	48.296	45.297	20.607
59	295.000	107.016	72.984	133.902	46.098	46.483	17.016
60	300.000	103.361	76.639	135.749	44.251	47.410	13.361
61	305.000	99.658	80.342	137.198	42.802	48.095	9.658
62	310.000	95.923	84.077	138.205	41.795	48.550	5.923
63	315.000	92.167	87.833	138.737	41.263	48.784	2.167
64	320.000	88.405	91.595	138.775	41.225	48.801	1.595
65	325.000	84.647	95.353	138.318	41.682	48.600	5.353
66	330.000	80.908	99.092	137.381	42.619	48.179	9.092
67	335.000	77.200	102.800	135.996	44.004	47.530	12.800
68	340.000	73.537	106.463	134.207	45.793	46.640	16.463
69	345.000	69.934	110.066	132.059	47.941	45.495	20.066
70	350.000	66.411	113.589	129.602	50.398	44.072	23.589
71	355.000	62.986	117.014	126.880	53.120	42.349	27.014
72	360.000	59.683	120.317	123.936	56.064	40.294	30.317

The following angles apply for FALL

38.361 Sun Angle to S/C Left Side
 141.639 Sun Angle to S/C Right Side

Point	OrbAng	SunFront	SunRear	SunTop	SunBot	S/A Rotate	SunSA
1	5.000	80.021	99.979	126.579	53.421	37.235	9.979
2	10.000	77.023	102.977	125.349	54.651	36.421	12.977
3	15.000	74.090	105.910	123.834	56.166	35.378	15.910
4	20.000	71.239	108.761	122.058	57.942	34.094	18.761
5	25.000	68.491	111.509	120.048	59.952	32.561	21.509
6	30.000	65.864	114.136	117.831	62.169	30.769	24.136
7	35.000	63.382	116.618	115.432	64.568	28.709	26.618
8	40.000	61.069	118.931	112.877	67.123	26.372	28.931
9	45.000	58.949	121.051	110.189	69.811	23.756	31.051
10	50.000	57.049	122.951	107.389	72.611	20.863	32.951
11	55.000	55.397	124.603	104.496	75.504	17.704	34.603
12	60.000	54.017	125.983	101.529	78.471	14.299	35.983
13	65.000	52.934	127.066	98.505	81.495	10.681	37.066
14	70.000	52.170	127.830	95.440	84.560	6.894	37.830
15	75.000	51.738	128.262	92.349	87.651	2.992	38.262
16	80.000	51.650	128.350	89.247	90.753	-0.960	38.350
17	85.000	51.905	128.095	86.148	93.852	-4.896	38.095
18	90.000	52.500	127.500	83.068	96.932	-8.750	37.500
19	95.000	53.421	126.579	80.021	99.979	-12.462	36.579
20	100.000	54.651	125.349	77.023	102.977	-15.981	35.349
21	105.000	56.166	123.834	74.090	105.910	-19.270	33.834
22	110.000	57.942	122.058	71.239	108.761	-22.302	32.058
23	115.000	59.952	120.048	68.491	111.509	-25.061	30.048
24	120.000	62.169	117.831	65.864	114.136	-27.541	27.831
25	125.000	64.568	115.432	63.382	116.618	-29.743	25.432
26	130.000	67.123	112.877	61.069	118.931	-31.672	22.877
27	135.000	69.811	110.189	58.949	121.051	-33.337	20.189
28	140.000	72.611	107.389	57.049	122.951	-34.748	17.389
29	145.000	75.504	104.496	55.397	124.603	-35.914	14.496
30	150.000	78.471	101.529	54.017	125.983	-36.844	11.529
31	155.000	81.495	98.505	52.934	127.066	-37.548	8.505
32	160.000	84.560	95.440	52.170	127.830	-38.032	5.440
33	165.000	87.651	92.349	51.738	128.262	-38.300	2.349
34	170.000	90.753	89.247	51.650	128.350	-38.354	0.753
35	175.000	93.852	86.148	51.905	128.095	-38.196	3.852
36	180.000	96.932	83.068	52.500	127.500	-37.824	6.932
37	185.000	99.979	80.021	53.421	126.579	-37.235	9.979
38	190.000	102.977	77.023	54.651	125.349	-36.421	12.977
39	195.000	105.910	74.090	56.166	123.834	-35.378	15.910
40	200.000	108.761	71.239	57.942	122.058	-34.094	18.761
41	205.000	111.509	68.491	59.952	120.048	-32.561	21.509
42	210.000	114.136	65.864	62.169	117.831	-30.769	24.136
43	215.000	116.618	63.382	64.568	115.432	-28.709	26.618
44	220.000	118.931	61.069	67.123	112.877	-26.372	28.931
45	225.000	121.051	58.949	69.811	110.189	-23.756	31.051
46	230.000	122.951	57.049	72.611	107.389	-20.863	32.951
47	235.000	124.603	55.397	75.504	104.496	-17.704	34.603
48	240.000	125.983	54.017	78.471	101.529	-14.299	35.983

49	245.000	127.066	52.934	81.495	98.505	-10.681	37.066
50	250.000	127.830	52.170	84.560	95.440	-6.894	37.830
51	255.000	128.262	51.738	87.651	92.349	-2.992	38.262
52	260.000	128.350	51.650	90.753	89.247	0.960	38.350
53	265.000	128.095	51.905	93.852	86.148	4.896	38.095
54	270.000	127.500	52.500	96.932	83.068	8.750	37.500
55	275.000	126.579	53.421	99.979	80.021	12.462	36.579
56	280.000	125.349	54.651	102.977	77.023	15.981	35.349
57	285.000	123.834	56.166	105.910	74.090	19.270	33.834
58	290.000	122.058	57.942	108.761	71.239	22.302	32.058
59	295.000	120.048	59.952	111.509	68.491	25.061	30.048
60	300.000	117.831	62.169	114.136	65.864	27.541	27.831
61	305.000	115.432	64.568	116.618	63.382	29.743	25.432
62	310.000	112.877	67.123	118.931	61.069	31.672	22.877
63	315.000	110.189	69.811	121.051	58.949	33.337	20.189
64	320.000	107.389	72.611	122.951	57.049	34.748	17.389
65	325.000	104.496	75.504	124.603	55.397	35.914	14.496
66	330.000	101.529	78.471	125.983	54.017	36.844	11.529
67	335.000	98.505	81.495	127.066	52.934	37.548	8.505
68	340.000	95.440	84.560	127.830	52.170	38.032	5.440
69	345.000	92.349	87.651	128.262	51.738	38.300	2.349
70	350.000	89.247	90.753	128.350	51.650	38.354	0.753
71	355.000	86.148	93.852	128.095	51.905	38.196	3.852
72	360.000	83.068	96.932	127.500	52.500	37.824	6.932

Appendix A.2

Program SUN_ANGLE3 Listing and Sample Output

C PHI: Angle between S/C position vector and sun vector
C RPERP: Component of S/C position vector perpendicular to sun
C vector

C COORDINATE SYSTEMS:

C System: Sun (Denoted by "S")
C Origin: Center of Earth
C Principle Axis: Directly at sun
C Second Axis: Complete Right Hand Coordinate System
C Third Axis: Perpendicular to Ecliptic (+ "North")
C Principle Plane: Ecliptic

C System: Sun (Denoted by "1")
C Origin: Center of Earth
C Principle Axis: Intersection of Ecliptic and Equator (where one
C dips below ecliptic when traveling eastward
C along equator
C Second Axis: Complete Right Hand Coordinate System
C Third Axis: Perpendicular to Ecliptic (+ "North")
C Principle Plane: Ecliptic

C System: Sun (Denoted by "2")
C Origin: Center of Earth
C Principle Axis: Intersection of Ecliptic and Equator (where one
C dips below ecliptic when traveling eastward
C along equator
C Second Axis: Along North Pole
C Third Axis: Complete Right Hand Coordinate System
C Principle Plane: Contains earth's spin axis and the intersection
C of the ecliptic plane with the equatorial plane

C System: Sun (Denoted by "3")
C Origin: Center of Earth
C Principle Axis: Ascending Node
C Second Axis: Along North Pole
C Third Axis: Complete Right Hand Coordinate System
C Principle Plane: Contains earth's spin axis and the ascending node

C System: Sun (Denoted by "4")
C Origin: Center of Earth
C Principle Axis: Ascending Node
C Second Axis: Complete Right Hand Coordinate System
C Third Axis: Perpendicular to S/C Orbital Plane (along orbit
C angular momentum vector)
C Principle Plane: S/C orbit plane

C System: Body (Denoted by "B")
C Origin: Center of S/C
C Principle Axis: Out S/C Top (Away from Earth) (Yaw)
C Second Axis: Out S/C Front (Along velocity vector) (Roll)
C Third Axis: Out S/C Left (Pitch)
C Principle Plane: Local Horizontal
C

C Echo check input values to output file and screen

C

.....

```
WRITE(8,1000)
WRITE(8,1010) ALT
WRITE(8,1020) INCL
WRITE(8,1030) OMEGA
WRITE(8,1040) POINTS
WRITE(8,1050) ORBTRIALS
```

.....

C

C Convert units

C

.....

```
ALT = ALT * NM2KM
INCL = INCL * DEG2RAD
OMEGA = OMEGA * DEG2RAD
```

.....

C

C Initialize the S/C position vector.

C Express it in body coordinates.

C

.....

```
R(1) = RE + ALT
R(2) = 0.0D0
R(3) = 0.0D0
CALL MAG(R)
```

.....

C

C Calculate the orbital period (min) and angular velocity (rad/min)

C

.....

```
PERIOD = (2.0D0 * PI / 60.0D0) * SQRT( R(4)**3 / MU)
OrbRate = 2.0D0 * PI / PERIOD
```

.....

C

C Initialize the vector normal to S/C left face

C

.....

```
LeftB(1) = 0.0D0
LeftB(2) = 0.0D0
LeftB(3) = 1.0D0
CALL MAG(LeftB)
```

.....


```

C
C The vector out the S/C left face remains in the same inertial
C direction as the S/C moves in its orbit. Once the sun vector
C is expressed in the "4" coordinate system, it can be compared to
C the vector out the left face. The angle between these two vectors
C is the sun angle on the S/C left face for this earth location.
C

```

```

SUNLEFT(I) = ANGLE(SUN4, LEFTB)
BETA = STEP * I

```

```

C
C Initialize Eclipse markers and counters for this earth location
C

```

```

BEGECL = 0.0D0
ENDECL = 0.0D0
LASTECL = 'N'
ECLBEG = 'N'
ECLEND = 'N'
ANYECL = 'N'
SAVEND = 'N'

```

```

C
C Begin the loop that advances the S/C in its orbit around earth
C

```

```

DO 20 J = 1,ORBTRIALS

```

```

C
C Express the sun vector in body coordinates for this S/C location.
C

```

```

INCREM = J * (2.0D0 * PI / ORBTRIALS)
CALL ROT3(SUN4, INCREM, SUNB)

```

```

C
C In order for the S/C to be in eclipse, it must be:
C 1) over the dark side of the earth
C and 2) in the earth's shadow
C

```

```

C
C   Find the angle between the sun vector and the S/C position vector.
C
C

```

$$PHI = ANGLE(R, SUNB)$$

```

C
C

```

```

C   Is the S/C over the dark side of the earth?
C       Yes if Phi is greater than 90 degrees
C       No if Phi is less than 90 degrees
C
C

```

```

IF (PHI .GT. PI/2.0D0) THEN

```

```

C
C

```

```

C   Find the component of S/C position perpendicular to sun vector.
C
C

```

$$RPERP = R(4) * DSIN(PHI)$$

```

C
C

```

```

C   Is the S/C in the earth's shadow?
C       Yes if RPerp is less than or equal to the radius of the earth
C       No if RPerp is greater than the radius of the earth
C
C

```

```

IF(RPERP .LE. RE) THEN

```

```

C
C

```

```

C   The remaining logic in this DO Loop, updates the appropriate
C   eclipse markers and counters to determine the start and stop
C   locations of the eclipse.
C
C

```

```

IF (LASTECL .EQ. 'Y') THEN
  IF (SAVEND .EQ. 'N') THEN
    ECLEND = 'Y'
    ENDECL = J
  ENDIF
ELSE
  IF (ANYECL .EQ. 'N') THEN
    ANYECL = 'Y'
    ECLEND = 'Y'
    ENDECL = J
  ENDIF

```



```

C
C   Return to outer DO LOOP (advance earth in orbit around sun)
C

```

```

40 CONTINUE

```

```

1000 FORMAT(///)
1010 FORMAT(15X,F7.3,' Orbit Altitude (nm)')
1020 FORMAT(15X,F7.3,' Orbit Inclination (deg)')
1030 FORMAT(15X,F7.3,' Orbit Longitude of the Ascending Node (deg) ',
+         14X,' on the first day of Winter')
1040 FORMAT(15X,I7,' Number of points to evaluate in one year')
1050 FORMAT(15X,I7,' Number of points to evaluate in one S/C orbit') 1070
    FORMAT(/,15X,'Point OrbAng SunLeft Eclipse (min)',
+         ' Entry (deg) Exit (deg)')
1080 FORMAT(15X,I4,3F10.3,7X,F10.3,F11.3)
END

```

```

SUBROUTINE ROT1(VIN, T, VOUT)

```

```

C
C   AUTHOR: Gary E. Yale
C
C   DATE: Nov 90
C
C   OBJECTIVE: Expresses a vector in a coordinate system which is
C               rotated T radians around the first axis as compared to the
C               original coordinate system
C
C   SUPPORT MODULES: MAG
C
C               ////////// VARIABLE DEFINITIONS //////////
C
C   All vectors have three components and their magnitude is in the
C   fourth position
C
C   INPUT VARIABLES:
C
C   VIN: Input vector
C   T:   Angle of rotation (rad)
C
C
C   OUTPUT VARIABLES:
C
C   VOUT: Output vector
C

```

```

C LOCAL VARIABLES:
C
C C: Cosine of the input angle, T
C S: Sine of the input angle, T
C TEMP: Temporary storage location
C

```

```

Ooooooooooooooooooooooooooooooooooooooooooooooooooooooooooooooooooooo

```

```

REAL*8 VIN(4), T, VOUT(4)
REAL*8 C, S, TEMP
TEMP = VIN(3)
C = DCOS(T)
S = DSIN(T)
VOUT(3) = C * VIN(3) - S * VIN(2)
VOUT(2) = C * VIN(2) + S * TEMP
VOUT(1) = VIN(1)
CALL MAG(VOUT)
RETURN
END

```

```

SUBROUTINE ROT2(VIN, T, VOUT)

```

```

Ooooooooooooooooooooooooooooooooooooooooooooooooooooooooooooooooooooo

```

```

C
C AUTHOR: Gary E. Yale
C
C DATE: Nov 90
C
C OBJECTIVE: Expresses a vector in a coordinate system which is
C rotated T radians around the second axis as compared to the
C original coordinate system
C
C SUPPORT MODULES: MAG
C
C ////////////// VARIABLE DEFINITIONS //////////////
C
C All vectors have three components and their magnitude is in the
C fourth position
C
C INPUT VARIABLES:
C
C VIN: Input vector
C T: Angle of rotation (rad)
C
C OUTPUT VARIABLES:
C
C VOUT: Output vector
C
C LOCAL VARIABLES:

```


450.000 Orbit Altitude (nm)
 98.750 Orbit Inclination (deg)
 37.500 Orbit Longitude of the Ascending Node (deg)
 on the first day of Winter
 72 Number of points to evaluate in one year
 360 Number of points to evaluate in one S/C orbit

Point	OrbAng	SunLeft	Eclipse (min)
1	5.000	38.340	23.137
2	10.000	37.878	22.573
3	15.000	37.391	22.009
4	20.000	36.895	21.726
5	25.000	36.410	21.444
6	30.000	35.954	20.598
7	35.000	35.549	20.316
8	40.000	35.215	20.034
9	45.000	34.971	19.751
10	50.000	34.834	19.469
11	55.000	34.819	19.469
12	60.000	34.935	19.751
13	65.000	35.189	20.034
14	70.000	35.581	20.316
15	75.000	36.105	20.880
16	80.000	36.753	21.444
17	85.000	37.510	22.291
18	90.000	38.361	23.137
19	95.000	39.285	23.702
20	100.000	40.262	24.266
21	105.000	41.272	25.112
22	110.000	42.292	25.959
23	115.000	43.302	26.241
24	120.000	44.281	26.805
25	125.000	45.212	27.370
26	130.000	46.077	27.934
27	135.000	46.862	27.934
28	140.000	47.552	28.216
29	145.000	48.138	28.498
30	150.000	48.608	28.781
31	155.000	48.958	29.063
32	160.000	49.182	29.063
33	165.000	49.279	29.063
34	170.000	49.249	29.063
35	175.000	49.094	29.063
36	180.000	48.820	28.781
37	185.000	48.434	28.781
38	190.000	47.945	28.498
39	195.000	47.365	28.216
40	200.000	46.707	27.934
41	205.000	45.986	27.652
42	210.000	45.217	27.370
43	215.000	44.419	27.088
44	220.000	43.609	26.241
45	225.000	42.806	25.959
46	230.000	42.027	25.395

47	235.000	41.290	25.112
48	240.000	40.612	24.548
49	245.000	40.006	24.266
50	250.000	39.484	23.702
51	255.000	39.055	23.702
52	260.000	38.725	23.419
53	265.000	38.494	22.855
54	270.000	38.361	23.137
55	275.000	38.318	23.137
56	280.000	38.357	22.855
57	285.000	38.465	22.855
58	290.000	38.628	23.137
59	295.000	38.829	23.419
60	300.000	39.051	23.419
61	305.000	39.279	23.702
62	310.000	39.496	23.984
63	315.000	39.687	23.984
64	320.000	39.839	23.984
65	325.000	39.939	24.266
66	330.000	39.980	24.266
67	335.000	39.954	24.266
68	340.000	39.856	24.266
69	345.000	39.686	23.984
70	350.000	39.444	23.702
71	355.000	39.134	23.419
72	360.000	38.763	23.137

Appendix A.3

Program ALTITUDE Listing and Sample Output


```

Write(8,910)Period
Write(8,920)Altp
Write(8,930)Step
Write(8,900)

```

```

C
C
C Calculate:
C     semimajor axis (km)
C     eccentricity
C     apogee altitude (km)
C

```

```

Semi = (((3600.0d0*Period)/(2.0d0*Pi))**2)*Mu**(1.0d0/3.0d0)
Ecc = (Semi - (Re + Altp))/Semi
Alta = 2.0d0 * Semi - 2.0d0 * Re - Altp

```

```

C
C Determine the index on the "DO" loop for calculating the output
C parameters.
C

```

```

Low = DINT(Altp/Step)
High = DINT(Alta/Step)
Index = 1 + (High - Low)

```

```

C
C Define the time of perigee passage to be the start of the orbit
C by setting T0 equal to zero.
C Initialize the Mean Anomaly at the low altitude portion of an
C altitude window to zero. The low altitude portion of the first
C window is perigee.
C

```

```

T0 = 0.0d0
T1 = 0.0d0

```

```

C
C Write the header for the output table.
C

```

```

WRITE(*,1000)
WRITE(8,1000)

```

```

C
C Initialize True Anomaly for the first point (perigee).
C Zero out the time spent in an altitude window.
C

```

```

Nu = 0.0d0
DT = 0.0d0

```

```

C
C Convert true anomaly from radians to degrees.
C Write the output variables to the output file for the first
C point (perigee).
C

```

```

WRITE(*,1010)AltP, Nu/DEG2RAD, DT, T0
WRITE(8,1010)AltP, Nu/DEG2RAD, DT, T0

```

```

C
C Begin the iteration to find the output variables for each of the
C altitude windows.
C

```

```

DO 500 I = 1, Index

```

```

C
C Look to see if this iteration is the last one or not.
C If it is the last iteration:
C   - the upper limit on the altitude window is the apogee altitude
C   - the true anomaly is  $\pi$  rad
C   - the mean anomaly is  $\pi$  rad
C If it is not the last iteration:
C   - the upper limit on the altitude window is the altitude step
C     size times the number of steps from the surface of the earth
C   - calculate the true anomaly at the upper altitude limit (rad)
C   - calculate the eccentric anomaly for the same point (rad)
C   - calculate the mean anomaly for the same point (rad)
C

```

```

IF (I .EQ. Index) THEN
  Alt = Alta
  Nu = Pi
  T2 = Pi
ELSE
  Alt = Step * (Low + I)
  R = Re + Alt
  Nu = DACOS((Semi*(1.0d0 - Ecc**2)/R - 1.0d0)/Ecc)

```

```

      EAnom = DACOS((Ecc + DCOS(Nu))/(1.0d0 + Ecc*DCOS(Nu)))
      T2 = EAnom - Ecc * DSIN(EAnom)
    ENDIF

```

```

    .....

```

```

    C
    C Calculate the time spent in this altitude window and convert to
    C minutes. (change in mean anomaly divided by mean motion)
    C
    C Calculate the time since perigee to reach the upper limit of this
    C altitude window and convert to minutes. (change in mean anomaly
    C from perigee divided by mean motion)
    C

```

```

    .....

```

```

      DT = DSQRT(Semi**3/Mu) * (T2 - T1) / 60.0d0
      TotalT = DSQRT(Semi**3/Mu) * (T2 - T0) / 60.0d0

```

```

    .....

```

```

    C
    C Convert true anomaly to degrees.
    C Write the the output variables to the output file.
    C

```

```

    .....

```

```

      WRITE(*,1010)Alt, Nu/DEG2RAD, DT, TotalT
      WRITE(8,1010)Alt, Nu/DEG2RAD, DT, TotalT

```

```

    .....

```

```

    C
    C The mean anomaly at the upper limit of this altitude window
    C becomes the mean anomaly at the lower limit of the next altitude
    C window.
    C

```

```

    .....

```

```

      T1 = T2

```

```

    .....

```

```

    C
    C Repeat the iteration.
    C

```

```

    .....

```

```

    500 CONTINUE

```

```

    .....

```

```

    C
    C See if there is another case.
    C

```

```

    .....

```

```

      Write(*,900)
      Write(*,*)'Do you have another case?'

```

```

Write(*,*) Enter "y" or "n"
Read(*,*)Again
IF ((AGAIN .EQ. "Y") .OR. (AGAIN .EQ. "y")) THEN
  GOTO 10
ENDIF

900 FORMAT (///)
910 FORMAT (10X,' Orbital Period (hrs) =',F9.3)
920 FORMAT (10X,' Perigee Altitude (km) =',F9.3)
930 FORMAT (10X,'Altitude Step Size (km) =',F9.3)
1000 FORMAT (26X,'True   Delta   Elapsed',/,12X,
+'Altitude   Anomaly   Time       Time',/,11X,
+' (km)      (deg)    (min)    (min)')
1010 FORMAT (11X,F9.3,4X,F7.3,4X,F5.2,4X,F7.3)

END

```

Orbital Period (hrs) = 8.000
 Perigee Altitude (km) = 500.000
 Altitude Step Size (km) = 100.000

Altitude (km)	True Anomaly (deg)	Delta Time (min)	Elapsed Time (min)
500.000	0.000	0.00	0.000
600.000	15.421	3.17	3.175
700.000	21.718	1.34	4.515
800.000	26.491	1.04	5.559
900.000	30.466	0.89	6.454
1000.000	33.926	0.80	7.255
1100.000	37.019	0.74	7.990
1200.000	39.830	0.69	8.677
1300.000	42.417	0.65	9.326
1400.000	44.820	0.62	9.944
1500.000	47.069	0.59	10.538
1600.000	49.184	0.57	11.111
1700.000	51.184	0.56	11.666
1800.000	53.083	0.54	12.207
1900.000	54.891	0.53	12.735
2000.000	56.617	0.52	13.251
2100.000	58.271	0.51	13.757
2200.000	59.858	0.50	14.255
2300.000	61.384	0.49	14.744
2400.000	62.855	0.48	15.227
2500.000	64.273	0.48	15.704
2600.000	65.644	0.47	16.175
2700.000	66.971	0.47	16.640
2800.000	68.256	0.46	17.102
2900.000	69.502	0.46	17.559
3000.000	70.712	0.45	18.013
3100.000	71.888	0.45	18.464
3200.000	73.032	0.45	18.911
3300.000	74.145	0.44	19.356
3400.000	75.230	0.44	19.799
3500.000	76.288	0.44	20.239
3600.000	77.319	0.44	20.677
3700.000	78.326	0.44	21.114
3800.000	79.310	0.43	21.549
3900.000	80.272	0.43	21.982
4000.000	81.212	0.43	22.415
4100.000	82.132	0.43	22.846
4200.000	83.033	0.43	23.276
4300.000	83.915	0.43	23.706
4400.000	84.780	0.43	24.134
4500.000	85.627	0.43	24.563
4600.000	86.458	0.43	24.990
4700.000	87.273	0.43	25.418
4800.000	88.073	0.43	25.845
4900.000	88.859	0.43	26.272
5000.000	89.631	0.43	26.698

5100.000	90.389	0.43	27.125
5200.000	91.134	0.43	27.552
5300.000	91.866	0.43	27.979
5400.000	92.587	0.43	28.406
5500.000	93.295	0.43	28.833
5600.000	93.992	0.43	29.261
5700.000	94.679	0.43	29.689
5800.000	95.354	0.43	30.117
5900.000	96.020	0.43	30.546
6000.000	96.675	0.43	30.975
6100.000	97.321	0.43	31.405
6200.000	97.957	0.43	31.836
6300.000	98.585	0.43	32.267
6400.000	99.203	0.43	32.699
6500.000	99.813	0.43	33.131
6600.000	100.415	0.43	33.565
6700.000	101.009	0.43	33.999
6800.000	101.594	0.44	34.434
6900.000	102.173	0.44	34.870
7000.000	102.743	0.44	35.307
7100.000	103.307	0.44	35.745
7200.000	103.863	0.44	36.184
7300.000	104.413	0.44	36.625
7400.000	104.956	0.44	37.066
7500.000	105.493	0.44	37.508
7600.000	106.023	0.44	37.951
7700.000	106.547	0.44	38.396
7800.000	107.065	0.45	38.842
7900.000	107.578	0.45	39.289
8000.000	108.084	0.45	39.737
8100.000	108.585	0.45	40.186
8200.000	109.081	0.45	40.637
8300.000	109.571	0.45	41.089
8400.000	110.056	0.45	41.543
8500.000	110.536	0.45	41.998
8600.000	111.011	0.46	42.454
8700.000	111.482	0.46	42.912
8800.000	111.947	0.46	43.372
8900.000	112.408	0.46	43.832
9000.000	112.865	0.46	44.295
9100.000	113.317	0.46	44.759
9200.000	113.765	0.47	45.224
9300.000	114.209	0.47	45.691
9400.000	114.648	0.47	46.160
9500.000	115.084	0.47	46.630
9600.000	115.515	0.47	47.102
9700.000	115.943	0.47	47.576
9800.000	116.367	0.48	48.051
9900.000	116.788	0.48	48.528
10000.000	117.204	0.48	49.007
10100.000	117.618	0.48	49.488
10200.000	118.027	0.48	49.970
10300.000	118.434	0.48	50.455
10400.000	118.837	0.49	50.941

10500.000	119.237	0.49	51.429
10600.000	119.633	0.49	51.919
10700.000	120.027	0.49	52.411
10800.000	120.418	0.49	52.905
10900.000	120.805	0.50	53.400
11000.000	121.190	0.50	53.898
11100.000	121.572	0.50	54.398
11200.000	121.951	0.50	54.900
11300.000	122.327	0.50	55.404
11400.000	122.700	0.51	55.910
11500.000	123.071	0.51	56.418
11600.000	123.440	0.51	56.928
11700.000	123.805	0.51	57.441
11800.000	124.169	0.51	57.956
11900.000	124.530	0.52	58.472
12000.000	124.888	0.52	58.991
12100.000	125.244	0.52	59.513
12200.000	125.598	0.52	60.036
12300.000	125.950	0.53	60.562
12400.000	126.299	0.53	61.091
12500.000	126.647	0.53	61.621
12600.000	126.992	0.53	62.154
12700.000	127.335	0.54	62.690
12800.000	127.676	0.54	63.228
12900.000	128.015	0.54	63.768
13000.000	128.352	0.54	64.311
13100.000	128.688	0.55	64.856
13200.000	129.021	0.55	65.404
13300.000	129.353	0.55	65.955
13400.000	129.682	0.55	66.508
13500.000	130.010	0.56	67.064
13600.000	130.336	0.56	67.622
13700.000	130.661	0.56	68.184
13800.000	130.984	0.56	68.747
13900.000	131.305	0.57	69.314
14000.000	131.625	0.57	69.884
14100.000	131.943	0.57	70.456
14200.000	132.260	0.58	71.031
14300.000	132.575	0.58	71.609
14400.000	132.889	0.58	72.190
14500.000	133.201	0.58	72.774
14600.000	133.512	0.59	73.361
14700.000	133.821	0.59	73.951
14800.000	134.130	0.59	74.544
14900.000	134.436	0.60	75.140
15000.000	134.742	0.60	75.739
15100.000	135.046	0.60	76.341
15200.000	135.350	0.61	76.947
15300.000	135.651	0.61	77.556
15400.000	135.952	0.61	78.168
15500.000	136.252	0.62	78.783
15600.000	136.551	0.62	79.402
15700.000	136.848	0.62	80.024
15800.000	137.144	0.63	80.650

15900.000	137.440	0.63	81.279
16000.000	137.734	0.63	81.911
16100.000	138.028	0.64	82.548
16200.000	138.320	0.64	83.188
16300.000	138.612	0.64	83.831
16400.000	138.903	0.65	84.478
16500.000	139.192	0.65	85.130
16600.000	139.481	0.65	85.784
16700.000	139.770	0.66	86.443
16800.000	140.057	0.66	87.106
16900.000	140.344	0.67	87.772
17000.000	140.630	0.67	88.443
17100.000	140.915	0.67	89.118
17200.000	141.199	0.68	89.797
17300.000	141.483	0.68	90.480
17400.000	141.767	0.69	91.167
17500.000	142.049	0.69	91.859
17600.000	142.331	0.70	92.555
17700.000	142.613	0.70	93.256
17800.000	142.894	0.71	93.961
17900.000	143.174	0.71	94.670
18000.000	143.454	0.71	95.384
18100.000	143.734	0.72	96.103
18200.000	144.013	0.72	96.827
18300.000	144.292	0.73	97.556
18400.000	144.570	0.73	98.289
18500.000	144.848	0.74	99.028
18600.000	145.126	0.74	99.772
18700.000	145.403	0.75	100.521
18800.000	145.680	0.75	101.275
18900.000	145.957	0.76	102.034
19000.000	146.234	0.76	102.799
19100.000	146.510	0.77	103.570
19200.000	146.786	0.78	104.346
19300.000	147.063	0.78	105.128
19400.000	147.339	0.79	105.916
19500.000	147.615	0.79	106.709
19600.000	147.891	0.80	107.509
19700.000	148.167	0.81	108.315
19800.000	148.443	0.81	109.127
19900.000	148.719	0.82	109.946
20000.000	148.995	0.83	110.771
20100.000	149.271	0.83	111.603
20200.000	149.548	0.84	112.441
20300.000	149.824	0.85	113.287
20400.000	150.101	0.85	114.139
20500.000	150.378	0.86	114.999
20600.000	150.656	0.87	115.866
20700.000	150.933	0.87	116.740
20800.000	151.212	0.88	117.622
20900.000	151.490	0.89	118.512
21000.000	151.769	0.90	119.411
21100.000	152.049	0.91	120.317
21200.000	152.329	0.91	121.231

21300.000	152.609	0.92	122.155
21400.000	152.890	0.93	123.086
21500.000	153.172	0.94	124.027
21600.000	153.455	0.95	124.978
21700.000	153.738	0.96	125.937
21800.000	154.022	0.97	126.906
21900.000	154.308	0.98	127.886
22000.000	154.594	0.99	128.875
22100.000	154.881	1.00	129.875
22200.000	155.169	1.01	130.886
22300.000	155.458	1.02	131.907
22400.000	155.748	1.03	132.940
22500.000	156.040	1.04	133.985
22600.000	156.333	1.06	135.042
22700.000	156.628	1.07	136.111
22800.000	156.923	1.08	137.194
22900.000	157.221	1.10	138.289
23000.000	157.520	1.11	139.398
23100.000	157.821	1.12	140.521
23200.000	158.124	1.14	141.659
23300.000	158.428	1.15	142.812
23400.000	158.735	1.17	143.980
23500.000	159.044	1.18	145.165
23600.000	159.355	1.20	146.367
23700.000	159.669	1.22	147.586
23800.000	159.985	1.24	148.823
23900.000	160.304	1.26	150.080
24000.000	160.626	1.28	151.356
24100.000	160.951	1.30	152.653
24200.000	161.279	1.32	153.971
24300.000	161.611	1.34	155.312
24400.000	161.946	1.36	156.677
24500.000	162.286	1.39	158.066
24600.000	162.629	1.42	159.482
24700.000	162.977	1.44	160.925
24800.000	163.329	1.47	162.398
24900.000	163.687	1.50	163.901
25000.000	164.050	1.54	165.437
25100.000	164.419	1.57	167.007
25200.000	164.794	1.61	168.615
25300.000	165.176	1.65	170.262
25400.000	165.566	1.69	171.952
25500.000	165.963	1.74	173.687
25600.000	166.369	1.78	175.472
25700.000	166.785	1.84	177.310
25800.000	167.211	1.90	179.207
25900.000	167.649	1.96	181.167
26000.000	168.100	2.03	183.199
26100.000	168.566	2.11	185.309
26200.000	169.048	2.20	187.507
26300.000	169.549	2.30	189.805
26400.000	170.071	2.41	192.218
26500.000	170.619	2.54	194.762
26600.000	171.197	2.70	197.462

26700.000	171.811	2.89	200.351
26800.000	172.471	3.12	203.471
26900.000	173.189	3.42	206.890
27000.000	173.987	3.82	210.712
27100.000	174.902	4.41	215.120
27200.000	176.015	5.39	220.510
27300.000	177.582	7.64	228.152
27358.544	180.000	11.85	240.000

Appendix A.4

Program ECLIPSE Listing and Sample Output

CHARACTER*1 Again

OPEN (Unit = 8, File = 'Eclipse.Out', Status = 'New')

```

C
C   Initialize useful constants.
C

```

```

Re = 6378.135d0
Mu = 398600.8d0
DEG2RAD = PI / 180.0D0

```

```

C
C   Get the orbital period and perigee altitude.
C   Echo check them to the output file.
C

```

```

10 Write(*,*)'Enter the orbital period in hours'
   Read(*,*)Period
   Write(*,*)'Enter the perigee altitude in kilometers'
   Read(*,*)Altp
   Write(*,900)
   Write(*,910)Period
   Write(*,920)Altp
   Write(8,900)
   Write(8,910)Period
   Write(8,920)Altp

```

```

C
C   Calculate semimajor axis and eccentricity
C

```

```

Semi = (((3600.0d0*Period)/(2.0d0*Pi))**2)*Mu**(1.0d0/3.0d0)
Ecc = (Semi - (Re + Altp))/Semi

```

```

C
C   Worst case eclipse occurs when the vector from the center of the
C   earth toward the sun lies in the same plane as the orbit plane.
C   Under these circumstances, the S/C must pass through the center
C   of the Earth's shadow. The situation gets worse when the point
C   of the orbit that passes through the center of the shadow
C   approaches apogee. Consequently, the geometry of the Earth's
C   tilt with respect to the plane of the ecliptic coupled with the
C   restriction that argument of perigee be at 270 deg lead to the
C   longest duration eclipse occurring when the point 113.5 deg from
C   perigee (90 + 23.5 for the tilt of the Earth's spin axis) passes

```

C through the center of the shadow.

C

.....

.....

C

C Iterative solution for true anomaly at eclipse entry.

C

C Because the center of the eclipse is for Nu = 113.5 deg, eclipse
C entry must occur for some value of Nu such that

C 23.5 deg < NuEnter < 113.5 deg

C Markers are used to hold low and high values for Nu. NuTest is
C half way between the low and high values. The radius is calculated
C for this value of NuTest. The solution has converged if the
C portion of the radius vector perpendicular to the sunline is
C within one kilometer of the radius of the earth. If the solution
C has not converged yet, the program selects which marker to update.

C If the portion of the radius vector perpendicular to the sunline is
C greater than the radius of the earth, the S/C is not in eclipse and
C the marker to update is the low value for Nu. The marker for the
C high value of Nu is updated if the portion of the radius vector
C perpendicular to the sunline is less than the radius of the
C earth. Finally, the eccentric anomaly at eclipse entry is
C calculated.

C

.....

```
NuCenter = 113.5d0 * DEG2RAD
NuEnter = NuCenter - Pi/2.0d0
NuLow = NuEnter
NuHigh = NuCenter
100 NuTest = (NuHigh + NuLow) / 2.0d0
RTest = Semi * ( 1.0d0 - Ecc**2) / (1.0d0 + Ecc * DCOS(NuTest))
RPerp = RTest * DSIN(NuCenter - NuTest)
Test = RPerp - Re
IF (DABS(Test) .GT. 1.0d0) THEN
  IF (Test .GT. 0.0) THEN
    NuLow = NuTest
  ELSE
    NuHigh = NuTest
  ENDIF
  GOTO 100
ELSE
  NuEnter = NuTest
ENDIF
EAnomB = DACOS((Ecc + DCOS(NuEnter))/(1.0d0 + Ecc*DCOS(NuEnter)))
```

.....

C

C Iterative solution for true anomaly at eclipse exit.

C

C Because the center of the eclipse is for Nu = 113.5 deg, eclipse
C exit must occur for some value of Nu such that

C 113.5 deg < NuExit < 203.5 deg

C

C Remaining logic parallels that for eclipse entry case.

C

.....

```
NuExit = NuCenter + Pi/2.0d0
NuLow = NuCenter
NuHigh = NuExit
200 NuTest = (NuHigh + NuLow) / 2.0d0
RTest = Semi * ( 1.0d0 - Ecc**2) / (1.0d0 + Ecc * DCOS(NuTest))
RPerp = RTest * DSIN(NuTest - NuCenter)
Test = RPerp - Re
IF (DABS(Test) .GT. 1.0d0) THEN
  IF (Test .GT. 0.0) THEN
    NuHigh = NuTest
  ELSE
    NuLow = NuTest
  ENDIF
  GOTO 200
ELSE
  NuExit = NuTest
ENDIF
EAnomF = DACOS((Ecc + DCOS(NuExit))/(1.0d0 + Ecc*DCOS(NuExit)))
```

.....

C

C Eclipse duration is based on the difference between the eccentric
C anomalies of eclipse entry and exit. Eclpdur holds temporary
C values for the eclipse duration because the equation is lengthy.
C The last line contains the true value for eclipse duration
C expressed in minutes.

C

.....

```
Eclpdur = EAnomB - Ecc * DSIN(EAnomB)
Eclpdur = EAnomF - Ecc * DSIN(EAnomF) - Eclpdur
Eclpdur = DSQRT(Semi**3/Mu) * Eclpdur / 60.0d0
```

.....

C

C Write eclipse duration to output file.
C Write true anomaly at eclipse entry and exit to output file.

C

.....

```
Write (*,1001) Eclpdur
Write (*,1002) NuEnter/DEG2RAD
Write (*,1003) NuExit/DEG2RAD
Write (8,1001) Eclpdur
Write (8,1002) NuEnter/DEG2RAD
Write (8,1003) NuExit/DEG2RAD
```

.....

C

C See if there is another case.

C



```
Write(*,*)'Do you have another case?'
Write(*,*)  Enter "y" or "n"
Read(*,*)Again
IF ((AGAIN .EQ. "Y") .OR. (AGAIN .EQ. "y")) THEN
  GOTO 10
ENDIF
```

```
900 FORMAT (///)
910 FORMAT (1X,'Orbital period (hrs) =',F6.3)
920 FORMAT (1X,'Perigee altitude (km) =',F8.3)
1001 FORMAT (1X,'Eclipse duration (min) =',F8.3)
1002 FORMAT (1X,'True Anomaly at eclipse entry (deg) =',F7.3)
1003 FORMAT (1X,'True Anomaly at eclipse exit (deg) =',F8.3)
```

END

```
Orbital period (hrs) = 8.000
Perigee altitude (km) = 500.000
Eclipse duration (min) = 52.079
True Anomaly at eclipse entry (deg) = 70.587
True Anomaly at eclipse exit (deg) = 131.715
```

APPENDIX B

A. BATTERY DESIGN

The batteries were sized on the eclipse load of the AVHRR payload. Having the requirement to operate the AVHRR 24 hours a day, it is not possible to turn off the mission instrument during eclipse to reduce power consumption. Therefore, the battery must supply all the power necessary to run the AVHRR and the bus during the 37 minute eclipse. The solar array must replace this 100.6 W in the approximately one hour of sunlight the AVHRR experiences. The equation used is:

$$P_{in} = \frac{(P_{discharged})(t_{discharged})}{(\eta)(\mu)(t_{recharge})} \quad (B.1)$$

where

P_{in} = Power required for recharge

η = efficiency of charging equipment

μ = 10 % margin for Low Earth Orbit

For the AVHRR:

$$P_{in} = \frac{(100.6)(37/60)}{(0.9)(0.9)(1)} = 76.5 \text{ W} \quad (B.2)$$

To calculate the charging rate the amp-hours utilized must first be determined. For the AVHRR, a discharge of 100.6 W at 17.6 V minimum consumes 3.52 amp-hours. The charging current required is then determined by dividing the amp-hours consumed by the amount of time the sun is available for charging. It was assumed that 90% of the sunlit portion of the orbit was used for recharging. For the AVHRR the charging current is 3.52 amps. The charging rate is then computed by dividing the cell capacity of the battery by the

charging current. The resultant charge rate is $C / 3.4$ where C is the battery capacity in amp-hours. This charge rate is only slightly lower than the maximum recommended rate of $C/3$.

For the EHF payload the above procedures resulted in the following calculations:

$$P_{in} = \frac{(150.3)(52/60)}{(0.9)(0.9)(6.5)} = 24.7 \text{ W} \quad (\text{B.3})$$

The amp-hours used are:

$$\frac{(150.3 \text{ W})(52/60)}{(17.6 \text{ V})} = 7.4 \text{ Amp-hour} \quad (\text{B.4})$$

The charge current is:

$$\frac{7.4 \text{ Amp-hour}}{6.5 \text{ hours}} = 1.1 \text{ Amps} \quad (\text{B.5})$$

The charge rate is: $\frac{C}{11}$

B. SOLAR ARRAY DEGRADATION

The solar cell radiation degradation was performed using the JPL Solar Cell Radiation Handbook. Analysis was done for both the circular low earth orbit and the 8-hour Molniya orbit. For the circular orbit, the first step was to determine the 1 MeV equivalent fluences for trapped protons and electrons at a 450 nm orbit. With the equivalent 1 MeV fluence, the electric power circuit parameters can be obtained from graphs in the radiation handbook. This data is shown in Tables B.6 TO B.9. For the 8-hour Molniya orbit, the satellite is traveling through several different altitudes at a changing speed. In order to determine the equivalent 1 MeV fluence, a summation must be performed in time increments over one orbit. The summation is shown in Equation B.6.

$$\phi_T = \sum \phi(h) \Delta t \quad (\text{B.6})$$

where:

ϕ_T = total fluence in one orbit

$\phi(h)$ = fluence interpolated for the average altitude h

Δt = time increment (5 minutes)

The 8-hour orbit was broken up into 5 minute increments. At each of these time increments, the equivalent fluence was determined for the average altitude during that time increment. This represents the fluence that the satellite sees during that 5 minutes. The fluence is multiplied by 5 minutes and then the product for each increment is summed to determine the equivalent fluence for the orbit. Then it is a simple matter to determine the equivalent fluence for 1 year and 3 years in order to enter the graphs and obtain circuit parameters. The numbers are shown in Tables B.1 TO B.5.

1. EHF Payload

Solar Cell: 10 Ohm-cm resistivity
 0.0203 cm (.008 in) thick

Dual AR, BSR, BSF, TEX

Coverglass: 0.015 cm (.006 in) thick

Fused silica, UV filter

Anti-reflecting coating

Backshielding: Infinite

Orbit: 8 hour Molniya (63.4 degree inclination)

Apogee = 2758 km

Perigee = 500 km

Eccentricity = .6612992

Assumptions: Solar maximum

3 year life

Time (min)	Alt (km)	Alt (nm)	Electrons (all)	Protons (Voc,Pm)	Protons (Isc)
0	500	273.40	2.57E + 11	2.98E + 12	1.76E +12
5	725	396.43	4.27E + 11	1.46E + 13	8.31E + 12
10	1415	773.73	1.96E + 12	1.79E + 13	1.05E + 14
15	2355	1287.73	9.42E + 12	2.11E + 15	1.15E + 15
20	3448	1885.39	1.61E + 13	1.15E + 16	5.68E + 15
25	4605	2518.04	1.80E + 13	2.81E + 16	1.27E + 16
30	5775	3157.81	1.62E + 13	3.57E + 16	1.52E + 16
35	6948	3799.21	1.51E + 13	3.27E + 16	1.33E + 16
40	8090	4423.67	1.62E + 13	2.61E + 16	1.03E + 16
45	9151	5003.83	1.82E + 13	1.84E + 16	7.08E + 15
50	10215	5585.63	2.17E + 13	1.26E + 16	4.79E + 15
55	11210	6129.70	2.60E + 13	7.57E + 15	2.83E + 15
60	12190	6665.57	3.16E + 13	4.40E + 15	1.63E + 15
65	13145	7187.77	3.63E + 13	2.06E + 15	7.51E + 14
70	14025	7668.96	3.94E + 13	1.14E + 15	4.14E + 14
75	14875	8133.75	4.28E + 13	4.48E + 14	1.60E + 14
80	15690	8579.40	4.66E + 13	2.47E + 14	8.84E + 13
85	16485	9014.11	5.04E + 13	5.73E + 13	2.01E + 13
90	12745	9429.68	5.26E + 13	3.52E + 13	1.24E + 13
95	17948	9814.09	5.49E + 13	1.48E + 13	5.18E + 12
100	18648	10196.85	5.51E + 13	4.04E + 12	1.39E + 12
105	19285	10545.17	5.40E + 13	2.38E + 12	8.18E + 11
110	19915	10889.65	5.29E + 13	7.44E + 11	2.55E + 11
115	20505	11212.27	5.11E + 13	1.73E + 11	5.87E + 10
120	21065	11518.48	4.89E + 13	1.05E + 11	3.59E + 10
125	21610	11816.49	4.68E + 13	4.02E + 10	1.37E + 10
130	22110	12089.9	4.51E + 13	8.76E - 03	8.76E - 03
135	22590	12352.36	4.38E + 13	6.24E - 03	6.42E - 03
140	23060	12609.36	4.26E + 13	3.76E - 03	3.76E - 03
145	23495	12847.22	4.14E + 13	1.47E - 03	1.47E - 03
150	23895	13065.94	4.01E + 13	3.80E + 00	3.80E +00
155	24278	13275.37	3.81E + 13	2.59E + 00	2.95E +00
160	24648	13477.69	3.62E + 13	2.13E + 00	2.13E +00
165	24975	13656.50	3.45E + 13	1.40E + 00	1.40E +00
170	25295	13831.47	3.28E + 13	6.86E - 01	6.86E - 01
175	25575	13984.58	3.13E + 13	6.28E - 02	6.82E - 02
180	25849	14134.41	2.98E + 13	0.00E + 00	0.00E + 00
185	26080	14260.72	2.86E + 13	0.00E + 00	0.00E + 00
190	26310	14386.48	2.73E + 13	0.00E + 00	0.00E + 00
200	26695	14597.00	2.52E + 13	0.00E + 00	0.00E + 00
205	26847	14680.12	2.43E + 13	0.00E + 00	0.00E + 00
210	26995	14761.05	2.35E + 13	0.00E + 00	0.00E + 00
215	27098	14817.37	2.29E + 13	0.00E + 00	0.00E + 00
220	27197	14871.50	2.24E + 13	0.00E + 00	0.00E + 00
225	27260	14905.95	2.20E + 13	0.00E + 00	0.00E + 00
230	27340	14949.69	2.16E + 13	0.00E + 00	0.00E + 00
235	27354	14957.35	2.15E + 13	0.00E + 00	0.00E + 00
240	27358	14959.54	2.15E + 13	0.00E + 00	0.00E + 00
	TOTALS	(per orbit)	2.90E+10	3.48E+12	1.45E+12
	TOTALS	(per year)	3.18E+13	3.82E+15	1.59E+15
	TOTALS	(life)	9.54E+13	1.15E+16	4.76E+15

TABLE B.1 Fluence Calculation for 8-hour Molniya Orbit

1 Me V Electron Fluence (per year)

Particle Type	I_{sc}	V_{oc}, P_{max}
Trapped Electrons	3.18E+13	3.18E+13
Trapped Protons	3.82E+15	1.59E+15
TOTAL FLUENCE e/cm ² -yr	3.85E+15	1.62E+15
FOR 3 YEARS e/cm ² -yr	1.15E+16	4.86E+15

TABLE B.2 Total 1 Mev Fluence for 8-hour Molniya Orbit

Solar Cell Output for EHF

a. BOL

Eq Fluence = 0

	Absolute	Relative
I_{sc}	44	1
V_{oc}	584	1
P_{max}	19.8	1
V_{mp}	492	1
I_{mp}	40.24	1

TABLE B.3 BOL Solar Cell Parameters

b. After 1 Year

Eq Fluence: $I_{sc} = 3.85E+15$

$V_{oc}, P_m = 1.62E+15$

	Absolute	Relative
I_{sc}	32.4	0.736
V_{oc}	502	0.860
P_{max}	13.1	0.663
V_{mp}	410	0.834
I_{mp}	31.9	0.792

TABLE B.4 One Year Solar Cell Parameters

c. After 3 Years

Eq Fluence: $I_{sc} = 1.15E+16$
 $V_{oc}, P_m = 4.86E+15$

	Absolute	Relative
I_{sc}	29.5	0.670
V_{oc}	483	0.827
P_{max}	11.3	0.571
V_{mp}	391	0.795
I_{mp}	28.9	0.72

TABLE B.5 EOL Solar Cell Parameters

2. AVHRR Payload

Solar Cell: 10 Ohm-cm resistivity
 0.0203 cm (.008 in) thick
 Dual AR, BSR, BSF, TEX

Coverglass: 0.015 cm (.006 in) thick
 Fused silica, UV filter
 Antireflecting coating

Backshielding: Infinite

Orbit: 450 NM Circular (Assumed 90° inclination)

Assumptions Solar Maximum
 3 Year Life

Particle Type	I_{sc}	V_{oc}, P_{max}
Trapped Electrons	4.59E+11	4.59E+11
Trapped Protons	8.64E+12	1.47E+13
TOTAL FLUENCE e/cm ² -yr	9.10E+12	1.52E+13

TABLE B.6 1 MeV Fluences for 450 NM Orbit

Solar Cell Output for AVHRR

a. BOL

Eq Fluence = 0

	Absolute	Relative
I_{sc}	44	1
V_{oc}	584	1
P_{max}	19.8	1
V_{mp}	492	1
I_{mp}	40.24	1

TABLE B.7 BOL Solar Cell Parameters

b. After 1 Year

Eq Fluence

$$I_{sc} = 9.1E+12$$

$$V_{oc}, P_m = 1.52E+13$$

	Absolute	Relative
I_{sc}	43.7	0.993
V_{oc}	571	0.978
P_{max}	19	0.959
V_{mp}	474	0.963
I_{mp}	39.8	0.989

TABLE B.8 One Year Solar Cell Parameters

c. After 3 Years

Eq Fluence

$$I_{sc} = 2.73E+13$$

$$V_{oc}, P_m = 4.55E+13$$

	Absolute	Relative
I_{sc}	42.7	0.97
V_{oc}	556	0.952
P_{max}	18	0.909
V_{mp}	461	0.937
I_{mp}	39	0.969

TABLE B.9 EOL Solar Cell Parameters

C. SOLAR ARRAY PANEL SIZING

	AVHRR	EHF
Cells in Series		
I_{mp}	0.624	0.624
α_I	0.00024	0.00024
K_a^I	0.96	0.96
K_d^I	0.969	0.72
K_s	0.8885	0.8885
I	0.517334	0.384397
I_t	11.25	8.5
Power	315	238
Bus voltage	28	28
T	33	33
$N_p = \frac{I_t}{I}$	21.74609	22.11256
Cells in Parallel		
V_{mp}	0.492	0.492
ΔV	0.005	0.005
α_V	-0.0022	-0.0022
T	33	33
K_e^V	0.937	0.795
V	0.439828	0.373173
Bus voltage	28	28
Bus voltage drop	1.8	1.8
$N_s = \frac{\text{bus} + \text{busdrop}}{V}$	67.75379	79.85572
Total # Cells	1473.38	1765.814
Cell width cm	2.5	2.5
Cell height cm	6.2	6.2
Cell area sq in	2.403101	2.403101
Area needed sq ft	24.58806	29.46826

TABLE B.10 Summary of Solar Array Sizing

APPENDIX C

ATTITUDE CONTROL CALCULATIONS

1. Moment of Inertia Calculations

The spacecraft is modeled as a simple assembly of individual components. Each component is represented as a simple geometric solid. Worst case is beginning of life with solar arrays deployed. The cross-products of inertia have been determined to contribute less than 0.5 kg-m² and are not shown here. The coordinate system is taken as the geometric center of the main body with the positive Z direction out of the earth face, positive X direction out of the west face and the positive Y direction out of the south face. The center of mass is measured from this reference.

Payload	mass kg	x cm	y cm	z cm	I _{xx} kg-m ²	I _{yy} kg-m ²	I _{zz} kg-m ²
AVHRR	157.01	1.68	4.47	13.23	14.16	45.4	39.75
EHF	175.51	-3.02	1.83	15.39	15.38	91.90	83.06

TABLE C.1 Mass and Inertia Summary

The component break-down and contribution to the total inertia is given in the following:

Item	a	b	c	mass (lbs)	x	y	z
RTU	8	8	8	5	11.5	-9.5	8.5
RCU	8	6	6	5	-12.5	-9.5	8.5
ESA	3.64	13.5	0	9	0	-8	10.75
Earth Face	0.375	28	32	0.786	0	0	11.5
Yaw RWA	4.5	0	4.7	5.23	-10.5	8.5	-9.15
AntiEarth Face	0.375	28	32	0.786	0	0	-11.5
Tank	8	0	0	8.16	0	0	-3.5
East SADM	3.15	4	0	8.8	-14	0	2
Roll RWA	4.63	4.7	0	5.23	-13.15	-1.58	-6.76
Gyros	4.49	2.95	0	2.64	-14	-11.25	2.88
ADACS	14.25	2.5	5.87	5.5	-14.25	6.38	8.57
East Face	0.375	23	28	0.565	-15.5	0	0
West SADM	3.15	4	0	8.8	14	0	2
Batteries	11.81	9.06	10.23	15.7	11	7.5	-6.38
Power Electronics	15.75	5.9	5.9	13.22	12.5	6	8.5
West Face	0.375	23	28	0.565	15.5	0	0
BU RWA	4.63	4.7	0	5.23	10.18	-7.83	-5.18
SSE	4.2	4	2	1.1	-2.3	-12.5	-2.16
SSU	5.2	5.5	1.6	0.98	-2.3	-15.13	-2.16
North Face	0.375	23	32	0.646	0	-13.5	0
Pitch RWA	4.63	4.7	0	5.23	-10.5	11.15	0
CSA	3	8.16	0	7	9.68	9.89	2.1
South Face	0.375	23	32	0.646	0	13.5	0
West Array	0.685	64	34	11.72	62	0.38	2
East Array	0.685	64	34	11.72	-62	0.38	2
Propellant	8	0	0	22	0	0	-3.5
AVHRR	11.5	31.5	14.5	62.4	-0.25	8.25	18.75

TABLE C.2 AVHRR Component Breakdown

Item	a	b	c	mass (lbs)	x	y	z
RTU	8	8	8	5	11.5	-9.5	8.5
RCU	8	6	6	5	-12.5	-9.5	8.5
ESA	3.64	13.5	0	9	0	-8	10.75
Earth Face	0.375	28	32	0.786	0	0	11.5
Yaw RWA	4.5	0	4.7	5.23	-10.5	8.5	-9.15
AntiEarth Face	0.375	28	32	0.786	0	0	-11.5
Tank	8	0	0	8.16	0	0	-3.5
East SADM	3.15	4	0	8.8	-14	0	2
Roll RWA	4.63	4.7	0	5.23	-13.15	-1.58	-6.76
Gyros	4.49	2.95	0	2.64	-14	-11.25	2.88
ADACS	14.25	2.5	5.87	5.5	-14.25	6.38	8.57
East Face	0.375	23	28	0.565	-15.5	0	0
West SADM	3.15	4	0	8.8	14	0	2
Batteries	11.81	9.06	10.23	15.7	11	7.5	-6.38
Power Electronics	15.75	5.9	5.9	13.22	12.5	6	8.5
West Face	0.375	23	28	0.565	15.5	0	0
BU RWA	4.63	4.7	0	5.23	10.18	-7.83	-5.18
SSE	4.2	4	2	1.1	-2.3	-12.5	-2.16
SSU	5.2	5.5	1.6	0.98	-2.3	-15.13	-2.16
North Face	0.375	23	32	0.646	0	-13.5	0
Pitch RWA	4.63	4.7	0	5.23	-10.5	11.15	0
CSA	3	8.16	0	7	9.68	9.89	2.1
South Face	0.375	23	32	0.646	0	13.5	0
West Array	0.685	64	34	11.72	62	0.38	2
East Array	0.685	64	34	11.72	-62	0.38	2
Propellant	8	0	0	22	0	0	-3.5
Feed Horn & Supports	10	18.78	13.68	10.73	-9.91	0	21.5
Reflector & Pedestal*	0	0	0	5.4	13.34	0	31.36
EHF Electronics	20	6	6	69.4	-12.63	-2.5	14.13
Box East	0.375	6	28	0.032	-15.63	0	14.31
Box West	0.375	6	28	0.032	15.63	0	14.31
Box North	0.375	6	32	0.032	0	-13.63	14.31
Box South	0.375	6	32	0.032	0	13.63	14.31

* Reflector and Pedestal considered as a point mass.

TABLE C.3 EHF Component Breakdown

2. Disturbance Torques

The disturbance torques consists of the solar pressure torque, the torque due to aerodynamic drag, the gravity gradient torque, internal torques, and the torques provided by the magnetic torque rods. The attitude control system senses these torques as a change in attitude and body rates from the sensors and gyros. The compensating torques are then provided by the RWA's. Cyclic torques will result in no net increase in wheel speeds, however the secular torques will. These secular torques will result in unacceptably high wheel speeds unless a desaturation scheme is used.

a. Solar Torque

In order to determine the effect of the solar torque over the orbit period, some simplifying assumptions are first made. The orbit is assumed to be exactly polar with a 3:30 PM ascending node. The 8:30 AM descending node case will be symmetric and is not modeled here. The spacecraft axis are frozen at the equatorial crossing and then considered 'inertial', (in fact, it is rotating at 1 deg per day). The vector from the sun to this axis is:

$$\mathbf{S} = \sin(\delta) \mathbf{I}_o + \cos(37.5) \mathbf{J}_o + \sin(37.5) \mathbf{K}_o$$

The antinormal vector to the solar arrays is (in body coordinates):

$$\mathbf{n} = \cos(38.766 \cos^2(\alpha-25^\circ))\mathbf{J} + \sin(38.766 \cos(\alpha-25^\circ))\mathbf{K}$$

The solar radiation pressure moment, M_s , is (see ref AGR):

$$\mathbf{M}_s = PA (\mathbf{n} \bullet \mathbf{S}) \mathbf{r} \times ((1-\rho_s)\mathbf{S} + 2(\rho_s + \frac{1}{3}\rho_d)\mathbf{n})$$

The solar vector is then transformed into the body coordinates resulting in the solar pressure moment (in body coordinates):

$$\mathbf{M}_s = \begin{pmatrix} y(BD+C\sin(38.766 \cos(\alpha-25^\circ)))-z (BH + CF) \mathbf{I} \\ PA (HF + \sin(38.766 \cos(\alpha-25^\circ)) D) z(BE) - x(BD+C\sin(38.766\cos(\alpha-25^\circ))) \mathbf{J} \\ x(BH + CF) - y(BE) \mathbf{K} \end{pmatrix}$$

where:

$$B = (1 - \rho_s)$$

$$C = 2(\rho_s + \frac{1}{3}\rho_d)$$

$$D = -\sin(\alpha) \sin(\delta) + \cos(\alpha) \sin(37.5)$$

$$E = \cos(\alpha) \sin(\delta) + \sin(\alpha) \sin(37.5)$$

$$F = \cos(38.766 \cos 2(\alpha))$$

$$G = \sin(37.5)$$

$$H = \cos(37.5)$$

α = orbit angle measured from equatorial crossing

δ = declination of the sun

ρ_s = coefficient of specular reflection

ρ_d = coefficient of diffuse reflection

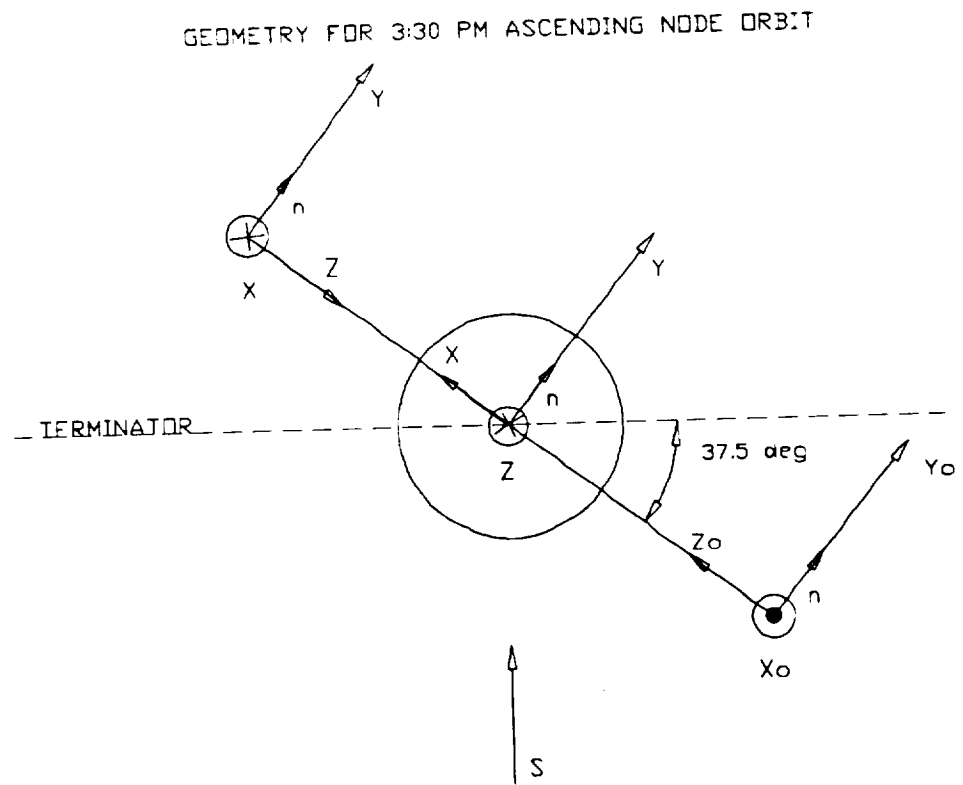


Figure C.1 Coordinate System

The solar pressure induced torque is plotted below for one orbit. Start time for the plot is at the ascending node.

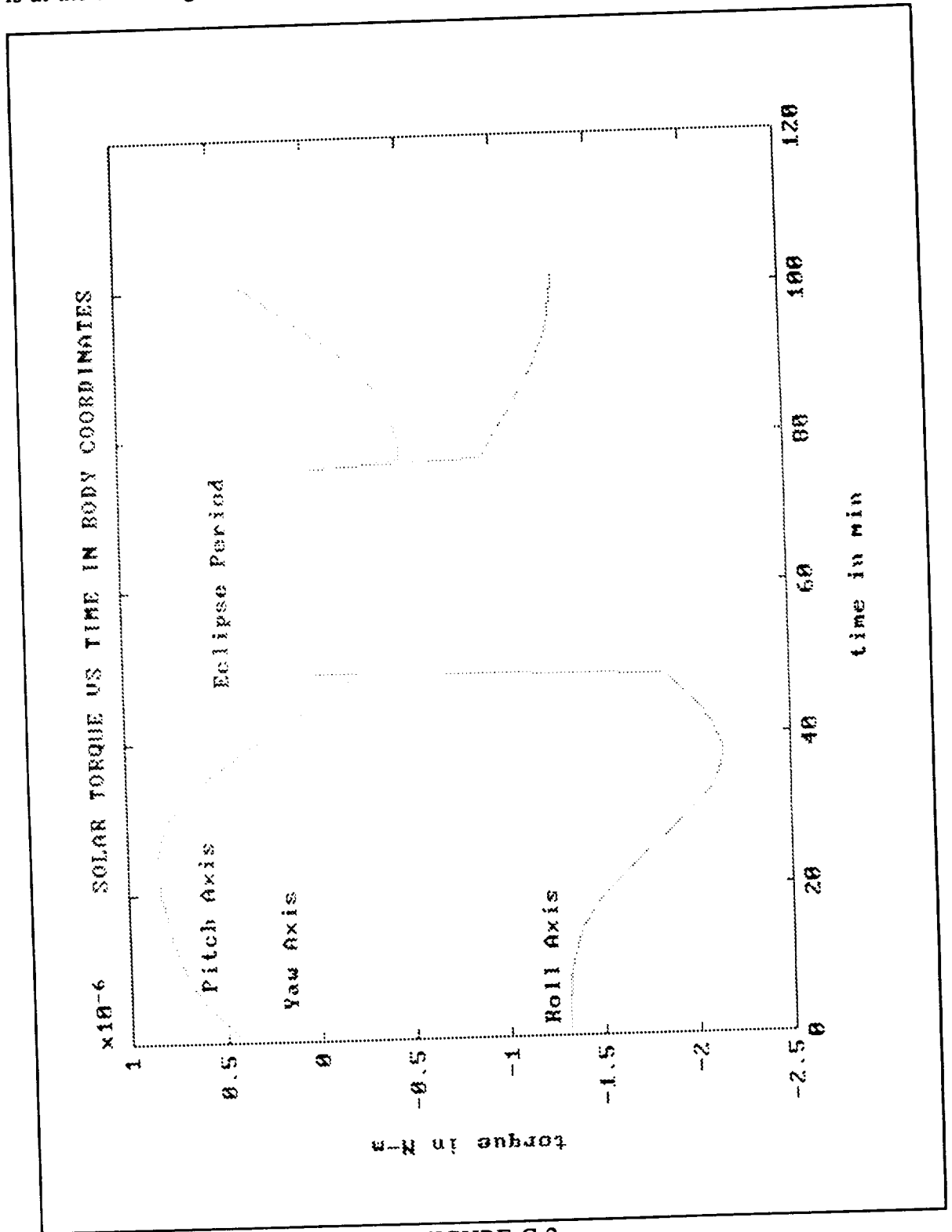


FIGURE C.2
198

b. Magnetic Torque

The magnetic torque rods provide a torque about the pitch and roll axis. Due to the roll-yaw coupling, this will be sufficient to desaturate all three RWA's. For this simulation, the earth's magnetic field is modeled as constant over the poles (within ± 30 degree), at 60 micro-Tesla and constant over the geomagnetic equator, (within ± 30 degree) at 30 micro-Tesla. The torque rods provide a 10 AMP-m² dipole. This results in a torque about the pitch axis of 0.006 N-m and 0.003 N-m about the roll. Since this is the worst case disturbance torque, the RWA gain and time constants are determined using these values. The closed loop transfer function for the wheel is derived in ref Agrawal and is provided below:

$$\frac{\theta(s)}{M_{sy}(s)} = \frac{1}{I_{yy} \left(s + \sqrt{\frac{K_{\theta}}{I_{yy}}} \right)}$$

Imposing a constant torque results in the time domain equation for the error:

$$\theta(t) = \frac{M_o}{I_{yy}} \left[\tau^2 - \exp \left(-\frac{t}{\tau} \right) \left(1 - 3\frac{t}{\tau} \right) \right]$$

This equation is solved analytically for tau for a 0.01 degree error. The gain is then calculated by the formula:

$$K_{\theta} = \frac{I_{yy}}{\tau^2}$$

The results for each axis is provided in the attitude control section of the report.

c. Aerodynamic Torque

The aerodynamic drag of the spacecraft results in a torque that is essentially about the positive pitch axis due to the displaced center of mass. The center of pressure for the spacecraft is again assumed to be the volumetric center of the main body. The atmospheric density is assumed to be constant at the value during solar maximum. The results are presented below:

Pressure	Area	Force	Moment
1.5E-08 N-m ²	0.415 m ²	6 E-09 N	8 E-10 N-m

TABLE C.4 Summary of Aerodynamic Torque

3. Equations of Motion

The equations of motion of a three-axis stabilized spacecraft have been derived by several authors. The ones presented here have been derived in ref Agrawal. These equations account for the gravity gradient torque in the right-hand side with the other disturbance torques on the left. The equations are presented below:

$$M_{x\text{dist}} = I_{xx} \frac{d^2\phi}{dt^2} + (4 \omega_o^2 (I_{yy} - I_{zz}) - \omega_o h_y) \phi + (-h_y - \omega_o (I_{xx} - I_{yy} + I_{zz})) \frac{d\psi}{dt} + h_z \frac{d\theta}{dt} - \omega_o h_z + \frac{dh_x}{dt}$$

$$M_{y\text{dist}} = I_{yy} \frac{d^2\theta}{dt^2} + 3 \omega_o^2 \theta (I_{xx} - I_{zz}) + \omega_o h_x \phi - h_z \frac{d\phi}{dt} + \omega_o h_z \psi + h_x \frac{d\psi}{dt} + \frac{dh_y}{dt}$$

$$M_{z\text{dist}} = I_{zz} \frac{d^2\psi}{dt^2} + (\omega_o^2 (I_{yy} - I_{xx}) - \omega_o h_y) \psi + (h_y + \omega_o (I_{xx} + I_{zz} - I_{yy})) \frac{d\phi}{dt} - h_x \frac{d\theta}{dt} + \omega_o h_x + \frac{dh_z}{dt}$$

where:

ϕ, θ, ψ are the attitude errors

ω_o is the orbital rate

h_x, h_y, h_z are the wheel momentum

I_{xx}, I_{yy}, I_{zz} are the spacecraft moment of inertias

The satellite's attitude control system is then modeled using the equations above and the disturbance torques previously described. The model is a PC-Matlab program given below:

```
% initialize variables for run
w_o = 1.032e-3; % orbital rate for 450 nmi circular, rad/sec
%
% coefficients of specular and diffuse reflections
rhos = 0.2; rhod = 0.0;
b_rho = (1-rhos); c_rho = 2*(rhos+1/3*rhod);
%
% read in inertia and center of mass (convert to MKS)
% note: inertia must be in lbm - ft^2
load a:\avhrr.spt; itot = avhrr.*0.04214;
load a:\avhrr.cen; cen = avhrr.*0.0254;
% coefficients for solar torque calcs
%
g_s = sin(0.6545); % offset of 37.5 deg;
h_s = cos(0.6545);
%
```

```

% input declination here in rads
%
s_del = sin(0.4102); % max declination
p_s = 4.644e-6; % solar pressure at 1 AU in N/m^2
% input solar array area
a_s = 4352; % area of solar arrays for AVHRR in sq. in.
a_s = a_s * 6.4516e-4; % convert to MKS
%
x_c = cen(1); y_c = cen(2); z_c = cen(3);
%
i_x = itot(1); i_y = itot(2); i_z = itot(3);
%
i_1 = 4*w_o^2*(i_y-i_z); i_2 = w_o*(i_x-i_y+i_z);
i_3 = 3*w_o^2*(i_x-i_z); i_4 = w_o^2*(i_y-i_x);
i_5 = w_o*(i_x+i_z-i_y);
torq_x = 0; torq_y = 0;
%
% define global variables (underscores)
global w_o g_s h_s s_del p_s a_s x_c y_c z_c i_x i_y i_z ...
      i_1 i_2 i_3 i_4 i_5 b_rho c_rho k_phi k_theta...
      k_psi t_phi t_theta t_psi torq_x torq_y;

function xdot = eqnmot(t,x)
% functions for solar torque
%
d = cos(w_o*t) .* g_s - sin(w_o*t) .* s_del;
e = cos(w_o*t) .* s_del + sin(w_o*t) .* g_s;

```

```

f = cos(0.67659434 .* cos(w_o*t) - 0.436332313);
g = sin(0.67659434 .* cos(w_o*t) - 0.436332313);
r = p_s * a_s .* (h_s .* f + g .* d);
aeroy = 8.e-10;
%
% solar and aero torque calculation
%
msx = r .* (y_c .* (b_rho .* d + c_rho .* g) - z_c .* ...
    (b_rho * h_s + c_rho .* f));
msy = r .* (z_c .* (b_rho .* e) - x_c .* (b_rho .* d + ...
    c_rho .* g)) + aeroy;
msz = r .* (x_c .* (b_rho * h_s + c_rho .* f) - y_c .* ...
    (b_rho .* e));
%
% determine if in eclipse and set Ms to zero
%
n = fix(w_o*t/(2*pi));
if ((w_o*t > (2.98+2*n*pi)) & (w_o*t < (4.76+2*n*pi))),
    msx = 0; msy = 0; msz = 0;
end
%
% check wheel speeds and desat if necessary
%
if x(7) > 10.47,
    torq_x = 1;
end
if x(8) > 10.47,

```

```

    torq_y = 1;
end
if x(7) < 0.1,
    torq_x = 0;
end
if x(8) < 0.1,
    torq_y = 0;
end
if torq_x == 1,
    if ((w_o*t > (5.76+2*n*pi)) & (w_o*t < (0.52+2*n*pi))),
        mmx = -0.0003;
    elseif ((w_o*t > (2.6+2*n*pi)) & (w_o*t < (3.67+2*n*pi))),
        mmx = -0.0003;
    else
        mmx = 0;
    end
else
    mmx = 0;
end
if torq_y == 1,
    if ((w_o*t > (1.0+2*n*pi)) & (w_o*t < (2.1+2*n*pi))),
        mmy = -0.0006;
    elseif ((w_o*t > (4.2+2*n*pi)) & (w_o*t < (5.2+2*n*pi))),
        mmy = -0.0006;
    else
        mmy = 0;
    end
end

```

```

else
    mmy = 0;
end

%
% differential equation matrix
%
% x(1) = phi    x(3) = theta    x(5) = psi
% x(2) = d/dt (phi)  x(4) = d/dt (theta)  x(6) = d/dt (psi)
% x(7) = roll wheel speed
% x(8) = pitch wheel speed
% x(9) = yaw wheel speed
% [xdot] = d/dt (x)
%
% roll error
%
xdot(1) = x(2);
xdot(2) = (i_x^(-1)) .* (((-i_1) + w_o .* x(8)) .* x(1) + ...
    (x(8) + i_2) .* x(6) - x(4) .* x(9) + w_o .* x(9) - ...
    k_phi .* (t_phi .* x(2) + x(1)) + msx+mmx);
%
% pitch error
%
xdot(3) = x(4);
xdot(4) = (i_y^(-1)) .* (((-i_3) .* x(3)) - w_o .* x(7) .* ...
    x(1) + x(9) .* x(2) - w_o .* x(9) .* x(5) - x(7) ...
    .* x(6) - k_theta .* (t_theta .* x(4) + x(3)) + msy+mmy);
%

```

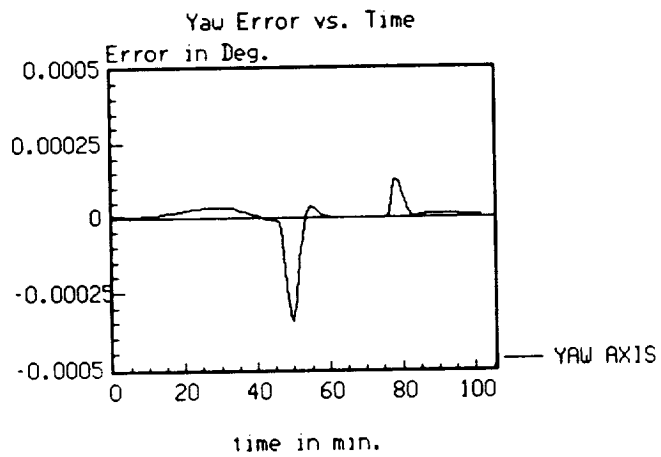
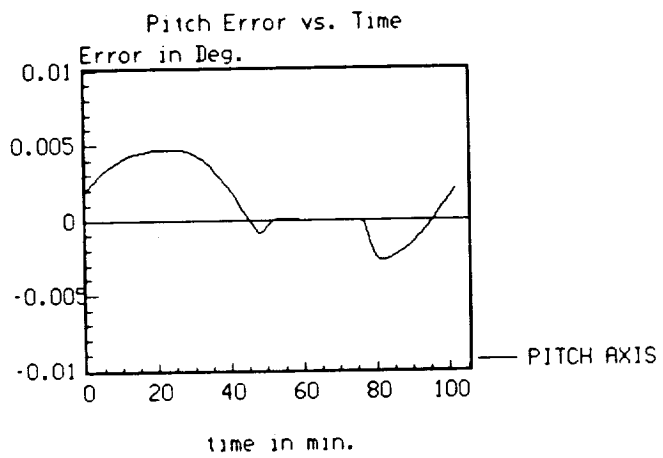
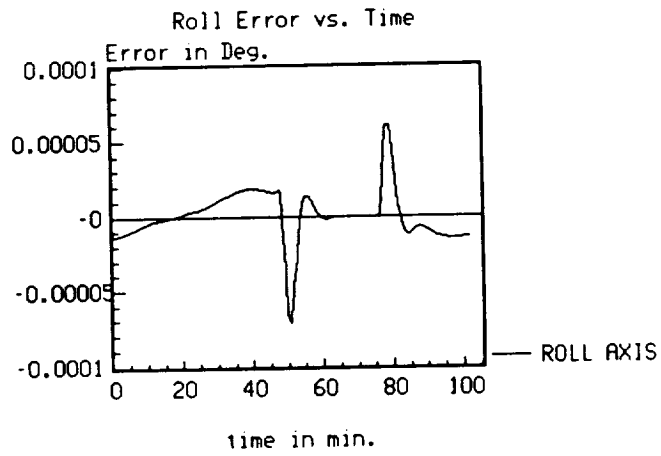
```

% yaw error
%
xdot(5) = x(6);
xdot(6) = (i_z^(-1)) .* (((-i_4) + w_o .* x(8)) .* x(5) - ...
    (x(8) + i_5) .* x(2) + x(7) .* x(4) - w_o .* x(7)...
    - k_psi .* (t_psi .* x(6) + x(5)) + msz);
%
% wheel control
% wheel inertias in kg-m^2
%
iwx = 0.009; iwy = 0.009; iwz = 0.009;
xdot(7) = k_phi .* (t_phi .* x(2) + x(1))./iwx;
xdot(8) = k_theta .* (t_theta .* x(4) + x(3))./iwy;
xdot(9) = k_psi .* (t_psi .* x(6) + x(5))./iwz;

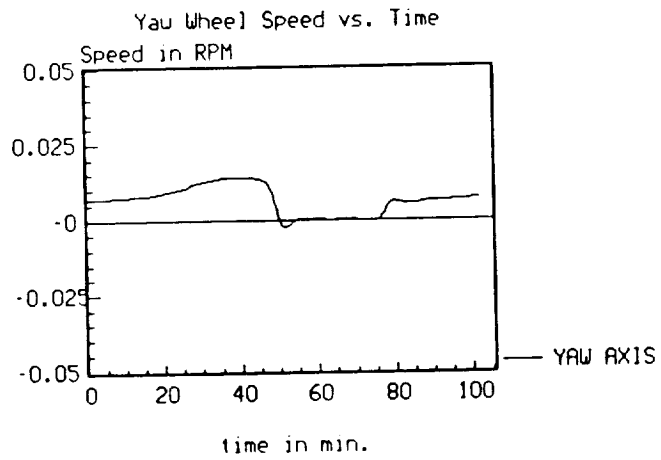
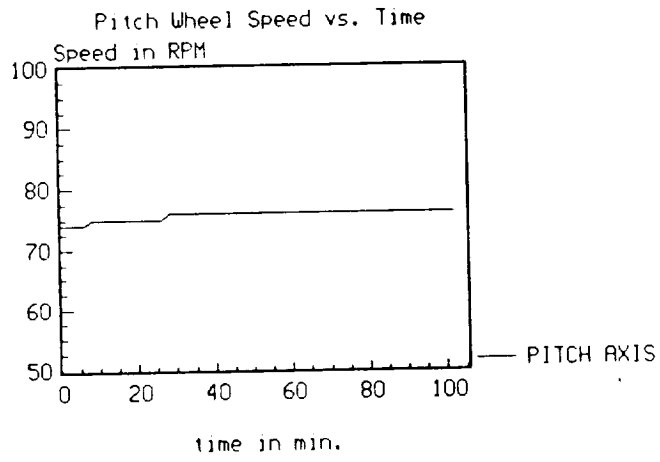
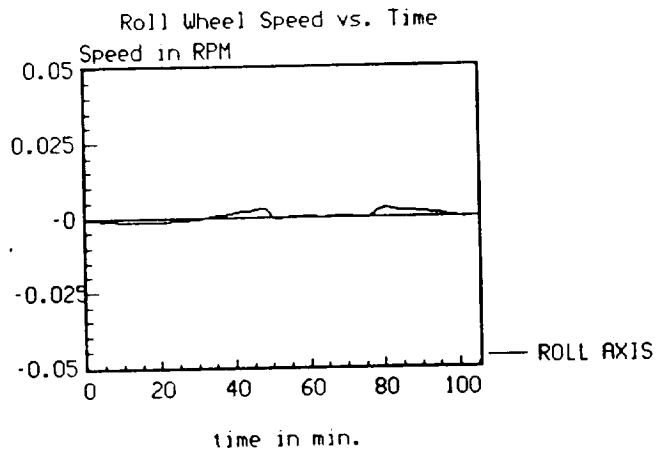
```

These equations are integrated using a Runge-Kutta-Fehlberg integration method provided with Matlab. The results are plotted for one orbit on the following pages. The simulation shows that the pitch wheel absorbs the angular momentum of the rotation of the spacecraft about the pitch axis due to its orbital motion. The roll and yaw wheel should only need desaturation if a change in the orbit is required.

Pointing Error for AVHRR Payload



Wheel Speed for AVHRR Payload



APPENDIX D

THERMAL CONTROL CALCULATIONS

The thermal control appendix contains a partial ITAS output for the AVHRR configured spacecraft. This partial output is in the form of steady state temperatures and is provided to show a sampling of the ITAS program's capability. The payload and the bus were modeled by approximately 150 nodes and several runs were completed for various orbits. Because the majority of the inputs into the ITAS model were assumed, the run should be considered as a bulk analysis. Very specific and detailed heat data, down to the circuit board level, would be required for more accurate temperatures. This data was unobtainable in the short time this project was completed.

 Date: 12/15/90 Time: 09:43:28.10

=====
 Thermal Analysis Parameters
 =====

1. Solution Method:1.Steady-State 2.Transient.....	1
2. Solution Time Step(minutes).....	0.10
3. Final Time (minutes);if <0 then no of orbs.....	123.80
4. Starting Temperature(Kelvin).....	300.00
5. Temperature Print Interval (minutes).....	20
6. Heat-Flow Print Interval (Iterations).....	9999
7. Temperature Unit 1:K, 2:C, 3:F, 4:R.....	2
8. Solution Accuracy Parameter.....	130
9. Solution Convergence Parameter.....	1.30
10. Solution Tolerance.....	0.00010
11. Transient Solution Stability Factor.....	0.850
12. Include User-Defined Network..... (Y/N).....	Y
13. Print RADK, POWER..... (Y/N).....	N
14. Print Transient Time/Temperature... (Y/N).....	N
15. Starting Temperatures Forced (No.4) (Y/N).....	Y

=====
 //
 ITAS THERMAL ANALYSIS
 //

ITAS ABSORBED HEAT RATES FROM ORBITAL INCIDENT & IR AND UV MARICES

 Date: 12/15/90 Time: 09:43:28.10

//
 ITAS ABSORBED HEAT-LOAD COMPUTATIONS
 //

Date: 12/15/90 Time: 09:43:28.10

=====
 Script-F Control Parameters
 =====

1. SPACE (SINK) Node Number.....	349
2. Cutoff Limit For Area*Script-F (Sq.cm.).....	0.1000E+01
3. Cutoff Limit For Blackbody Viewfactors.....	0.0000
4. SPACE (SINK) Node Emissivity.....	0.9999
5. SPACE (SINK) Node Temperature (Kelvin).....	0.0000
6. SINDA Interface File To Be Generated (Y/N).....	Y
7. SINDA Radiation Conductor Number At Start.....	100000
8. Print control: 0:No,do not print, 1:Yes, print all.....	0

Seq	Surface No	Node No	Alpha	Emiss	T/Mass	Dissip	Matr ID
1	1.01	1	0.30	0.80	1.00	0.00	153
2	1.02	2	0.30	0.80	1.00	0.00	153
3	1.03	3	0.30	0.80	1.00	0.00	153
4	1.04	4	0.30	0.80	1.00	0.00	153
5	1.05	5	0.30	0.80	1.00	0.00	153
6	2.01	6	0.42	0.21	1.00	0.10	118
7	2.02	7	0.42	0.21	1.00	0.10	118
8	2.03	8	0.42	0.21	1.00	0.10	118
9	2.04	9	0.42	0.21	1.00	0.10	118
10	2.05	10	0.42	0.21	1.00	0.10	118
11	2.06	11	0.42	0.21	1.00	0.10	118
12	3.01	12	0.38	0.19	1.00	9.00	210
13	3.02	13	0.38	0.19	1.00	9.00	210
14	3.03	14	0.38	0.19	1.00	9.00	210
15	3.04	15	0.38	0.19	1.00	9.00	210
16	3.05	16	0.38	0.19	1.00	9.00	210
17	3.06	17	0.38	0.19	1.00	9.00	210
18	4.01	18	0.42	0.21	1.00	0.30	118
19	4.02	19	0.42	0.21	1.00	0.30	118
20	4.03	20	0.42	0.21	1.00	0.30	118
21	4.04	21	0.42	0.21	1.00	0.30	118
22	4.05	22	0.42	0.21	1.00	0.30	118
23	4.06	23	0.42	0.21	1.00	0.30	118
24	5.01	24	0.44	0.05	1.00	0.20	34
25	5.02	25	0.44	0.05	1.00	0.20	34
26	5.03	26	0.44	0.05	1.00	0.20	34
27	5.04	27	0.44	0.05	1.00	0.20	34
28	5.05	28	0.44	0.05	1.00	0.20	34
29	5.06	29	0.44	0.05	1.00	0.20	34
30	5.07	30	0.44	0.05	1.00	0.20	34
31	5.08	31	0.44	0.05	1.00	0.20	34
32	5.09	32	0.44	0.05	1.00	0.20	34
33	5.10	33	0.44	0.05	1.00	0.20	34
34	5.11	34	0.44	0.05	1.00	0.20	34
35	5.12	35	0.44	0.05	1.00	0.20	34
36	5.13	36	0.44	0.05	1.00	0.20	34
37	5.14	37	0.44	0.05	1.00	0.20	34
38	5.15	38	0.44	0.05	1.00	0.20	34
39	5.16	39	0.44	0.05	1.00	0.20	34
40	5.17	40	0.44	0.05	1.00	0.20	34
41	5.18	41	0.44	0.05	1.00	0.20	34
42	6.01	42	0.25	0.72	1.00	1.50	173
43	6.02	43	0.25	0.72	1.00	1.50	173
44	6.03	44	0.25	0.72	1.00	1.50	173
45	6.04	45	0.25	0.72	1.00	1.50	173
46	6.05	46	0.25	0.72	1.00	1.50	173
47	7.01	47	0.42	0.21	1.00	0.30	118

48	7.02	48	0.42	0.21	1.00	0.30	118
	7.03	49	0.42	0.21	1.00	0.30	118
50	7.04	50	0.42	0.21	1.00	0.30	118
51	7.05	51	0.42	0.21	1.00	0.30	118
52	7.06	52	0.42	0.21	1.00	0.30	118
53	8.01	53	0.42	0.21	1.00	0.30	118
54	8.02	54	0.42	0.21	1.00	0.30	118
55	8.03	55	0.42	0.21	1.00	0.30	118
56	8.04	56	0.42	0.21	1.00	0.30	118
57	8.05	57	0.42	0.21	1.00	0.30	118
58	8.06	58	0.42	0.21	1.00	0.30	118
59	9.00	59	0.19	0.08	1.00	0.00	175
60	10.00	60	0.25	0.72	1.00	0.50	173
61	11.00	61	0.25	0.72	1.00	0.50	173
62	12.00	62	0.05	0.80	1.00	0.00	36
63	13.00	63	0.05	0.80	1.00	0.00	36
64	14.01	64	0.68	0.48	1.00	0.50	116
65	14.02	65	0.68	0.48	1.00	0.50	116
66	14.03	66	0.68	0.48	1.00	0.50	116
67	14.04	67	0.68	0.48	1.00	0.50	116
68	14.05	68	0.68	0.48	1.00	0.50	116
69	14.06	69	0.68	0.48	1.00	0.50	116
70	14.07	70	0.68	0.48	1.00	0.50	116
71	14.08	71	0.68	0.48	1.00	0.50	116
72	14.09	72	0.68	0.48	1.00	0.50	116
73	14.10	73	0.68	0.48	1.00	0.50	116
74	14.11	74	0.68	0.48	1.00	0.50	116
75	14.12	75	0.68	0.48	1.00	0.50	116
76	14.13	76	0.68	0.48	1.00	0.50	116
77	14.14	77	0.68	0.48	1.00	0.50	116
78	14.15	78	0.68	0.48	1.00	0.50	116
79	14.16	79	0.68	0.48	1.00	0.50	116
80	14.17	80	0.68	0.48	1.00	0.50	116
81	14.18	81	0.68	0.48	1.00	0.50	116
82	14.19	82	0.68	0.48	1.00	0.50	116
83	14.20	83	0.68	0.48	1.00	0.50	116
84	14.21	84	0.68	0.48	1.00	0.50	116
85	14.22	85	0.68	0.48	1.00	0.50	116
86	14.23	86	0.68	0.48	1.00	0.50	116
87	14.24	87	0.68	0.48	1.00	0.50	116
88	15.01	88	0.68	0.48	1.00	0.50	116
89	15.02	89	0.68	0.48	1.00	0.50	116
90	15.03	90	0.68	0.48	1.00	0.50	116
91	15.04	91	0.68	0.48	1.00	0.50	116
92	15.05	92	0.68	0.48	1.00	0.50	116
93	15.06	93	0.68	0.48	1.00	0.50	116
94	15.07	94	0.68	0.48	1.00	0.50	116
95	15.08	95	0.68	0.48	1.00	0.50	116
96	15.09	96	0.68	0.48	1.00	0.50	116
97	15.10	97	0.68	0.48	1.00	0.50	116
98	15.11	98	0.68	0.48	1.00	0.50	116
99	15.12	99	0.68	0.48	1.00	0.50	116

100	15.13	100	0.68	0.48	1.00	0.50	116
	15.14	101	0.68	0.48	1.00	0.50	116
102	15.15	102	0.68	0.48	1.00	0.50	116
103	15.16	103	0.68	0.48	1.00	0.50	116
104	15.17	104	0.68	0.48	1.00	0.50	116
105	15.18	105	0.68	0.48	1.00	0.50	116
106	15.19	106	0.68	0.48	1.00	0.50	116
107	15.20	107	0.68	0.48	1.00	0.50	116
108	15.21	108	0.68	0.48	1.00	0.50	116
109	15.22	109	0.68	0.48	1.00	0.50	116
110	15.23	110	0.68	0.48	1.00	0.50	116
111	15.24	111	0.68	0.48	1.00	0.50	116
112	16.01	112	0.68	0.48	1.00	0.50	116
113	16.02	113	0.68	0.48	1.00	0.50	116
114	16.03	114	0.68	0.48	1.00	0.50	116
115	16.04	115	0.68	0.48	1.00	0.50	116
116	16.05	116	0.68	0.48	1.00	0.50	116
117	16.06	117	0.68	0.48	1.00	0.50	116
118	16.07	118	0.68	0.48	1.00	0.50	116
119	16.08	119	0.68	0.48	1.00	0.50	116
120	16.09	120	0.68	0.48	1.00	0.50	116
121	16.10	121	0.68	0.48	1.00	0.50	116
122	16.11	122	0.68	0.48	1.00	0.50	116
123	16.12	123	0.68	0.48	1.00	0.50	116
124	16.13	124	0.68	0.48	1.00	0.50	116
125	16.14	125	0.68	0.48	1.00	0.50	116
126	16.15	126	0.68	0.48	1.00	0.50	116
127	16.16	127	0.68	0.48	1.00	0.50	116
128	16.17	128	0.68	0.48	1.00	0.50	116
129	16.18	129	0.68	0.48	1.00	0.50	116
130	16.19	130	0.68	0.48	1.00	0.50	116
131	16.20	131	0.68	0.48	1.00	0.50	116
132	16.21	132	0.68	0.48	1.00	0.50	116
133	16.22	133	0.68	0.48	1.00	0.50	116
134	16.23	134	0.68	0.48	1.00	0.50	116
135	16.24	135	0.68	0.48	1.00	0.50	116
136	22.00	136	0.30	0.80	1.00	0.00	153
137	23.01	137	0.68	0.48	1.00	0.70	116
138	23.02	138	0.68	0.48	1.00	0.70	116
139	23.03	139	0.68	0.48	1.00	0.70	116
140	23.04	140	0.68	0.48	1.00	0.70	116
141	23.05	141	0.68	0.48	1.00	0.70	116
142	24.01	142	0.68	0.48	1.00	0.70	116
143	24.02	143	0.68	0.48	1.00	0.70	116
144	24.03	144	0.68	0.48	1.00	0.70	116
145	24.04	145	0.68	0.48	1.00	0.70	116
146	24.05	146	0.68	0.48	1.00	0.70	116

////////////////////////////////////
 ITAS SCRIPT-F (RADK) COMPUTATIONS
 //////////////////////////////////////

147 IS A FIXED TEMPERATURE NODE

WARNING ITAS HAS DIFFERENT NUMBER OF SURFACES THAN CONTROL CARD SPECIFIED

CONTROL CARD VALUE SET TO ITAS(148)

SCRIPT-F CALC CPU TIME (second) = 223.820

Date: 12/15/90 Time: 09:47:15.10

=====

Orbital Control Parameters

=====

- 0. Print:0:Summary;1:Detail;2:Individual Tables;3:Options 1+2. 0
- 1. Power Units In The Output 0:Watt, 1:Btu/hr, 2:Btu/min..... 2
- 2. Orbit And Attitude Remain Constant Throughout Run (Y/N).... Y
- 3. Spacecraft Is 0:Stationary, 1:Spinning..... 0
- 4. Spacecraft Geometry Is:
 - 0:Fixed, or 1:Changing Throughout Orbit..... 0
- 5. Shadow Entry/Exit Point Calculation Accuracy Factor..... 5
- 6. Earth and Albedo Flux Computation Accuracy Factor-1..... 6
- 7. Earth and Albedo Flux Computation Accuracy Factor-2..... 10
- Spacecraft Attitude:
- 8. Spacecraft Is 1:Earth-Oriented, 2:Sun-Oriented..... 1
- 9. Spacecraft Is Orbiting Around 1:Earth, or 2:Moon..... 1
- Select Option (A or B) For Beta Angle:
- Option Selected..... A

- Option A:
- 10. Longitude of the Ascending Node (Degrees)..... 52.50
- 11. Sun Declination (Degrees)..... 0.00
- 12. Sun Right Ascension (Degrees)..... 0.00
- 13. Orbit Inclination (Degrees)..... 98.75
- 14. Argument of Perifocus (Degrees)..... 0.00

- Option B:
- 15. Beta Angle (Degrees), Orbit Normal & Sun Vector..... 90.00
- 16. Cigma Angle (Degrees), 0.00
(Orbit XO & Sun vector Projection in Orbit Plane)

- 17. Angular Increment of the True Anomaly (Degrees)..... 30.00
- 18. Starting Point in the Orbit (Degrees)..... 0.00
- 19. Rotation Angles (Degrees):
 - X-ROT..... 0.00
 - Y-ROT..... 0.00
 - Z-ROT..... 0.00
- 20. Radiation Constants:Solar, Albedo, Earth-IR:
 - SOLAR..... 429.50
 - ALBEDO..... 0.30
 - EARTH-IR..... 75.12
- 21. Orbit Altitude At Apogee(=0 Circular Orb)NM (-ve for KM).. 0.00
- 22. Orbit Altitude At Perigee(Closest Point);NM (-ve for KM).. 450.00
- 23. Satellite Travelling 1:North, 2:South At Perigee..... 1
- Earth-Effects (IR and Albedo) Computation Options:
- 31. Altitude Above Which All Earth Inputs Are Ignored 225.00

2. Albedo & Earth-IR Computation Options (A/B/C)..... C
 A: Detailed (Accurate) Computation, The Real Thing!
 B: Approximation (Faster), No Blockage, For Parametric
 C: Approximation (Fastest), No Alb/E-IR, For Parametric Studies ONLY

////////////////////////////////////
 ITAS ORBITAL INCIDENT FLUX COMPUTATIONS
 //////////////////////////////////////

ITAS ORBIT CONTROL PARAMETERS:
 NUMBER OF SURFACES= 146
 ENERGY UNITS = 2 REF. ITAS ORBITAL SETUP MENU
 SPIN = 0 =0 NO; =1 YES
 VARIABLE GEOMETRY = 0 =0 NO; =1 YES

NUMBER OF SURFACES IDENTIFIED IN THE BLOCKAGE TABLES= 146

NOTE: SURFACE AREAS ARE IN CENTIMETERS
 DP & TP CALCULATED FROM THE ST CARD: 80.170 -8.500
 ITAS ORBITAL PARAMETERS INITIAL CONDITIONS:

S/C ORIENTATION MODE= 1 =1 EARTH; =2 STAR; =3 SUN
 ALBEDO, EARTH-SHINE, SOLAR CONSTANT= 0.30 75.12 429.50

- o Angle from the ascending node to perigee,
 measured in the orbit plane at the center
 of the earth = 0.00000E+00 Degrees
- o Longitude of the ascending node in X, Y, Z,
 angle past equinox, measured in the
 equatorial = 5.25014E+01 Degrees
- o Sun position In Celestial Coordinates :
 COS (AS) = 1.00000E+00-->Equinox
 COS (BS) = -2.60943E-05
 COS (GS) = -1.13442E-05-->North

 AS = 1.63027E-03 Degrees
 BS = 9.00015E+01 Degrees
 GS = 9.00006E+01 Degrees
- o Mean anomaly of the sun central angle from
 perihelion = 7.60605E+01 Degrees
- o Approximation to Kepler s solution for the
 sun central = -1.63024E-03 Degrees; Measured
 In The Ecliptic Plane From Line Of Nodes
- o Sun RA = 0.00000E+00 Degrees
- o Sun DEC = 0.00000E+00 Degrees

~ Sun Vector Direction Cosines In Orbit Plane:

COS (alfa) = 6.08743E-01
 o COS (gama) = 1.20690E-01
 o COS (BETA) = 7.84134E-01

 o (alfa) = 5.25014E+01 Degrees
 o (gama) = 8.30681E+01 Degrees
 o * (BETA) = 3.83593E+01 Degrees <---- *Note

 o BETA * = 3.83593E+01 Degrees <---- *Note
 o CIGMA * = 1.12141E+01 Degrees

* Note: BETA: The Angle Between The Sun Vector
 And The Orbit Normal, And
 CIGMA: The Angle Between The Projection Of
 The Sun Vector In The Orbit Plane
 From Perigee (=0 for Circular Orb)

			ECC	INC(DEG)	LATP(DEG)	LONG(DEG)	RP(NM)			
			0.0000	98.750	0.000	0.000	450.000			
DP(DAY)	TP(HRS)	DT(MIN)	DETA(DEG)	ROT1(DEG)	ROT2(DEG)	ROT3(DEG)				
80.170	-8.500	0.000	30.00	0.00	0.00	0.00				
SURF	NODE	BTAB	AREA	ABSORB	EMIT	ALPHA	BETA	GAMMA	COMMENT	
1	1	1	6.22	1.0	1.0	1.0	0.0	0.0	1.01	
2	2	4	4.47	1.0	1.0	0.0	1.0	0.0	1.02	
3	3	3	5.11	1.0	1.0	0.0	0.0	1.0	1.03	
4	4	2	6.22	1.0	1.0	-1.0	0.0	0.0	1.04	
5	5	5	4.47	1.0	1.0	0.0	-1.0	0.0	1.05	
6	6	20	0.63	1.0	1.0	1.0	0.0	0.0	2.01	
7	7	21	0.63	1.0	1.0	0.0	1.0	0.0	2.02	
8	8	43	0.25	1.0	1.0	0.0	0.0	1.0	2.03	
9	9	22	0.63	1.0	1.0	-1.0	0.0	0.0	2.04	
10	10	23	0.63	1.0	1.0	0.0	-1.0	0.0	2.05	
11	11	44	0.25	1.0	1.0	0.0	0.0	-1.0	2.06	
12	12	17	0.72	1.0	1.0	1.0	0.0	0.0	3.01	
13	13	15	0.94	1.0	1.0	0.0	1.0	0.0	3.02	
14	14	26	0.58	1.0	1.0	0.0	0.0	1.0	3.03	
15	15	18	0.72	1.0	1.0	-1.0	0.0	0.0	3.04	
16	16	16	0.94	1.0	1.0	0.0	-1.0	0.0	3.05	
17	17	27	0.58	1.0	1.0	0.0	0.0	-1.0	3.06	
18	18	51	0.25	1.0	1.0	1.0	0.0	0.0	4.01	
19	19	24	0.59	1.0	1.0	0.0	1.0	0.0	4.02	
20	20	65	0.10	1.0	1.0	0.0	0.0	1.0	4.03	
21	21	52	0.25	1.0	1.0	-1.0	0.0	0.0	4.04	
22	22	25	0.59	1.0	1.0	0.0	-1.0	0.0	4.05	
23	23	66	0.10	1.0	1.0	0.0	0.0	-1.0	4.06	
24	24	59	0.17	1.0	1.0	0.8	0.3	-0.5	5.01	
25	25	64	0.17	1.0	1.0	0.8	0.6	0.0	5.02	
26	26	62	0.17	1.0	1.0	0.8	0.3	0.5	5.03	

27	27	63	0.17	1.0	1.0	0.8	-0.3	0.5	5.04
28	28	61	0.17	1.0	1.0	0.8	-0.6	0.0	5.05
29	29	60	0.17	1.0	1.0	0.8	-0.3	-0.5	5.06
30	30	31	0.38	1.0	1.0	0.0	0.5	-0.9	5.07
31	31	32	0.38	1.0	1.0	0.0	1.0	0.0	5.08
32	32	29	0.38	1.0	1.0	0.0	0.5	0.9	5.09
33	33	33	0.38	1.0	1.0	0.0	-0.5	0.9	5.10
34	34	28	0.38	1.0	1.0	0.0	-1.0	0.0	5.11
35	35	30	0.38	1.0	1.0	0.0	-0.5	-0.9	5.12
36	36	58	0.17	1.0	1.0	-0.8	0.3	-0.5	5.13
37	37	57	0.17	1.0	1.0	-0.8	0.6	0.0	5.14
38	38	54	0.17	1.0	1.0	-0.8	0.3	0.5	5.15
39	39	55	0.17	1.0	1.0	-0.8	-0.3	0.5	5.16
40	40	53	0.17	1.0	1.0	-0.8	-0.6	0.0	5.17
41	41	56	0.17	1.0	1.0	-0.8	-0.3	-0.5	5.18
42	42	8	2.52	1.0	1.0	1.0	0.0	0.0	6.01
43	43	13	1.16	1.0	1.0	0.0	1.0	0.0	6.02
44	44	7	3.17	1.0	1.0	0.0	0.0	1.0	6.03
45	45	9	2.52	1.0	1.0	-1.0	0.0	0.0	6.04
46	46	14	1.16	1.0	1.0	0.0	-1.0	0.0	6.05
47	47	35	0.33	1.0	1.0	1.0	0.0	0.0	7.01
48	48	36	0.33	1.0	1.0	0.0	1.0	0.0	7.02
49	49	45	0.25	1.0	1.0	0.0	0.0	1.0	7.03
50	50	37	0.33	1.0	1.0	-1.0	0.0	0.0	7.04
51	51	38	0.33	1.0	1.0	0.0	-1.0	0.0	7.05
52	52	46	0.25	1.0	1.0	0.0	0.0	-1.0	7.06
53	53	39	0.33	1.0	1.0	1.0	0.0	0.0	8.01
54	54	40	0.33	1.0	1.0	0.0	1.0	0.0	8.02
55	55	47	0.25	1.0	1.0	0.0	0.0	1.0	8.03
56	56	41	0.33	1.0	1.0	-1.0	0.0	0.0	8.04
57	57	42	0.33	1.0	1.0	0.0	-1.0	0.0	8.05
58	58	48	0.25	1.0	1.0	0.0	0.0	-1.0	8.06
59	59	12	1.19	1.0	1.0	-1.0	0.0	0.0	9.00
60	60	34	0.35	1.0	1.0	0.0	0.0	-1.0	10.00
61	61	19	0.65	1.0	1.0	0.0	0.0	1.0	11.00
62	62	10	2.16	1.0	1.0	0.0	0.0	1.0	12.00
63	63	11	1.33	1.0	1.0	0.0	0.0	1.0	13.00
64	64	93	0.08	1.0	1.0	0.0	0.3	-1.0	14.01
65	65	107	0.08	1.0	1.0	0.0	0.7	-0.7	14.02
66	66	94	0.08	1.0	1.0	0.0	1.0	-0.3	14.03
67	67	101	0.08	1.0	1.0	0.0	1.0	0.3	14.04
68	68	84	0.08	1.0	1.0	0.0	0.7	0.7	14.05
69	69	102	0.08	1.0	1.0	0.0	0.3	1.0	14.06
70	70	85	0.08	1.0	1.0	0.0	-0.3	1.0	14.07
71	71	103	0.08	1.0	1.0	0.0	-0.7	0.7	14.08
72	72	95	0.08	1.0	1.0	0.0	-1.0	0.3	14.09
73	73	96	0.08	1.0	1.0	0.0	-1.0	-0.3	14.10
74	74	97	0.08	1.0	1.0	0.0	-0.7	-0.7	14.11
75	75	98	0.08	1.0	1.0	0.0	-0.3	-1.0	14.12
76	76	118	0.04	1.0	1.0	-1.0	0.0	0.0	14.13
77	77	139	0.04	1.0	1.0	-1.0	0.0	0.0	14.14
78	78	135	0.04	1.0	1.0	-1.0	0.0	0.0	14.15

79	79	136	0.04	1.0	1.0	-1.0	0.0	0.0	14.16
80	80	119	0.04	1.0	1.0	-1.0	0.0	0.0	14.17
81	81	120	0.04	1.0	1.0	-1.0	0.0	0.0	14.18
82	82	121	0.04	1.0	1.0	-1.0	0.0	0.0	14.19
83	83	140	0.04	1.0	1.0	-1.0	0.0	0.0	14.20
84	84	122	0.04	1.0	1.0	-1.0	0.0	0.0	14.21
85	85	123	0.04	1.0	1.0	-1.0	0.0	0.0	14.22
86	86	124	0.04	1.0	1.0	-1.0	0.0	0.0	14.23
87	87	125	0.04	1.0	1.0	-1.0	0.0	0.0	14.24
88	88	86	0.08	1.0	1.0	1.0	0.3	0.0	15.01
89	89	87	0.08	1.0	1.0	0.7	0.7	0.0	15.02
90	90	79	0.08	1.0	1.0	0.3	1.0	0.0	15.03
91	91	99	0.08	1.0	1.0	-0.3	1.0	0.0	15.04
92	92	88	0.08	1.0	1.0	-0.7	0.7	0.0	15.05
93	93	100	0.08	1.0	1.0	-1.0	0.3	0.0	15.06
94	94	80	0.08	1.0	1.0	-1.0	-0.3	0.0	15.07
95	95	108	0.08	1.0	1.0	-0.7	-0.7	0.0	15.08
96	96	77	0.08	1.0	1.0	-0.3	-1.0	0.0	15.09
97	97	104	0.08	1.0	1.0	0.3	-1.0	0.0	15.10
98	98	89	0.08	1.0	1.0	0.7	-0.7	0.0	15.11
99	99	81	0.08	1.0	1.0	1.0	-0.3	0.0	15.12
100	100	126	0.04	1.0	1.0	0.0	0.0	1.0	15.13
101	101	127	0.04	1.0	1.0	0.0	0.0	1.0	15.14
102	102	128	0.04	1.0	1.0	0.0	0.0	1.0	15.15
103	103	137	0.04	1.0	1.0	0.0	0.0	1.0	15.16
104	104	114	0.04	1.0	1.0	0.0	0.0	1.0	15.17
105	105	129	0.04	1.0	1.0	0.0	0.0	1.0	15.18
106	106	130	0.04	1.0	1.0	0.0	0.0	1.0	15.19
107	107	141	0.04	1.0	1.0	0.0	0.0	1.0	15.20
108	108	113	0.04	1.0	1.0	0.0	0.0	1.0	15.21
109	109	142	0.04	1.0	1.0	0.0	0.0	1.0	15.22
110	110	131	0.04	1.0	1.0	0.0	0.0	1.0	15.23
111	111	132	0.04	1.0	1.0	0.0	0.0	1.0	15.24
112	112	105	0.08	1.0	1.0	1.0	0.0	0.3	16.01
113	113	82	0.08	1.0	1.0	0.7	0.0	0.7	16.02
114	114	90	0.08	1.0	1.0	0.3	0.0	1.0	16.03
115	115	75	0.08	1.0	1.0	-0.3	0.0	1.0	16.04
116	116	110	0.08	1.0	1.0	-0.7	0.0	0.7	16.05
117	117	91	0.08	1.0	1.0	-1.0	0.0	0.3	16.06
118	118	83	0.08	1.0	1.0	-1.0	0.0	-0.3	16.07
119	119	78	0.08	1.0	1.0	-0.7	0.0	-0.7	16.08
120	120	109	0.08	1.0	1.0	-0.3	0.0	-1.0	16.09
121	121	106	0.08	1.0	1.0	0.3	0.0	-1.0	16.10
122	122	76	0.08	1.0	1.0	0.7	0.0	-0.7	16.11
123	123	92	0.08	1.0	1.0	1.0	0.0	-0.3	16.12
124	124	143	0.04	1.0	1.0	0.0	1.0	0.0	16.13
125	125	111	0.04	1.0	1.0	0.0	1.0	0.0	16.14
126	126	138	0.04	1.0	1.0	0.0	1.0	0.0	16.15
127	127	115	0.04	1.0	1.0	0.0	1.0	0.0	16.16
128	128	146	0.04	1.0	1.0	0.0	1.0	0.0	16.17
129	129	133	0.04	1.0	1.0	0.0	1.0	0.0	16.18
130	130	134	0.04	1.0	1.0	0.0	1.0	0.0	16.19

131	131	116	0.04	1.0	1.0	0.0	1.0	0.0	16.20
2	132	145	0.04	1.0	1.0	0.0	1.0	0.0	16.21
133	133	144	0.04	1.0	1.0	0.0	1.0	0.0	16.22
134	134	112	0.04	1.0	1.0	0.0	1.0	0.0	16.23
135	135	117	0.04	1.0	1.0	0.0	1.0	0.0	16.24
136	136	6	3.78	1.0	1.0	0.0	0.0	1.0	22.00
137	137	67	0.08	1.0	1.0	1.0	0.0	0.0	23.01
138	138	49	0.25	1.0	1.0	0.0	1.0	0.0	23.02
139	139	68	0.08	1.0	1.0	0.0	0.0	1.0	23.03
140	140	69	0.08	1.0	1.0	-1.0	0.0	0.0	23.04
141	141	70	0.08	1.0	1.0	0.0	0.0	-1.0	23.05
142	142	71	0.08	1.0	1.0	1.0	0.0	0.0	24.01
143	143	72	0.08	1.0	1.0	0.0	0.0	1.0	24.02
144	144	73	0.08	1.0	1.0	-1.0	0.0	0.0	24.03
145	145	50	0.25	1.0	1.0	0.0	-1.0	0.0	24.04
146	146	74	0.08	1.0	1.0	0.0	0.0	-1.0	24.05

FINAL ORBITAL TIME-AVERAGED FLUXES (A=E=1) IN BTU/HR/SQ.FT. or WATT/SqCm

ORBIT SUN-TIME (PERCENT) = 76.95

SURF	NODE	SOLAR(S)	ALBEDO(A)	EAR-IR(E)	S+A+E	S+A (ABS)	IR (ABS)	
1	1	85.63	0.00	0.00	85.63	85.63	0.00	1.01
2	2	74.04	0.00	0.00	74.04	74.04	0.00	1.02
3	3	259.18	0.00	0.00	259.18	259.18	0.00	1.03
4	4	18.18	0.00	0.00	18.18	18.18	0.00	1.04
5	5	73.78	0.00	0.00	73.78	73.78	0.00	1.05
6	6	0.00	0.00	0.00	0.00	0.00	0.00	2.01
7	7	74.04	0.00	0.00	74.04	74.04	0.00	2.02
8	8	0.00	0.00	0.00	0.00	0.00	0.00	2.03
9	9	8.19	0.00	0.00	8.19	8.19	0.00	2.04
10	10	0.00	0.00	0.00	0.00	0.00	0.00	2.05
11	11	0.00	0.00	0.00	0.00	0.00	0.00	2.06
12	12	85.63	0.00	0.00	85.63	85.63	0.00	3.01
13	13	74.04	0.00	0.00	74.04	74.04	0.00	3.02
14	14	0.00	0.00	0.00	0.00	0.00	0.00	3.03
15	15	0.00	0.00	0.00	0.00	0.00	0.00	3.04
16	16	0.00	0.00	0.00	0.00	0.00	0.00	3.05
17	17	0.00	0.00	0.00	0.00	0.00	0.00	3.06
18	18	0.00	0.00	0.00	0.00	0.00	0.00	4.01
19	19	0.00	0.00	0.00	0.00	0.00	0.00	4.02
20	20	0.00	0.00	0.00	0.00	0.00	0.00	4.03
21	21	6.02	0.00	0.00	6.02	6.02	0.00	4.04
22	22	73.78	0.00	0.00	73.78	73.78	0.00	4.05
23	23	0.00	0.00	0.00	0.00	0.00	0.00	4.06
24	24	0.00	0.00	0.00	0.00	0.00	0.00	5.01
25	25	0.00	0.00	0.00	0.00	0.00	0.00	5.02
26	26	0.00	0.00	0.00	0.00	0.00	0.00	5.03
27	27	0.00	0.00	0.00	0.00	0.00	0.00	5.04
28	28	0.00	0.00	0.00	0.00	0.00	0.00	5.05
29	29	0.00	0.00	0.00	0.00	0.00	0.00	5.06
30	30	0.00	0.00	0.00	0.00	0.00	0.00	5.07
31	31	0.00	0.00	0.00	0.00	0.00	0.00	5.08

32	32	0.00	0.00	0.00	0.00	0.00	0.00	0.00	5.09
33	33	0.00	0.00	0.00	0.00	0.00	0.00	0.00	5.10
34	34	0.00	0.00	0.00	0.00	0.00	0.00	0.00	5.11
35	35	0.00	0.00	0.00	0.00	0.00	0.00	0.00	5.12
36	36	0.00	0.00	0.00	0.00	0.00	0.00	0.00	5.13
37	37	0.00	0.00	0.00	0.00	0.00	0.00	0.00	5.14
38	38	0.00	0.00	0.00	0.00	0.00	0.00	0.00	5.15
39	39	0.00	0.00	0.00	0.00	0.00	0.00	0.00	5.16
40	40	0.00	0.00	0.00	0.00	0.00	0.00	0.00	5.17
41	41	0.00	0.00	0.00	0.00	0.00	0.00	0.00	5.18
42	42	0.00	0.00	0.00	0.00	0.00	0.00	0.00	6.01
43	43	71.85	0.00	0.00	71.85	71.85	0.00	0.00	6.02
44	44	172.93	0.00	0.00	172.93	172.93	0.00	0.00	6.03
45	45	30.81	0.00	0.00	30.81	30.81	0.00	0.00	6.04
46	46	73.78	0.00	0.00	73.78	73.78	0.00	0.00	6.05
47	47	0.00	0.00	0.00	0.00	0.00	0.00	0.00	7.01
48	48	0.00	0.00	0.00	0.00	0.00	0.00	0.00	7.02
49	49	0.00	0.00	0.00	0.00	0.00	0.00	0.00	7.03
50	50	30.81	0.00	0.00	30.81	30.81	0.00	0.00	7.04
51	51	0.00	0.00	0.00	0.00	0.00	0.00	0.00	7.05
52	52	0.00	0.00	0.00	0.00	0.00	0.00	0.00	7.06
53	53	0.00	0.00	0.00	0.00	0.00	0.00	0.00	8.01
54	54	0.00	0.00	0.00	0.00	0.00	0.00	0.00	8.02
55	55	0.00	0.00	0.00	0.00	0.00	0.00	0.00	8.03
56	56	30.81	0.00	0.00	30.81	30.81	0.00	0.00	8.04
57	57	0.00	0.00	0.00	0.00	0.00	0.00	0.00	8.05
58	58	0.00	0.00	0.00	0.00	0.00	0.00	0.00	8.06
59	59	30.81	0.00	0.00	30.81	30.81	0.00	0.00	9.00
60	60	0.00	0.00	0.00	0.00	0.00	0.00	0.00	10.00
61	61	0.00	0.00	0.00	0.00	0.00	0.00	0.00	11.00
62	62	0.00	0.00	0.00	0.00	0.00	0.00	0.00	12.00
63	63	0.00	0.00	0.00	0.00	0.00	0.00	0.00	13.00
64	64	0.00	0.00	0.00	0.00	0.00	0.00	0.00	14.01
65	65	0.00	0.00	0.00	0.00	0.00	0.00	0.00	14.02
66	66	0.00	0.00	0.00	0.00	0.00	0.00	0.00	14.03
67	67	0.00	0.00	0.00	0.00	0.00	0.00	0.00	14.04
68	68	0.00	0.00	0.00	0.00	0.00	0.00	0.00	14.05
69	69	0.00	0.00	0.00	0.00	0.00	0.00	0.00	14.06
70	70	0.00	0.00	0.00	0.00	0.00	0.00	0.00	14.07
71	71	0.00	0.00	0.00	0.00	0.00	0.00	0.00	14.08
72	72	0.00	0.00	0.00	0.00	0.00	0.00	0.00	14.09
73	73	0.00	0.00	0.00	0.00	0.00	0.00	0.00	14.10
74	74	0.00	0.00	0.00	0.00	0.00	0.00	0.00	14.11
75	75	0.00	0.00	0.00	0.00	0.00	0.00	0.00	14.12
76	76	0.00	0.00	0.00	0.00	0.00	0.00	0.00	14.13
77	77	0.00	0.00	0.00	0.00	0.00	0.00	0.00	14.14
78	78	0.00	0.00	0.00	0.00	0.00	0.00	0.00	14.15
79	79	0.00	0.00	0.00	0.00	0.00	0.00	0.00	14.16
80	80	0.00	0.00	0.00	0.00	0.00	0.00	0.00	14.17
81	81	0.00	0.00	0.00	0.00	0.00	0.00	0.00	14.18
82	82	0.00	0.00	0.00	0.00	0.00	0.00	0.00	14.19
83	83	0.00	0.00	0.00	0.00	0.00	0.00	0.00	14.20

84	84	0.00	0.00	0.00	0.00	0.00	0.00	14.21
85	85	0.00	0.00	0.00	0.00	0.00	0.00	14.22
86	86	0.00	0.00	0.00	0.00	0.00	0.00	14.23
87	87	0.00	0.00	0.00	0.00	0.00	0.00	14.24
88	88	0.00	0.00	0.00	0.00	0.00	0.00	15.01
89	89	0.00	0.00	0.00	0.00	0.00	0.00	15.02
90	90	0.00	0.00	0.00	0.00	0.00	0.00	15.03
91	91	0.00	0.00	0.00	0.00	0.00	0.00	15.04
92	92	0.00	0.00	0.00	0.00	0.00	0.00	15.05
93	93	0.00	0.00	0.00	0.00	0.00	0.00	15.06
94	94	0.00	0.00	0.00	0.00	0.00	0.00	15.07
95	95	0.00	0.00	0.00	0.00	0.00	0.00	15.08
96	96	0.00	0.00	0.00	0.00	0.00	0.00	15.09
97	97	0.00	0.00	0.00	0.00	0.00	0.00	15.10
98	98	0.00	0.00	0.00	0.00	0.00	0.00	15.11
99	99	0.00	0.00	0.00	0.00	0.00	0.00	15.12
100	100	0.00	0.00	0.00	0.00	0.00	0.00	15.13
101	101	0.00	0.00	0.00	0.00	0.00	0.00	15.14
102	102	0.00	0.00	0.00	0.00	0.00	0.00	15.15
103	103	0.00	0.00	0.00	0.00	0.00	0.00	15.16
104	104	0.00	0.00	0.00	0.00	0.00	0.00	15.17
105	105	0.00	0.00	0.00	0.00	0.00	0.00	15.18
106	106	0.00	0.00	0.00	0.00	0.00	0.00	15.19
107	107	0.00	0.00	0.00	0.00	0.00	0.00	15.20
108	108	0.00	0.00	0.00	0.00	0.00	0.00	15.21
109	109	0.00	0.00	0.00	0.00	0.00	0.00	15.22
110	110	0.00	0.00	0.00	0.00	0.00	0.00	15.23
111	111	0.00	0.00	0.00	0.00	0.00	0.00	15.24
112	112	0.00	0.00	0.00	0.00	0.00	0.00	16.01
113	113	0.00	0.00	0.00	0.00	0.00	0.00	16.02
114	114	0.00	0.00	0.00	0.00	0.00	0.00	16.03
115	115	0.00	0.00	0.00	0.00	0.00	0.00	16.04
116	116	0.00	0.00	0.00	0.00	0.00	0.00	16.05
117	117	0.00	0.00	0.00	0.00	0.00	0.00	16.06
118	118	0.00	0.00	0.00	0.00	0.00	0.00	16.07
119	119	0.00	0.00	0.00	0.00	0.00	0.00	16.08
120	120	0.00	0.00	0.00	0.00	0.00	0.00	16.09
121	121	0.00	0.00	0.00	0.00	0.00	0.00	16.10
122	122	0.00	0.00	0.00	0.00	0.00	0.00	16.11
123	123	0.00	0.00	0.00	0.00	0.00	0.00	16.12
124	124	0.00	0.00	0.00	0.00	0.00	0.00	16.13
125	125	0.00	0.00	0.00	0.00	0.00	0.00	16.14
126	126	0.00	0.00	0.00	0.00	0.00	0.00	16.15
127	127	0.00	0.00	0.00	0.00	0.00	0.00	16.16
128	128	0.00	0.00	0.00	0.00	0.00	0.00	16.17
129	129	0.00	0.00	0.00	0.00	0.00	0.00	16.18
130	130	0.00	0.00	0.00	0.00	0.00	0.00	16.19
131	131	0.00	0.00	0.00	0.00	0.00	0.00	16.20
132	132	0.00	0.00	0.00	0.00	0.00	0.00	16.21
133	133	0.00	0.00	0.00	0.00	0.00	0.00	16.22
134	134	0.00	0.00	0.00	0.00	0.00	0.00	16.23
135	135	0.00	0.00	0.00	0.00	0.00	0.00	16.24

136	136	0.00	0.00	0.00	0.00	0.00	0.00	0.00	22.00
.37	137	0.00	0.00	0.00	0.00	0.00	0.00	0.00	23.01
138	138	0.00	0.00	0.00	0.00	0.00	0.00	0.00	23.02
139	139	0.00	0.00	0.00	0.00	0.00	0.00	0.00	23.03
140	140	0.00	0.00	0.00	0.00	0.00	0.00	0.00	23.04
141	141	0.00	0.00	0.00	0.00	0.00	0.00	0.00	23.05
142	142	0.00	0.00	0.00	0.00	0.00	0.00	0.00	24.01
143	143	0.00	0.00	0.00	0.00	0.00	0.00	0.00	24.02
144	144	0.00	0.00	0.00	0.00	0.00	0.00	0.00	24.03
145	145	0.00	0.00	0.00	0.00	0.00	0.00	0.00	24.04
146	146	0.00	0.00	0.00	0.00	0.00	0.00	0.00	24.05

 ORBITAL CALC CPU TIME (second) = 105.290

NO. OF THERMAL NODES= 147
 WARNING NO. OF THERMAL NODES CHANGED
 TEMPERATURE (DEGREES CENTIGRADE), POWER IN WATTS

=====

TIME= 0.000 NO. OF ITERATIONS= 1 (STEADY-STATE SOLUTION)

T	1=	26.84	T	2=	26.84	T	3=	26.84	T	4=	26.84
T	5=	26.84	T	6=	26.84	T	7=	26.84	T	8=	26.84
T	9=	26.84	T	10=	26.84	T	11=	26.84	T	12=	26.84
-	13=	26.84	T	14=	26.84	T	15=	26.84	T	16=	26.84
-	17=	26.84	T	18=	26.84	T	19=	26.84	T	20=	26.84
T	21=	26.84	T	22=	26.84	T	23=	26.84	T	24=	26.84
T	25=	26.84	T	26=	26.84	T	27=	26.84	T	28=	26.84
T	29=	26.84	T	30=	26.84	T	31=	26.84	T	32=	26.84
T	33=	26.84	T	34=	26.84	T	35=	26.84	T	36=	26.84
T	37=	26.84	T	38=	26.84	T	39=	26.84	T	40=	26.84
T	41=	26.84	T	42=	26.84	T	43=	26.84	T	44=	26.84
T	45=	26.84	T	46=	26.84	T	47=	26.84	T	48=	26.84
T	49=	26.84	T	50=	26.84	T	51=	26.84	T	52=	26.84
T	53=	26.84	T	54=	26.84	T	55=	26.84	T	56=	26.84
T	57=	26.84	T	58=	26.84	T	59=	26.84	T	60=	26.84
T	61=	26.84	T	62=	26.84	T	63=	26.84	T	64=	26.84
T	65=	26.84	T	66=	26.84	T	67=	26.84	T	68=	26.84
T	69=	26.84	T	70=	26.84	T	71=	26.84	T	72=	26.84
T	73=	26.84	T	74=	26.84	T	75=	26.84	T	76=	26.84
T	77=	26.84	T	78=	26.84	T	79=	26.84	T	80=	26.84
T	81=	26.84	T	82=	26.84	T	83=	26.84	T	84=	26.84
T	85=	26.84	T	86=	26.84	T	87=	26.84	T	88=	26.84
T	89=	26.84	T	90=	26.84	T	91=	26.84	T	92=	26.84
T	93=	26.84	T	94=	26.84	T	95=	26.84	T	96=	26.84
T	97=	26.84	T	98=	26.84	T	99=	26.84	T	100=	26.84
T	101=	26.84	T	102=	26.84	T	103=	26.84	T	104=	26.84
T	105=	26.84	T	106=	26.84	T	107=	26.84	T	108=	26.84
T	109=	26.84	T	110=	26.84	T	111=	26.84	T	112=	26.84
T	113=	26.84	T	114=	26.84	T	115=	26.84	T	116=	26.84

T	117=	26.84	T	118=	26.84	T	119=	26.84	T	120=	26.84
	121=	26.84	T	122=	26.84	T	123=	26.84	T	124=	26.84
T	125=	26.84	T	126=	26.84	T	127=	26.84	T	128=	26.84
T	129=	26.84	T	130=	26.84	T	131=	26.84	T	132=	26.84
T	133=	26.84	T	134=	26.84	T	135=	26.84	T	136=	26.84
T	137=	26.84	T	138=	26.84	T	139=	26.84	T	140=	26.84
T	141=	26.84	T	142=	26.84	T	143=	26.84	T	144=	26.84
T	145=	26.84	T	146=	26.84	T	147=	-273.16	T		

TEMPERATURE (DEGREES CENTIGRADE), POWER IN WATTS

=====

TIME= 101.540 NO. OF ITERATIONS= 17 (STEADY-STATE SOLUTION)

T	1=	-67.59	T	2=	-74.95	T	3=	-2.03	T	4=	-87.84
T	5=	-75.10	T	6=	-72.25	T	7=	29.37	T	8=	-124.71
T	9=	-42.48	T	10=	-118.11	T	11=	-135.26	T	12=	111.86
T	13=	92.15	T	14=	84.50	T	15=	69.34	T	16=	50.35
T	17=	80.05	T	18=	-58.91	T	19=	-96.66	T	20=	-37.81
T	21=	-38.39	T	22=	31.94	T	23=	-47.27	T	24=	-4.39
T	25=	-10.66	T	26=	-15.84	T	27=	-15.17	T	28=	-9.11
T	29=	-3.91	T	30=	-27.12	T	31=	-36.66	T	32=	-61.30
T	33=	-60.08	T	34=	-38.07	T	35=	-37.46	T	36=	-3.64
T	37=	2.02	T	38=	-8.54	T	39=	-8.90	T	40=	-0.38
T	41=	4.99	T	42=	-101.36	T	43=	-68.08	T	44=	-22.69
T	45=	-107.56	T	46=	-68.15	T	47=	-101.04	T	48=	-104.12
T	49=	-91.68	T	50=	9.86	T	51=	-99.44	T	52=	-80.95
T	53=	-99.51	T	54=	-99.56	T	55=	-91.68	T	56=	9.21
T	57=	-104.25	T	58=	-78.32	T	59=	-20.60	T	60=	-134.09
T	61=	-154.03	T	62=	-143.75	T	63=	-117.85	T	64=	-31.55
T	65=	-32.28	T	66=	-34.64	T	67=	-36.06	T	68=	-37.64
T	69=	-35.83	T	70=	-29.52	T	71=	-35.19	T	72=	-45.76
T	73=	-46.20	T	74=	-39.63	T	75=	-32.61	T	76=	30.55
T	77=	27.85	T	78=	27.70	T	79=	26.30	T	80=	25.50
T	81=	24.59	T	82=	23.58	T	83=	21.92	T	84=	20.42
T	85=	26.85	T	86=	25.30	T	87=	27.81	T	88=	-4.43
T	89=	-27.42	T	90=	-30.01	T	91=	-31.14	T	92=	-32.36
T	93=	-32.07	T	94=	-32.08	T	95=	-35.23	T	96=	-43.45
T	97=	-44.61	T	98=	-36.85	T	99=	-7.86	T	100=	34.87
T	101=	26.85	T	102=	20.08	T	103=	18.90	T	104=	22.71
T	105=	21.82	T	106=	21.45	T	107=	25.91	T	108=	23.58
T	109=	23.72	T	110=	27.14	T	111=	31.93	T	112=	-47.33
T	113=	-47.33	T	114=	-47.25	T	115=	-46.41	T	116=	-43.77
T	117=	-30.44	T	118=	-22.36	T	119=	-26.32	T	120=	-26.99
T	121=	-27.50	T	122=	-38.60	T	123=	-46.63	T	124=	11.51
T	125=	10.35	T	126=	10.38	T	127=	11.84	T	128=	15.04
T	129=	19.78	T	130=	18.58	T	131=	20.00	T	132=	19.52
T	133=	17.46	T	134=	18.10	T	135=	13.94	T	136=	-100.29
T	137=	-7.27	T	138=	-73.98	T	139=	-28.85	T	140=	-15.21
T	141=	-17.21	T	142=	-3.83	T	143=	-30.39	T	144=	-12.38
T	145=	-63.59	T	146=	-12.41	T	147=	-273.16	T		

APPENDIX E

PROPULSION CALCULATIONS

The requirements for the amount of fuel for corrections to the initial orbit insertions were determined using:

$$V = \sqrt{\frac{\mu}{a}}$$

where

$$\mu = 398.602$$

a = altitude in kilometers

The initial insertion altitude is 450 nmi (7211 km) and the safety margin is 50 nmi (92.6 km). If Pegasus can only get the spacecraft to 400 nmi (7118.8 km), then using the above equation the following values are calculated:

$$V_{450} = 7.435 \text{ km/s}$$

$$V_{400} = 7.483 \text{ km/s}$$

$$\Delta V = 7.483 - 7.435 = 0.048 \text{ km/s}$$

This value is substituted in the following equation to determine the mass of propellant required:

$$m_p = m_i \left[1 - \exp \left(\frac{\Delta V}{I_{sp} g} \right) \right]$$

where

m_p = mass propellant

m_i = mass spacecraft

I_{sp} = specific impulse

Substituting this value for ΔV in the above equation yields the fuel required to be 3.344 kilograms.

APPENDIX F

AXIAL LOADS

1. Frame Beams

The frame axial members were modelled as columns under compression. A factor of safety of 1.5 was used. Worst case load was the EHF payload structure at 135 lbs. The honeycomb panels were assumed to have an additional 130 lbs load in the axial direction, modeling the weight of the equipment panels.

$$F_C = (8.5g) (265 \text{ lbs}) (1.5) = 3378 \text{ lbf}$$

$$\text{Area} = (4) (0.9375 \text{ in}^2) = 3.75 \text{ in}^2$$

$$\sigma = \frac{3378 \text{ lbf}}{3.75 \text{ in}^2} = 900 \text{ psi}$$

$$\text{M.S.} = \frac{\text{yield strength}}{\text{limit load}} - 1$$

$$\text{M.S.} = \frac{37000 \text{ psi}}{900 \text{ psi}} - 1 = 40$$

2. Honeycomb Panel

The earth face honeycomb panel with the AVHRR attached was checked for stress during launch loads.

Facing stress

$$a = 32 \text{ (in.)}$$

$$b = 14 \text{ (in.)}$$

where a and b are footprint dimensions of AVHRR

$$K = \text{constant}$$

p = load (lbs/in²)

h = half thickness of panel (in.)

t_f = faceskin thickness (in.)

$$\sigma_f = \frac{K p b^2}{h t_f}$$

$$\sigma_f = \frac{(0.05) \left(\frac{62}{448} \right) (14)^2 (1.5) (8.5)}{(0.379) (0.004)}$$

$$\sigma_f = 11,406 \text{ psi}$$

$$\text{M.S.} = \frac{24000}{11406} - 1 = 1.1$$

BENDING LOADS

The axial rectangular tubing (1.5 in. x 2 in.) was designed to withstand the 3.5 g pullup maneuver the Pegasus performs. The worse case payload was the EHF payload and a factor of safety of 1.5 was used. The tubing was modelled as a cantilever beam rigidly fixed at the anti-earth face.

1. Maximum Deflection

$$\delta_t = \delta_{\text{uniform load}} + \delta_{\text{payload}}$$

$$\delta_t = \frac{P l^3}{8 E I} + \frac{P l^3}{3 E I}$$

$$\delta_t = \frac{(1.5) (25) (3.5) (23)^3}{8 (9.9(10^6)) (0.442)} + \frac{(1.5) (135) (3.5) (23)^3}{3 (9.9(10^6)) (0.442)}$$

$$\delta_t = 0.178 \text{ inch}$$

2. Maximum Bending Stress

For distributed load per beam:

$$S_{b1} = \frac{M_{\perp} C}{I}$$

$$M_{\perp \max} = \frac{W L}{2}$$

$$M_{\perp \max} = \frac{(25) (23 \text{ in.}) (3.5) (1.5)}{2}$$

$$M_{\perp \max} = 1509 \text{ lbf-in}$$

$$= \frac{(1509 \text{ lbf-in}) (1 \text{ in.})}{0.442} = 9219 \text{ psi}$$

For concentrated loads per beam:

$$S_{b2} = \frac{M_2 C}{I}$$

$$M_2 = \frac{(135) (3.5) (1.5) (23)}{4} = 4075 \text{ lbf-in}$$

$$S_{b2} = \frac{(4075 \text{ lbf-in}) (1 \text{ in.})}{0.442} = 9219 \text{ psi}$$

$$S_{bT} = S_{b1} + S_{b2} = 3414.8 + 9219 = 12633 \text{ psi}$$

$$\text{M.S.} = \frac{37000}{12633} - 1 = 1.9$$

3. Maximum Shear Stress

The general formula for horizontal shearing stress is:

$$S_h = \frac{Q V}{I b}$$

where

Q = area moment

V = vertical shear force

I = moment of inertia of cross section

b = width across the beam

therefore:

$$S_h = \frac{(0.8026 \text{ in}^3) (800 \text{ lbf})}{(0.442 \text{ in}^4) (1.5 \text{ in})}$$

$$S_h = 968 \text{ psi}$$

$$\text{M.S.} = \frac{30000 \text{ psi}}{1000 \text{ psi}} - 1 = 29$$

HONEYCOMB PANELS

The honeycomb panels are designed for stiffness to meet design criteria for minimum natural frequency and for stress due to dynamic loads.

1. Fundamental Natural Frequency Calculations

To avoid coupling with the primary structure, the fundamental natural frequency is assumed to be 30 Hz. The fundamental natural frequency of the panel is given by:

$$f = \frac{1}{2\pi} \beta \sqrt{\frac{D}{\gamma a^4}}$$

where

$$a = 23 \text{ in.}$$

$$b = 28 \text{ in.}$$

$$\beta = 19$$

$$\gamma = 28.92 \text{ kg/m}^2$$

$$D = 3.84(10^{10}) \text{ t h}^2$$

$$h = 3/8 \text{ in}$$

$$t = 0.1 \text{ mm}$$

2. Stress Due to Dynamic Acceleration

Assuming a uniform dynamic acceleration of 20g across the panel, the maximum stress in the face skin of the center of the panel is:

$$\sigma_{\max} = \beta \frac{W a^2}{6 t h}$$

$$= \frac{(0.3453) \left(\frac{(26)(20)}{(28)(32)} \right) (28)^2}{(6) (0.004) (0.375)}$$

$$\sigma_{\max} = 17456 \text{ psi}$$

$$\text{F.S.} = \frac{37000}{17456} = 2.1$$

APPENDIX H

COMMUNICATIONS SUBSYSTEM TABLES

beam	gain
4	32.00
5	30.75
6	29.50
7	28.25
8	27.00
9	26.25
10	25.50
11	24.75
12	24.00
13	23.80
14	23.60
15	23.40
16	23.20
17	23.00
18	22.80
19	22.60
20	22.40
21	22.20
22	22.00
23	21.67
24	21.33
25	21.00
26	20.67
27	20.33
28	20.00

TABLE H.1. Supplement To Figure 3.6.

Swath Width =>		1000	2000	4000	6000	Swath Width =>		1000	2000	4000	6000
Alt	Time	beam1	beam2	beam3	beam4	Alt	Time	beam1	beam2	beam3	beam4
500	0.00	28.00	28.00	28.00	28.00	14500	72.77	4.00	7.89	15.71	23.38
750	5.06	28.00	28.00	28.00	28.00	14750	74.25	4.00	7.76	15.44	22.99
1000	7.25	28.00	28.00	28.00	28.00	15000	75.74	4.00	7.63	15.19	22.62
1250	9.00	28.00	28.00	28.00	28.00	15250	77.25	4.00	7.50	14.94	22.26
1500	10.54	28.00	28.00	28.00	28.00	15500	78.78	4.00	7.38	14.70	21.91
1750	11.94	28.00	28.00	28.00	28.00	15750	80.34	4.00	7.27	14.47	21.57
2000	13.25	28.00	28.00	28.00	28.00	16000	81.91	4.00	7.15	14.25	21.24
2250	14.50	25.06	28.00	28.00	28.00	16250	83.51	4.00	7.04	14.03	20.92
2500	15.70	22.62	28.00	28.00	28.00	16500	85.13	4.00	6.94	13.82	20.61
2750	16.87	20.61	28.00	28.00	28.00	16750	86.77	4.00	6.83	13.62	20.31
3000	18.01	18.92	28.00	28.00	28.00	17000	88.44	4.00	6.73	13.42	20.02
3250	19.13	17.49	28.00	28.00	28.00	17250	90.14	4.00	6.64	13.23	19.73
3500	20.24	16.26	28.00	28.00	28.00	17500	91.86	4.00	6.54	13.04	19.46
3750	21.33	15.19	28.00	28.00	28.00	17750	93.61	4.00	6.45	12.86	19.19
4000	22.41	14.25	28.00	28.00	28.00	18000	95.38	4.00	6.36	12.68	18.92
4250	23.49	13.42	26.48	28.00	28.00	18250	97.19	4.00	6.27	12.51	18.67
4500	24.56	12.68	25.06	28.00	28.00	18500	99.03	4.00	6.19	12.34	18.42
4750	25.63	12.02	23.78	28.00	28.00	18750	100.90	4.00	6.11	12.18	18.18
5000	26.70	11.42	22.62	28.00	28.00	19000	102.80	4.00	6.03	12.02	17.95
5250	27.76	10.88	21.57	28.00	28.00	19250	104.74	4.00	5.95	11.86	17.72
5500	28.83	10.39	20.61	28.00	28.00	19500	106.71	4.00	5.87	11.71	17.49
5750	29.90	9.94	19.73	28.00	28.00	19750	108.72	4.00	5.80	11.56	17.27
6000	30.97	9.53	18.92	28.00	28.00	20000	110.77	4.00	5.72	11.42	17.06
6250	32.05	9.15	18.18	28.00	28.00	20250	112.86	4.00	5.65	11.28	16.85
6500	33.13	8.80	17.49	28.00	28.00	20500	115.00	4.00	5.59	11.14	16.65
6750	34.22	8.47	16.85	28.00	28.00	20750	117.18	4.00	5.52	11.01	16.45
7000	35.31	8.17	16.26	28.00	28.00	21000	119.41	4.00	5.45	10.88	16.26
7250	36.40	7.89	15.71	28.00	28.00	21250	121.69	4.00	5.39	10.75	16.07
7500	37.51	7.63	15.19	28.00	28.00	21500	124.03	4.00	5.33	10.63	15.89
7750	38.62	7.38	14.70	28.00	28.00	21750	126.42	4.00	5.26	10.51	15.71
8000	39.74	7.15	14.25	28.00	28.00	22000	128.87	4.00	5.21	10.39	15.53
8250	40.86	6.94	13.82	27.25	28.00	22250	131.39	4.00	5.15	10.27	15.36
8500	42.00	6.73	13.42	26.48	28.00	22500	133.98	4.00	5.09	10.16	15.19
8750	43.14	6.54	13.04	25.75	28.00	22750	136.65	4.00	5.03	10.05	15.02
9000	44.29	6.36	12.68	25.06	28.00	23000	139.40	4.00	4.98	9.94	14.86
9250	45.46	6.19	12.34	24.40	28.00	23250	142.23	4.00	4.93	9.83	14.70
9500	46.63	6.03	12.02	23.78	28.00	23500	145.16	4.00	4.87	9.73	14.55
9750	47.81	5.87	11.71	23.18	28.00	23750	148.20	4.00	4.82	9.63	14.40
10000	49.01	5.72	11.42	22.62	28.00	24000	151.35	4.00	4.77	9.53	14.25
10250	50.21	5.59	11.14	22.08	28.00	24250	154.64	4.00	4.72	9.43	14.10
10500	51.43	5.45	10.88	21.57	28.00	24500	158.06	4.00	4.67	9.33	13.96
10750	52.66	5.33	10.63	21.08	28.00	24750	161.66	4.00	4.63	9.24	13.82
11000	53.90	5.21	10.39	20.61	28.00	25000	165.43	4.00	4.58	9.15	13.69
11250	55.15	5.09	10.16	20.16	28.00	25250	169.43	4.00	4.54	9.06	13.55
11500	56.42	4.98	9.94	19.73	28.00	25500	173.68	4.00	4.49	8.97	13.42
11750	57.70	4.87	9.73	19.32	28.00	25750	178.25	4.00	4.45	8.88	13.29
12000	58.99	4.77	9.53	18.92	28.00	26000	183.20	4.00	4.41	8.80	13.16
12250	60.30	4.67	9.33	18.55	27.52	26250	188.64	4.00	4.36	8.71	13.04
12500	61.62	4.58	9.15	18.18	26.99	26500	194.76	4.00	4.32	8.63	12.92
12750	62.96	4.49	8.97	17.83	26.48	26750	201.87	4.00	4.28	8.55	12.80
13000	64.31	4.41	8.80	17.49	25.99	27000	210.71	4.00	4.24	8.47	12.68
13250	65.68	4.32	8.63	17.17	25.52	27250	223.86	4.00	4.20	8.40	12.56
13500	67.06	4.24	8.47	16.85	25.06	27358	238.72	4.00	4.19	8.36	12.52
13750	68.46	4.17	8.32	16.55	24.62						
14000	69.88	4.09	8.17	16.26	24.19						
14250	71.32	4.02	8.03	15.98	23.78						

TABLE H.2. Supplement To Figures 3.7 & 3.8.

Swath Width= >		1000	2000	4000	6000	Swath Width= >		1000	2000	4000	6000
Alt	Time	Gain1	Gain2	Gain3	Gain4	Alt	Time	Gain1	Gain2	Gain3	Gain4
500	0.00	20.00	20.00	20.00	20.00	14250	71.32	31.98	26.98	23.20	21.41
750	5.06	20.00	20.00	20.00	20.00	14500	72.77	32.00	27.14	23.26	21.54
1000	7.25	20.00	20.00	20.00	20.00	14750	74.25	32.00	27.30	23.31	21.67
1250	9.00	20.00	20.00	20.00	20.00	15000	75.74	32.00	27.46	23.36	21.79
1500	10.54	20.00	20.00	20.00	20.00	15250	77.25	32.00	27.62	23.41	21.91
1750	11.94	20.00	20.00	20.00	20.00	15500	78.78	32.00	27.77	23.46	22.02
2000	13.25	20.00	20.00	20.00	20.00	15750	80.34	32.00	27.92	23.51	22.09
2250	14.50	20.98	20.00	20.00	20.00	16000	81.91	32.00	28.06	23.55	22.15
2500	15.70	21.79	20.00	20.00	20.00	16250	83.51	32.00	28.20	23.59	22.22
2750	16.87	22.28	20.00	20.00	20.00	16500	85.13	32.00	28.33	23.64	22.28
3000	18.01	22.62	20.00	20.00	20.00	16750	86.77	32.00	28.46	23.68	22.34
3250	19.13	22.90	20.00	20.00	20.00	17000	88.44	32.00	28.58	23.72	22.40
3500	20.24	23.15	20.00	20.00	20.00	17250	90.14	32.00	28.71	23.75	22.45
3750	21.33	23.36	20.00	20.00	20.00	17500	91.86	32.00	28.82	23.79	22.51
4000	22.41	23.55	20.00	20.00	20.00	17750	93.61	32.00	28.94	23.83	22.56
4250	23.49	23.72	20.51	20.00	20.00	18000	95.38	32.00	29.05	23.86	22.62
4500	24.56	23.86	20.98	20.00	20.00	18250	97.19	32.00	29.16	23.90	22.67
4750	25.63	24.00	21.41	20.00	20.00	18500	99.03	32.00	29.26	23.93	22.72
5000	26.70	24.43	21.79	20.00	20.00	18750	100.90	32.00	29.37	23.96	22.76
5250	27.76	24.84	22.09	20.00	20.00	19000	102.80	32.00	29.47	24.00	22.81
5500	28.83	25.21	22.28	20.00	20.00	19250	104.74	32.00	29.57	24.10	22.86
5750	29.90	25.55	22.45	20.00	20.00	19500	106.71	32.00	29.66	24.22	22.90
6000	30.97	25.85	22.62	20.00	20.00	19750	108.72	32.00	29.75	24.33	22.95
6250	32.05	26.14	22.76	20.00	20.00	20000	110.77	32.00	29.84	24.43	22.99
6500	33.13	26.40	22.90	20.00	20.00	20250	112.86	32.00	29.93	24.54	23.03
6750	34.22	26.65	23.03	20.00	20.00	20500	115.00	32.00	30.02	24.64	23.07
7000	35.31	26.87	23.15	20.00	20.00	20750	117.18	32.00	30.10	24.74	23.11
7250	36.40	27.14	23.26	20.00	20.00	21000	119.41	32.00	30.18	24.84	23.15
7500	37.51	27.46	23.36	20.00	20.00	21250	121.69	32.00	30.26	24.93	23.19
7750	38.62	27.77	23.46	20.00	20.00	21500	124.03	32.00	30.34	25.03	23.22
8000	39.74	28.06	23.55	20.00	20.00	21750	126.42	32.00	30.42	25.12	23.26
8250	40.86	28.33	23.64	20.25	20.00	22000	128.87	32.00	30.49	25.21	23.29
8500	42.00	28.58	23.72	20.51	20.00	22250	131.39	32.00	30.57	25.30	23.33
8750	43.14	28.82	23.79	20.75	20.00	22500	133.98	32.00	30.64	25.38	23.36
9000	44.29	29.05	23.86	20.98	20.00	22750	136.65	32.00	30.71	25.46	23.40
9250	45.46	29.26	23.93	21.20	20.00	23000	139.40	32.00	30.78	25.55	23.43
9500	46.63	29.47	24.00	21.41	20.00	23250	142.23	32.00	30.84	25.63	23.46
9750	47.81	29.66	24.22	21.61	20.00	23500	145.16	32.00	30.91	25.70	23.49
10000	49.01	29.84	24.43	21.79	20.00	23750	148.20	32.00	30.97	25.78	23.52
10250	50.21	30.02	24.64	21.97	20.00	24000	151.35	32.00	31.04	25.85	23.55
10500	51.43	30.18	24.84	22.09	20.00	24250	154.64	32.00	31.10	25.93	23.58
10750	52.66	30.34	25.03	22.18	20.00	24500	158.06	32.00	31.16	26.00	23.61
11000	53.90	30.49	25.21	22.28	20.00	24750	161.66	32.00	31.22	26.07	23.64
11250	55.15	30.64	25.38	22.37	20.00	25000	165.43	32.00	31.27	26.14	23.66
11500	56.42	30.78	25.55	22.45	20.00	25250	169.43	32.00	31.33	26.21	23.69
11750	57.70	30.91	25.70	22.54	20.00	25500	173.68	32.00	31.39	26.27	23.72
12000	58.99	31.04	25.85	22.62	20.00	25750	178.25	32.00	31.44	26.34	23.74
12250	60.30	31.16	26.00	22.69	20.16	26000	183.20	32.00	31.49	26.40	23.77
12500	61.62	31.27	26.14	22.76	20.34	26250	188.64	32.00	31.55	26.46	23.79
12750	62.96	31.39	26.27	22.83	20.51	26500	194.76	32.00	31.60	26.53	23.82
13000	64.31	31.49	26.40	22.90	20.67	26750	201.87	32.00	31.65	26.59	23.84
13250	65.68	31.60	26.53	22.97	20.83	27000	210.71	32.00	31.70	26.65	23.86
13500	67.06	31.70	26.65	23.03	20.98	27250	223.86	32.00	31.75	26.70	23.89
13750	68.46	31.79	26.76	23.09	21.13	27358	238.72	32.00	31.77	26.73	23.90
14000	69.88	31.89	26.87	23.15	21.27						

TABLE H.3. Supplement To Figures 3.9 & 3.10.

Gain vs. Off Angle		
Angle	Gain	Relative
0	32.00	0.00
0.1	31.99	-0.01
0.2	31.97	-0.03
0.3	31.93	-0.07
0.4	31.88	-0.12
0.5	31.82	-0.18
0.6	31.73	-0.27
0.7	31.64	-0.36
0.8	31.53	-0.47
0.9	31.40	-0.60
1	31.26	-0.74
1.1	31.11	-0.89
1.2	30.94	-1.06
1.3	30.75	-1.25
1.4	30.55	-1.45
1.5	30.34	-1.66
1.6	30.11	-1.89
1.7	29.87	-2.13
1.8	29.61	-2.39
1.9	29.33	-2.67
2	29.05	-2.95
2.1	28.74	-3.26
2.2	28.43	-3.57
2.3	28.09	-3.91
2.4	27.75	-4.25
2.5	27.39	-4.61
2.6	27.01	-4.99
2.7	26.62	-5.38
2.8	26.21	-5.79
2.9	25.79	-6.21
3	25.36	-6.64
3.1	24.90	-7.10
3.2	24.44	-7.56
3.3	23.96	-8.04
3.4	23.47	-8.53
3.5	22.96	-9.04
3.6	22.43	-9.57
3.7	21.89	-10.11
3.8	21.34	-10.66
3.9	20.77	-11.23
4	20.19	-11.81

Gain vs. Off Angle		
Angle	Gain	Relative
4	20.19	-11.81
4.1	19.59	-12.41
4.2	18.98	-13.02
4.3	18.35	-13.65
4.4	17.71	-14.29
4.5	17.05	-14.95
4.6	16.38	-15.62
4.7	15.69	-16.31
4.8	14.99	-17.01
4.9	14.27	-17.73
5	13.54	-18.46

TABLE H.4. Supplement To Figure 3.12.

YAW ERROR ->	0.1	0.3	0.5	0.7	0.9	1	1.5	2	3
Scan Angle (degrees)	GAIN VS. SCAN ANGLE OFF OF NADIR FOR VARIOUS YAW ERRORS (ALL IN dB)								
0	0.00E+00	0.00E+00	0.00E+00	0.00E+00	0.00E+00	0.00E+00	0.00E+00	0.00E+00	0.00E+00
1	-6.9E-10	-6.2E-09	-1.7E-08	-3.4E-08	-5.5E-08	-6.8E-08	-1.5E-07	-2.7E-07	-2.5E-06
2	-2.7E-09	-2.5E-08	-6.8E-08	-1.3E-07	-2.2E-07	-2.7E-07	-6.2E-07	-1.1E-06	-5.5E-06
3	-6.2E-09	-5.5E-08	-1.5E-07	-3.0E-07	-5.0E-07	-6.2E-07	-1.4E-06	-2.5E-06	-9.8E-06
4	-1.1E-08	-9.8E-08	-2.7E-07	-5.4E-07	-8.9E-07	-1.1E-06	-2.5E-06	-4.4E-06	-9.8E-06
5	-1.7E-08	-1.5E-07	-4.3E-07	-8.4E-07	-1.4E-06	-1.7E-06	-3.8E-06	-6.8E-06	-1.5E-05
6	-2.5E-08	-2.2E-07	-6.1E-07	-1.2E-06	-2.0E-06	-2.5E-06	-5.5E-06	-9.8E-06	-2.2E-05
7	-3.3E-08	-3.0E-07	-8.4E-07	-1.6E-06	-2.7E-06	-3.3E-06	-7.5E-06	-1.3E-05	-3.0E-05
8	-4.4E-08	-3.9E-07	-1.1E-06	-2.1E-06	-3.5E-06	-4.4E-06	-9.8E-06	-1.7E-05	-3.9E-05
9	-5.5E-08	-5.0E-07	-1.4E-06	-2.7E-06	-4.5E-06	-5.5E-06	-1.2E-05	-2.2E-05	-5.0E-05
10	-6.8E-08	-6.1E-07	-1.7E-06	-3.3E-06	-5.5E-06	-6.8E-06	-1.5E-05	-2.7E-05	-6.1E-05
11	-8.2E-08	-7.4E-07	-2.0E-06	-4.0E-06	-6.6E-06	-8.2E-06	-1.8E-05	-3.3E-05	-7.4E-05
12	-9.7E-08	-8.7E-07	-2.4E-06	-4.8E-06	-7.9E-06	-9.7E-06	-2.2E-05	-3.9E-05	-8.7E-05
13	-1.1E-07	-1.0E-06	-2.8E-06	-5.6E-06	-9.2E-06	-1.1E-05	-2.6E-05	-4.6E-05	-1.0E-04
14	-1.3E-07	-1.2E-06	-3.3E-06	-6.4E-06	-1.1E-05	-1.3E-05	-3.0E-05	-5.3E-05	-1.2E-04
15	-1.5E-07	-1.4E-06	-3.8E-06	-7.4E-06	-1.2E-05	-1.5E-05	-3.4E-05	-6.0E-05	-1.4E-04
16	-1.7E-07	-1.5E-06	-4.3E-06	-8.4E-06	-1.4E-05	-1.7E-05	-3.8E-05	-6.8E-05	-1.5E-04
17	-1.9E-07	-1.7E-06	-4.8E-06	-9.4E-06	-1.6E-05	-1.9E-05	-4.3E-05	-7.7E-05	-1.7E-04
18	-2.1E-07	-1.9E-06	-5.4E-06	-1.1E-05	-1.7E-05	-2.1E-05	-4.8E-05	-8.6E-05	-1.9E-04
19	-2.4E-07	-2.1E-06	-6.0E-06	-1.2E-05	-1.9E-05	-2.4E-05	-5.4E-05	-9.5E-05	-2.1E-04
20	-2.6E-07	-2.4E-06	-6.6E-06	-1.3E-05	-2.1E-05	-2.6E-05	-5.9E-05	-1.1E-04	-2.4E-04
21	-2.9E-07	-2.6E-06	-7.2E-06	-1.4E-05	-2.3E-05	-2.9E-05	-6.5E-05	-1.2E-04	-2.6E-04
22	-3.2E-07	-2.8E-06	-7.9E-06	-1.5E-05	-2.6E-05	-3.2E-05	-7.1E-05	-1.3E-04	-2.8E-04
23	-3.4E-07	-3.1E-06	-8.6E-06	-1.7E-05	-2.8E-05	-3.4E-05	-7.7E-05	-1.4E-04	-3.1E-04
24	-3.7E-07	-3.3E-06	-9.3E-06	-1.8E-05	-3.0E-05	-3.7E-05	-8.4E-05	-1.5E-04	-3.3E-04
25	-4.0E-07	-3.6E-06	-1.0E-05	-2.0E-05	-3.3E-05	-4.0E-05	-9.0E-05	-1.6E-04	-3.6E-04
26	-4.3E-07	-3.9E-06	-1.1E-05	-2.1E-05	-3.5E-05	-4.3E-05	-9.7E-05	-1.7E-04	-3.9E-04
27	-4.6E-07	-4.2E-06	-1.2E-05	-2.3E-05	-3.8E-05	-4.6E-05	-1.0E-04	-1.9E-04	-4.2E-04
28	-5.0E-07	-4.5E-06	-1.2E-05	-2.4E-05	-4.0E-05	-5.0E-05	-1.1E-04	-2.0E-04	-4.5E-04
29	-5.3E-07	-4.8E-06	-1.3E-05	-2.6E-05	-4.3E-05	-5.3E-05	-1.2E-04	-2.1E-04	-4.8E-04
30	-5.6E-07	-5.1E-06	-1.4E-05	-2.8E-05	-4.6E-05	-5.6E-05	-1.3E-04	-2.2E-04	-5.1E-04
31	-6.0E-07	-5.4E-06	-1.5E-05	-2.9E-05	-4.8E-05	-6.0E-05	-1.3E-04	-2.4E-04	-5.4E-04
32	-6.3E-07	-5.7E-06	-1.6E-05	-3.1E-05	-5.1E-05	-6.3E-05	-1.4E-04	-2.5E-04	-5.7E-04
33	-6.7E-07	-6.0E-06	-1.7E-05	-3.3E-05	-5.4E-05	-6.7E-05	-1.5E-04	-2.7E-04	-6.0E-04
34	-7.0E-07	-6.3E-06	-1.8E-05	-3.4E-05	-5.7E-05	-7.0E-05	-1.6E-04	-2.8E-04	-6.3E-04
35	-7.4E-07	-6.7E-06	-1.8E-05	-3.6E-05	-6.0E-05	-7.4E-05	-1.7E-04	-3.0E-04	-6.7E-04
36	-7.8E-07	-7.0E-06	-1.9E-05	-3.8E-05	-6.3E-05	-7.8E-05	-1.7E-04	-3.1E-04	-7.0E-04
37	-8.1E-07	-7.3E-06	-2.0E-05	-4.0E-05	-6.6E-05	-8.1E-05	-1.8E-04	-3.3E-04	-7.3E-04
38	-8.5E-07	-7.7E-06	-2.1E-05	-4.2E-05	-6.9E-05	-8.5E-05	-1.9E-04	-3.4E-04	-7.7E-04
39	-8.9E-07	-8.0E-06	-2.2E-05	-4.4E-05	-7.2E-05	-8.9E-05	-2.0E-04	-3.6E-04	-8.0E-04
40	-9.3E-07	-8.4E-06	-2.3E-05	-4.6E-05	-7.5E-05	-9.3E-05	-2.1E-04	-3.7E-04	-8.4E-04
41	-9.7E-07	-8.7E-06	-2.4E-05	-4.7E-05	-7.8E-05	-9.7E-05	-2.2E-04	-3.9E-04	-8.7E-04
42	-1.0E-06	-9.1E-06	-2.5E-05	-4.9E-05	-8.2E-05	-1.0E-04	-2.3E-04	-4.0E-04	-9.1E-04
43	-1.0E-06	-9.4E-06	-2.6E-05	-5.1E-05	-8.5E-05	-1.0E-04	-2.4E-04	-4.2E-04	-9.4E-04
44	-1.1E-06	-9.8E-06	-2.7E-05	-5.3E-05	-8.8E-05	-1.1E-04	-2.4E-04	-4.3E-04	-9.8E-04
45	-1.1E-06	-1.0E-05	-2.8E-05	-5.5E-05	-9.1E-05	-1.1E-04	-2.5E-04	-4.5E-04	-1.0E-03
46	-1.2E-06	-1.0E-05	-2.9E-05	-5.7E-05	-9.4E-05	-1.2E-04	-2.6E-04	-4.7E-04	-1.0E-03
47	-1.2E-06	-1.1E-05	-3.0E-05	-5.9E-05	-9.7E-05	-1.2E-04	-2.7E-04	-4.8E-04	-1.1E-03
48	-1.2E-06	-1.1E-05	-3.1E-05	-6.1E-05	-1.0E-04	-1.2E-04	-2.8E-04	-5.0E-04	-1.1E-03
49	-1.3E-06	-1.2E-05	-3.2E-05	-6.3E-05	-1.0E-04	-1.3E-04	-2.9E-04	-5.1E-04	-1.2E-03
50	-1.3E-06	-1.2E-05	-3.3E-05	-6.5E-05	-1.1E-04	-1.3E-04	-3.0E-04	-5.3E-04	-1.2E-03

TABLE H.5. Supplement To Figure 3.13.

APPENDIX J

LINK ANALYSIS

Each of the various transmission frequencies, altitudes, modulation techniques and antenna gains must be examined to insure that a proper carrier-to-noise ratio (C/N) is maintained. For the design of the links in this satellite, a maximum bit error rate (BER) of 10^{-6} was desired. In order to achieve this BER, a C/N of 14 dB must be achieved for FSK modulation or 11 dB for PSK modulation. Since the majority of the carriers are FSK due to the Frequency Hopping of the carrier, the link analysis assumes FSK modulation. Along with the 14 dB, a link margin of 4 dB was added for weather and atmospheric attenuation as well as any other losses that may not have been considered. A "Closed Link" in this satellite is one in which a total C/N of 18 dB is achieved.

Several worst case assumptions were made for this analysis. The ground station elevation angle was assumed to be 20° for EHF frequencies and 5° for lower frequencies. The worst case altitude is at apogee except for the variable beamwidth antenna which must be analyzed for the entire orbit. The ground station for the EHF frequencies was assumed to be the SCAMP Terminal. Figure J.1 shows the EHF link. The ground station for SHF TT&C was assumed to be channel 1 of the space ground link subsystem (SGLS) of the Air Force Satellite Control Facility (AFSCF) at Thule, Greenland (Thule Tracking Station - TTS). The ground station for the AVHRR payload was assumed to be the TIROS-N earth terminals. Data for each earth station follows:

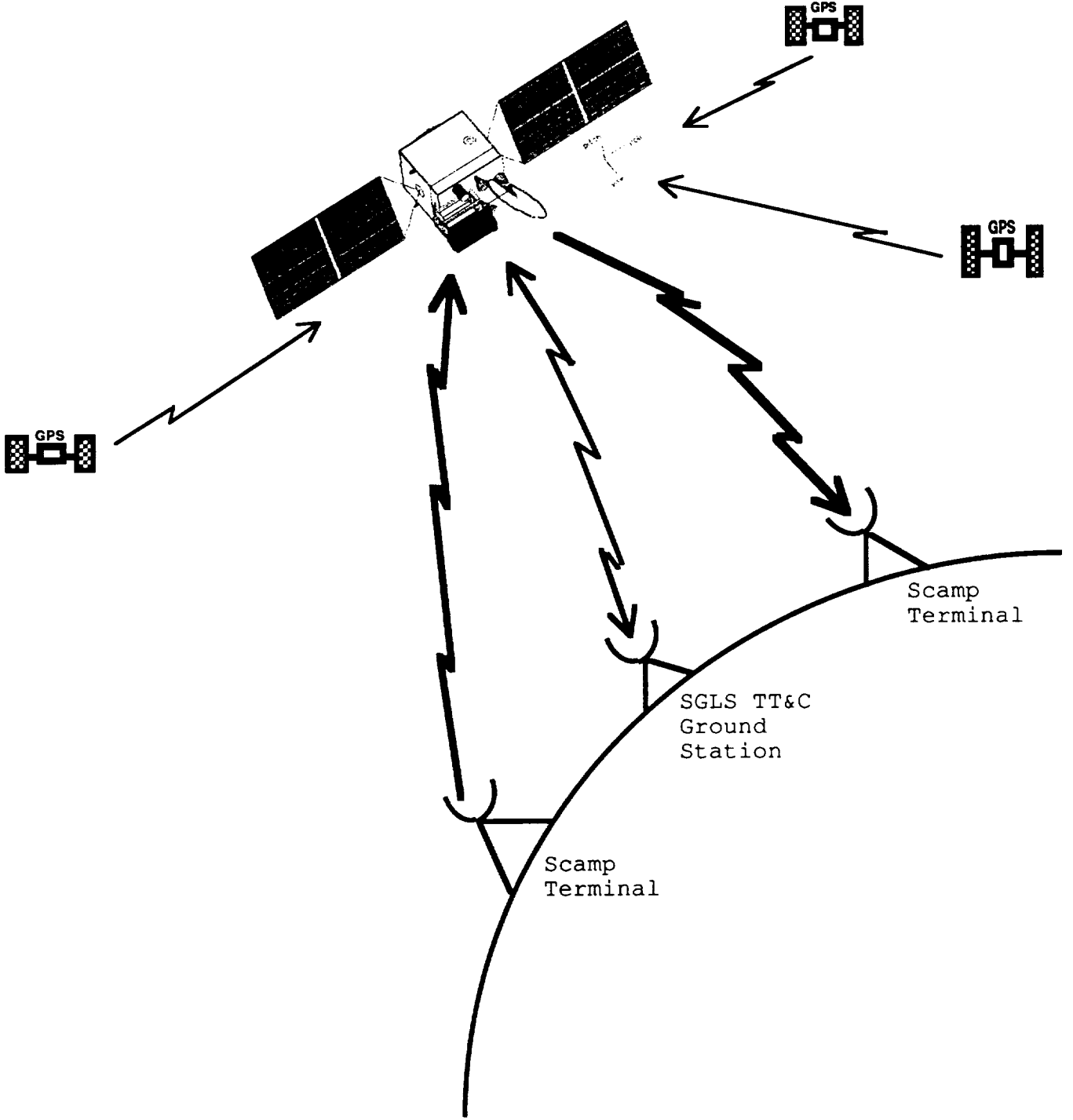


FIGURE J.1. EHF Link Diagram

SCAMP

Data Rate: 2.4 kbps
Rcv Gain: 39.92 dB
Transmit EIRP: 48 dB
Uplink Freq: 44 GHz
Downlink Freq: 20 GHz

SGLS (Thule):

Data Rate: 300 bps
Rcv Gain: 48.2 dB
Transmit EIRP: 39.69 dB
Uplink Freq: 1.763721 GHz
Downlink Freq: 2.2 GHz

TIROS-N (HRPT)

Data Rate: 665 kbps
Rcv Gain: 30 dB
Transmit EIRP: NA
Uplink Freq: NA
Downlink Freq: 1.71 GHz

TIROS-N (APT)

Data Rate:	2000 bps
Rcv Gain:	30 dB
Transmit EIRP:	NA
Uplink Freq:	NA
Downlink Freq:	137.5 MHz

TIROS-N (TT&C)

Data Rate:	8.32 kbps
Rcv Gain:	30 dB
Transmit EIRP:	NA
Uplink Freq:	NA
Downlink Freq:	137.77 MHz

TIROS-N (Command Uplink)

Data Rate:	1000 bps
Rcv Gain:	NA
Transmit EIRP:	27 dB
Uplink Freq:	148.56 MHz
Downlink Freq:	NA

Given the above data and the orbital information and design characteristics of the MPS satellite bus and payloads, link analysis was done for all channels and is listed in Tables J.1 and J.2. An example of the link analysis calculations follows:

1. The carrier-to-noise ratio is the amount of signal energy which reaches the receiver divided by the noise level at the receiver. Equation J.1 is a simple formula for calculating the C/N for the uplink. Equation J.2 is for the downlink.

$$\frac{C}{N} = \frac{P_t G_t G_u}{L_u k T_u B} \quad (J.1)$$

$$\frac{C}{N} = \frac{P_s G_d G_r}{L_d k T_d B} \quad (J.2)$$

Equation J.3 and J.4 are for calculating C/N when all the data is in decibels.

$$\frac{C}{N} = P_t + G_t + G_u - L_u - k - T_u - B \quad (J.3)$$

$$\frac{C}{N} = P_s + G_d + G_r - L_d - k - T_d - B \quad (J.4)$$

where:

P_t = power transmitted

G_t = gain of transmitting antenna

G_u = gain of uplink antenna

L_u = free space losses in uplink

k = Boltzmann's constant (-228.6 dB)

T_u = noise temperature in uplink

B = noise bandwidth

P_s = transmitted power from satellite

G_d = gain of downlink antenna

G_r = gain of receive antenna

L_d = free space losses in downlink

T_d = noise temperature in downlink

2. Before calculating C/N, the different parameters must be obtained. Equation J.5 is the general formula to obtain the gain of an antenna.

$$G = \eta \left(\frac{\pi f D}{c} \right)^2 \quad (J.5)$$

where:

η = efficiency of the antenna

f = frequency

D = antenna diameter

c = speed of light

3. Free space loss can be obtained with equation J.6.

$$L = \left(\frac{4\pi f d}{c} \right)^2 \quad (J.6)$$

where:

d = slant range (use Equation J.7)

$$d^2 = (R_e + H)^2 + R_e^2 - 2 R_e (R_e + H) \sin \left[E + \sin^{-1} \left(\frac{R_e \cos E}{R_e + H} \right) \right] \quad (J.7)$$

where:

R_e = radius of the earth (6378 km)

H = altitude

E = elevation angle earth antenna

4. Once the C/N is known for both uplink and downlink, they are combined with Equation J.8 to determine the total C/N. This number must be higher than 18 dB to close the link and insure a 10^{-6} BER.

$$\left(\frac{C}{N} \right)^{-1} = \left(\frac{C}{N} \right)_u^{-1} + \left(\frac{C}{N} \right)_d^{-1} \quad (J.8)$$

Table J.1 and J.2 show the link analysis for the MPS satellite. None of the C/N's fall below 18 dB and therefore all of the links have suitable margins to insure a maximum BER of 10^{-6} . For the variable beamwidth antenna, the analysis had to be done over the entire orbit. Figure J.1 shows the C/N versus altitude and Figure J.2 shows the C/N versus time after perigee.

As a final note on the advantage of variable beamwidth antennas, Figure J.3 shows a comparison between a fixed beamwidth antenna and a variable beamwidth antenna for maintaining a 2000 km swath width. The fixed beamwidth antenna has a 28° beamwidth for the entire orbit. The variable beamwidth varies from 28° to 4° as necessary. Figure J.3 shows that the variable beamwidth has a definite advantage that increases with altitude. At apogee, the variable beamwidth antenna has almost a 10 dB advantage over fixed beamwidth antennas.

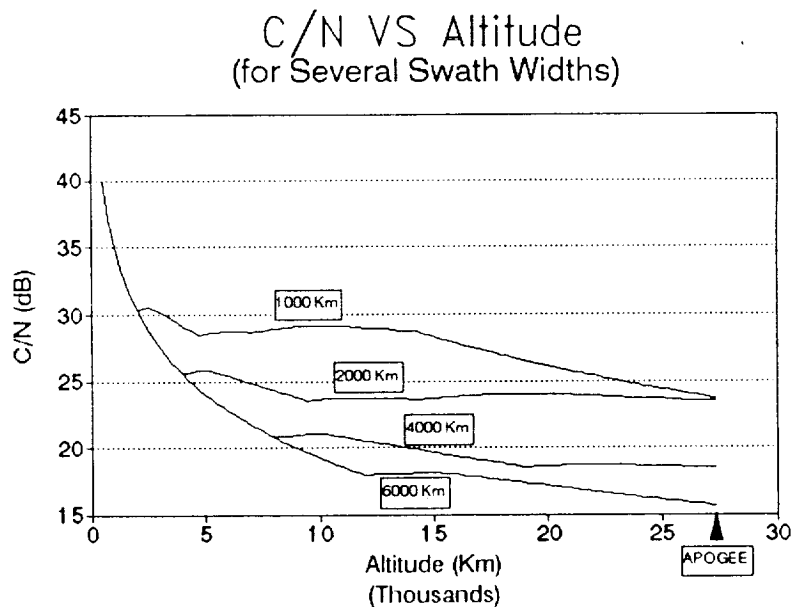


FIGURE J.1. C/N Versus Altitude

EHF Communications Sample Link Analysis	EHF TTC (VBWA)						(E/C Horns) (A-E Ant)	
	Apogee	15000 km	20 degs	Apogee	15000	20 degs	Apogee	Apogee
Freq Up (Hz)	4.4E +10	4.4E +10	4.4E +10	4.3E +10	4.3E +10	4.3E +10	1.76E +09	1760000000
Freq Down (Hz)	2E +10	2E +10	2E +10	1.9E +10	1.9E +10	1.9E +10	2.20E +09	2200000000
Data Rate (bps)	2400	2400	2400	300	300	300	300	300
Alt (km)	27358	15000	4050	27358	15000	4050	27358	27358
Slant Ang(rads)	0.35	0.35	0.35	0.35	0.35	0.35	0.35	0.35
Slant Range(km)	31017.95	18339.28	6352.225	31017.95	18339.28	6352.22	31017.95	31017.95
UPLINK (in dB)								
EIRPt	48	48	48	48	48	48	39.69	39.69
Xmit Power	1.5	1.5	1.5	1.5	1.5	1.5	-3.01	-3.01
Xmit Gain	46.5	46.5	46.5	46.5	46.5	46.5	42.7	42.7
FS LOSS	215.14	210.58	201.37	214.94	210.38	201.17	187.20	187.18
Rcv Gain	31.9	27.5	20	31.9	27.5	20	2	2
Boltz Const	-228.6	-228.6	-228.6	-228.6	-228.6	-228.6	-228.6	-228.6
Noise Temp	31	31	31	31	31	31	31	31
NOISE BW	36.81	36.81	36.81	27.78	27.78	27.78	27.78	27.78
DOWNLINK (in dB)								
Xmit Power	1.76	1.76	1.76	1.76	1.76	1.76	1.76	1.76
Xmit Gain	31.9	27.5	20	31.9	27.5	20	2	2
FS LOSS	208.29	203.73	194.52	207.85	203.28	194.08	189.12	189.12
Rcv Gain	39.92	39.92	39.92	39.92	39.92	39.92	48.2	48.2
BOLTZ CONST	-228.6	-228.6	-228.6	-228.6	-228.6	-228.6	-228.6	-228.6
Noise Temp	29	29	29	29	29	29	29	29
NOISE BW	36.81	36.81	36.81	27.78	27.78	27.78	27.78	27.78
C/N UP	25.54	25.71	27.42	34.78	34.94	36.65	24.31	24.32
C/N DOWN	28.07	28.24	29.95	37.55	37.71	39.42	34.66	34.66
C/N TOTAL	23.62	23.78	25.49					

TABLE J.1. Link Analysis Data For EHF Payload

	HRPT	APT	TT&C	Command
Freq Up (Hz)				1.49E+08
Freq Down (Hz)	1.71E+09	1.38E+08	1.37E+08	
Data Rate (bps)	665000	2000	8320	1000
Alt (km)	824	824	824	824
Slant Ang(rads)	0.35	0.09	0.09	0.09
Slant Range(km)	1812.15	2835.13	2835.13	2835.13
UPLINK (in dB)				
EIRPt				27.00
Xmit Power				-3.00
Xmit Gain				30
FS LOSS				144.93
Rcv Gain				0
Boltz Const				-228.6
Noise Figure				29
NOISE BW				33.01
DOWNLINK (in dB)				
Xmit Power	11.76	-3.01	-3.01	
Xmit Gain	4.05	0	0	
FS LOSS	162.25	144.26	144.21	
Rcv Gain	30	30	30	
BOLTZ CONST	-228.6	-228.6	-228.6	
Noise Figure	29	29	29	
NOISE BW	61.24	36.02	42.21	
C/N UP				48.66
C/N DOWN	21.92	46.31	40.17	

TABLE J.2. Link Analysis Data For AVHRR Payload

C/N VS Time after Perigee (for Several Swath Widths)

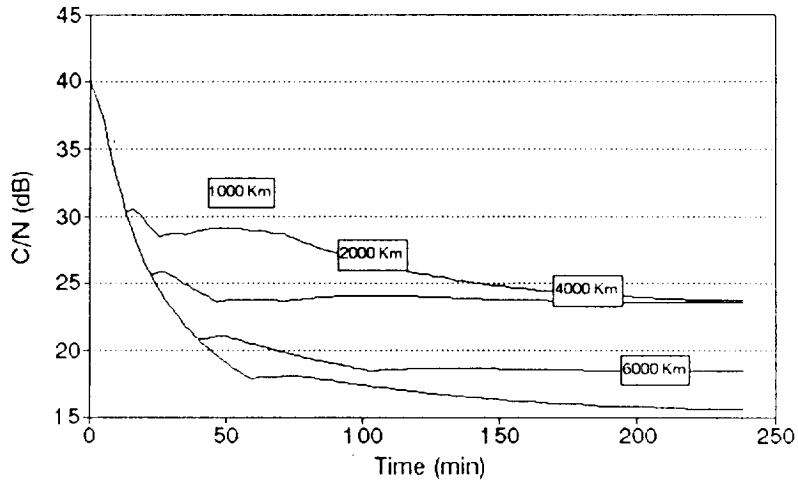


FIGURE J.2. C/N Versus Time After Perigee

C/N vs Altitude (Swath Width Greater Than 2000 KM)

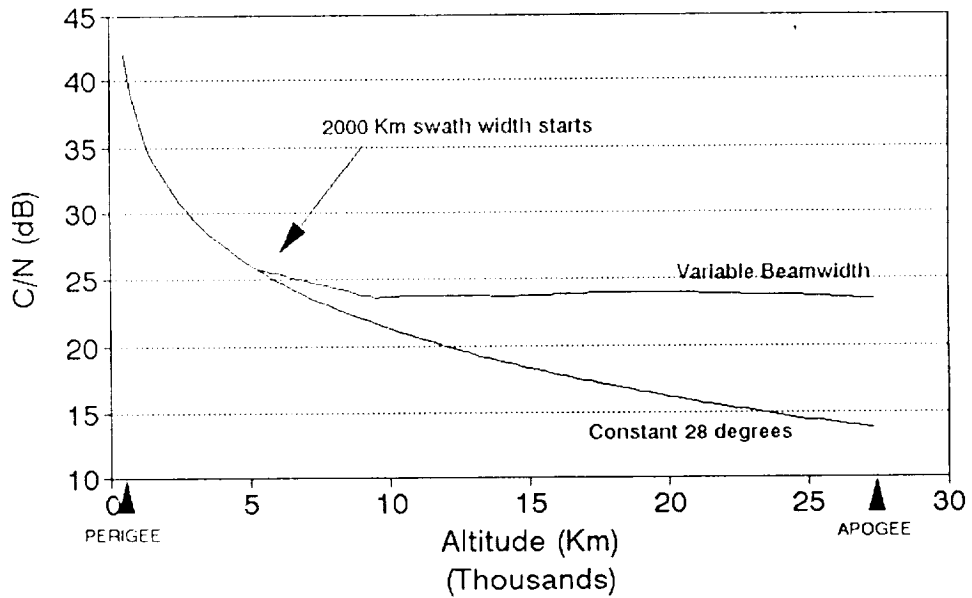


FIGURE J.3. Comparison of C/N Versus Altitude for Fixed and Variable Antennas

Swath Width =>		1000		2000		4000		6000		1000		2000		4000		6000	
All	Time	C/N(up)1	C/N(up)2	C/N(up)3	C/N(up)4	C/N(down)1	C/N(down)2	C/N(down)3	C/N(down)4	C/N(tot)1	C/N(tot)2	C/N(tot)3	C/N(tot)4				
500	0 00	41 94	41 94	41 94	41 94	44 47	44 47	44 47	44 47	40 02	40 02	40 02	40 02				
750	5 06	38 99	38 99	38 99	38 99	41 51	41 51	41 51	41 51	37 06	37 06	37 06	37 06				
1000	7 25	36 94	36 94	36 94	36 94	39 47	39 47	39 47	39 47	35 02	35 02	35 02	35 02				
1250	9 00	35 39	35 39	35 39	35 39	37 92	37 92	37 92	37 92	33 46	33 46	33 46	33 46				
1500	10 54	34 13	34 13	34 13	34 13	36 66	36 66	36 66	36 66	32 21	32 21	32 21	32 21				
1750	11 94	33 08	33 08	33 08	33 08	35 61	35 61	35 61	35 61	31 16	31 16	31 16	31 16				
2000	13 25	32 18	32 18	32 18	32 18	34 71	34 71	34 71	34 71	30 25	30 25	30 25	30 25				
2250	14 50	32 36	31 38	31 38	31 38	34 89	33 91	33 91	33 91	30 43	29 45	29 45	29 45				
2500	15 70	32 46	30 67	30 67	30 67	34 99	33 20	33 20	33 20	30 54	28 74	28 74	28 74				
2750	16 87	32 31	30 03	30 03	30 03	34 84	32 56	32 56	32 56	30 38	28 10	28 10	28 10				
3000	18 01	32 06	29 44	29 44	29 44	34 69	31 97	31 97	31 97	30 13	27 52	27 52	27 52				
3250	19 13	31 81	28 90	28 90	28 90	34 33	31 43	31 43	31 43	29 88	26 98	26 98	26 98				
3500	20 24	31 55	28 40	28 40	28 40	34 08	30 93	30 93	30 93	29 62	26 48	26 48	26 48				
3750	21 33	31 30	27 84	27 84	27 84	33 83	30 47	30 47	30 47	29 37	26 01	26 01	26 01				
4000	22 41	31 05	27 50	27 50	27 50	33 58	30 03	30 03	30 03	29 13	25 58	25 58	25 58				
4250	23 49	30 81	27 60	27 09	27 09	33 34	30 13	29 62	29 62	28 88	25 67	25 67	25 67				
4500	24 56	30 57	27 68	26 70	26 70	33 10	30 21	29 23	29 23	28 64	25 76	24 78	24 78				
4750	25 63	30 33	27 74	26 34	26 34	32 86	30 27	28 87	28 87	28 41	25 82	24 41	24 41				
5000	26 70	30 42	27 78	25 99	25 99	32 95	30 31	28 52	28 52	28 49	25 85	24 06	24 06				
5250	27 76	30 49	27 74	25 65	25 65	33 02	30 27	28 18	28 18	28 57	25 81	23 73	23 73				
5500	28 83	30 54	27 61	25 34	25 34	33 07	30 14	27 86	27 86	28 62	25 69	23 41	23 41				
5750	29 90	30 58	27 48	25 03	25 03	33 11	30 01	27 56	27 56	28 65	25 56	23 10	23 10				
6000	30 97	30 59	27 35	24 74	24 74	33 12	29 88	27 27	27 27	28 66	25 43	22 81	22 81				
6250	32 05	30 60	27 22	24 46	24 46	33 12	29 75	26 99	26 99	28 67	25 29	22 53	22 53				
6500	33 13	30 59	27 09	24 19	24 19	33 12	29 62	26 71	26 71	28 66	25 16	22 26	22 26				
6750	34 22	30 57	26 95	23 92	23 92	33 10	29 48	26 45	26 45	28 64	25 03	22 00	22 00				
7000	35 31	30 54	26 82	23 67	23 67	33 07	29 35	26 20	26 20	28 62	24 89	21 74	21 74				
7250	36 40	30 56	26 69	23 43	23 43	33 09	29 21	25 96	25 96	28 64	24 76	21 50	21 50				
7500	37 51	30 65	26 55	23 19	23 19	33 18	29 08	25 72	25 72	28 73	24 62	21 26	21 26				
7750	38 62	30 73	26 42	22 96	22 96	33 26	28 95	25 49	25 49	28 80	24 49	21 03	21 03				
8000	39 74	30 80	26 29	22 74	22 74	33 33	28 82	25 27	25 27	28 87	24 36	20 81	20 81				
8250	40 86	30 85	26 16	22 77	22 77	33 38	28 69	25 30	25 30	28 92	24 23	20 84	20 59				
8500	42 00	30 90	26 03	22 82	22 31	33 42	28 56	25 35	24 84	28 97	24 10	20 89	20 38				
8750	43 14	30 93	25 90	22 86	22 11	33 46	28 43	25 39	24 64	29 00	23 97	20 93	20 18				
9000	44 29	30 96	25 77	22 89	21 91	33 49	28 30	25 42	24 44	29 03	23 84	20 96	19 98				
9250	45 46	30 98	25 64	22 91	21 71	33 51	28 17	25 44	24 24	29 05	23 72	20 99	19 79				
9500	46 63	30 99	25 52	22 93	21 52	33 52	28 05	25 46	24 05	29 06	23 59	21 00	19 60				
9750	47 81	31 00	25 55	22 94	21 34	33 53	28 08	25 47	23 87	29 07	23 63	21 02	19 41				
10000	49 01	31 00	25 59	22 95	21 16	33 53	28 12	25 48	23 69	29 07	23 66	21 02	19 23				
10250	50 21	31 00	25 62	22 95	20 98	33 53	28 15	25 48	23 51	29 07	23 70	21 03	19 05				
10500	51 43	30 99	25 65	22 89	20 81	33 52	28 18	25 42	23 34	29 07	23 72	20 97	18 88				
10750	52 66	30 98	25 67	22 82	20 64	33 51	28 20	25 35	23 17	29 05	23 74	20 90	18 71				
11000	53 90	30 97	25 68	22 75	20 47	33 50	28 21	25 28	23 00	29 04	23 75	20 82	18 55				
11250	55 15	30 95	25 69	22 68	20 31	33 48	28 22	25 21	22 84	29 02	23 77	20 75	18 38				
11500	56 42	30 93	25 70	22 61	20 15	33 46	28 23	25 14	22 68	29 00	23 77	20 68	18 23				
11750	57 70	30 91	25 70	22 53	20 00	33 43	28 23	25 06	22 53	28 98	23 77	20 61	18 07				
12000	58 99	30 88	25 70	22 46	19 84	33 41	28 23	24 99	22 37	28 95	23 77	20 53	17 92				
12250	60 30	30 85	25 69	22 39	19 65	33 38	28 22	24 92	22 38	28 92	23 77	20 46	17 93				
12500	61 62	30 82	25 69	22 31	19 88	33 35	28 22	24 84	22 41	28 89	23 76	20 38	17 96				
12750	62 96	30 79	25 68	22 24	19 91	33 32	28 21	24 77	22 44	28 86	23 75	20 31	17 98				
13000	64 31	30 76	25 66	22 16	19 93	33 28	28 19	24 69	22 46	28 83	23 74	20 24	18 00				
13250	65 68	30 72	25 65	22 09	19 95	33 25	28 18	24 62	22 48	28 79	23 72	20 16	18 02				
13500	67 06	30 68	25 63	22 01	19 97	33 21	28 16	24 54	22 50	28 76	23 70	20 09	18 04				
13750	68 46	30 64	25 61	21 94	19 98	33 17	28 14	24 47	22 51	28 72	23 68	20 01	18 05				
14000	69 88	30 60	25 59	21 87	19 99	33 13	28 12	24 40	22 52	28 68	23 66	19 94	18 06				
14250	71 32	30 56	25 57	21 79	20 00	33 09	28 10	24 32	22 52	28 64	23 64	19 86	18 07				
14500	72 77	30 46	25 60	21 72	20 00	32 99	28 13	24 25	22 53	28 53	23 67	19 79	18 07				
14750	74 25	30 33	25 64	21 64	20 00	32 86	28 17	24 17	22 53	28 41	23 71	19 72	18 08				
15000	75 74	30 21	25 67	21 57	20 00	32 74	28 20	24 10	22 53	28 28	23 75	19 64	18 08				
15250	77 25	30 09	25 71	21 50	20 00	32 62	28 24	24 03	22 53	28 16	23 78	19 57	18 07				
15500	78 78	29 97	25 74	21 43	19 98	32 50	28 27	23 95	22 51	28 04	23 81	19 50	18 06				
15750	80 34	29 85	25 76	21 35	19 93	32 38	28 29	23 88	22 46	27 92	23 84	19 43	18 01				
16000	81 91	29 73	25 79	21 28	19 88	32 26	28 32	23 81	22 41	27 80	23 86	19 35	17 96				
16250	83 51	29 61	25 81	21 21	19 83	32 14	28 34	23 74	22 36	27 69	23 88	19 28	17 90				
16500	85 13	29 50	25 83	21 14	19 78	32 03	28 36	23 67	22 31	27 57	23 90	19 21	17 85				
16750	86 77	29 39	25 85	21 06	19 73	31 92	28 38	23 59	22 26	27 46	23 92	19 14	17 80				
17000	88 44	29 28	25 86	20 99	19 67	31 81	28 39	23 52	22 20	27 35	23 93	19 07	17 75				
17250	90 14	29 17	25 87	20 92	19 62	31 70	28 40	23 45	22 15	27 24	23 95	19 00	17 69				
17500	91 86	29 06	25 88	20 85	19 57	31 59	28 41	23 38	22 10	27 13	23 96	18 93	17 64				
17750	93 61	28 95	25 89	20 78	19 52	31 48	28 42	23 31	22 05	27 03	23 97	18 86	17 59				
18000	95 38	28 85	25 90	20 71	19 46	31 38	28 43	23 24	21 99	26 92	23 97	18 79	17 54				
18250	97 19	28 75	25 90	20 64	19 41	31 27	28 43	23 17	21 94	26 82	23 98	18 72	17 48				
18500	99 03	28 64	25 91	20 57	19 36	31 17	28 44	23 10	21 89	26 72	23 98	18 65	17 43				
18750	100 90	28 54	25 91	20 51	19 31	31 07	28 44	23 04	21 83	26 61	23 98	18 58	17 38				

TABLE J.1. Supplement To Figures J.1 & J.2.

19000	102 80	28 44	25 91	20 44	19 25	30 97	28 44	22 97	21 78	26 51	23 98	18 51	17 33
19250	104 74	28 34	25 91	20 45	19 20	30 87	28 44	22 97	21 73	26 42	23 98	18 52	17 27
19500	106 71	28 24	25 91	20 46	19 15	30 77	28 44	22 99	21 68	26 32	23 98	18 53	17 22
19750	108 72	28 15	25 90	20 47	19 09	30 68	28 43	23 00	21 62	26 22	23 97	18 55	17 17
20000	110 77	28 05	25 90	20 49	19 04	30 58	28 43	23 02	21 57	26 13	23 97	18 56	17 11
20250	112 86	27 96	25 89	20 50	18 99	30 49	28 42	23 03	21 52	26 03	23 96	18 57	17 06
20500	115 00	27 87	25 88	20 51	18 94	30 39	28 41	23 04	21 46	25 94	23 96	18 58	17 01
20750	117 18	27 77	25 88	20 51	18 88	30 30	28 40	23 04	21 41	25 85	23 95	18 59	16 96
21000	119 41	27 68	25 87	20 52	18 83	30 21	28 40	23 05	21 36	25 75	23 94	18 59	16 90
21250	121 69	27 59	25 86	20 53	18 78	30 12	28 39	23 06	21 31	25 66	23 93	18 60	16 85
21500	124 03	27 50	25 84	20 53	18 73	30 03	28 37	23 06	21 25	25 58	23 92	18 60	16 80
21750	126 42	27 41	25 83	20 53	18 67	29 94	28 36	23 06	21 20	25 49	23 91	18 61	16 75
22000	128 87	27 33	25 82	20 54	18 62	29 86	28 35	23 06	21 15	25 40	23 89	18 61	16 69
22250	131 39	27 24	25 81	20 54	18 57	29 77	28 34	23 07	21 10	25 31	23 88	18 61	16 64
22500	133 98	27 15	25 79	20 54	18 52	29 68	28 32	23 06	21 05	25 23	23 87	18 61	16 59
22750	136 65	27 07	25 78	20 53	18 47	29 60	28 31	23 06	20 99	25 14	23 85	18 61	16 54
23000	139 40	26 99	25 76	20 53	18 41	29 52	28 29	23 06	20 94	25 06	23 83	18 60	16 49
23250	142 23	26 90	25 75	20 53	18 36	29 43	28 28	23 06	20 89	24 98	23 82	18 60	16 43
23500	145 16	26 82	25 73	20 52	18 31	29 35	28 26	23 05	20 84	24 89	23 80	18 60	16 38
23750	148 20	26 74	25 71	20 52	18 26	29 27	28 24	23 05	20 79	24 81	23 78	18 59	16 33
24000	151 35	26 66	25 69	20 51	18 21	29 19	28 22	23 04	20 74	24 73	23 77	18 59	16 28
24250	154 64	26 58	25 68	20 51	18 16	29 11	28 20	23 04	20 69	24 65	23 75	18 58	16 23
24500	158 06	26 50	25 66	20 50	18 11	29 03	28 19	23 03	20 64	24 57	23 73	18 57	16 18
24750	161 66	26 42	25 64	20 49	18 06	28 95	28 17	23 02	20 59	24 49	23 71	18 56	16 13
25000	165 43	26 34	25 62	20 48	18 01	28 87	28 15	23 01	20 54	24 42	23 69	18 56	16 08
25250	169 43	26 27	25 60	20 47	17 96	28 80	28 13	23 00	20 49	24 34	23 67	18 55	16 03
25500	173 68	26 19	25 58	20 46	17 91	28 72	28 11	22 99	20 44	24 26	23 65	18 54	15 98
25750	178 25	26 11	25 56	20 45	17 86	28 64	28 08	22 98	20 39	24 19	23 63	18 53	15 93
26000	183 20	26 04	25 53	20 44	17 81	28 57	28 06	22 97	20 34	24 11	23 61	18 51	15 88
26250	188 64	25 97	25 51	20 43	17 76	28 50	28 04	22 96	20 29	24 04	23 58	18 50	15 83
26500	194 76	25 89	25 49	20 42	17 71	28 42	28 02	22 95	20 24	23 97	23 56	18 49	15 78
26750	201 87	25 82	25 47	20 41	17 66	28 35	28 00	22 93	20 19	23 89	23 54	18 48	15 73
27000	210 71	25 75	25 44	20 39	17 61	28 28	27 97	22 92	20 14	23 82	23 52	18 47	15 68
27250	223 86	25 68	25 42	20 38	17 56	28 20	27 95	22 91	20 09	23 75	23 49	18 45	15 64
27358	238 72	25 64	25 41	20 37	17 54	28 17	27 94	22 90	20 07	23 72	23 48	18 45	15 61

TABLE J.2. Continuation of Supplement To Figures J.1 & J.2.

alt	C/N(28 deg)	C/N(var)	alt	C/N(28 deg)	C/N(var)
500	42.06	42.06	15000	18.33	23.75
750	39.10	39.10	15250	18.20	23.78
1000	37.06	37.06	15500	18.08	23.81
1250	35.51	35.51	15750	17.96	23.84
1500	34.25	34.25	16000	17.85	23.86
1750	33.20	33.20	16250	17.73	23.88
2000	32.29	32.29	16500	17.62	23.90
2250	31.50	31.50	16750	17.51	23.92
2500	30.79	30.79	17000	17.39	23.93
2750	30.15	30.15	17250	17.29	23.95
3000	29.56	29.56	17500	17.18	23.96
3250	29.02	29.02	17750	17.07	23.97
3500	28.52	28.52	18000	16.97	23.97
3750	28.06	28.06	18250	16.86	23.98
4000	27.62	27.62	18500	16.76	23.98
4250	27.21	27.21	18750	16.66	23.98
4500	26.82	26.82	19000	16.56	23.98
4750	26.45	26.45	19250	16.46	23.98
5000	26.10	26.10	19500	16.36	23.98
5250	25.77	25.81	19750	16.27	23.97
5500	25.45	25.69	20000	16.17	23.97
5750	25.15	25.56	20250	16.08	23.96
6000	24.85	25.43	20500	15.98	23.96
6250	24.57	25.29	20750	15.89	23.95
6500	24.30	25.16	21000	15.80	23.94
6750	24.04	25.03	21250	15.71	23.93
7000	23.79	24.89	21500	15.62	23.92
7250	23.54	24.76	21750	15.53	23.91
7500	23.31	24.62	22000	15.44	23.89
7750	23.08	24.49	22250	15.36	23.88
8000	22.85	24.36	22500	15.27	23.87
8250	22.64	24.23	22750	15.19	23.85
8500	22.43	24.10	23000	15.10	23.83
8750	22.22	23.97	23250	15.02	23.82
9000	22.02	23.84	23500	14.94	23.80
9250	21.83	23.72	23750	14.86	23.78
9500	21.64	23.59	24000	14.78	23.77
9750	21.45	23.63	24250	14.70	23.75
10000	21.27	23.66	24500	14.62	23.73
10250	21.10	23.70	24750	14.54	23.71
10500	20.92	23.72	25000	14.46	23.69
10750	20.76	23.74	25250	14.38	23.67
11000	20.59	23.75	25500	14.31	23.65
11250	20.43	23.77	25750	14.23	23.63
11500	20.27	23.77	26000	14.16	23.61
11750	20.11	23.77	26250	14.08	23.58
12000	19.96	23.77	26500	14.01	23.56
12250	19.81	23.77	26750	13.94	23.54
12500	19.66	23.76	27000	13.86	23.52
12750	19.52	23.75	27250	13.79	23.49
13000	19.38	23.74	27358	13.76	23.48
13250	19.24	23.72			
13500	19.10	23.70			
13750	18.97	23.68			
14000	18.83	23.66			
14250	18.70	23.64			
14500	18.58	23.67			
14750	18.45	23.71			

TABLE J.3. Supplement To Figure J.3.

ALT	Slnt Rng	Lu	Ld	ALT	Slnt Rng	Lu	Ld	ALT	Slnt Rng	Lu	Ld
500	1192 99	186 84	180 00	9400	12413 97	207 19	200 34	18300	21757 75	212 06	205 21
500	1392 41	188 19	181 34	9500	12622 01	207 26	200 42	18400	21860 83	212 10	205 26
600	1583 93	189 31	182 46	9600	12629 95	207 34	200 49	18500	21963 88	212 15	205 30
700	1768 70	190 26	183 42	9700	12737 77	207 41	200 56	18600	22066 90	212 19	205 34
800	1947 63	191 10	184 25	9800	12845 48	207 49	200 64	18700	22169 89	212 23	205 38
900	2121 45	191 84	185 00	9900	12953 09	207 56	200 71	18800	22272 87	212 27	205 42
1000	2290 75	192 51	185 66	10000	13060 59	207 63	200 78	18900	22375 81	212 31	205 46
1100	2456 02	193 12	186 27	10100	13168 00	207 70	200 85	19000	22478 74	212 35	205 50
1200	2617 69	193 67	186 82	10200	13275 30	207 77	200 92	19100	22581 64	212 39	205 54
1300	2776 11	194 18	187 33	10300	13382 51	207 84	200 99	19200	22684 51	212 43	205 58
1400	2931 57	194 65	187 80	10400	13489 62	207 91	201 06	19300	22787 36	212 46	206 62
1500	3084 35	195 09	188 25	10500	13596 63	207 98	201 13	19400	22890 19	212 50	206 66
1600	3234 66	195 51	188 66	10600	13703 56	208 05	201 20	19500	22993 00	212 54	206 69
1700	3382 71	195 90	189 05	10700	13810 40	208 11	201 27	19600	23095 78	212 58	205 73
1800	3528 67	196 26	189 41	10800	13917 15	208 18	201 33	19700	23198 54	212 62	205 77
1900	3672 70	196 61	189 76	10900	14023 81	208 25	201 40	19800	23301 28	212 66	205 81
2000	3814 94	196 94	190 09	11000	14130 39	208 31	201 47	19900	23404 00	212 70	205 85
2100	3955 51	197 25	190 41	11100	14236 88	208 38	201 53	20000	23506 70	212 73	205 89
2200	4094 53	197 55	190 71	11200	14343 30	208 44	201 60	20100	23609 37	212 77	205 92
2300	4232 09	197 84	190 99	11300	14449 63	208 51	201 66	20200	23712 03	212 81	205 96
2400	4368 29	198 12	191 27	11400	14555 89	208 57	201 72	20300	23814 66	212 85	206 00
2500	4503 21	198 38	191 53	11500	14662 07	208 63	201 79	20400	23917 27	212 89	206 04
2600	4636 93	198 64	191 79	11600	14768 17	208 70	201 85	20500	24019 87	212 92	206 07
2700	4769 52	198 88	192 03	11700	14874 20	208 76	201 91	20600	24122 44	212 96	206 11
2800	4901 03	199 12	192 27	11800	14980 16	208 82	201 97	20700	24224 99	213 00	206 15
2900	5031 54	199 34	192 50	11900	15086 05	208 88	202 03	20800	24327 52	213 03	206 18
3000	5161 08	199 57	192 72	12000	15191 87	208 94	202 09	20900	24430 03	213 07	206 22
3100	5289 72	199 78	192 93	12100	15297 62	209 00	202 15	21000	24532 53	213 11	206 26
3200	5417 50	199 99	193 14	12200	15403 30	209 06	202 21	21100	24635 01	213 14	206 29
3300	5544 46	200 19	193 34	12300	15508 91	209 12	202 27	21200	24737 47	213 18	206 33
3400	5670 64	200 38	193 54	12400	15614 46	209 18	202 33	21300	24839 91	213 21	206 37
3500	5796 07	200 57	193 73	12500	15719 95	209 24	202 39	21400	24942 33	213 25	206 40
3600	5920 80	200 76	193 91	12600	15825 38	209 30	202 45	21500	25044 73	213 29	206 44
3700	6044 85	200 94	194 09	12700	15930 74	209 36	202 51	21600	25147 12	213 32	206 47
3800	6168 26	201 11	194 27	12800	16036 04	209 41	202 56	21700	25249 49	213 36	206 51
3900	6291 05	201 29	194 44	12900	16141 28	209 47	202 62	21800	25351 84	213 39	206 54
4000	6413 25	201 45	194 60	13000	16246 47	209 53	202 68	21900	25454 17	213 43	206 58
4100	6534 89	201 62	194 77	13100	16351 60	209 58	202 73	22000	25556 49	213 46	206 61
4200	6656 62	202 08	195 24	13200	16456 64	209 75	202 90	22100	25658 33	213 50	206 65
4300	6776 21	202 23	195 38	13300	16561 55	209 80	202 95	22200	25760 58	213 54	206 69
4400	6894 34	202 38	195 53	13400	16666 21	209 86	203 01	22300	25863 02	213 58	206 73
4500	7011 50	202 52	195 67	13500	16771 55	209 91	203 06	22400	25965 58	213 62	206 77
4600	7128 28	202 66	195 81	13600	16876 41	209 96	203 12	22500	26068 24	213 66	206 81
4700	7244 03	202 80	195 95	13700	16981 21	209 99	203 17	22600	26170 82	213 70	206 85
4800	7359 28	202 93	196 09	13800	17085 96	209 96	203 22	22700	26272 42	213 74	206 89
4900	7474 03	203 07	196 23	13900	17190 66	210 02	203 27	22800	26374 02	213 78	206 93
5000	7588 78	203 20	196 37	14000	17295 31	210 07	203 32	22900	26475 59	213 82	206 97
5100	7702 53	203 33	196 51	14100	17399 92	210 12	203 37	23000	26577 15	213 86	207 01
5200	7816 28	203 46	196 65	14200	17504 47	210 17	203 42	23100	26678 71	213 90	207 05
5300	7929 03	203 59	196 79	14300	17608 98	210 22	203 47	23200	26780 27	213 94	207 09
5400	8041 78	203 72	196 93	14400	17713 44	210 28	203 52	23300	26881 83	213 98	207 13
5500	8154 53	203 85	197 07	14500	17817 86	210 33	203 57	23400	26983 39	214 02	207 17
5600	8267 28	203 98	197 21	14600	17922 23	210 38	203 62	23500	27084 95	214 06	207 21
5700	8379 03	204 11	197 35	14700	18026 56	210 43	203 67	23600	27186 51	214 10	207 25
5800	8490 78	204 24	197 49	14800	18130 84	210 48	203 72	23700	27288 07	214 14	207 29
5900	8602 53	204 37	197 63	14900	18235 08	210 53	203 77	23800	27389 63	214 18	207 33
6000	8714 28	204 50	197 77	15000	18339 28	210 58	203 82	23900	27491 19	214 22	207 37
6100	8826 03	204 63	197 91	15100	18443 44	210 63	203 87	24000	27592 75	214 26	207 41
6200	8937 78	204 76	198 05	15200	18547 55	210 68	203 92	24100	27694 31	214 30	207 45
6300	9049 53	204 89	198 19	15300	18651 63	210 73	203 97	24200	27795 87	214 34	207 49
6400	9161 28	205 02	198 33	15400	18755 67	210 78	204 02	24300	27897 43	214 38	207 53
6500	9273 03	205 15	198 47	15500	18859 62	210 83	204 07	24400	27998 99	214 42	207 57
6600	9384 78	205 28	198 61	15600	18963 54	210 88	204 12	24500	28099 55	214 46	207 61
6700	9496 53	205 41	198 75	15700	19067 42	210 92	204 17	24600	28200 11	214 50	207 65
6800	9608 28	205 54	198 89	15800	19171 26	210 97	204 22	24700	28300 67	214 54	207 69
6900	9719 03	205 67	199 03	15900	19275 17	211 01	204 27	24800	28401 23	214 58	207 73
7000	9829 78	205 80	199 17	16000	19379 08	211 06	204 32	24900	28501 79	214 62	207 77
7100	9940 53	205 93	199 31	16100	19482 85	211 10	204 37	25000	28602 35	214 66	207 81
7200	10051 28	206 06	199 45	16200	19586 59	211 15	204 42	25100	28702 91	214 70	207 85
7300	10162 03	206 19	199 59	16300	19690 30	211 20	204 47	25200	28803 47	214 74	207 89
7400	10272 78	206 32	199 73	16400	19793 97	211 24	204 52	25300	28904 03	214 78	207 93
7500	10383 53	206 45	199 87	16500	19897 60	211 29	204 57	25400	29004 59	214 82	207 97
7600	10494 28	206 58	199 99	16600	20001 20	211 33	204 62	25500	29105 15	214 86	208 01
7700	10605 03	206 71	200 13	16700	20104 77	211 38	204 67	25600	29205 71	214 90	208 05
7800	10715 78	206 84	200 27	16800	20208 31	211 42	204 72	25700	29306 27	214 94	208 09
7900	10826 53	206 97	200 41	16900	20311 82	211 47	204 77	25800	29406 83	214 98	208 13
8000	10937 28	207 10	200 55	17000	20415 29	211 51	204 82	25900	29507 39	215 02	208 17
8100	11048 03	207 23	200 69	17100	20518 73	211 55	204 87	26000	29607 95	215 06	208 21
8200	11158 78	207 36	200 83	17200	20622 14	211 60	204 92	26100	29708 51	215 10	208 25
8300	11269 53	207 49	200 97	17300	20725 52	211 64	204 97	26200	29809 07	215 14	208 29
8400	11380 28	207 62	201 11	17400	20828 87	211 68	205 02	26300	29909 63	215 18	208 33
8500	11491 03	207 75	201 25	17500	20932 20	211 73	205 07	26400	30010 19	215 22	208 37
8600	11601 78	207 88	201 39	17600	21035 49	211 77	205 12	26500	30110 75	215 26	208 41
8700	11712 53	208 01	201 53	17700	21138 75	211 81	205 17	26600	30211 31	215 30	208 45
8800	11823 28	208 14	201 67	17800	21241 99	211 85	205 22	26700	30311 87	215 34	208 49
8900	11934 03	208 27	201 81	17900	21345 20	211 90	205 27	26800	30412 43	215 38	208 53
9000	12044 78	208 40	201 95	18000	21448 38	211 94	205 32	26900	30512 99	215 42	208 57
9100	12155 53	208 53	202 09	18100	21551 53	211 98	205 37	27000	30613 55	215 46	208 61
9200	12266 28	208 66	202 23	18200	21654 65	212 02	205				

Alt	32			27			24			22			20		
	C/Up	C/Down	C/Ntot												
500	54 87645	61 72491	54 06078	49 87645	56 72491	49 06078	46 87645	53 72491	46 06078	44 87645	51 72491	44 06078	42 87645	49 72491	42 06078
750	51 91802	58 76647	51 10234	46 91802	53 76647	46 10234	43 91802	50 76647	43 10234	41 91802	48 76647	41 10234	39 91802	46 76647	39 10234
1000	49 87653	56 72499	49 06086	44 87653	51 72499	44 06086	41 87653	48 72499	41 06086	39 87653	46 72499	39 06086	37 87653	44 72499	37 06086
1250	48 32179	55 17024	47 50612	43 32179	50 17024	42 50612	40 32179	47 17024	39 50612	38 32179	45 17024	37 50612	36 32179	43 17024	35 50612
1500	47 06716	53 91562	46 25149	42 06716	48 91562	41 25149	39 06716	45 91562	38 25149	37 06716	43 91562	36 25149	35 06716	41 91562	34 25149
1750	46 01536	52 86382	45 19969	41 01536	47 86382	40 19969	38 01536	44 86382	37 19969	36 01536	42 86382	35 19969	34 01536	40 86382	33 19969
2000	45 10947	51 95792	44 29379	40 10947	46 95792	39 29379	37 10947	43 95792	36 29379	35 10947	41 95792	34 29379	33 10947	39 95792	32 29379
2250	44 31341	51 16186	43 49774	39 31341	46 16186	38 49774	36 31341	43 16186	35 49774	34 31341	41 16186	33 49774	32 31341	39 16186	31 49774
2500	43 60294	50 45139	42 78727	38 60294	45 45139	37 78727	35 60294	42 45139	34 78727	33 60294	40 45139	32 78727	31 60294	38 45139	30 78727
2750	42 961	49 80946	42 14533	37 961	44 80946	37 14533	34 961	41 80946	34 14533	32 961	39 80946	32 14533	30 961	37 80946	30 14533
3000	42 37516	49 22361	41 55949	37 37516	44 22361	36 55949	34 37516	41 22361	33 55949	32 37516	39 22361	31 55949	30 37516	29 55949	29 22361
3250	41 83607	48 68452	41 02039	36 83607	43 68452	36 02039	33 83607	40 68452	33 02039	31 83607	38 68452	31 02039	29 83607	36 68452	29 02039
3500	41 33654	48 18499	40 52087	36 33654	43 18499	35 52087	33 33654	40 18499	32 52087	31 33654	38 18499	30 52087	29 33654	36 18499	28 52087
3750	40 87093	47 71938	40 05525	35 87093	42 71938	35 05525	32 87093	39 71938	32 05525	30 87093	37 71938	30 05525	28 87093	35 71938	28 05525
4000	40 43471	47 28316	39 61903	35 43471	42 28316	34 61903	32 43471	39 28316	31 61903	30 43471	37 28316	29 61903	28 43471	35 28316	27 61903
4250	40 02422	46 87268	39 20855	35 02422	41 87268	34 20855	32 02422	38 87268	31 20855	30 02422	36 87268	29 20855	28 02422	34 87268	27 20855
4500	39 63645	46 4849	38 82077	34 63645	41 4849	33 82077	31 63645	38 4849	30 82077	29 63645	36 4849	28 82077	27 63645	26 82077	26 82077
4750	39 26888	46 11733	38 4532	34 26888	41 11733	33 4532	31 26888	38 11733	30 4532	29 26888	36 11733	28 4532	27 26888	34 11733	26 4532
5000	38 91939	45 76784	38 10372	33 91939	40 76784	33 10372	30 91939	37 76784	30 10372	28 91939	35 76784	28 10372	26 91939	33 76784	26 10372
5250	38 5862	45 43465	37 77052	33 5862	40 43465	32 77052	30 5862	37 43465	29 77052	28 5862	35 43465	27 77052	26 5862	33 43465	25 77052
5500	38 26776	45 11621	37 45208	33 26776	40 11621	32 45208	30 26776	37 11621	29 45208	28 26776	35 11621	27 45208	26 26776	33 11621	25 45208
5750	37 96274	44 8112	37 14707	32 96274	39 8112	32 14707	29 96274	36 8112	29 14707	27 96274	34 8112	27 14707	25 96274	32 8112	25 14707
6000	37 67	44 51846	36 85433	32 67	39 51846	31 85433	29 67	36 51846	28 85433	27 67	34 51846	26 85433	25 67	32 51846	24 85433
6250	37 38853	44 23698	36 57285	32 38853	39 23698	31 57285	29 38853	36 23698	28 57285	27 38853	34 23698	26 57285	25 38853	32 23698	24 57285
6500	37 11743	43 96588	36 30175	32 11743	39 96588	31 30175	29 11743	35 96588	28 30175	27 11743	33 96588	26 30175	25 11743	31 96588	24 30175
6750	36 85592	43 70438	36 04025	31 85592	38 70438	31 04025	28 85592	35 70438	28 04025	26 85592	33 70438	26 04025	24 85592	31 70438	24 04025
7000	36 60331	43 45177	35 78764	31 60331	38 45177	30 78764	28 60331	35 45177	27 78764	26 60331	33 45177	25 78764	24 60331	31 45177	23 78764
7250	36 35898	43 20743	35 5433	31 35898	38 20743	30 5433	28 35898	35 20743	27 5433	26 35898	33 20743	25 5433	24 35898	31 20743	23 5433
7500	36 12236	42 97081	35 30668	31 12236	37 97081	30 30668	28 12236	34 97081	27 30668	26 12236	32 97081	25 30668	24 12236	30 97081	23 30668
7750	35 89295	42 7414	35 07727	30 89295	37 7414	30 07727	27 89295	34 7414	27 07727	25 89295	32 7414	25 07727	23 89295	30 7414	23 07727
8000	35 6703	42 51875	34 85462	30 6703	37 51875	29 85462	27 6703	34 51875	26 85462	25 6703	32 51875	24 85462	23 6703	30 51875	22 85462
8250	35 454	42 30245	34 63832	30 454	37 30245	29 63832	27 454	34 30245	26 63832	25 454	32 30245	24 63832	23 454	30 30245	22 63832
8500	35 24367	42 09212	34 42799	30 24367	37 09212	29 42799	27 24367	34 09212	26 42799	25 24367	32 09212	24 42799	23 24367	30 09212	22 42799
8750	35 03897	41 88743	34 2233	30 03897	36 88743	29 2233	27 03897	33 88743	26 2233	25 03897	31 88743	24 2233	23 03897	29 88743	22 2233
9000	34 8396	41 68805	34 02392	29 8396	36 68805	29 02392	26 8396	33 68805	26 02392	24 8396	31 68805	24 02392	22 8396	29 68805	22 02392
9250	34 64526	41 49371	33 82958	29 64526	36 49371	28 82958	26 64526	33 49371	25 82958	24 64526	31 49371	23 82958	22 64526	29 49371	21 82958
9500	34 45569	41 30414	33 64002	29 45569	36 30414	28 64002	26 45569	33 30414	25 64002	24 45569	31 30414	23 64002	22 45569	29 30414	21 64002
9750	34 27065	41 11191	33 45498	29 27065	36 11191	28 45498	26 27065	33 11191	25 45498	24 27065	31 11191	23 45498	22 27065	29 11191	21 45498
10000	34 08992	40 93837	33 27424	29 08992	35 93837	28 27424	26 08992	32 93837	25 27424	24 08992	30 93837	23 27424	22 08992	28 93837	21 27424
10250	33 91328	40 76173	33 0976	28 91328	35 76173	28 0976	25 91328	32 76173	25 0976	23 91328	30 76173	23 0976	21 91328	28 76173	21 0976
10500	33 74055	40 589	32 92487	28 74055	35 589	27 92487	25 74055	32 589	24 92487	23 74055	30 589	22 92487	21 74055	28 589	20 92487
10750	33 57154	40 41999	32 75586	28 57154	35 41999	27 75586	25 57154	32 41999	24 75586	23 57154	30 41999	22 75586	21 57154	28 41999	20 75586
11000	33 40609	40 25455	32 59042	28 40609	35 25455	27 59042	25 40609	32 25455	24 59042	23 40609	30 25455	22 59042	21 40609	28 25455	20 59042
11250	33 24405	40 09251	32 42838	28 24405	35 09251	27 42838	25 24405	32 09251	24 42838	23 24405	30 09251	22 42838	21 24405	28 09251	20 42838
11500	33 08527	39 93372	32 2696	28 08527	34 93372	27 2696	25 08527	31 93372	24 2696	23 08527	29 93372	22 2696	21 08527	27 93372	20 2696
11750	32 92961	39 77807	32 11394	27 92961	34 77807	27 11394	24 92961	31 77807	24 11394	22 92961	29 77807	22 11394	20 92961	27 77807	20 11394
12000	32 77695	39 62541	31 96128	27 77695	34 62541	26 96128	24 77695	31 62541	24 96128	22 77695	29 62541	22 96128	20 77695	27 62541	19 96128
12250	32 62717	39 47562	31 81149	27 62717	34 47562	26 81149	24 62717	31 47562	23 81149	22 62717	29 47562	22 81149	20 62717	27 47562	19 81149
12500	32 48015	39 3286	31 66448	27 48015	34 3286	26 66448	24 48015	31 3286	23 66448	22 48015	29 3286	22 66448	20 48015	27 3286	19 66448
12750	32 33579	39 18425	31 52012	27 33579	34 18425	26 52012	24 33579	31 18425	23 52012	22 33579	29 18425	22 52012	20 33579	27 18425	19 52012
13000	32 19399	39 04245	31 37832	27 19399	34 04245	26 37832	24 19399	31 04245	23 37832	22 19399	29 04245	22 37832	20 19399	27 04245	19 37832
13250	32 05466	38 90312	31 23899	27 05466	33 90312	26 23899	24 05466	30 90312	23 23899	22 05466	28 90312	21 23899	20 05466	26 90312	19 23899
13500	31 91771	38 76616	31 10203	26 91771	33 76616	26 10203	24 91771	30 76616	23 10203	22 91771	28 76616	21 10203	19 91771	26 76616	19 10203
13750	31 78305	38 6315	30 96738	26 78305	33 6315	25 96738	23 78305	30 6315	22 96738	21 78305	28 6315	20 96738	19 78305	26 6315	18 96738
14000	31 65061	38 49906	30 83493	26 65061	33 49906	25 83493	23 65061	30 49906	22 83493	21 65061	28 49906	20 83493	19 65061	26 49906	18 83493
14250	31 5203	38 36875	30 70463	26 5203	33 36875	25 70463	23 5203	30 36875	22 70463	21 5203	28 36875	20 70463	19 5203	26 36875	18 70463
14500	31 39206	38 24052	30 57639	26 39206	33 24052	25 57639	23 39206	30 24052	22 57639	21 39206	28 24052	20 57639	19 39206	26 24052	18 57639
14750	31 26583	38 11428	30 45015	26 26583	33 11428	25 45015	23 26583	30 11428	22 45015	21 26583	28 11428	20 45015	19 26583	26 11428	18 45015
15000	31 14153	37 98998	30 32585	26 14153	33 98998	25 32585	23 14153	29 989							

22750	28 00236	34 85081	27.18668	23 00236	29 85081	22 18668	20 00236	26 85081	19 18668	18 00236	24 85081	17 18668	16 00236	22 85081	15 18668
23000	27 91848	34 76694	27.10281	22 91848	29 76694	22 10281	19 91848	26 76694	19 10281	17 91848	24 76694	17 10281	15 91848	22 76694	15 10281
23250	27 83544	34 6839	27 01977	22 83544	29 6839	22 01977	19 83544	26 6839	19 01977	17 83544	24 6839	17 01977	15 83544	22 6839	15 01977
23500	27 75322	34 60167	26 93754	22 75322	29 60167	21 93754	19 75322	26 60167	18 93754	17 75322	24 60167	16 93754	15 75322	22 60167	14 93754
23750	27 67179	34 52024	26 85612	22 67179	29 52024	21 85612	19 67179	26 52024	18 85612	17 67179	24 52024	16 85612	15 67179	22 52024	14 85612
24000	27 59115	34 4396	26 77547	22 59115	29 4396	21 77547	19 59115	26 4396	18 77547	17 59115	24 4396	16 77547	15 59115	22 4396	14 77547
24250	27 51127	34 35973	26 6956	22 51127	29 35973	21 6956	19 51127	26 35973	18 6956	17 51127	24 35973	16 6956	15 51127	22 35973	14 6956
24500	27 43215	34 28061	26 61648	22 43215	29 28061	21 61648	19 43215	26 28061	18 61648	17 43215	24 28061	16 61648	15 43215	22 28061	14 61648
24750	27 35377	34 20223	26 5381	22 35377	29 20223	21 5381	19 35377	26 20223	18 5381	17 35377	24 20223	16 5381	15 35377	22 20223	14 5381
25000	27 27612	34 12457	26 46044	22 27612	29 12457	21 46044	19 27612	26 12457	18 46044	17 27612	24 12457	16 46044	15 27612	22 12457	14 46044
25250	27 19917	34 04763	26 3835	22 19917	29 04763	21 3835	19 19917	26 04763	18 3835	17 19917	24 04763	16 3835	15 19917	22 04763	14 3835
25500	27 12292	33 97138	26 30725	22 12292	28 97138	21 30725	19 12292	25 97138	18 30725	17 12292	23 97138	16 30725	15 12292	21 97138	14 30725
25750	27 04736	33 89582	26 23169	22 04736	28 89582	21 23169	19 04736	25 89582	18 23169	17 04736	23 89582	16 23169	15 04736	21 89582	14 23169
26000	26 97247	33 82093	26 1568	21 97247	28 82093	21 1568	18 97247	25 82093	18 1568	16 97247	23 82093	16 1568	14 97247	21 82093	14 1568
26250	26 89824	33 7467	26 08257	21 89824	28 7467	21 08257	18 89824	25 7467	18 08257	16 89824	23 7467	16 08257	14 89824	21 7467	14 08257
26500	26 82466	33 67312	26 00899	21 82466	28 67312	21 00899	18 82466	25 67312	18 00899	16 82466	23 67312	16 00899	14 82466	21 67312	14 00899
26750	26 75172	33 60017	25 93604	21 75172	28 60017	20 93604	18 75172	25 60017	17 93604	16 75172	23 60017	15 93604	14 75172	21 60017	13 93604
27000	26 6794	33 52786	25 86373	21 6794	28 52786	20 86373	18 6794	25 52786	17 86373	16 6794	23 52786	15 86373	14 6794	21 52786	13 86373
27250	26 6077	33 45615	25 79202	21 6077	28 45615	20 79202	18 6077	25 45615	17 79202	16 6077	23 45615	15 79202	14 6077	21 45615	13 79202
27358	26 57691	33 42537	25 76124	21 57691	28 42537	20 76124	18 57691	25 42537	17 76124	16 57691	23 42537	15 76124	14 57691	21 42537	13 76124

TABLE J.5. Carrier -To-Noise Ratios For Fixed Antenna Gains.

APPENDIX K

**DEFENSE ADVANCED RESEARCH PROJECTS AGENCY
STATEMENT OF WORK**

**DEFENSE ADVANCED RESEARCH PROJECTS AGENCY (DARPA)
ADVANCED SPACE TECHNOLOGY PROGRAM (ASTP)
ADVANCED SATELLITE SUBSYSTEM TECHNOLOGIES DEMONSTRATION
STATEMENT OF WORK**

1.0 PURPOSE

This Statement of Work (SOW) defines the tasks to be performed by the Contractor to develop the system designs for a multi-mission-capable small standard spacecraft bus and a meteorological satellite based on the standard spacecraft bus. In addition, the Contractor is tasked to develop a system design for a spacecraft to incorporate and demonstrate advanced technology spacecraft and payload subsystems and components currently being developed for DARPA.

2.0 BACKGROUND

The Defense Advanced Research Projects Agency (DARPA) Advanced Space Technology Program (ASTP) is defining, developing and demonstrating high payoff advanced technology applications to improve space system operational support to military commanders. The focus of the program is to advance the state-of-the-art for more capable, smaller and lighter satellite systems, subsystems and components.

The current program includes: the development, launch and demonstration of small, lightweight UHF communications satellites; the flight test of the PEGASUS Air Launched Vehicle (ALV) to evaluate its launch flexibility, practicality and utility to place small payloads into orbit; and the development and demonstration of the ground launched Standard Small Launch Vehicle (SSLV) which is to be capable of placing a minimum payload of 1000 pounds into a 400 nautical mile circular polar orbit. Both the ALV and SSLV are to enable delivery of a small spacecraft to low earth orbit within 72 hours of the launch command (i.e., vehicle/spacecraft integration, final vehicle assembly, checkout and launch activities are to occur within this 72 hour period).

Consistent with the ASTP objectives is the pursuit of advanced space system technologies that will enable the DoD to acquire lightweight, cost-effective military satellites which can be dedicated to Theater commanders to assure availability and reconstitution after attack. Subsystem and component innovations are included in this pursuit.

Proposals addressing advanced technology space systems, subsystems and components have been received in response to a Broad Agency Announcement (BAA #88-13) issued by DARPA. This SOW is a formalization to a proposal selected for consideration.

The proposal is to design a small, low-cost, lightweight, general purpose spacecraft bus capable of accommodating any of a variety of mission payloads. Such a bus is expected to provide major benefits to the military, as well as the scientific and technical community. Typical payloads envisioned include those associated with meteorological, communications, surveillance and tracking, target location, and navigation mission areas. Specific emphasis is given in the proposal to using a multi-spectral meteorological payload to demonstrate the military utility and benefits of a general purpose multi-mission capable spacecraft bus.

As separate efforts, DARPA is sponsoring the development of advanced technology spacecraft and payload subsystems and components. A small standard spacecraft provides the opportunity to integrate the results of these efforts for subsequent on-orbit system demonstrations.

3.0 SCOPE

The Contractor's activities are directed towards the following objectives:

- * Defining the system requirements for a small, standard spacecraft bus as imposed by potential tactical mission areas which include meteorology, communications, surveillance and tracking, target location, navigation, and crosslinking.
- * Developing the system design for a small, standard spacecraft bus.
- * Developing the system design for a meteorological satellite using the small, standard spacecraft bus, and
- * Developing the system design for a communications satellite using subsystem and component technologies being developed by DARPA.

The small, standard spacecraft bus shall be capable of accommodating any of several potential mission payloads. The spacecraft shall be compatible with the ALV and SSLV (and comparable launch vehicles), and capable of being inserted into and operating in any of a variety of potential mission orbits, including low earth circular (i.e., less than 400 nautical mile altitude), higher earth circular (i.e., greater than 400 nautical mile altitude), and Molniya-type elliptical orbits.

The spacecraft bus shall possess sufficient space and power to enable implementation of appropriate hardware and software to support duplex crosslink communications with suitably-equipped satellites. The duplex crosslink communications capability shall be inherent in the spacecraft bus design, but shall permit optional implementation of hardware/software. Besides supporting payload and Telemetry, Tracking and Command (TT&C) operations, the crosslink capability shall also support pass-through relay communications.

The TT&C and communications subsystems shall include appropriate hardware/software for embedded encryption/decryption and communications security (COMSEC).

The meteorological satellite portion of the program requires the Contractor to develop the system-level design for a meteorological satellite system using the Advanced Very High Resolution Radiometer (AVHRR) or equivalent multi-spectral meteorological payload. The satellite shall be capable of being launched using either the ALV or SSLV. The meteorological satellite mission data shall be compatible with the capabilities of existing tactical weather terminals.

The communications satellite portion of the program requires the Contractor to develop a system-level design for integrating and demonstrating advanced technology spacecraft and payload subsystems and components which are being developed under DARPA sponsorship. The payload technologies, when integrated, comprise an advanced technology Extremely High Frequency (EHF) communications package capable of operating in 6, 8 and/or 12 hour Molniya-type elliptical orbits. The satellite shall be capable of being launched using either the ALV or SSLV.

4.0 CONTRACTOR TASKS

The Contractor shall provide all management, technical and administrative personnel, facilities, equipment, supplies, material and services to accomplish the following tasks:

4.1 TASK 1: MANAGEMENT

The Contractor shall appoint a Program Manager who shall be responsible for all aspects of this program and who shall serve as the single point of contact. The Contractor's Program Manager shall coordinate all contract activities with the Government Project Officer (hereafter referred to as the Project Officer). The Contractor's Program Manager shall be responsible for direction of his Project Staff and for timely submission of CDRL items.

4.1.1 Kick-Off Meeting. Within 30 calendar days following contract initiation, the Contractor shall meet at DARPA with the DARPA Program Manager, the Project Officer, and members of the ASTP Systems Engineering and Technical Assistance (SETA) team. Principle matters to be discussed will include project goals, ASTP-SETA-Contractor interaction, and resolution of any technical questions.

4.1.2 Monthly Progress And Expenditure Reports. The Contractor shall prepare a monthly Progress Report and an Expenditure Report which summarize the previous month's results of all work performed, expenses incurred, problems encountered and recommendations. The Progress Report shall also identify the Contractor's plan/schedule for accomplishing the contract requirements for the next two months. (CDRL A001, A002)

4.1.3 Informal Working Meetings. The Contractor shall provide technical participation during informal working meetings to be held monthly (typically, one day per meeting) at the Contractor's facility. These sessions are intended to cause as little impact as possible to the Contractor's efforts, yet enable sufficient insight to maintain awareness of the program activities and progress, and to assist with the resolution of any problems or issues that may arise.

4.1.4 Advanced Technology Meetings. The Contractor shall provide technical participation in meetings which are arranged by the Project Officer to address the DARPA-sponsored projects involving advanced technology spacecraft and payload subsystems and components. (For planning purposes, approximately 16 one-day meetings are anticipated with 75% being in the Los Angeles area and the remainder being at east coast locations.)

4.1.5 Quarterly Status Reviews. The Contractor shall present oral reports to the Project Officer and DARPA Program Manager summarizing the status/results of contract activity on a quarterly basis. The Quarterly Status Reviews shall alternately be held between the Contractor's facility and DARPA (Arlington, VA). The Contractor shall prepare presentation material and conference minutes for these reviews. (CDRL A003, A004)

4.1.6 Mid-Term Review. The Contractor shall present an oral Mid-Term Review to the Project Officer and DARPA Program Manager summarizing the technical investigations, status and results since contract start. The Mid-Term Review shall be held at the Contractor's facility. The Mid-Term Review will be attended by a larger Government audience to include representatives from the Military Services and other Government agencies. The Contractor shall prepare presentation material and conference minutes for this review. (The Quarterly Status Review is not required in the quarter for which the Mid-Term Review is scheduled.) (CDRL A003, A004)

4.1.7 Final Review. The Contractor shall present an oral Final Review to the Project Officer and DARPA Program Manager summarizing the technical investigations, status and results since the Mid-Term Review. The Final Review shall be held at the Contractor's facility. The Final Review will be attended by a larger Government audience to include representatives from the Military Services and other Government agencies. The Contractor shall prepare presentation material and conference minutes for this review. (The Quarterly Status Review is not required in the quarter for which the Final Review is scheduled.) (CDRL A003, A004)

4.1.8 Final Engineering Report. The Contractor shall prepare a final engineering report. (CDRL A005)

4.2 TASK 2: SYSTEM REQUIREMENTS DEFINITION

The contractor shall conduct analyses and trade studies to determine the system performance requirements and operational characteristics for a multi-mission adaptable small standard spacecraft bus. The Contractor shall perform trade-offs of the overall system architecture to determine: (1) which payloads, from potential mission areas which include meteorology, communications, surveillance and tracking, target location, navigation, and crosslinking can be accommodated by the spacecraft bus; (2) alternative orbits (including circular and Molniya-type elliptical) useful for the various missions and their effect on spacecraft bus design; (3) one-year (with a goal of eighteen months) and three-year (with a goal of 4 years) design lives on orbit and their impact as schedule and cost drivers; (4) use of ALV, SSLV, and other optional launch vehicles; (5) system adaptability and flexibility for quick-response launch; (6) orbit insertion and orbit transfer requirements; (7) autonomous spacecraft operations; (8) on-board data

handling (including processor and mass memory) to support spacecraft requirements and reserve capacity for payloads; (9) mission data communications requirements; (10) interoperability and compatibility with the Air Force Satellite Control Network (AFSCN); (11) embedded COMSEC for the TT&C and data links; and (12) any other factors affecting system performance.

The crosslink (including pass-through communications relay) trades shall include the advantages and disadvantages for alternative frequency bands which as a minimum include S- and K-Bands.

The Contractor shall also include the applicable mission ground segments as part of the system requirements trade-off activities. The trade-offs may consider employment of a multi-mission capable Common Data Link (CDL).

4.3 TASK 3: SPACECRAFT BUS SYSTEM DESIGN

Based on the results of the system requirements definition task, the Contractor shall perform systems engineering and design of a small, standard multi-mission adaptable spacecraft bus. The systems engineering and design activities shall include, but are not limited to the following:

- Structure and mechanical subsystem
- Attitude Determination and Control
- Orbit Determination and Control
- TT&C with embedded Encryption/Decryption (Including Satellite/AFSCN Interface and Control for SGLS Compatibility)
- Spacecraft Data Handling
- Software
- Electrical Power
- Payload Interfaces and Integration
- Communications and COMSEC
- Optionally Implemented Crosslinks
- Thermal Control
- Propulsion System
- Orbit Insertion
- Orbit Transfer
- ALV and SSLV Compatibility (and Compatibility with Other Launchers)
- Ground Support Equipment (GSE)

The Contractor shall address all external and internal system interfaces. The Contractor shall provide an assessment of the technical, schedule and cost risks of each subsystem and the overall spacecraft.

4.4 TASK 4: METEOROLOGICAL SATELLITE SYSTEM DESIGN

Based upon the spacecraft bus design developed in paragraph 4.3 (including optionally implemented crosslink), the Contractor shall develop the system design for the meteorological satellite, including the design of the following subsystems/segments:

- Any Adaptation of the Spacecraft Bus Unique to the Multi-Spectral Meteorological Payload and Mission
- Multi-Spectral Meteorological Payload Integration and Interfaces
- Mission Unique Equipment/Mission Unique Software (MUE/MUS), if required
- Satellite Checkout After Integration into the ALV and SSLV, and
- Unique GSE Required for the Meteorological Spacecraft

The Contractor shall accomplish performance analyses in support of the design and integration activities for the meteorological spacecraft.

The Contractor shall address all external and internal system interfaces unique to the meteorological satellite, including the mission ground segment. The meteorological satellite mission data shall be compatible with the capabilities of existing tactical weather terminals.

The Contractor shall provide an assessment of the technical, schedule and cost risks of each subsystem and the overall spacecraft.

4.5 TASK 5: ADVANCED TECHNOLOGY DEMONSTRATION SATELLITE SYSTEM DESIGN

Based upon the spacecraft bus design developed in paragraph 4.3 (including optionally implemented crosslink) and using DARPA-supplied data on advanced technology spacecraft and communications payload subsystems and components, the Contractor shall develop the system design for an advanced technology demonstration satellite capable of being placed into a Molniya-type elliptical orbit.

5.0 REPORTS, DATA AND OTHER DELIVERABLES

All reports and data shall be generated and submitted in accordance with the attached DD Form 1423 (or equivalent), Contract Data Requirements List (CDRL).

6.0 SPECIAL CONSIDERATIONS

6.1 DOCUMENTS

The Contractor shall use the following documents for guidance purposes only:

AFSCF-TR-86-204	MUS Generic Interface Description Document for Data System Modernization, 14 May 1986
DOD-HDBK-343	Design, Construction, and Testing Requirements For One of a Kind Space Equipment, 1 February 1986
MIL-HDBK-340	Applications Guidelines for MIL-STD-1540B, Test Requirements for Space Vehicles
MIL-STD-1540	Test Requirements for Space Vehicles
TOR-0059(6110-01)-3	Air Force Control Facility Space/Ground Interface, June 1987